

Central European Geology

Acta Geologica Hungarica

Editor-in-Chief
Attila DEMÉNY

Vice Editor-in-Chief
Elemér PÁL-MOLNÁR

Guest Editor
István FÓRIZS

Editorial Board

Applied and Environmental Earth Sciences – Ákos TÖRÖK

Economic Geology – Ferenc MOLNÁR

Fossils and Stratigraphic Records – József PÁLFY

Geochemistry – Gábor DOBOSI

Geodynamics – Emő MÁRTON

Mineralogy, Petrology – Tivadar M. TÓTH

Petroleum Geology – György POGÁCSÁS

Regional Geology and Sedimentology – János HAAS

Ágnes KRIVÁN-HORVÁTH &

Gábor SCHMIEDL (Co-ordinating Editors),

Henry M. LIEBERMAN (Language Editor)

Advisory Board

György BÁRDOSSY (Chairman), Tamás BUDAI, Géza CSÁSZÁR,

László CSONTOS, János FÖLDESSY, Magdolna HETÉNYI,

Judit MÁDLNÉ SZÓNYI, Mihály PÓSFAL, Attila VÖRÖS,

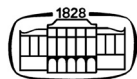
Ioan BUCUR (Romania), Sorin FILIPESCU (Romania), Ron FODOR (USA),

Wolfgang FRISCH (Germany), Friedrich KOLLER (Austria),

Robert MORITZ (Switzerland), Richard PRIKRYL (Czech Republic),

Gábor TARI (Austria), Dario ZAMPIERI (Italy)

Volume 54, Numbers 1–2, March 2011



AKADÉMIAI KIADÓ
MEMBER OF WOLTERS KLUWER GROUP

Published by the financial support of the
Committee on Publishing Scientific Books and Periodicals,
Hungarian Academy of Sciences

Front cover
House of Parliament in Budapest (Hungary) on the left bank of the River
Danube. Photo: János Miskolczy

Cover design: xfer grafikai műhely

European Society for Isotope Research

Isotope Workshop XI

4th–8th July 2011
Budapest, Hungary

Organized by

European Society for Isotope Research
<http://www.esir.org.pl>



Institute for Geochemical Research,
Hungarian Academy of Sciences, Budapest, Hungary
<http://www.geochem.hu>

Local Organizing Committee

Chair: **István Fórizs** – Ph.D., senior research fellow
Secretary: **Sándor Kele** – Ph.D., research fellow
György Czuppon – Ph.D., junior research fellow
Attila Demény – corresponding member of the Academy, director
József Fekete – Ph.D. student, junior research fellow
Krisztina Kármán – Ph.D. student, junior research fellow
Zoltán Kern – Ph.D., junior research fellow
Gabriella Schöll-Barna – Ph.D. student, junior research fellow
Zoltán Siklósy – Ph.D. student, junior research fellow

Members of the Advisory Board (2009–2011)

István Fórizs – President of the ESIR (Budapest, Hungary)
Marion Tichomirowa – Vice President of the ESIR (Freiberg, Germany)
Zwjezdana Roller-Lutz – Vice President of the ESIR (Rijeka, Croatia)
Adriana Trojanowska – past president (Wrocław, Poland)
Bogdan P. Onac – past president (Cluj, Romania)
Gerhard Strauch – past president (Leipzig, Germany)
Ana-Voica Bojar – past president (Graz, Austria)
Rein Vaikmäe – past president (Tallinn, Estonia)
Nada Miljević – elected member (Belgrade, Serbia)
Mariusz-Orion Jędrysek – elected member (Wrocław, Poland)

Contents

Editorial A. Demény, I. Fórizs	1
BIOGEOCHEMISTRY	
H and C isotope trends and anomalies in hot and mature oils from the Pannonian Basin. J. Fekete, Cs. Sajgó	5
Compound-specific isotope analysis for assessing sources and fate of aromatic hydrocarbons in contaminated aquifers. M. Blessing, E. Proust, D. Widory	15
Metabolic origin of $\delta^{13}\text{C}$ in dark-respired CO_2 : Comparison between leaves and roots. J. Ghashghaie, C. Bathellier, G. Tcherkez, F. W. Badeck	16
The use of stable isotopes for assessing Portuguese wine genuineness. A. I. Janeiro, L. Ramalho, B. Henriques, L. Santos, F. Alvarrão, F. Costa, A. J. R. Teixeira	17
<i>Mytilus galloprovincialis</i> as a bioindicator of environmental conditions: the case of the eastern coast of the Adriatic Sea. T. Kanduč, D. Medaković, B. Hamer	18
Tracing biogeochemical processes and pollution sources with stable isotopes in river systems: Kamniška Bistrica (Slovenia) case study. T. Kanduč, M. Šturm, S. Žigon, D. Kocman, J. C. McIntosh	19
Application of geochemical and isotopic analysis and their role in the examination of coal gas genesis. J. Pezdič, S. Zavšek, J. Žula, T. Kanduč	20
Carbon and hydrogen isotopic variations in a low pressure methane-poor hydrocarbons deposit. L. Plešniak, M. Bucha, M.-O. Jędrysek	21
Bone collagen in mammals from the outskirts of the Early Roman Empire. C. M. Puscas, Z. Bedaso, C. Roman, I. Ferencz, C. C. Stremtan	22
Deuterium depletion as a new approach in cancer treatment and prevention. G. Somlyai, A. Kovács, I. Guller, Z. Gyöngyi, K. Kremfels, I. Somlyai, M. Szabó, T. Berkényi, M. Molnár	23
Tracing the stable isotope composition of oxygen and hydrogen in precipitation from tree ring cellulose – examples from an oak and two pine tree sites in Finland. E. Sonninen	24
Organic matter sources in sediments of Szczecin Lagoon (NW Poland) indicated by C and N isotopic composition. A. Trojanowska, P. Jezierski, A. Skowronek	25
The carbon isotopic composition of dried and carbonized plant samples. P. Vreča, M. Šturm, I. Krajcar Bronić	26
ENVIRONMENTAL GEOCHEMISTRY AND ECOLOGY	
Groundwater nitrate sources in alluvial aquifers: Isotope case study in Savinja Valley (Slovenia). J. Uhan, S. Lojen, M. Pintar, J. Pezdič	29
C, N isotopic ratios in <i>P. oceanica</i> meadows of Alexandroupolis Gulf, NE Greece. M.-V. Apostolopoulou, P. Roose, P. Kosmas, F. Dehairs	35

Stable isotope distribution in deep-sea hydrothermal barnacle, Manus Basin, Papua New Guinea: a key in understanding their ecology. <i>A.-V. Bojar, H.-P. Bojar, W. Tufar</i>	36
Chemical and isotopic yearly seasonal observations of the ammonium and nitrate in Wrocław (SW Poland) precipitation. <i>M. Ciężka, M. Górka, M. Modelska, M.-O. Jędrysek, S. Stacko</i>	37
Apportionment of carbon dioxide over central Europe: insights from combined measurements of atmospheric CO ₂ mixing ratios and carbon isotope composition. <i>M. Galkowski, D. Jelen, M. Zimnoch, T. Kuc, J. Necki, Ł. Chmura, Z. Gorczyca, A. Jasek, K. Rózanski</i>	38
5-years (2004–2009) isotopic seasonal observations of the sulphates in Wrocław (SW Poland) precipitation. <i>M. Górka, S. Halas, D. Strapoć, D. Kufka, M.-O. Jędrysek</i>	39
Triple oxygen isotope composition as a potential tracer for mixing ratios of carbon dioxide sources in urban air. <i>B. Horváth, M. E. G. Hofmann, A. Pack</i>	40
Sulphur and oxygen isotopes in dissolved sulphates as tracers of sea and river water mixing in the Szczecin Lagoon (Poland). <i>P. Jezierski, A. Trojanowska, A. Skowronek</i>	41
Methanogenesis in the Pliocene Velenje Coal Basin, Slovenia, inferred from stable carbon isotopes. <i>T. Kanduč, M. Markič, S. Zavšek, J. McIntosh</i> . . .	42
Carbon isotopic variation in $\delta^{13}\text{C}_{\text{DIC}}$ and $\delta^{13}\text{C}_{\text{CO}_2}$ during early anaerobic decomposition of organic agriculture wastes. <i>D. Kufka, B. Biega, M.-O. Jędrysek</i>	43
Recent paleolimnological changes in small carbonate rich hypertrophic lake. <i>A. Mikomägi, T. Martma, A. Marzecova</i>	44
Use of light stable isotopes, dissolved gas constituents, and microbial community abundances to characterize biodegradation of chlorinated ethenes in a fractured-rock aquifer. <i>K. Révész, B. Sherwood Lollar, A. M. Shapiro, J. Kirshtein, M. Voytek, T. E. Imbrigiotta, E. Busenberg, C. R. Tiedeman, D. J. Goode</i>	45
Distribution and origin of organic matter in the Baltic sediments based on $\delta^{13}\text{C}$ profiles in sediment cores dated with ²¹⁰ Pb and ¹³⁷ Cs. <i>A. Szczepanska, A. Maciejewska, K. Kulinski, J. Pempkowiak</i>	46
Carbon and nitrogen isotopic analysis coupled with palynological data of PM10 dust in Wrocław city (SW Poland) – assessment of anthropogenic impact. <i>E. Zwolińska, M. Górka, M. Malkiewicz, D. Lewicka-Szczebak, M.-O. Jędrysek</i>	47
GENERAL ISOTOPE GEOCHEMISTRY	
Hydrogen isotope compositions in carbonado diamond: constraints on terrestrial formation. <i>A. Demény, G. Nagy, J. Garai, B. Bajnóczy, T. Németh, V. Drozd, E. Hegner</i>	51
Carbon isotope study on Celtic graphite-tempered archaeological ceramics from the South Transdanubian region (Hungary). <i>I. Havancsák, J. Fekete, B. Bajnóczy</i>	75

Experimental study of D/H fractionation between water and hydrogen gas during the oxidation of Fe-bearing silicates at high temperatures (600 °C–1200 °C). <i>L. Simon, C. Lécuyer, F. Robert, F. Martineau</i>	81
$\delta^2\text{H}$ and $\delta^{13}\text{C}$ of methane in lignite fermentation. <i>M. Bucha, L. Plešniak, K. Kubiak, M. Blaszczyk, M.-O. Jędrysek</i>	95
Calculation of chlorine and bromine isotope fractionation factors in aqua-gas system. <i>M. Czarnacki, S. Halas, A. Pelc</i>	96
Dissolving halite for H, C and S isotopic analysis of fluid inclusions. <i>W. Drzewicki, S. Burliga, J. Krajniak, L. Plešniak, M.-O. Jędrysek</i>	97
Origin of Precambrian carbonate rocks of the Ukrainian Shield by geological-structural peculiarities and isotopic signatures. <i>V. Guliy, V. Zagnitko, R. Bochevar</i>	98
Anomalous $\delta^{18}\text{O}$ isotope composition of minerals from North Karelia (Russia). <i>A. V. Ignatiev, V. I. Levitskiy, S. V. Vysotskiy, S. Yu. Budnitskiy, T. A. Velivetskaya</i>	99
INERT GAS AND RADIOGENIC ISOTOPES	
Noble gases in mantle derived xenoliths from Eastern Australia and their implications for the tectonic evolution: Summary. <i>Gy. Czuppon, T. Matsumoto, J. Matsuda, M. R. Handler, J. Everard, L. Sutherland</i>	103
Helium isotopes distribution in NW Iberian peninsula: evidences of a local neotectonic activity. <i>F. Grassa, G. Capasso, P. M. Carreira, M. R. Carvalho, J. M. Marques, M. A. da Silva</i>	104
Deep groundwater age dating with noble gases (He) and chlorine-36: The Continental Intercalaire aquifer from the Sahara basin. <i>A. Guendouz, A. S. Moulla, J.-L. Michelot</i>	105
Study of the behavior of radon isotope in Pál-völgy show cave (Budapest, Hungary). <i>H. É. Nagy, Cs. Szabó, Á. Horváth, A. Kiss</i>	106
Uranium, radium and ^{222}Rn isotopes in thermal waters from Podhale Trough (Polish Inner Carpathians). <i>C. D. Nguyen, J. Nowak, P. Jodłowski</i>	107
^{222}Rn concentration measurements of soil gas in Hungary. <i>K. Zs. Szabó, Á. Horváth, Cs. Szabó</i>	108
Testing of fast ^{222}Rn and ^{220}Rn exhalation measurements of high number of Hungarian adobe building material samples. <i>Zs. Szabó, Cs. Szabó, Á. Horváth</i>	109
Isotopic constraints on genesis of the multistacked $\text{CO}_2\text{-CH}_4\text{-N}_2$ Répcelak gas field (Pannonian Basin System, W Hungary). <i>I. Vétő, L. Palcsu, I. Futó, G. Vodila, L. Papp, Z. Major</i>	110
Examination of radiogenic isotopes and chemical composition of coal slag and fly ash bearing building materials. <i>P. Völgyesi, H. É. Nagy, Cs. Szabó</i>	111
ISOTOPE HYDROLOGY	
Comparison of the isotope hydrogeological features of thermal and cold karstic waters in the Denizli Basin (Turkey) and Buda Thermal Karst (Hungary). <i>I. Fórizs, A. Gökgöz, S. Kele, M. Özkul, J. Deák, M. O. Baykara, M. C. Alçiçek</i>	115

Study of the bank filtered groundwater system of the Sava River at Zagreb (Croatia) using isotope analyses. <i>N. Horvatinčić, J. Barešić, K. Kármán, I. Fórizs, I. K. Bronić, B. Obelić</i>	121
Isotopic study of nitrates and bicarbonates in mineral waters of the Southeast Poland. <i>A. Baran</i>	129
Error in variables regression model for meteoric water line determination. <i>M. Brenčić</i>	130
Stable isotope feature of groundwaters from Graciosa volcanic Island (Azores) – preliminary results. <i>P. M. Carreira, J. M. Marques, M. R. Carvalho, F. Grassa, G. Capasso, D. Nunes, J. C. Nunes</i>	131
Determining forest turbulent transport and evapotranspiration partition with the help of a new soil water isotope model. <i>M. Cuntz, V. Haverd, D. W. Griffith, C. Keitel, C. Tadros, J. Twining</i>	132
Stable isotope composition of carbon dioxide and TDIC reservoir associated with mineral waters of the Polish Flysch Carpathians. <i>M. Dulinski, L. Rajchel, J. Rajchel</i>	133
Assessing the impacts of anthropogenic activities on groundwater quality using nitrogen isotopes – Alter do Chão-Monforte (Portugal). <i>P. Galego Fernandes, M. R. Carvalho, C. Silva</i>	134
$\delta^{18}\text{O}$ spatial distribution of precipitation in Croatia. <i>T. Hunjak, D. Mance, H. O. Lutz, Z. Roller-Lutz</i>	135
The effect of the mutual interaction between climate change and the land-use pattern on the hydrologic regime under dry-land conditions. <i>J. R. Gat</i>	136
Hydrogeochemistry of Alpine springs from North Slovenia: insights from stable isotopes. <i>T. Kanduč, N. Mori, D. Kocmanan, V. Stibilj, F. Grassa</i> . . .	137
Estimation of groundwater transit time by lumped parameter model using $\delta^{18}\text{O}$ on Szentendre Island, Hungary. <i>K. Kármán, P. Maloszewski, I. Fórizs, J. Deák, Cs. Szabó</i>	138
Isotopic investigations on some mineral waters from Corund, Harghita County, Romania. <i>B. M. Kis, K. Kármán, C. Baciú</i>	139
Quantitative assessment of lake water balance components: new calculation approach. <i>D. Lewicka-Szczebak, M.-O. Jędrysek</i>	140
Strontium isotopic ($^{87}\text{Sr}/^{86}\text{Sr}$) and geochemical signatures of CO_2 -rich thermal and mineral waters (N-Portugal). <i>J. M. Marques, P. M. Carreira, H. G. M. Eggenkamp, M. A. da Silva, L. Aires-Barros</i>	141
Application of isotopes for assessment of pollution probability of drinking water resources in Georgia. <i>G. I. Melikadze</i>	142
Relationship between atmospheric circulation and stable isotope composition of Belgrade daily precipitation. <i>N. Miljević, A. Pešić, D. Golobočanin, Z. Gršić, M. Unkašević, I. Tošić</i>	143
Hydrogeochemical and isotopic assessment of seawater intrusion into alluvial aquifers in the Western Algiers coastal area (Tipasa, Algeria). <i>A. S. Moulla, A. Guendouz, M. Belaid, H. Maamar, S. Ouarezki</i>	144

Isotopic composition of sulphates dissolved in waters of deep aquifers associated with copper ore deposits: implications for sulphate source and water-rock interaction. <i>A. Porowski, J. Dowgiallo, S. Halas, R. Becker</i>	145
Badenian salinity crisis in Carpathian foredeep: new insights from stable isotope composition of fluid inclusions in halite deposits of Wieliczka and Bochnia, southern Poland. <i>K. Rózanski, M. Dulinski, K. Bukowski</i>	146
Oxygen isotope variations in shallow lake water and bivalve shells: application of the isotope mass balance model. <i>G. Schöll-Barna, A. Demény, T. Cserny, I. Fórizs, P. Sümegi</i>	147
Sulphate reduction in deep groundwater. <i>G. Strauch, K. Al-Mashaikhi, K. Knöller</i>	148
Radiocarbon age study of Slovenian–Hungarian transboundary groundwater. <i>T. Szócs, N. Rman, M. Süveges</i>	149
Preliminary geochemical and isotope results in a hydrogeologic complex volcanic system aquifer in Tumbaco – Cumbayá region (Ecuador). <i>J.-D. Taupin, C. Manciat, T. Munoz, N. Arias, O. Larrea, R. Alulema, C. Leduc</i>	150
Tritium level in several European surface waters. <i>C. Varlam, I. Stefanescu, A. Soare, I. Faurescu</i>	151
A 9-year record of stable isotope ratios of precipitation in Eastern Hungary: implications on isotope hydrology and regional palaeoclimatology. <i>G. Vodila, L. Palcsu, Zs. Szántó, I. Futó</i>	152
Detailed isotopic mapping of the karstic Savica River, NW Slovenia. <i>P. Vreča, M. Brenčič</i>	153
PALEOCLIMATE	
Calculation of temperature and $\delta^{18}\text{O}$ of depositing water by measured $\delta^{18}\text{O}$ of recent travertines deposited from the Budapest thermal karst water. <i>J. Deák, S. Kele, I. Fórizs, A. Demény, Gy. Scheuer</i>	157
Sedimentary changes vs. climate signals in bivalve shell and bulk rock compositions in a Late Pleistocene to Early Holocene fluvial section at Körösladány, SE-Hungary. <i>A. Demény, P. Sümegi, G. Schöll-Barna, P. Sipos, B. R. Balázs</i>	167
Stable isotope studies of secondary carbonates of the Süttő loess-paleosoil sequence, Hungary. <i>G. Barta, P. Koeniger, E. Horváth, M. Frechen, B. Bajnóczy</i>	173
Calcite carbon and oxygen stable isotopes in riverine tufas as paleoclimatic records of Interglacials: the sequence of Condat-sur-Vézère (MIS 5, South-western France). <i>J. Dabkowski, N. Limondin-Lozouet, P. Antoine, A. Marca-Bell, J. Andrews, P. Dennis</i>	174
Isotope hydrological and geophysical studies on the perennial cave ice deposit of Saarlhale (Mammuthöhle, Dachstein Mts, Austria). <i>Z. Kern, I. Fórizs, L. Palcsu, M. Behm, H. Hausmann, R. Pavuza</i>	175

Stable O-isotope record of Holocene freshwater tufa in Lake Valgejärve, Estonia – an interpretation of postglacial climate changes. <i>L. Laumets, V. Kalm</i>	176
The isotopic memory of fossils. <i>C. Lécuyer</i>	177
Semi-continuous online isotope and elemental ratio measurements of high time resolution on Greenland ice cores for temperature reconstruction. <i>M. Leuenberger, P. Kindler, C. Huber</i>	179
Carbon and oxygen isotopes in Baltic Early Palaeozoic geology: some results and trends. <i>T. Martma, D. Kaljo</i>	181
Stable isotopes of rainfall and dripwater at Ursilor Cave (Romania): the path to reliable speleothems paleoclimate reconstructions. <i>B. P. Onac, T. Tămaş, I. Vişan</i>	182
Modelling the effects of melting and refreezing on the original isotopic signal in cave ice. <i>A. Perşoiu</i>	183
Correlating $\delta^{18}\text{O}$ values of Barbary sheep tooth enamel and environmental waters: Implications for North African palaeoclimate reconstructions. <i>H. Reade, G. Barker, T. Legge, T. O'Connell, R. Stevens</i>	184
Recent achievements and future prospects of ice core science. <i>R. Vaikmäe</i> ..	185
Pleistocene seasonal temperature reconstructions from $\delta^{18}\text{O}$ of bison teeth, Ural Russia. <i>T. A. Velivetskaya, N. G. Smirnov, S. I. Kiyashko, A. V. Ignatiev, A. I. Ulitko</i>	186

TECHNICAL DEVELOPEMENTS

Reduced partition function ratios for isotopes of hydrated alkali and alkaline earth ions calculated by a simple electrostatic model. <i>M. Czarnacki, S. Halas</i>	189
<i>Ab initio</i> calculations of sulfur isotope fractionation factor for H_2S in aqua-gas system. <i>M. Czarnacki, S. Halas</i>	199
Rapid ^2H analysis of small H_2O samples by CF-IRMS. <i>E. M. Galimov, V. S. Sevastyanov, N. E. Babulevich, A. A. Arzhannikov</i>	200
Innovations in technical developments of stable isotope analyses. <i>S. Halas</i> ..	201
UV laser ablation microanalysis of $\delta^{34}\text{S}$. <i>A. V. Ignatiev, T. A. Velivetskaya</i>	202
Noble gas measurements from 1 μL of water: fluid inclusions of speleothems. <i>L. Palcsu, L. Papp, Z. Major</i>	203
Chlorine stable isotope ratio analysis by the negative surface ionization of chloromethane. <i>A. Pelc, S. Halas, M. Czarnacki</i>	204
Isotope Ratio Mass Spectrometry for tracing the origin of cyanide for forensic investigation. <i>I. Tea, I. Antheaum, B.-L. Zhang</i>	205
Simultaneous measurements of carbon and oxygen isotopologues of carbon dioxide using a mid-IR laser based platform. <i>E. Wapelhorst, H.-J. Jost, J. J. Scherer, J. B. Paul</i>	206
Index of authors	207

To the Reader,

This issue of Central European Geology contains papers describing presentations of the 11th Isotope Workshop of the European Society for Isotope Research held in Budapest. Conference volumes of earlier workshops contained usually abstracts or extended abstracts. However, several participants sent inquiries if longer papers could be published beside the usual conference abstracts. The organizers and the editors decided to provide the possibility of publication of short and regular papers. Some of the submitted manuscripts were not presented at the meeting, but all of them were related to isotope research. Thus, the publishers and the editors decided to insert these papers in the special issue after the regular review process and merge two issues in a double one in order to produce a coherent compilation of papers.

The compilation of the issue was mainly conducted by the guest editor and president of the Society, István Fórizs, with the help of the local organizing team. The team had a hard job to arrange reviewing, pursue authors to revise the papers and edit the final versions, so their work is gratefully thanked. Finally I would like to express my gratitude to the reviewers. The special issue greatly benefitted from their help as they provided their opinions in very short course. I hope the readers will like the issue and find interesting ideas in the papers, and if they do, the investment of the authors, the organizers and the reviewers will pay off.

Kind regards,

Attila Demény
Editor-in-Chief

Introduction

It was in 1991 when late István Cornides, the father of isotope geochemistry in Hungary, gave us a printed invitation for an Isotope Workshop to be held in Lublin in May 1992. Our stable isotope laboratory was established just in the preceding year, we were two years after the political turnover in the Eastern European Block, and we were young, so in 1992 with a great enthusiasm together with my colleague Attila Demény (now director of our institute) we drove happily to Lublin, Poland. And our expectations were more than fulfilled. We could make fruitful contacts with well-known researchers and good friendships. We were so enthusiastic that we decided to establish an international society. And we did it under the name International Isotope Society registered in Poland. Soon I noticed that there was another society with exactly the same name. Although they offered the fusion of these two societies, we wanted to go on our way; therefore in 1996 we changed the name to European Society for Isotope Research (ESIR). Our intention was to organize biannual meetings in Europe, mostly in Central Europe providing an opportunity for researchers living in the former

communist countries to come together on moderate costs and to meet colleagues living in other part of Europe and of the world.

Anyway, the 'Isotope Workshop I' held in 1992 in Lublin was a starting point of a series of workshops with slightly increasing number of attendees and firmly developing in quality. Let's recall the venues and organizers of these workshops: 1st in Lublin, Poland, 1992 (Mariusz-Orion Jędrysek, Stanislaw Halas); 2nd in Ksiaz, Poland, 1994 (Mariusz-Orion Jędrysek); 3rd in Budapest, Hungary, 1996 (Attila Demény, István Fórizs); 4th in Portorož, Slovenia, 1998 (Jože Pezdic); 5th in Cracow, Poland, 2000 (Przemislaw Wachniew); 6th in Tallinn, Estonia, 2002 (Rein Vaikmäe); 7th in Seggau, Austria, 2004 (Ana-Voica Bojar); 8th in Leipzig, Germany, 2005 (Gerhard Strauch); 9th in Cluj, Romania, 2007 (Bogdan P. Onac); 10th in Zlotniki Lubanski, Poland, 2009 (Adriana Trojanowska); and now the 11th in Budapest, Hungary, 2011 (István Fórizs).

This time the number of registered participants is 95 – the biggest so far – indicating the success of previous Isotope Workshops and the increasing need for the research dealing with environmental isotopes. The meeting is based on 50 oral and 44 poster presentations with a wide range of scopes, including two invited speakers and seven key note lecturers. Reflecting the modern trends the two invited speakers present review papers on paleoclimate: "*Isotopic memory of fossils*" (Christophe Lécuyer) and "*Semi-continuous online isotope and elemental ratio measurements of high time resolution on Greenland ice cores for temperature reconstruction*" (Markus Leuenberger). The presentations are arranged into seven chapters (Biogeochemistry, Environmental Geochemistry and Ecology, General Isotope Geochemistry, Inert Gas and Radiogenic Isotopes, Isotope Hydrology, Paleoclimate, Technical Developments), among which the section of Isotope Hydrology is the biggest one with 27 presentations underlining the growing importance of water research.

I wish a joyful time for the readers while reading this Volume.

István Fórizs
Guest Editor

President of the European Society for Isotope Research
Senior research fellow, Institute for Geochemical Research,
Hungarian Academy of Sciences

BIOGEOCHEMISTRY

H and C isotope trends and anomalies in hot and mature oils from the Pannonian Basin

József Fekete, Csanád Sajgó
Institute for Geochemical Research,
Hungarian Academy of Sciences, Budapest

Crude oil samples from uncommonly hot ($>170^{\circ}\text{C}$) reservoirs of the SE-Pannonian Basin were studied for stable carbon and hydrogen isotope compositions of their different fractions. From two fields, 15 samples of different depths and temperatures were chosen for this study. The aim was to study the impact of extreme reservoir conditions on the isotope ratios of the different fractions and to find the ratios that show correlation with increasing depth and temperature.

We have shown that the behaviour of isotopes in these very hot oils differs from those from lower temperatures. The combined application of carbon and hydrogen isotope techniques is useful and may provide approximate information on reservoir conditions.

Key words: crude oil, oil fractions, δD , $\delta^{13}\text{C}$, hot reservoirs

Introduction

Stable isotope ratios have always been among the best tools of organic geochemists studying oil generation, migration, maturation, oil-to-oil and oil-to-source rock correlation. The stable isotopic compositions of crude oil fractions (e.g. saturated, aliphatic, aromatic etc.) are proven to be very informative and useful techniques and so are the isotope type-curves (e.g. Galimov 1973; Stahl 1978). The application of D/H ratios is also a well-known tool in determining the source, maturity and biodegradation of crude oils. The use of isotopic compositions of oil fractions is a reliable isotope technique.

Addresses: J. Fekete, Cs. Sajgó: H-1112 Budapest, Budaörsi út 45, Hungary,
e-mail: feketej@sparc.core.hu

Received: May 9, 2011; accepted: May 19, 2011

Oil traces of the Makó–Hódmezővásárhely-trough (M–H-trough), Pannonian Basin have been studied recently (Fekete et al. 2009, 2010, 2011). The isotope type-curves formed from the stable carbon and hydrogen isotope compositions of different oil fractions were found to be good tools to group these oils of different origins. However, the carbon and hydrogen stable isotopic compositions of fractions in these oils are not obvious.

In this paper we study the stable carbon and hydrogen isotope ratios in different fractions of very hot oils from two sites from the M–H-trough. Ten of the fifteen samples was investigated former (Fekete et al. 2011). Our aim is to present the isotopic features of high temperature oils (from 170°C to 215°C) and we also try to briefly interpret the effects of the extreme reservoir conditions.

Geological setting and samples

The M–H-trough is one of the deepest subbasins of the Pannonian Basin. It is filled with Neogene and Quaternary sediments (silts, fine grained marls, calcareous marls, sandstones and shales of brackish and lacustrine environments) up to the thickness of 7000 meters. However, giant Algyó oil and gas field is located adjacent to the area, up to now, identification of proven source rocks has been unsuccessful; candidates are shales from the basal part of the basin fill (Koncz et al. 1999). The geothermal gradient is varying around 40°C/km depending on depth (Dövényi and Horváth 1988; Sajgó 1980; 2000; Sajgó et al. 1988; Hetényi et al. 1993).

Samples were chosen from four (SI1; SI2-3; SII; SI4–9) wells of two fields close to each other and located in the M–H-trough. For proprietary reasons the names of the wells and fields are changed and also the exact depth and temperature values are not presented. "SI" and "SII" represent the two sites and increasing numbers represent the increasing depths and temperatures. The oils are mature or very mature ones and show no signs of biodegradation (Sajgó 2000). SI4 and SII1 are so-called "kick" samples that were taken when the drill reached the first oil reservoir. These samples can be contaminated by the drilling mud and the formation waters.

Sample preparation and methods

The oil samples are 'topped' oils not containing any $<C_{14}$ compounds.

Separation of oil fractions was carried out on the basis of the method used by Sajgó (1980). The fractions and their abbreviations (between brackets) are as follows: n-alkanes (n-alk), saturated aliphatic (sat), n-alkane-free saturated (isoalkanes, in our case predominantly isoprenoid alkanes; iso), aromatic hydrocarbon (aro) fraction, resin (heteroaromatic) compounds (NSO), asphaltenes (asph).

The samples were oxidized with copper-oxide in evacuated and flame-sealed pyrex tubes at 480°C based on the method of Sofer (1980). The evolved H₂O and CO₂ were separated by means of vacuum distillation using liquid nitrogen and ethyl-alcohol cooled below -80 °C. H₂ gas was produced from H₂O using the zinc reduction method (Coleman et al. 1982; Demény 1995).

The D/H and ¹³C/¹²C ratios were determined using a Finnigan MAT delta S mass spectrometer. The results are given in the conventional δ value ($\delta = (R_{\text{sample}}/R_{\text{standard}}) \cdot 1000$, where R_{sample} and R_{standard} are the D/H and ¹³C/¹²C ratios in the sample and standard, respectively) relative to V-SMOW (H) and V-PDB (C) in ‰. Based on sample reproducibility and differences in δD and δ¹³C values obtained for standards from their theoretical values, the results are accurate at ±3‰ for δD and better than ±0.1‰ for δ¹³C. See Fekete et al. (2011) for detailed description.

Results and discussion

The carbon isotopic composition of oils is basically determined by the composition of the original organic matter (i.e. contribution of different biota: higher plants to algae), salinity of the depositing water body and climate. During deposition and burial, diagenesis and maturation processes the carbon isotopic composition may change (Galimov 2006). It can be greatly changed by biodegradation and partly by maturation processes but is assumed to remain constant during migration. Maturation causes saturated fraction to be enriched and asphaltenes (and NSO compounds) to become depleted in ¹³C (Galimov 2006). Aromatic hydrocarbons are the most resistant fractions to isotope change (Stahl 1980; Schoell 1984).

The D/H ratio of oil is determined by the hydrogen isotope compositions of the initial organic matter and that of the formation water at the time of deposition and the subsequent rock-water-oil interactions at high temperatures during migration or in the reservoir rocks. The oils may become enriched in D due to their interaction with formation waters, as suggested by pyrolysis experiments (Schimmelmann et al. 2001). The hydrogen exchange with water mainly affects the NSO compounds and mildly other aromatics.

Our results are listed in Table 1. ¹³C/¹²C and D/H ratios of the fractions are presented in aliphatic and non-aliphatic separate plots (Figures 1–4). δD_{aro}/δD_{NSO} and δD_{asph}/δD_{NSO} ratios are plotted in Figure 5.

The δ¹³C values of n-alkanes slightly decrease and those of isoalkanes increase in the middle sample set (SII), while that of the saturated fraction does not show a definite trend. The least hot and the hottest samples of the other sample set (SI) do not show any obvious trend. The δ¹³C of the saturated fraction varies slightly between -27.8 and 27.0‰ with one extremely high value of -25.5‰ (Figure 1). The isoalkanes are distinctively enriched in ¹³C compared to n-alkanes, the SI5

sample excepted. Bjoroy et al. (1991) also reported that isoprenoids were generally heavier than n-alkanes in oils.

The $\delta^{13}\text{C}$ values of the three non-aliphatic fractions (Figure 2) do not show any significant trend. The values are more scattered than those of aliphatic fractions. Asphaltene $\delta^{13}\text{C}$ values show the largest variability with two outliers (SI3 and SI9) which shows the instability of this fraction. The $\delta^{13}\text{C}_{\text{aro}}$ is generally 1–2‰ less negative than $\delta^{13}\text{C}_{\text{NSO}}$ and $\delta^{13}\text{C}_{\text{asph}}$. This is the effect of maturation (Galimov 2006). Similar phenomenon was found by e.g. Cortes et al (2010). The two "kick" samples do not show regular deviation; however, SII1 $\delta^{13}\text{C}_{\text{NSO}}$ and $\delta^{13}\text{C}_{\text{asph}}$ values are more negative compared to those of SII2–SII6.

The δD of aliphatic fractions vary in a relatively narrow range of -135 – -115 ‰ (Fig. 3) and shows a slight increase towards greater depths and temperatures. It is notable that δD of isoalkanes is the same or somewhat less negative than that of n-alkanes in the first (SI1–SI3) group, and in the others (SII and SI4 – SI9) n-alkanes are enriched in D compared to isoalkanes. In SII the correlation is good between $\delta\text{D}_{\text{n-alk}}$ and $\delta\text{D}_{\text{iso}}$, and exists in SI.

Relationship between hydrogen isotopic compositions of non-aliphatic fractions is rather complicated (Fig. 4). The values are scattered between ~ -90 and -160 ‰. We can observe that with one exception the δD values of aromatic and asphaltene fractions run close to each other, and that of NSO compounds is far more negative. The $\delta\text{D}_{\text{aro}}$ and $\delta\text{D}_{\text{asph}}$ decrease and $\delta\text{D}_{\text{NSO}}$ increases with increasing depths and temperatures in SI. In SII this phenomenon cannot be observed.

$\delta\text{D}_{\text{aro}}/\delta\text{D}_{\text{NSO}}$ and $\delta\text{D}_{\text{asph}}/\delta\text{D}_{\text{NSO}}$ increase in both groups (Fig. 5). As stated former, the NSO compounds are the most affected by hydrogen exchange processes, but this increase in the mentioned values is unexpected. As Figures 4 and 5 show, "kick" samples are exceptions, because their NSO compounds are enriched in D.

On the basis of the results discussed former we can state the following:

1. The $\delta^{13}\text{C}$ of the isoalkane fraction is less negative than that of the n-alkanes. The extreme high temperature has not affected the general difference between the two fractions. At high temperatures the non-aliphatic fractions are not resistant to isotope fractionation and their δ values are more variable. The $\delta^{13}\text{C}$ of aromatic fraction is 1–2‰ less negative than that of asphaltene and NSO compounds.

2. The δD of aliphatic fractions is less variable than that of non-aliphatic fractions. A slight enrichment of D may be observed in the fractions towards greater depths and temperatures, but δD values do not show strong temperature dependence. Aromatic and asphaltene fractions represent the least negative δD values, and in negative direction n-alkanes, isoalkanes and NSO compounds follow, which are strongly depleted in D. In one sample set (SII) the $\delta^{13}\text{C}_{\text{n-alk}}$ decreases and $\delta^{13}\text{C}_{\text{iso}}$ increases with increasing depth and temperature, in the

other (SI) δD_{aro} and δD_{asph} decrease and D_{NSO} increases with increasing depths and temperature.

3. In high temperature reservoirs the application of carbon and hydrogen stable isotopes is limited. The inherited isotopic features were partly preserved in the oils, and the temperature dependent isotopic trends are exhibited clearly only by oils of the same organic facies.

4. Our results corroborate the observation, that NSO compounds are the most affected by hydrogen exchange processes. The samples studied show the relative deuterium depletion of NSO fraction.

5. "Kick" samples differ from the others mainly in their increased δD_{NSO} values. A contamination effect is not excluded.

Table 1
C and H stable isotopic compositions of the oil fractions

Sample	$\delta^{13}\text{C}$ (‰)						δD (‰)					
	<i>n</i> -alk	sat	iso	aro	NSO	asph	<i>n</i> -alk	sat	iso	aro	NSO	asph
SI 1	-27.9	-27.3	-26.3	-25.9	-27.5	-26.7	-117	-118	-121	-106	-149	-105
SI 2	-27.8	-27.2	-26.0	-25.6	-28.3	-27.6	-130	-127	-120	-116	-142	-114
SI 3	-27.8	-27.4	-26.5	-26.0	-27.1	-23.3	-124	-124	-127	-121	-147	-116
SII 1	-28.0	-27.3	-26.5	-26.3	-29.8	-29.5	-128	-130	-133	-105	-119	-110
SII 2	-28.0	-27.4	-26.6	-25.1	-27.8	-27.4	-124	-124	-123	-103	-149	-109
SII 3	-28.1	-27.4	-26.5	-26.0	-27.2	-27.5	-119	-121	-124	-100	-157	-125
SII 4	-28.3	-27.3	-26.4	-25.4	-27.4	-27.1	-122	-125	-128	-97	-144	-102
SII 5	-28.2	-27.3	-26.5	-25.4	-27.2	-28.1	-119	-122	-124	-102	-138	-104
SII 6	-28.5	-27.6	-26.3	-25.3	-26.7	-27.2	-128	-126	-121	-127	-152	-125
SI 4	-28.3	-27.8	-26.9	-27.4	-28.5	-28.4	-124	-124	-122	-101	-100	-90
SI 5	-25.5	-25.5	-25.4	-26.2	-26.8	-27.8	-116	-116	-115	-98	-140	-101
SI 6	-28.2	-27.4	-26.3	-26.1	-28.4	-27.6	-116	-118	-122	-108	-134	-101
SI 7	-27.0	-27.0	-26.7	-26.8	-28.0	-27.7	-116	-116	-119	-103	-127	-102
SI 8	-27.3	-27.1	-26.5	-25.6	-27.8	-28.0	-121	-121	-121	-101	-126	-109
SI 9	-27.6	-27.2	-26.4	-26.2	-27.9	-25.6	-119	-120	-123	-117	-129	-117

6. Crude oils from similar depths and adjacent localities have shown different isotopic behaviour. The reason for this may be the different heritage of the oils (^{13}C) and the different hydrogeological conditions (D).

Conclusions

This study has demonstrated that the combined application of $\delta^{13}\text{C}$ and δD data of different fractions is useful and may carry information on relative reservoir conditions and crude oil relationships; however, the interpretation of

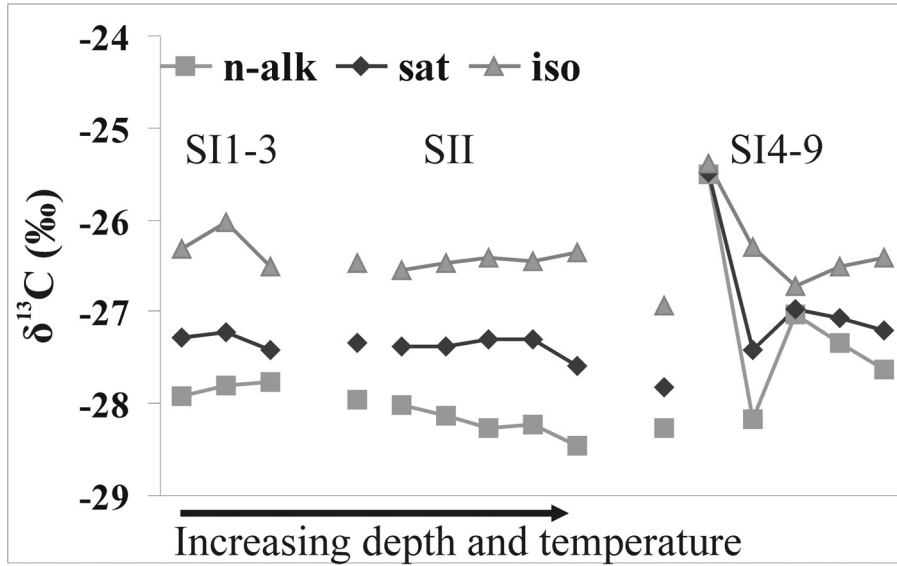


Fig. 1
 $\delta^{13}\text{C}$ of the aliphatic fractions

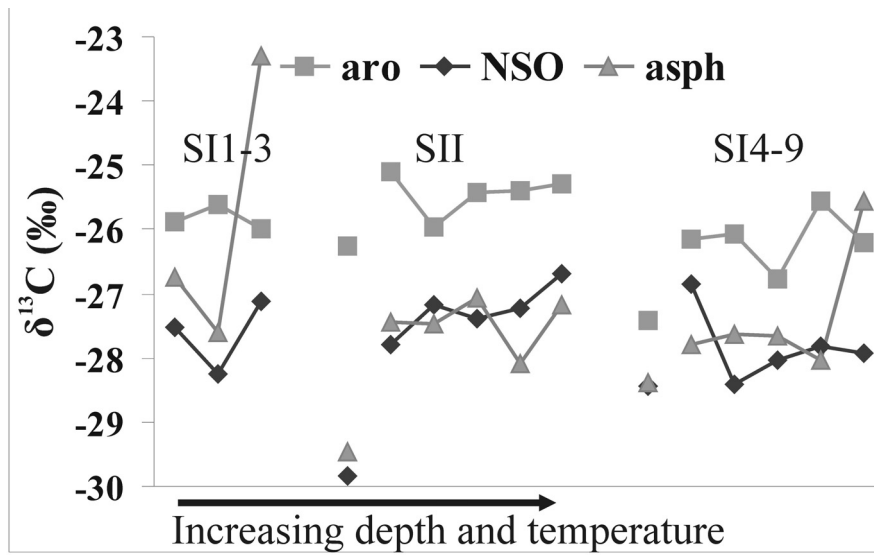


Fig. 2
 $\delta^{13}\text{C}$ of the non-aliphatic fractions

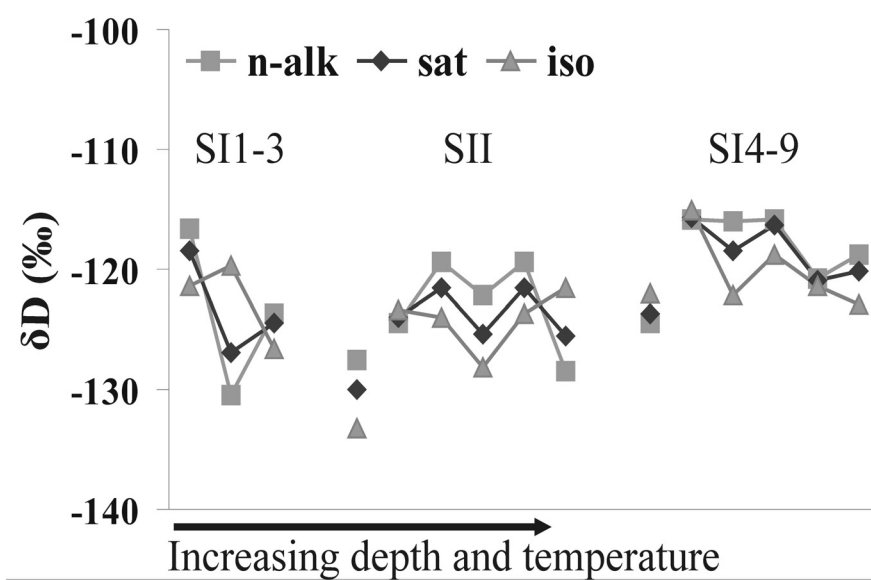


Fig. 3
δD of the aliphatic fractions

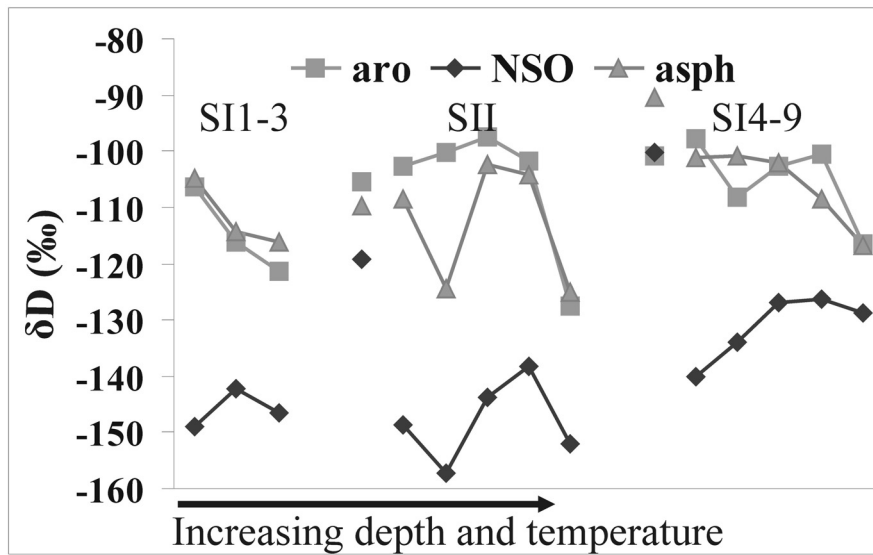


Fig. 4
δD of the non-aliphatic fractions

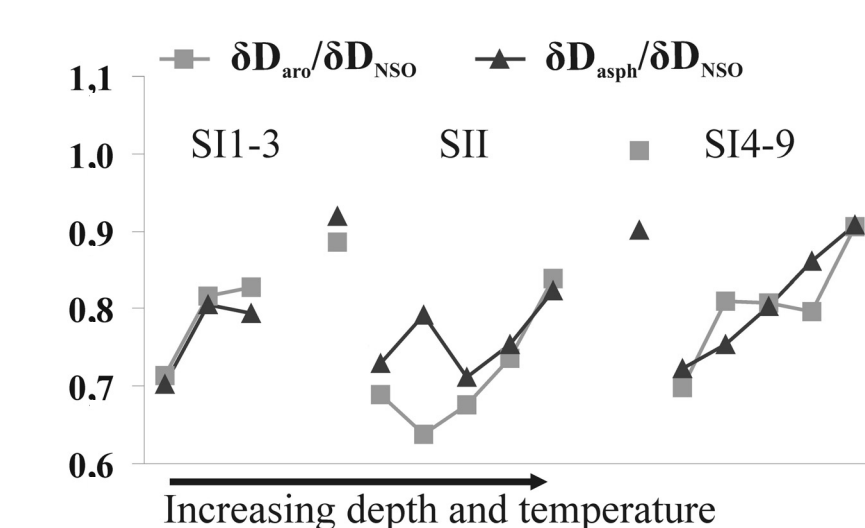


Fig. 5
 δD ratios of the non-aliphatic fractions

carbon and hydrogen isotope ratios is rather complicated in very hot and mature crude oils. In the case of some fractions trends can be observed: the inherited isotopic composition is slightly overprinted by the effect of temperature.

Acknowledgements

This work was funded by the Hungarian Scientific Research Fund (OTKA K84086). The authors thank I. Vető and G. Abbott for improving the article.

References

- Bjoroy, M., K. Hall, P. Gillyon, J. Jumeau 1991: Carbon isotope variations in n-alkanes and isoprenoids of whole oils. – *Chemical Geology*, 93/1–2, pp. 13–20.
- Coleman, M.L., T.J. Shepard, J.J. Durham, J.E. Rouse, G.R. Moore 1982: Reduction of water with zinc for hydrogen isotope analysis. – *Analytical Chemistry*, 54/6, pp. 993–995.
- Cortes, J.E., J.M. Rincon, J.M. Jaramillo, R.P. Philp, J. Allen 2010: Biomarkers and compound-specific stable carbon isotope of n-alkanes in crude oils from Eastern Llanos Basin, Colombia. – *Journal of South American Earth Sciences*, 29/2, pp. 198–213.
- Demény, A. 1995: H isotope fractionation due to hydrogen-zinc reactions and its implications on D/H analysis of water samples. – *Chemical Geology*, 121/1–4, pp. 19–25.
- Dövényi, P., F. Horváth 1988: A review of temperature; thermal conductivity; heat flow data from the Pannonian basin. – In: Royden, L., F. Horváth (eds): *The Pannonian Basin: a study in basin evolution*, AAPG Memoir, 45. Tulsa Oklahoma, pp. 195–233.

- Fekete, J., Cs. Sajgó 2009: Variation of D and ^{13}C isotope ratios in bulk components of high temperature oils from the Pannonian basin. – In: Hinrichs, K.-U. et al. (Eds): 24th International Meeting on Organic Geochemistry, Bremen, Germany. September 6th–11th, 2009; P-326, 421 p.
- Fekete, J., Cs. Sajgó 2010: Stable isotopic composition of mature crude oil fractions. Introduction of deuterium type-curves. – In: Pál-Molnár, E. (Ed.): Medencefejlődés és geológiai erőforrások GeoLitera, pp. 52–55. (In Hungarian.)
- Fekete, J., Cs. Sajgó, A. Demény 2011: Hydrogen isotope type-curves of very hot crude oils. – Rapid Communications in Mass Spectrometry, 25/1, pp. 191–198.
- Galimov, E.M. 1973: Carbon isotopes in Oil-Gas Geology. – Nedra, Moscow, 1973; p. (In Russian.)
- Galimov, E.M. 2006: Isotope Organic Geochemistry. – Organic Geochemistry, 37/10, pp. 1200–1262.
- Hetényi, M., I. Koncz, Á. Szalay 1993: Organic geochemical evaluation of the Makó-3 borehole. – Acta Geologica Hungarica, 36/2, pp. 211–222.
- Koncz, I., T. Lukacs, C.S. Molnar 1999: Carbon isotopic evidences of genetic heterogeneity in a multiple-zone oil field, Hungary. – (abs.): 19th International Meeting on Organic Geochemistry, Istanbul, Turkey, Abstracts Part II: Istanbul, Tubitak Marmara Research Center, Earth Sciences Research Institute, pp. 605–606.
- Sajgó, Cs. 1980: Hydrocarbon generation in a super-thick Neogene sequence in South-east Hungary. A study of the extractable organic matter. – Advances in Organic Geochemistry, 1979. Pergamon Press, pp. 103–113.
- Sajgó, Cs., Z.A. Horváth, J. Lefler 1988: An organic maturation study of the Hód-I borehole (Pannonian Basin). – In: Royden, L., F. Horváth (eds): The Pannonian Basin: a study in basin evolution. AAPG Memoir, 45. Tulsa Oklahoma, pp. 297–310.
- Sajgó, Cs. 2000: Assessment of generation temperatures of crude oils. – Organic Geochemistry, 31/12, pp. 1301–1323.
- Schimmelmann, A., J.-P. Boudou, M.D. Lewan, R.P. Wintsch 2001: Experimental controls on D/H and $^{13}\text{C}/^{12}\text{C}$ ratios of kerogen, bitumen and oil during hydrous pyrolysis. – Organic Geochemistry, 32/8, pp. 1009–1018.
- Schoell, M. 1984: Stable isotopes in petroleum research. – In: Brooks, J., D.H. Welte (Eds): Advances in Petroleum Geochemistry, 1, Academic Press.
- Sofer, Z. 1980: Preparation of carbon dioxide for stable carbon isotope analysis of petroleum fractions. – Analytical Chemistry, 52/8, pp. 1389–1391.
- Stahl, W.J. 1978: Source rock-crude oil correlation by isotopic type-curves. – Geochimica et Cosmochimica Acta, 42/10, pp. 1573–1577.
- Stahl, W.J. 1980: Compositional changes and $\delta^{13}\text{C}/^{12}\text{C}$ fractionations during the degradation of hydrocarbons by bacteria. – Geochimica et Cosmochimica Acta, 44/11, pp. 1903–1907.

Compound-specific isotope analysis for assessing sources and fate of aromatic hydrocarbons in contaminated aquifers

Michaela Blessing, Eric Proust, David Widory

Bureau de Recherches Géologiques et Minières (BRGM), MMA-ISO, Orléans, France

Organic compounds deriving from industry, oil spills, improper disposal and/or leaking storage tanks, landfill leachates, household use, motor vehicle emissions as well as agricultural fertilizers and pesticides are responsible for widespread soil and aquifer pollution. The fate and behavior of such compounds in the subsurface depend on a number of physicochemical and biological processes, which may lead to 'natural attenuation'. Determination and quantification of these processes are crucial for contamination risk assessment and sustainable groundwater management. Compound-specific isotope analysis (CSIA) by online-coupling of capillary gas chromatography and isotope ratio mass spectrometry (GC-IRMS) offers a versatile tool to study the origin and to assess degradation processes of organic pollutants in the environment.

The aim of the present work is to demonstrate the potential of CSIA for studying sources and fate of aromatic hydrocarbons in aquifer systems. Headspace solid-phase micro extraction (hsSPME) was applied as sample pre-concentration and extraction technique allowing for compound-specific carbon and hydrogen isotope analysis ($\delta^{13}\text{C}$ and δD) of volatile compounds, even at concentrations in the low ppb-range. The analytical approach was thoroughly evaluated in terms of its precision, linearity and reproducibility.

Our study focuses on carbon and hydrogen isotope fractionation of aromatic hydrocarbons such as benzene and toluene (BTEX), and the possibility how to evaluate biodegradation processes *in situ* according to the Rayleigh-equation. Results obtained at sites with two different contamination scenarios will be presented: The first location is situated at a former coal carbonization plant; the second site represents a typical contamination due to a leaking underground storage tank at a fuel station. In addition to the possibility for assessing the extent of biodegradation of organic contaminants in soil and groundwater systems, we will demonstrate how isotope signatures can help revealing different pollution sources. Limitations and challenging aspects of the method will be critically addressed.

Address of corresponding author: M. Blessing: 3 Avenue Claude Guillemin, BP 36009, 45060 Orléans cedex 2, France, e-mail: m.blessing@brgm.fr

Metabolic origin of $\delta^{13}\text{C}$ in dark-respired CO_2 : Comparison between leaves and roots

Jaleh Ghashghaie, Camille Bathellier
*Laboratoire d'Ecologie, Systématique et Evolution
Univ. Paris-Sud, Orsay*

Guillaume Tcherkez
*Plateforme Métabolisme-Métabolome, Institut
de Biologie des Plantes, Univ. Paris-Sud, Orsay*

Franz W. Badeck
*Potsdam Institute for Climate Impact Research,
Potsdam*

The photosynthetic discrimination against ^{13}C leads to a ^{13}C -depletion of plant organic matter while the CO_2 left in the atmosphere gets ^{13}C -enriched. Thus, records of the variation of the isotopic composition of CO_2 above ecosystems are used to distinguish between photosynthetic and respiratory fluxes. However, the generally accepted hypothesis in such studies that no discrimination occur downstream photosynthetic fixation is now questioned. We have shown that the CO_2 respired by leaves in the dark is ^{13}C -enriched compared to organic matter, while it is ^{13}C -depleted in the case of roots. Although the relation between the metabolism and the ^{13}C of respired CO_2 has been explored in leaves, no such metabolic rationale is available for roots. To address this issue, we conducted ^{13}C -analysis on CO_2 and metabolites in typical conditions or in continuous darkness, both under natural abundance and following labelling with ^{13}C -enriched glucose or pyruvate (in specific carbon atom positions) using IRMS and NMR techniques. Surprisingly, the $\delta^{13}\text{C}$ of root-respired CO_2 remained constant under continuous darkness, despite the decrease in the respiration rate and respiratory quotient (RQ). Indeed, we have previously shown that the $\delta^{13}\text{C}$ of leaf-respired CO_2 decreased together with the decrease in RQ leading to a linear relationship between these 2 parameters. This strongly suggested that the variation in $\delta^{13}\text{C}$ is a consequence of a substrate switch to feed respiration: carbohydrate oxidation producing ^{13}C -enriched CO_2 and β -oxidation of fatty acids producing ^{13}C -depleted CO_2 compared to organic matter. This is consistent with the assumption that the $\delta^{13}\text{C}$ of dark-respired CO_2 in the leaves is determined by relative contribution of the 2 major decarboxylation processes in the dark: pyruvate dehydrogenase activity and Krebs cycle. Labelling on roots allowed us to infer, in typical conditions, an important contribution of the pentose phosphate pathway to respiration (22%). Continuous darkness mainly affected the Krebs cycle which seemed to become notably reduced. It is concluded that the invariance in the isotope composition of root respired CO_2 under continuous darkness is driven by compensations between both the different fractionating steps and the composition of the respiratory substrate mix.

Address of corresponding author: J. Ghashghaie: CNRS-UMR 8079, Bât 362, Univ. Paris-Sud 11,
F-91405, Orsay cedex, France, e-mail: jaleh.ghashghaie@u-psud.fr

The use of stable isotopes for assessing Portuguese wine genuineness

Ana Isabel Janeiro
*Departamento de Geologia, Faculdade de Ciências
da Universidade de Lisboa, Lisboa*

Luís Ramalho
*Laboratório Nacional de Energia e Geologia, LNEG,
Lisboa*

Bruno Henriques
Hovione, Loures, Lisboa

Lina Santos, Fernanda Alvarrão,
Filomena Costa
*Autoridade de Segurança Alimentar e Económica,
ASAE, Lisboa*

Adriano J. R. Teixeira
Exagium Solutions, Ltd, Lisboa

Wine is one of the most important beverages with an increasing role in international trading and economic income, being authenticity a key factor in establishing its effective cost.

The chemical composition of wine is affected by several factors including production area, grape variety, soil type, climate, oenological practices among others. These factors play an important role in discriminating wines according to their geographic origin and year of harvest, and in wine authentication as a proof of chaptalization, addition of water and sweetening with sugar.

By applying multivariate analysis techniques to stable isotope (^{13}C , ^{18}O , $(\text{D}/\text{H})_{\text{I}}$ and $(\text{D}/\text{H})_{\text{II}}$) data obtained from authentic wines from several Portuguese grape growing areas, the influence of geographical origin, climate, year and date of vintage are discussed.

Address of corresponding author: A. I. Janeiro: Bloco C6, Piso 1, Campo Grande, 1749-016, Lisboa, Portugal, e-mail: aiferreira@fc.ul.pt

Mytilus galloprovincialis
as a bioindicator of environmental conditions:
the case of the eastern coast of the Adriatic Sea

Tjaša Kanduč
Department of Environmental Science,
Jožef Stefan Institute, Ljubljana

Davorin Medaković, Bojan Hamer
Ruđer Bošković Institute, Center for Marine
Research, Rovinj

The marine mussel (*Mytilus galloprovincialis*) lives attached to the surface of hard substrata, where its exposure and relative immobility allows it to record changes in ambient seawater. It is also found along the Eastern coast of the Adriatic Sea.

Oxygen and carbon isotopes were analyzed for calcite and aragonite in separate shell layers, while major, minor and trace elements in the bulk shell were analyzed to evaluate environmental conditions, such as the temperature of carbonate deposition, freshwater influence and locations of anthropogenic pollution. We found that, on average, aragonite is enriched by 1.1‰ in ^{13}C and by 0.2‰ in ^{18}O compared to calcite. The calculated temperatures for *M. galloprovincialis* shell growth from the investigated area range from 13.4 – 20.9°C for calcite and 16.6 – 23.1°C for aragonite. According to the $\delta^{18}\text{O}$ and $\delta^{13}\text{C}$ values of shell layers, we can separate the investigated area into three locations: those with more influence of fresh water, those with less influence of fresh water and those with marine environments. The highest concentrations of manganese, barium, boron, arsenic, nickel, chromium were observed in shells from Omiš, Bačvice, Zablace (Central Adriatic) and Sv. Ivan (South Adriatic), where chemical and heavy industries are located, and where sewage is known to be discharged into coastal areas. The highest concentrations of zinc, lead and copper were measured in samples from Pula, Rijeka and Gruz, where there are also ports in addition to industry.

Address of corresponding author: T. Kanduč: Jamova cesta 39, Ljubljana 1000, Slovenia,
e-mail: Tjasa.kanduc@ijs.si

Tracing biogeochemical processes and pollution sources with stable isotopes in river systems: Kamniška Bistrica (Slovenia) case study

Tjaša Kanduč, Martina Šturm
*Department of Environmental Science
Jožef Stefan Institute, Ljubljana*

Stojan Žigon, David Kocman
*Department of Environmental Science
Jožef Stefan Institute, Ljubljana*

Jennifer C. McIntosh
*Department of Hydrology and Water Resources,
University of Arizona, Tucson*

The geochemical study of river water allows important information to be obtained on chemical weathering of rocks/soil and to determine biogeochemical processes in water. Few studies have attempted to identify sources of nitrate in surface water using stable isotopic ratios.

The River Kamniška Bistrica has an HCO_3^- - Ca^{2+} - Mg^{2+} type water. Its $\text{Ca}^{2+}/\text{Mg}^{2+}$ molar ratio indicates that calcite weathering prevails in the watershed. The River Kamniška Bistrica and its tributaries are oversaturated with respect to calcite and dolomite. The pCO_2 pressure is on average up to 4 times over atmospheric pressure and represents a source of CO_2 to the atmosphere. $\delta^{18}\text{O}$ values of river water indicate primary control from precipitation and enrichment of the heavy oxygen isotope of infiltrating water recharging the Kamniška Bistrica from its slopes. The $\delta^{13}\text{C}_{\text{DIC}}$ values range from -3.6‰ to -10.7‰ and are controlled by biogeochemical processes in terrestrial environments and in stream: (1) exchange with atmospheric CO_2 , (2) degradation of organic matter, (3) dissolution of carbonates, and (4) tributaries. The most important process in the upper flow of the river is carbonate dissolution, and combination of carbonate dissolution and organic degradation in lower flow. The most important contributions will be further calculated in detail according to steady-state equations at the mouth of the river. $\delta^{15}\text{N}$ ranges from -1.9‰ (source) to 8.0‰ (lower flow) in autumn sampling season and from -5.2‰ (source) to 4.5‰ (lower flow) in winter sampling season, respectively. Higher $\delta^{15}\text{N}$ values in the lower flow of the river indicate anthropogenic pollution activity.

Address of corresponding author: T. Kanduč: Jamova cesta 39, Ljubljana 1000, Slovenia
e-mail: tjasa.kanduc@ijs.si

Application of geochemical and isotopic analysis and their role in the examination of coal gas genesis

Jože Pezdič
Georis, Radovljica

Simon Zavšek
*Georis, Radovljica
Velenje Coal Mine, Velenje*

Janja Zula
Velenje Coal Mine, Velenje

Tjaša Kanduč
*Department of Environmental Science, Jožef Stefan
Institute, Ljubljana*

Coal gas is the gas of various origins that resides in the coal structure. It is composed of CO₂, methane, nitrogen, higher hydrocarbons (ethane, propane, butane). In general three main sources of gases can be distinguished: 1) abiogenic, 2) biogenic and 3) thermogenic. During migration, the gases of different origin may mix.

The major components of coal gases in the Velenje lignite seam are CO₂, methane and nitrogen. Concentrations of CO₂ vary from 18 to 98.8%, of methane from 1.1 to 100%, and of nitrogen from 7.2 to 67.3%. Ratio between CO₂ and CH₄ concentrations varies over a wide range and is crucial at higher values. Variations of concentration and isotopic composition indicate various sources of coal gases with possible mixing and other physico-chemical processes during migration, as diffusion and sorption.

During mining of lignite in the Velenje coalmine drastic changes of all measured gas parameters occur. At each working face short and long boreholes are placed to monitor gas concentrations and isotopic composition as well as mechanical parameters with the distance of the working face. Especially important is the drop of concentration of excess nitrogen with approaching of the working face – the excess nitrogen being formed in the coal seam. Change of two typical values of $\delta^{13}\text{C}_{\text{CH}_4}$ during approaching of working face toward boreholes indicates the emptying of at least two reservoirs. The utmost positive $\delta^{13}\text{C}_{\text{CO}_2}$ values (–5‰) and the utmost negative $\delta^{13}\text{C}_{\text{CH}_4}$ values (–72.8‰) were measured when the working face was already far ahead. Monitoring of coal gases in Velenje coalmine at working faces is important since beside other measured parameters, e.g. petrological, geomechanical and structural, can assure safety and eventually prevent sudden coal and gas outbursts.

Address of corresponding author: J. Pezdic: Gradiška pot 3, 4240 Radovljica, Slovenia
e-mail: joze.pezdic@georis.si

Carbon and hydrogen isotopic variations in a low pressure methane-poor hydrocarbons deposit

Łukasz Pleśniak, Michal Bucha, Mariusz-Orion Jędrysek
Laboratory of Isotope Geology and Geoecology, University of Wrocław, Wrocław

In order to increase recovery of gas and oil from deposits technologies called Enhanced Gas Recovery with injection of CO₂ are used. In this process isotopic effects are expected. Therefore we have analysed isotopic composition of carbon and hydrogen in methane in one EGR object.

Carbon and hydrogen stable isotopic observations of methane from the EGR object have been carried out since September 2009. Gas samples (n=60) have been prepared manually on the lines, where the methane was separated from other carbohydrate gases by cryogenic purification using molecular sieves, a dry ice/ethanol mixture, and liquid nitrogen. The methane was passed through a copper oxide furnace (850°), where it was completely combusted to CO₂ and H₂O, which were then separated cryogenically. Carbon stable isotopic composition of methane was analysed off-line on dual inlet system (Finnigan MAT delta E IRMS) and hydrogen stable isotope composition of methane was analysed off-line on Delta V Advantage IRMS.

Isotopic composition of carbon in methane varied from -35.05 to -36.76‰ and isotopic composition of hydrogen in that methane varied from -96.5 to -134.7‰. Both spatial and temporal variations in carbon and hydrogen isotopic ratios in methane show that the system is very dynamic. It has been observed clearly that there are some preferential paths of methane transportation through the deposit, what resulted in isotopic effects. Namely, the carbon and hydrogen isotopic ratios show that the front of the highest velocity of methane movement is marked by the lowest isotopic ratios.

The studies are supported by the Lower Silesian Marshal Department, project "Entrepreneurial PhD student – an investment in the innovative development of the region", Operational Programme Human Capital, and from commercial studies.

Address of corresponding author: Ł. Pleśniak: 30 Cybulskiego St., 50-205 Wrocław, Poland
e-mail: lukasz.plesniak@ing.uni.wroc.pl

Bone collagen in mammals from the outskirts of the Early Roman Empire

Cristina M. Puscas
*Department of Geology,
University of South Florida, Tampa*

Zelalem Bedaso
*Department of Geology,
University of South Florida, Tampa*

Babes-Bolyai University, Geology, Cluj-Napoca

Cristian Roman
Corvins Castle Museum, Hunedoara

Iosif Ferencz
Dacian and Roman Civilization Museum, Deva

Ciprian C. Stremtan
Department of Geology, University of South Florida, Tampa

Stable isotopes from bone collagen are a valuable and widely utilized tool in reconstructing paleodiets of human and animal populations as $\delta^{13}\text{C}$ in bone collagen is controlled by the type of diet (e.g. C_3 vs. C_4 plants), while $\delta^{15}\text{N}$ is constrained by the trophic level. Little such work has been carried out on samples from the outskirts of the Early Roman Empire.

Artifacts collected at the Ardeu site (SE limb of the Apuseni Mountains, Romanian Western Carpathians) indicate that this settlement was inhabited from the Eneolithic to the Bronze Age, during the Dacian Kingdom, and through the Middle Ages. The mammalian tooth samples used for collagen extraction were found along with items dating back to the Dacian Kingdom, centuries I BC–I AD.

The values of $\delta^{13}\text{C}$ of collagen ($n=21$) range between -21.9 and -17.1‰ (PDB), while $\delta^{15}\text{N}$ vary between 3.9 and 8.5‰ (AIR). Jaw bone and tooth root from a single individual yielded $\delta^{13}\text{C}$ and $\delta^{15}\text{N}$ in close agreement. The teeth belonged to omnivores (*Suus*) and herbivores (*Equus*, *Ovis*, *Capra*, *Bos* and *Cervus*) bred or hunted by Dacians. Isotope data show no clear patterns of distribution, which could indicate either frequent changes in agricultural/grazing habits over a few centuries, or the effects of seasonal transhumance on the animals' diet. The majority of plants in the Dacian Kingdom 2 Ky ago belonged to the C_3 (e.g. barley, legumes) group, with few C_4 staple crops (e.g. sorghum and millet), which explains the variation in $\delta^{13}\text{C}$ values.

Address of corresponding author: C. M. Puscas: 4202 E. Fowler Ave., SCA 528 Tampa, FL 33620, USA
e-mail: cpuscas@mail.usf.edu

Deuterium depletion as a new approach in cancer treatment and prevention

Gábor Somlyai
HYD LLC for Cancer Research and Drug
Development, Budapest

András Kovács, Imre Guller
Saint John's Hospital, Budapest

Zoltán Gyöngyi
Department of Public Health,
University Medical School of Pécs, Pécs

Krisztina Krempels, Ildikó Somlyai
HYD LLC for Cancer Research and Drug
Development, Budapest

Mariann Szabó
Private Veterinary Surgeon, Budapest

Tamás Berkényi
Alpha-Vet Veterinary Hospital, Székesfehérvár

Miklós Molnár
Semmelweis University of Medicine, Budapest

It is known that the deuterium/hydrogen (D/H) mass ratio is the largest of stable isotopes of the same element, causing differences in the physical and chemical behaviour between the two hydrogen isotopes. Although the concentration of D is more than 10 mM in living organisms the possible role of D had not been investigated for 6 decades after its discovery in the early 30s.

In order to investigate the possible role of naturally occurring D in living organisms, in cell growth, tumor development and prevention, D-depleted water (DDW) was used. DDW caused tumor regression in xenotransplanted mice (MDA and MCF-7, human breast; PC-3, human prostate) and induced apoptosis *in vitro* and *in vivo*. Deuterium depletion inhibited the expression of certain genes (c-myc, H-ras, Bcl-2, K-Ras, COX-2) having key role in tumor development and prevented the appearance of cancer in mice after tumor induction with DMBA. During the four-month-long DDW administration in the phase II, double blind clinical trial, 7 out of 22 prostate cancer patients achieved partial response (PR), while only one patient out of 22 showed PR in the control group ($p=0.027$). In the treated group, net decrease in the prostate volume was three times higher (160.3 cm^3 vs. 54.0 cm^3 , $p=0.0019$). The one year survival was significantly higher in patients treated with DDW (logrank test, $p = 0.029$). The mortality rate decreased substantially in the treated group by the end of the first year ($p=0.034$).

In a retrospective study with breast cancer patients the relapse rate, within five years after the tumor was removed by surgery, was reduced to 22% from the expected 50%.

We suggest that cells are able to regulate D/H ratio and its changes can trigger molecular mechanisms having key role in cell cycle regulation. The decrease in D-concentration can intervene in the signal transduction pathways thus leading to tumor regression.

Address of corresponding author: G. Somlyai: H-1539 Budapest, Pf. 695, Hungary
e-mail: gsomlyai@hyd.hu

Tracing the stable isotope composition of oxygen and hydrogen in precipitation from tree ring cellulose – examples from an oak and two pine tree sites in Finland

Eloni Sonninen

Radiocarbon Dating Laboratory, University of Helsinki, Helsinki

Records of oxygen and hydrogen isotope ratios in tree rings are used to trace past environmental and climate conditions. Change in the isotope composition of precipitation, source water for trees, is connected to atmospheric air mass circulations, and is known to correlate with the temperature at the precipitation site for mid- and high latitudes.

We have studied the relationships between $\delta^{18}\text{O}$ ($\delta^2\text{H}$) values in tree ring α -cellulose (nitrated cellulose) and precipitation at three sites for the period 1989–2002. Pines (*Pinus sylvestris*) are from northern and eastern Finland and oak (*Quercus robur*) from southern Finland.

The $\delta^{18}\text{O}$ signal in tree ring cellulose has the highest correlation with summer (monthly average JJA) precipitation for oaks in southern and with previous year autumn (SON) precipitation for pines in eastern Finland. A lower correlation is obtained for pines in northern Finland.

Address of corresponding author: E. Sonninen: POB 64, FI-00014 University of Helsinki, Finland,
e-mail: eloni.sonninen@helsinki.fi

Organic matter sources in sediments of Szczecin Lagoon (NW Poland) indicated by C and N isotopic composition

Adriana Trojanowska, Piotr Jezierski
*Laboratory of Isotope Geology and Geoecology,
University of Wrocław, Wrocław*

Artur Skowronek
*Department of Geology and Paleogeography,
University of Szczecin, Szczecin*

The C/N and stable C and N isotope ratios ($\delta^{13}\text{C}$ and $\delta^{15}\text{N}$) of sedimentary organic matter (OM) were determined in the Szczecin Lagoon – the area of the Odra River discharge into the Baltic Sea –, where gradual mixing of riverine and seawater occurs.

Organic matter content in sediments achieved maximum value in central part of the lagoon (22%) and decreased closer to the shore (0.2%). Carbon isotopic composition of OM ranged from -29.4‰ in central part to -26.4‰ in the mouth of the Dziwna river channel. $\delta^{15}\text{N}$ varied between 5.6‰ in the central area to 12.9‰ near the shore, while the C/N was changing in a narrow range from 9.7 to 11.9. $\delta^{13}\text{C}$ and C/N ratio of riverine suspended OM from Odra river ($\delta^{13}\text{C} = -30.6\text{‰}$; C/N = 9.6) and cyanobacteria ($\delta^{13}\text{C} = -30.2\text{‰}$; C/N=9.4) from the central part of the lagoon were characteristic for freshwater phytoplankton, however in the areas of seawater inflow contribution of marine algae to suspended organic matter was proved by OM enrichment in ^{13}C ($\delta^{13}\text{C} = -25.8\text{‰}$; C/N = 9.2).

Significant correlation have been found between $\delta^{13}\text{C}$ and OM content ($r = -0.54$, $p = 0.002$) as well as between $\delta^{15}\text{N}$ and both: organic nitrogen content ($r = 0.65$, $p = 0.012$) and organic carbon content ($r = 0.70$, $p = 0.006$) in sediments.

Our data indicate that OM in sediments of the lagoon is originated mostly from freshwater algae and cyanobacterial cells ($\delta^{13}\text{C} \sim -29\text{‰}$; $\delta^{15}\text{N} \sim 10\text{‰}$, C/N ~ 10). In the area of seawater inflow carbon isotopic composition of sedimentary OM was somewhat changed due to contribution of marine algae ($\delta^{13}\text{C} \sim -27\text{‰}$; $\delta^{15}\text{N} \sim 10\text{‰}$, C/N ~ 10). Occurrence of terrestrial OM in sediments was not confirmed.

Address of corresponding author: A. Trojanowska: ulica Cybulskiego 30, 50-205 Wrocław, Poland
e-mail: adriana.trojanowska@ing.uni.wroc.pl

The carbon isotopic composition of dried and carbonized plant samples

Polona Vreča, Martina Šturm
Jožef Stefan Institute, Ljubljana

Ines Krajcar Bronić
Rudjer Bošković Institute, Zagreb

Monitoring ^{14}C activity in plant samples in the vicinity of the Nuclear power plant Krško (NPPK) is performed regularly since 2006 to estimate the possible influence on environmental ^{14}C levels and the possible contribution to the effective dose of local population through food chain. When reporting ^{14}C activity (Bqkg^{-1}C) of the samples, it is necessary to consider the stable isotopic composition of carbon ($\delta^{13}\text{C}$) and the fractionation that occurs during photosynthesis. In addition, isotopic fractionation can occur also during sample preparation. Therefore, the aim of our study was to analyse selected C3 and C4 plant samples in order to (1) determine their actual $\delta^{13}\text{C}$ values to be used for correction of ^{14}C activity and (2) investigate eventual isotopic fractionation which might occur during sample carbonization process, i.e. pyrolysis by analysing dried and carbonized counterparts of selected plant samples.

In this study $\delta^{13}\text{C}$ of 37 dried and 34 carbonized samples of apples, maize (leaves and grain) and wheat collected in four sampling campaigns (2008 and 2009) in the vicinity of NPPK was determined. Carbonized samples were ground to powder and homogenized. The dried samples were ground using different grinding methods. Apple samples were ground to powder and homogenized in an agate mortar. Maize and wheat samples were lyophilized after being frozen in liquid nitrogen. Four lyophilized samples were ground in a mill. During this process it was not possible to obtain completely homogenized samples, therefore, the rest of maize and wheat samples were ground and homogenized in an agate mortar. $\delta^{13}\text{C}$ was determined using a Europa 20–20 isotope ratio mass spectrometer (IRMS). The mean $\delta^{13}\text{C}$ value for analysed C3 plant samples (i.e. apple and wheat) and for C4 plant samples (i.e. maize) was close to -27‰ and -12‰ , respectively. In wheat, apple and maize samples, no significant differences (at $p < 0.05$) were observed between the dried and carbonized samples, however, an up to 2.2‰ and 1.8‰ difference was observed for particular apple and maize leaves samples, respectively. The influence of variability of $\delta^{13}\text{C}$ values on reported ^{14}C activity will be discussed.

Address of corresponding author: P. Vreca: Jamova 39, 1000 Ljubljana, Slovenia
e-mail: Polona.Vreca@ijs.si

ENVIRONMENTAL GEOCHEMISTRY
AND ECOLOGY

Groundwater nitrate sources in alluvial aquifers: Isotope case study in Savinja Valley (Slovenia)

Jože Uhan
Georis, Radovljica, Slovenia
Environmental Agency of the Republic of Slovenia,
Ljubljana

Sonja Lojen
Jožef Stefan Institute, Ljubljana

Marina Pintar
Biotechnical Faculty, University of Ljubljana,
Ljubljana

Jože Pezdíč
Georis, Radovljica, Slovenia

The chemical status of the shallow alluvial Savinja Valley groundwater body in Slovenia is poor, mainly due to the high concentration of nitrate in groundwater. This case study is therefore oriented in the assessment of groundwater vulnerability to nitrate pollution, as a base for the measurement processes. The article describes the use of isotope information of surface water and groundwater for the determination of possible sources of groundwater nitrate pollution. The isotope information of predominant soil and manure/septic waste nitrate origin, associated with other local physical and chemical boundary conditions and land use data, offers an interpretative support in the delineation of nitrate vulnerable zones.

Key words: groundwater nitrate, denitrification, Savinja Valley

The knowledge of geochemical processes and pollution sources is necessary for interpretation of the groundwater vulnerability results also in case of a process-based model results application (Uhan et al. 2010a; Uhan et al. 2010b). Alluvial aquifer of Lower Savinja Valley was selected as an isotopic case study of groundwater nitrate pollution sources identification (Uhan 2011). It is less than 100 square kilometre shallow alluvial aquifer system with about 5 percent of the total groundwater reserves of all Slovenian alluvial aquifers. An important part of the regional water demand in the Savinja Valley is met by pumping groundwater from vulnerable Pleistocene and Holocene sandy gravel aquifers of the plain with population pressure and intensive agricultural production. The average depth to the groundwater is between 4 and 5 metres.

Address of corresponding author: J. Uhan: ARSO, Vojkova 1b, 1000 Ljubljana, Slovenia,
e-mail: joze.uhan@gov.si

Received: April 26, 2011; accepted: May 17, 2011

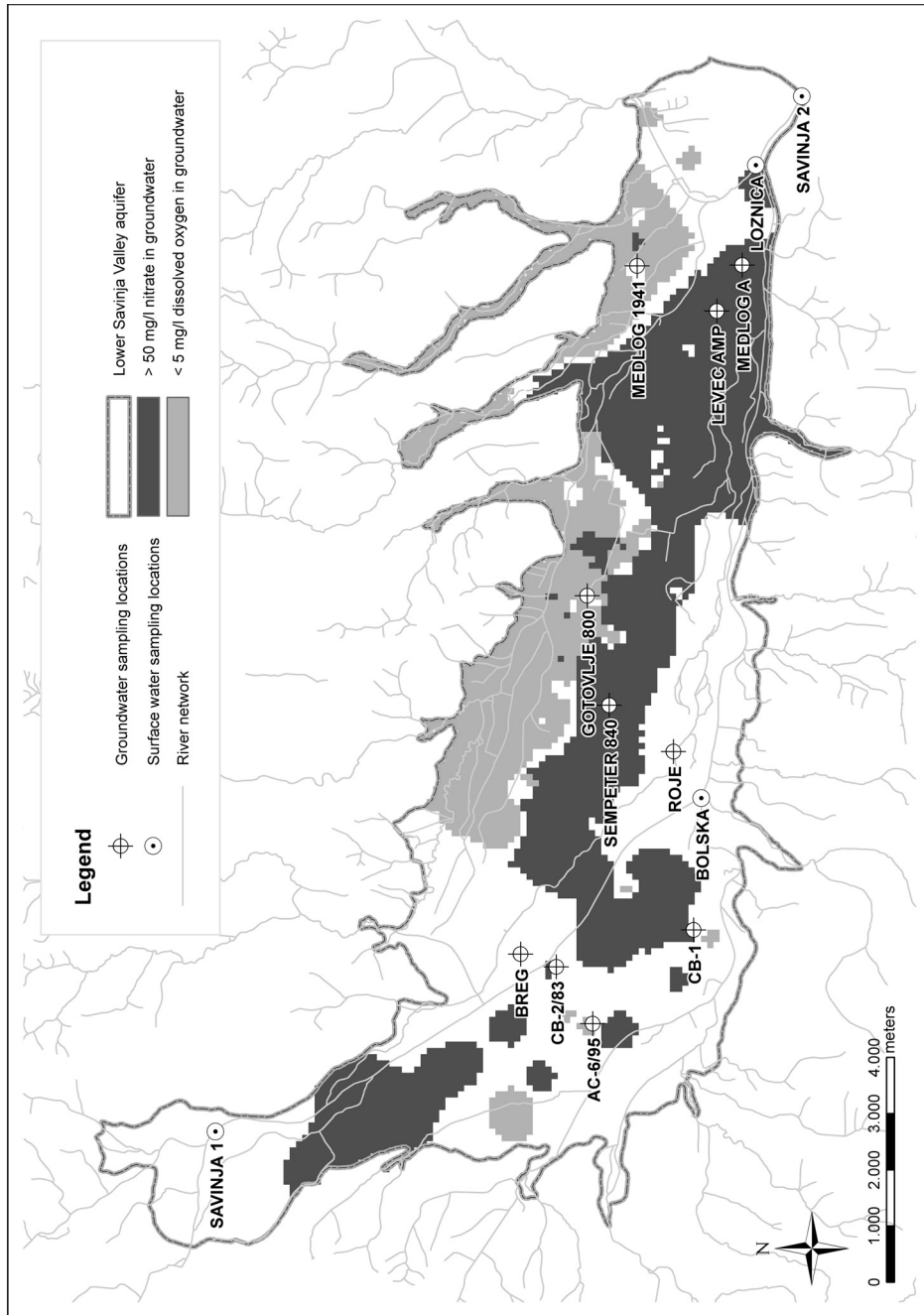
In order to meet the requirements of the EU Water Framework Directive, the Lower Savinja Valley groundwater quality and quantity status assessment were made in the year 2008 (Uhan et al. 2010c). Adequate quantity, but poor chemical status was assessed for Savinja Valley groundwater body. The reason for the bad chemical status of the groundwater was that high nitrate concentrations were found beside pesticides. Through measurements performed in the year 2009, two distinct areas of the aquifer were identified: the central parts, where the concentrations of nitrate in the groundwater surpassed 50 mg/l, and the northern marginal part, characterized by the concentrations of dissolved oxygen lower than 5 mg/l (Fig. 1).

Correlation between the groundwater nitrate concentrations and $\delta^{15}\text{N}$ in groundwater nitrate (Fig. 2a) suggests that part of the aquifer was influenced by denitrification, especially at measurement points in the northern clay-rich soils area of the aquifer. In these areas, decreased dissolved oxygen was measured. According to Kendall's ranges of $\delta^{15}\text{N}$ values for the major sources of nitrogen in the hydrosphere (1998), the $\delta^{15}\text{N}$ in Lower Savinja Valley groundwater nitrate suggests predominant soil (cultivation) sources and/or manure/septic waste nitrate sources. The range of $\delta^{15}\text{N}_{\text{NO}_3^-}$ values in the groundwater of Lower Savinja Valley is between +5.11‰ and +21.90‰, which falls inside the range found in areas with comparable hydrogeological setting and land use in the northeastern part of Slovenia (Pintar 1996; Pezdic 1999). The $\delta^{15}\text{N}_{\text{NO}_3^-}$ values in the samples from the rivers in Lower Savinja Valley ranged between +3‰ and +13‰ and were grouped together with some groundwater samples from locations where the hydrological impact of the surface water on the groundwater flow regime was significant.

The $\delta^{15}\text{N}_{\text{NO}_3^-}$ and $\delta^{13}\text{C}_{\text{DIC}}$ relation (Fig. 2b) reflects the importance of internal and external sources of dissolved carbon and nitrogen and the hydrochemical evolution of groundwater in the aquifer. The shift in $\delta^{13}\text{C}_{\text{DIC}}$ toward the more negative values was indicative of an isotopically light carbon source, such as leaching of soil CO_2 . The isotope information of predominant soil and manure/septic waste nitrate origin, associated with other local physical and chemical boundary conditions and land use data, offered an interpretative support in the delineation of nitrate vulnerable zones. To achieve a more precise determination of nitrate sources or mixing processes, a more complex isotopic investigation (e.g. groundwater nitrate oxygen and boron) would be needed (Widory 2009). The results, obtained in this case study, lead us to envisage additional monitoring programs, focused on a field measurements technique and water sampling for isotopes.

Fig. 1 →

Map of nitrate and dissolved oxygen distribution in groundwater of Lower Savinja Valley aquifer with sampling locations for isotope analysis



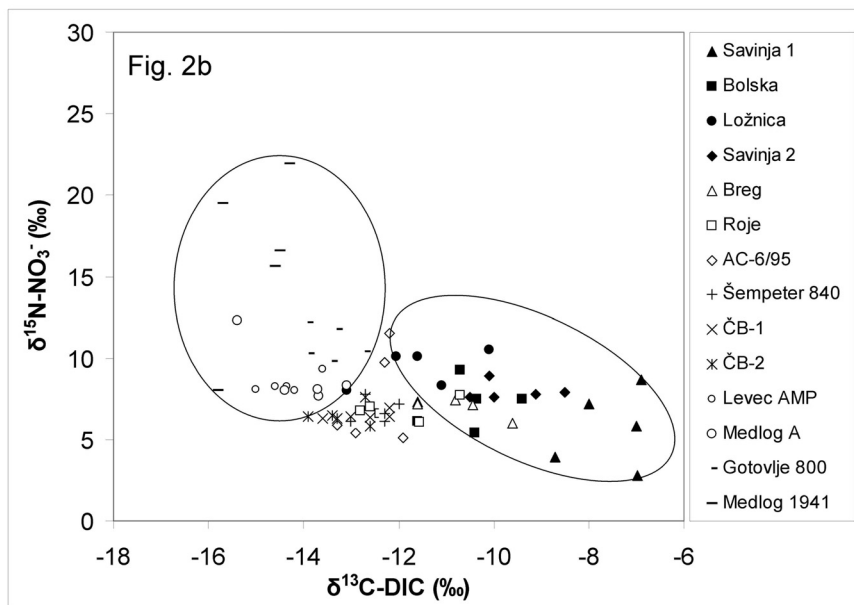
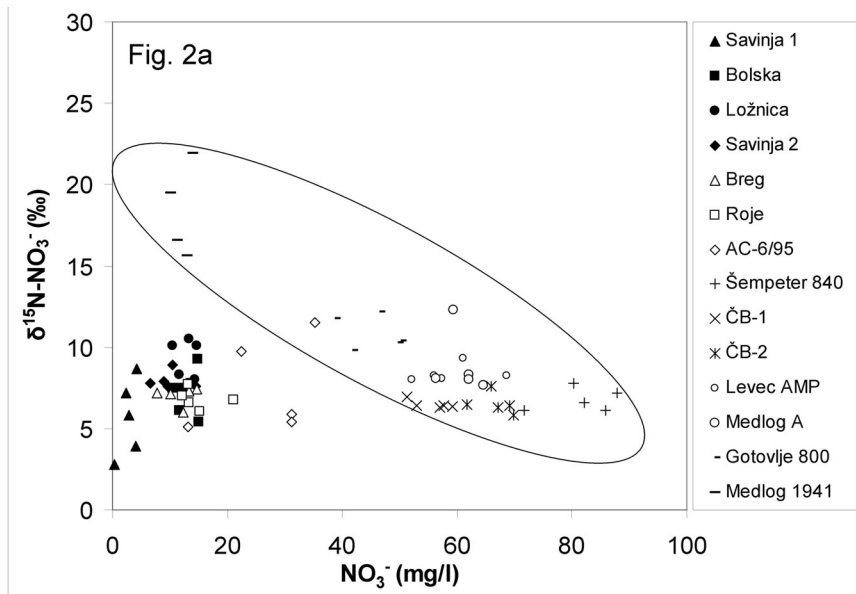


Fig. 2
 $\delta^{15}\text{N-NO}_3^-$ vs. nitrate NO_3^- concentration (Fig. 2a) and $\delta^{15}\text{N-NO}_3^-$ vs. $\delta^{13}\text{C-DIC}$ (Fig. 2b) in groundwater of Lower Savinja Valley in period 2008–2009

References

- Kendall, C. 1998: Tracing nitrogen sources and cycling in catchments – In: Kendall, C., J.J. McDonnell (Eds): *Isotope tracers in catchment hydrology*, Elsevier, pp. 519–576.
- Pezdic, J. 1999: *Izotopi in geokemijski procesi*. – Univerza v Ljubljani, Naravoslovnotehniška fakulteta, Oddelek za geologijo, 269 p.
- Pintar, M. 1996: *Vpliv kemijske dejavnosti na koncentracijo nitratov in atrazina v vodah Apaškega polja*. – M.Sc. Thesis, University of Ljubljana, Biotechnical Faculty, 106 p.
- Uhan, J., G. Vizintin, J. Pezdic 2010a: *Groundwater nitrate vulnerability assessment in alluvial aquifer using process-based models and weights-of-evidence method – Lower Savinja Valley case study (Slovenia)*. – *Groundwater quality sustainability*, Abstract book of XXXVIII IAH Congress, Krakow, pp. 47–48.
- Uhan, J., G. Vizintin, J. Pezdic 2010b: *Groundwater nitrate vulnerability assessment in alluvial aquifer using proces-based models and weihgts-of-evidence method – Lower Savija valley case study (Slovenia)*. *Environmental earth sciences*, doi: 10.1007/s12665-010-0821-y, 9 p.
- Uhan, J., M. Dobnikar Tehovnik, U. Pavlic 2010c: *Vode v Sloveniji – Ocena stanja voda za obdobje 2006–2008 po določilih okvirne direktive o vodah*, Agencija RS za okolje, 62 p.
- Uhan, J. 2011: *Ranljivost podzemne vode na nitratno onesnazenje v aluvialnih vodonosnikih Slovenije*. – Ph.D. Thesis, University of Ljubljana, Faculty of natural sciences, 163 p.
- Widory, D. 2009: *Towards new methods to manage nitrate pollution within the Water Framework Directive*. – *International Workshop of the ISONITRATE project programme*, Paris, 54 p.

C, N isotopic ratios in *P. oceanica* meadows of Alexandroupolis Gulf, NE Greece

Maria-Venetia Apostolopoulou
Analytical and Environmental Chemistry
Vrije Universiteit Brussel, Brussels

Patrick Roose
Management Unit of the North Sea Mathematical
Models and the Scheldt Estuary, Ostend

Pavlopoulos Kosmas
Geography, Harokopio University, Athens

Frank Dehairs
Analytical and Environmental Chemistry,
Vrije Universiteit, Brussel

We investigated the stable C, N isotopic composition of seagrass and sediments to track effects of pollution, as part of a study to assess 'base-line' conditions for seagrass meadows in Alexandroupolis Gulf (north-east Aegean Sea, Greece) where the construction of an oil-tanker terminal is being planned. *Posidonia oceanica* seagrasses and ambient sediment substrate were sampled at 4 different sites along the coast line during the summers of 2007, 2009, and 2010 and leaves, roots and rhizomes were analysed for C and N isotopic composition. Whole plant ^{15}N values increased over the years (2007: $+3.61 \pm 1.40\text{‰}$; 2009: $+5.99 \pm 2.32\text{‰}$; 2010: $+8.40 \pm 2.94\text{‰}$), while whole plant $\delta^{13}\text{C}$ values showed a slight depletion in ^{13}C for 2010 compared to 2007 and 2009 (2007: $-12.67 \pm 1.97\text{‰}$; 2009: $-12.65 \pm 1.27\text{‰}$; 2010: $-13.81 \pm 0.82\text{‰}$). Such trends possibly reflect increased impact of domestic and industrial wastes via river and groundwater inputs. This temporal trend is detected in leaves, roots and rhizomes alike. Overall, leaves, roots and rhizomes do not show a significant difference between their $\delta^{13}\text{C}$ values, while leaves were less ^{15}N enriched compared to roots and rhizomes. Comparing additional parameters and biomarkers such as 16 PAHs (EPA610) in the ambient sediment substrate, it appeared that these values also had significantly increased over the years, corroborating a possible pollution effect.

Address of corresponding author: M. V. Apostolopoulou: Pleinlaan 2, B-1050, Brussels, Belgium
e-mail: mapostol@vub.ac.be

Stable isotope distribution in deep-sea hydrothermal barnacle, Manus Basin, Papua New Guinea: a key in understanding their ecology

Ana-Voica Bojar

Department of Geology, Salzburg University, Salzburg

Department of Natural Sciences,
Universal Museum Joanneum, Graz

Hans-Peter Bojar, Werner Tufar

Department of Geology, Salzburg University,
Salzburg

One of the most extended and active hydrothermal fields of the Manus Spreading Center is the Hydrothermal field 1, Vienna Woods. In this study we present around 60 stable isotope data on carbonates and shell structure investigations of barnacles collected during the Olga 2 expedition. The heterogeneous faunal composition found at this site consists of gastropods, barnacles, bythograeid crabs, bresiliid shrimps, vestimentiferans, and sea anemones.

For this study, 5 specimens of a hydrothermal vent barnacle, *Eochionelasmus ohtai manusensis* were collected at depth of c. 2500 m.

Stable oxygen isotope data of *Eochionelasmus ohtai manusensis* were performed from the centre to the border of the calcitic shells, along profiles. Within one shell, the isotope values show variations of max. 0.6‰. The temperatures calculated from the stable isotope data consistently indicate that *Eochionelasmus* precipitated their shell carbonate at low temperature, up to a few °C. The calculated temperatures from the isotope data are also in agreement with the reported habitat from the North Fiji and Lau Basins, where temperatures of max. 6°C were measured at sites populated by *Eochionelasmus*. Both calculated and measured temperatures of a few degree °C indicate that at the sites where *Eochionelasmus* lives, hydrothermal fluid input is present, as ambient temperatures are around 1.5°C. Carbon stable isotope composition of *Eochionelasmus* show lower $\delta^{13}\text{C}$ values than for littoral barnacles, supporting the idea of input of a vent carbon source.

Address of corresponding author: A.-V. Bojar: Hellbrunnerstrasse 34, A-5020, Salzburg, Austria
e-mail: Ana-Voica.Bojar@sbg.ac.at

Chemical and isotopic yearly seasonal observations of the ammonium and nitrate in Wrocław (SW Poland) precipitation

Monika Ciezka, Maciej Górka
Mariusz-Orion Jędrysek
*Laboratory of Isotope Geology and Geoecology,
Department Applied Geology and Geochemistry,
Institute of Geological Sciences,
University of Wrocław, Wrocław*

Magdalena Modelska
Stanisław Stacko
*Department of General Hydrogeology,
Institute of Geological Sciences,
University of Wrocław, Wrocław*

Major ion constituents and nitrogen isotopic ratios of ammonium ($\delta^{15}\text{N-NH}_4^+$) and nitrate ($\delta^{15}\text{N-NO}_3^-$) were measured in order to investigate the sources of NH_4^+ and NO_3^- in precipitation. Precipitation (41 samples) was collected from January 2010 to December 2010 in Wrocław (SW Poland) via a funnel in 5L plastic containers covered by plastic grid. Chemical analysis were carried out using Alliance Waters HPLC. For isotopic analyses nitrate and ammonium were absorbed by ion exchanging resins columns and isotopic ratios were measured using Delta V Advantage mass spectrometer.

The pH values ranged from 6.56 to 7.9 and electrical conductivity from $12 \mu\text{S/cm}$ to $162 \mu\text{S/cm}$. Concentrations of Ca^{2+} varied from 0.14 mg/L to 6.93 mg/L, Mg^{2+} from 0.05 mg/L to 0.97 mg/L, K^+ from 0.00 mg/L to 22.95 mg/L, Na^+ from 0.00 mg/L to 9.15 mg/L, SO_4^{2-} from 0.00 mg/L to 24.51 mg/L, Cl^- from 0.70 mg/L to 18.63 mg/L. Nitrate concentration ranged from 0.00 mg/L to 16.48 mg/L with average value 3.71 mg/L, ammonium from 0.00 mg/L to 7.92 mg/L with average value 2.46 mg/L.

Concentrations of ammonium and nitrate show weak positive correlation (0.57). There were no correlation observed between nitrogen forms and pH, Cl^- , Na^+ , K^+ , Mg^{2+} . Both ammonium and nitrate concentrations correlated positively with electrical conductivity, SO_4^{2-} and Ca^{2+} . Ammonium ions and atmospheric NO_x (analysed in Wrocław air in the same period of time) concentrations were negatively correlated (-0.36). The seasonal variations of ammonium and nitrate ions concentrations corresponded with each other. The concentrations of both compounds were higher in spring and summer – 19.42 mgNO_3^-/L and 7.92 mgNH_4^+/L than in autumn and winter – 3.88 mgNO_3^-/L and 0.39 mgNH_4^+/L .

The $\delta^{15}\text{N}$ values of ammonium oscillated from -11.5 to 2.2‰ in cold season and from -4.6 to 10.2‰ in warm season. Selected samples for $\delta^{15}\text{N}$ nitrate isotopic analyses show the values from -2.8‰ to 1.7‰. Ammonium $\delta^{15}\text{N}$ values show wide range of variations probably due to different origins of dissolved ions in precipitation. Conversely, we do not observe such significant variations in nitrate $\delta^{15}\text{N}$ values.

Address of corresponding author: M. Cieżka: Cybulskiego 30, 50-205 Wrocław, Poland
e-mail: monika.ciezka@wp.pl

Apportionment of carbon dioxide over central Europe: insights from combined measurements of atmospheric CO₂ mixing ratios and carbon isotope composition

Michał Galkowski, Dorota Jelen, Mirosław Zimnoch, Tadeusz Kuc, Jarosław Necki, Łukasz Chmura, Zbigniew Gorczyca, Alina Jasek, Kazimierz Rozanski
AGH University of Science and Technology, Faculty of Physics and Applied Computer Science, Kraków

Carbon isotope composition of atmospheric CO₂ constitutes an important source of information on circulation of carbon between the atmosphere, biosphere and the ocean. It also helps to quantify anthropogenic disturbances of the carbon cycle. The European continent, with high population density and numerous sources of anthropogenic CO₂ emissions, plays an important role in the global carbon budget. Observations of atmospheric CO₂ mixing ratios alone cannot provide information on apportionment of biogenic and fossil-fuel related contributions to the overall CO₂ burden of the regional atmosphere. In order to perform such apportionment, additional information is required. Such information can be obtained from measurements of carbon isotope signatures (¹⁴C/¹²C and ¹³C/¹²C ratios) of atmospheric carbon dioxide.

Regular observations of carbon isotope composition of atmospheric CO₂ are performed in Krakow, southern Poland (19°55'E, 50°04'N, 220 m asl) since 1983. Analogous data are available for the past decade also for Kasprowy Wierch (High Tatra Mountains, at 19°56'E, 49°14'N, 1987 m asl), a regional reference site relatively free of local anthropogenic influences. The available data on atmospheric mixing ratios and carbon isotope composition of atmospheric CO₂ at both sites for the period 2005–2009 (and monthly composite samples) were used to quantify biogenic and fossil-fuel related contributions to the overall CO₂ load of the regional atmosphere using isotope and mass balance approach. In addition, the ¹³C signature of fossil-fuel component at both sites has been evaluated and used for assessing long-term trends and changes in the internal structure of fossil CO₂ emissions. The results of this apportionment clearly indicate distinct seasonal changes in the local CO₂ budget at both locations as well as large differences between them in terms of impact of anthropogenic CO₂ emissions. The average load of urban atmosphere of Krakow with fossil-fuel derived CO₂ is approximately five times larger than that derived or Kasprowy Wierch site.

Address of corresponding author: M. Galkowski: al. Mickiewicza 30, 30-059 Kraków, Poland
e-mail: galek1@poczta.onet.pl

5-year (2004–2009) isotopic seasonal observations of the sulphates in Wrocław (SW Poland) precipitation

Maciej Górka

*Laboratory of Isotope Geology and Geoecology,
Institute of Geological Sciences,
University of Wrocław, Wrocław*

Stanisław Halas

*Department of Mass Spectrometry, Marie Curie-
Sklódowska University, Lublin*

Dariusz Strapoć

*Department of Geological Sciences,
Indiana University, Bloomington*

Dominika Kufka, Mariusz-Orion Jędrysek

*Laboratory of Isotope Geology and Geoecology,
Institute of Geological Sciences
University of Wrocław, Wrocław*

The aim of this study was to observe the seasonal variations in concentration and isotopic composition of sulphates in precipitation in relation to other parameters (air temperature, air SO₂ concentration, etc.). The field studies taking place in Wrocław (SW Poland) started from 25th May 2004 and finished on 25th May 2009. The precipitation samples were collected after each rain episode. The sulphates were precipitated from filtered water using barium chloride method. The concentration of sulphates was calculated from weight of sulphates samples and water amounts.

The concentration of sulphates vary between 0.93 mg·dm⁻³ (1st August 2005) and 98.39 mg·dm⁻³ (12th April 2007) with average 12.79±13.10 mg·dm⁻³. The δ³⁴S_{SO₄} values vary between 0.3‰ (13th June 2005) and 5.4‰ (16th May 2007) with average 2.8±0.9‰. The δ¹⁸O_{SO₄} values vary between 4.7‰ (12th December 2005) and 19.1‰ (18th March 2008) with average 13.5±2.0‰. Statistically significant positive correlations have been noted between: (i) SO₄²⁻ concentration and air SO₂ (R=0.22, p=0.008); (ii) SO₄²⁻ concentration and δ¹⁸O_{SO₄} (R=0.24, p=0.002); (iii) δ¹⁸O_{SO₄} and δ¹⁸O_{H₂O} (R=0.27, p=0.000), while statistically significant negative correlations have been observed between: (i) SO₄²⁻ concentration and air temperature (R=-0.21, p=0.005); (ii) SO₄²⁻ concentration and δ³⁴S_{SO₄} (R=-0.21, p=0.007); (iii) δ¹⁸O_{SO₄} and δ³⁴S_{SO₄} (R=-0.27, p=0.001).

Moreover, the dominant sulphate sources have been identified based on the samples showing the highest sulphate concentration. These sources show the isotopic signature of sulphur ca. 2.7‰ and oxygen ca. 17.3‰.

Probably for lower concentrations of sulphate the dominant signal has been masked by the multiple sources of sulphur and oxygen.

Finally, we conclude that in 5-year observation period the fluctuation of isotopic signals in sulphates are distinct for S and O, which is probably caused by different sources and processes influencing the final isotopic composition of sulphates in precipitation.

Address of corresponding author: M. Górka: ul. Cybulskiego 30, 50-205 Wrocław, Poland
e-mail: maciej.gorka@ing.uni.wroc.pl

Triple oxygen isotope composition as a potential tracer for mixing ratios of carbon dioxide sources in urban air

Balázs Horváth, Magdalena E. G. Hofmann, Andreas Pack
Georg-August-University, Geoscience Centre, Isotope Geology Section, Göttingen

Urban air investigations are important, as urban regions are the main sources of anthropogenic CO₂. The ¹³C/¹²C and ¹⁸O/¹⁶O ratios are traditionally used to distinguish between CO₂ sources. However, the number and variability of sources are large, thus unambiguous determination of different fluxes need further tracers. The ratio ¹⁷O/¹⁶O to ¹⁸O/¹⁶O is a potential new tracer. Atmospheric O₂ has an anomaly in its triple oxygen isotope ratio. During combustion, O is transferred from O₂ to CO₂. Hence, CO₂ from combustion should carry the isotope anomaly of air O₂. In this study, we present the triple oxygen isotope data of CO₂ with different anthropogenic (combustion) provenance and we compare the results to local atmospheric CO₂.

Carbon dioxide from laboratory combustion experiments and air CO₂ were isolated cryogenically. The triple oxygen isotope composition of CO₂ was determined by equilibration with CeO₂, and subsequent analysis of Δ¹⁷O and ¹⁸O of CeO₂ by means of IR laser fluorination GC-CF-irmMS. The oxygen isotope anomalies are reported as Δ¹⁷O relative to the terrestrial fractionation line. The CO₂ concentrations were measured by gas chromatography.

High temperature combustion (>900 °C) resulted in CO₂, which inherited the isotope signature of tropospheric O₂. Combustion at lower temperatures (biomass) was accompanied by kinetic fractionation between the starting material (O₂) and the product (CO₂). As result of the kinetic fractionation, δ¹⁸O values of CO₂ decreased and Δ¹⁷O values increased. The CO₂ from car exhaust pipe line was also significantly different from atmospheric O₂, which we interpret by partial equilibration with water in the exhaust fume. These results suggest that each combustion process yields CO₂ with a characteristic triple oxygen isotope signature.

Atmospheric CO₂ samples were collected on the campus of the University of Göttingen (NW Germany), between June 2010 and March 2011. The Δ¹⁷O shows variations of 0.045‰ (SD) without correlation between Δ¹⁷O and 1/[CO₂]. Variance analysis suggests a small difference in Δ¹⁷O (0.07‰) between summer and winter. The small variation could be due to differences in the mixing ratio of anomalous anthropogenic and isotopically normal natural CO₂.

Address of corresponding author: B. Horváth: Goldschmidtstrasse 3, D-37077 Göttingen, Germany
e-mail: bhorvat@gwdg.de

Sulphur and oxygen isotopes in dissolved sulphates as tracers of sea and river water mixing in the Szczecin Lagoon (Poland)

Piotr Jezierski, Adriana Trojanowska
*Laboratory of Isotope Geology and Geoecology,
University of Wrocław, Wrocław*

Artur Skowronek
*Department of Geology and Paleogeography, University
of Szczecin, Szczecin*

Sulphur and oxygen isotope ratios ($\delta^{34}\text{S}_{\text{SO}_4}$, $\delta^{18}\text{O}_{\text{SO}_4}$) in dissolved SO_4^{2-} ions and concentration of sulphates in water were analyzed in the Szczecin Lagoon (SW Baltic Sea) – an area of inland and coastal water mixing. This reservoir receives from the south the Odra River water, whereas, in its northern part, the lagoon connects via straits with the Baltic Sea. Therefore, mixing of marine and riverine waters is an important feature of the lagoon hydrodynamics and its hydrochemistry as well. Frequent storms in this shallow lagoon promote oxygenation of waters and the redox stability of SO_4^{2-} ions, which is the important property of the good geochemical tracer. The proportion of sea and river waters in the lagoon depends on several hydrological and weather factors that determine the direction and distribution of water current (wind direction and strength, the relationship of sea level to the level of water in the lagoon, etc.).

Interpretation of the chemical and isotope data allowed to recognize two main sources of SO_4^{2-} ions: riverine (the Odra River) and marine (Baltic Sea). Marine sulphates were characterized by distinctly higher concentration and higher values of $\delta^{18}\text{O}_{\text{SO}_4}$ and $\delta^{34}\text{S}_{\text{SO}_4}$ than riverine ones. Concentration of SO_4^{2-} ions varied from 202 to 571 mg/l, values of $\delta^{18}\text{O}_{\text{SO}_4}$ from 3.6 to 8.9‰ and $\delta^{34}\text{S}_{\text{SO}_4}$ from 2.9 to 14.9‰. It was found that the concentration of sulphate ions and $\delta^{34}\text{S}_{\text{SO}_4}$ values were increasing from south to north. The significant correlations between SO_4^{2-} conc. ($r=0.893$, $p=0.000$) and $\delta^{34}\text{S}_{\text{SO}_4}$ ($r=0.537$, $p=0.039$) versus sample points latitude were noted.

The results showed that sulphur and oxygen isotopes in dissolved sulphates are good tracers of sea and river water mixing in the Szczecin Lagoon. It seems that studies of similar scope may be helpful for simple and quick quantitative estimation of inland and marine waters contribution in other coastal reservoirs as well.

Address of corresponding author: P. Jezierski: Ul. Cybulskiego 30, 50-205 Wrocław, Poland
e-mail: piotr.jezierski@ing.uni.wroc.pl

Methanogenesis in the Pliocene Velenje Coal Basin, Slovenia, inferred from stable carbon isotopes

Tjaša Kanduč
*Department of Environmental Sciences,
Jožef Stefan Institute, Ljubljana*

Miloš Markič
Geological Survey of Slovenia, Ljubljana

Simon Zavšek
Velenje Coal Mine, Velenje

Jennifer McIntosh
*Department of Hydrology and Water Resources,
University of Arizona, Tucson*

In this study, stable isotopes of carbon were used to trace organic and inorganic carbon cycles and biogeochemical processes, especially methanogenesis within different geological media of the Pliocene lignite-bearing Velenje Basin in northern Slovenia. The study is based on investigations of carbon isotopic composition of the following geological media: 1.) lithotypes of lignite, 2.) coalbed gases, 3.) calcified woods (xylites) and carbonate-rich sediments, and 4.) groundwaters in various aquifers. For different lignite lithotypes it was found that $\delta^{13}\text{C}$ values ranged from -28.1 to -23.0‰ , the variability is being a consequence of original isotopic heterogeneity of the source plant ingredients and of biogeochemical processes (gelification, fusinitization, mineralization of organic matter) at the early stage of biomass accumulation and its early diagenesis. In the lignite seam the major gas components were found to be CO_2 and CH_4 with small amounts of N_2 . The carbon isotope compositions of carbon in CO_2 ($\delta^{13}\text{C}_{\text{CO}_2}$) and CH_4 ($\delta^{13}\text{C}_{\text{CH}_4}$) were very variable and ranged from -9.7 to 0.6‰ and from -70.5 to -34.2‰ , respectively. The presence of thermogenic gases is unlikely due to the low rank of the coal and lack of higher chain hydrocarbons. Calcified xylite enriched with ^{13}C ($\delta^{13}\text{C}$ values up to 17.1‰) indicated that CO_2 reduction process was present at the time of formation of the basin. The $\delta^{13}\text{C}_{\text{DIC}}$ values (from -17.4 to -3.2‰) of groundwaters recharging the basin from the Triassic aquifer were consistent with degradation of organic matter and dissolution of dolomite. Groundwaters from the Pliocene sandy and Lithotamnium carbonate aquifers had $\delta^{13}\text{C}_{\text{DIC}}$ values (from -9.1 to 0.2‰) suggestive of degradation of organic matter and biogenic CO_2 reduction.

Address of corresponding author: T. Kanduč: Jamova 39, 1000 Ljubljana, Slovenia
e-mail: tjasa.kanduc@ijs.si

Carbon isotopic variation in $\delta^{13}\text{C}_{\text{DIC}}$ and $\delta^{13}\text{C}_{\text{CO}_2}$ during early anaerobic decomposition of organic agriculture wastes

Dominika Kufka, Beata Biega, Mariusz Orion Jędrysek
*Laboratory of Isotope Geology and Geoecology Institute of Geological Sciences,
University of Wrocław, Wrocław*

This abstract reports carbon isotopic variation in $\delta^{13}\text{C}_{\text{DIC}}$ and $\delta^{13}\text{C}_{\text{CO}_2}$ formed during anaerobic decomposition of grass and corn silage. This study is an initial part of a larger experiment regarding methanogenic processes in incubated conditions. Decomposed biomass was incubated in batch approach (closed system) at temperature 32 °C. Experiments were started at 14th February 2011. Fermented biomass has been located in a half litter bottle with rubber septum. In the first bottle (B1) 40 g of biomass was placed and filled up with distilled water up to 350 ml – the remaining volume was air. Another bottle (B 2) has been filled with 10 g of biomass, and 350 ml of distilled water – the remaining volume was completed with gaseous nitrogen.

DIC (10 ml of water) and CO_2 (7 ml gas) has been sampled daily since 23rd March 2011 to 1st April 2011. Five samples of gaseous CO_2 and five samples of DIC from the B1 have been sampled. Four respective samples have been collected from the B2. The sampled volume has been substituted with distilled water each time. Additionally the analyses of $\delta^{13}\text{C}$ from unfermented organic matter (prior to the experiment) have been carried out. The method of DIC and CO_2 analyses was based on conversion all of DIC forms to gaseous CO_2 under acidic condition. The analyses of concentrations of gaseous and dissolved CO_2 were not carried out. However, visual judgement shows that the production of carbon dioxide decreased along experiment. Measurements of carbon isotope composition have been made using a mass spectrometer Finnigan Mat Delta E.

In the B1 $\delta^{13}\text{C}_{\text{DIC}}$ and $\delta^{13}\text{C}_{\text{CO}_2}$ varied from 9.05 to 12.90‰ and 8.82 to 9.72‰, respectively. In the B2 $\delta^{13}\text{C}_{\text{DIC}}$ and $\delta^{13}\text{C}_{\text{CO}_2}$ varied from 7.55 to 10.54‰ and 1.90 to 8.69‰, respectively. The $\delta^{13}\text{C}$ value of the initial organic load was –12.65‰. In the B1 $\delta^{13}\text{C}_{\text{CO}_2}$ increased with time while in the B2 $\delta^{13}\text{C}_{\text{CO}_2}$ and both in B1 and B2 $\delta^{13}\text{C}_{\text{DIC}}$ values have shown chaotic variations. These suggest the experiment was too short to observe isotopic effect in anaerobic conditions, but selective oxidation of C isotopes took place when atmospheric O_2 was available.

Address of corresponding author: D. Kufka: Cybulskiego 30 Str; 50-205 Wrocław; Poland
e-mail: ominika.kufka@ing.uni.wroc.pl

Recent paleolimnological changes in small carbonate rich hypertrophic lake

Annika Mikomägi
Institute of Ecology, Tallinn University, Tallinn

Tonu Martma
*Institute of Geology, Tallinn University of
Technology, Tallinn*

Agata Marzecova
*Institute of Mathematics and Natural Sciences,
Tallinn University, Tallinn*

In paleolimnological studies oxygen and carbon isotopes have been used for reconstructions of climate changes and productivity within the lake. This study presents the use of stable isotopes from lacustrine carbonates in a multi-proxy approach to track environmental changes and associated anthropogenic impacts in lake. The main objective was to combine different indicators and to detect how they correspond to the documented history of the lake. Sedimentary pigments were used because they are known as good indicators of changes in lake primary production. Geochemical composition of lake sediment is influenced by processes taking place in lake and also by the surrounding catchment therefore XRF analysis can be used as a supportive tool to understand how human activities affect the natural ecosystem. For this study, two short sediment cores from Lake Verevi littoral zone were collected. The study site L. Verevi is small, hard-water and intermittently open/closed lake. Lake is situated in town Elva (Estonia) and during the last 100 years it has been highly popular recreation area. Town located in the vicinity of the lake contaminates the lake from various sources (discharge of urban wastewater, infiltrated water from farms, swimming pool). Carbon and oxygen stable isotopes in carbonates ($\delta^{13}\text{C}_{\text{Carb}}$ and $\delta^{18}\text{O}_{\text{Carb}}$) were analysed, sediment pigment markers were identified using high-performance liquid chromatography (HPLC) and bulk geochemistry determined by XRF spectroscopy. The sediment record covers last 150 years (based on ^{210}Pb dating). XRF chemistry reflects increase of the pollution and significant changes in the lithology of the sediment which changes from organic-rich to mineral sediment. Changes in sediment pigment markers show strong eutrophication. Isotopic values at the same time show increase in the amount of heavier isotopes. We were able to link these results with collected historical and monitoring data which confirmed that at the beginning of 20th century the lake was moderately eutrophic and during 1970s and 1980s the distinctive changes in lake productivity occurred and lake became hypertrophic. In addition, the results of our multi-proxy analysis show drastic changes in lake carbonate precipitation processes after extensive human impact has started. Based on shift in carbon isotope values we conclude that a change in lake sediment has been caused by excessive eutrophication.

Address of corresponding author: A. Mikomägi: Uus-Sadama 5, 10120 Tallinn, Estonia
e-mail: annikam@tlu.ee

Use of light stable isotopes, dissolved gas constituents, and microbial community abundances to characterize biodegradation of chlorinated ethenes in a fractured-rock aquifer

Kinga Révész
U.S. Geological Survey, USA

Barbara Sherwood Lollar
University of Toronto, Canada

Allen M. Shapiro, Julie Kirshtein, Mary Voytek, Thomas E. Imbrigiotta,
Eurybiades Busenberg, Claire R. Tiedeman, Daniel J. Goode
U.S. Geological Survey, USA

The $\delta^{13}\text{C}_{\text{VPDB}}$ and concentration results of TCE are qualitatively consistent with kinetic isotope fractionation by natural microbial TCE dehalogenation and indicate clearly that TCE microbial dehalogenation has occurred in a fracture rock aquifer at the former Naval Air Warfare Center (NAWC) site in West Trenton, New Jersey. The estimated value of the isotope fractionation factor (α) obtained from the borehole interval with the lowest transmissivity was 0.99345, which is in the range of published values. With the knowledge of the site-specific α the original TCE concentration that degraded microbiologically can be calculated in the various monitored intervals. The data from the same low-transmissivity well also could be used to determine the site-specific, first-order reaction kinetic constant. It is also close to published values.

Bioaugmentation was used to accelerate the dechlorination of TCE in groundwater at NAWC site. Water enriched in deuterium was used as a tracer. The $\delta^2\text{H}$ of water and the concentration of H_2 gas were more sensitive indicators of bioremediation than the $\delta^{13}\text{C}$ of the chlorinated hydrocarbons and the abundance of the microbial communities. The combined evidence suggests that the effects of bioaugmentation were detectable up to 15 m from the injection well, and that the effect of it might have occurred to a lesser extent up to 26 m. Data also showed that the sum of the molar chlorinated hydrocarbon concentrations was higher than the sum of the background molar concentration in those wells where the bioaugmentation was intensive. The concentration ratios of TCE/(cDCE+VC) and the carbon isotope mass balance calculation of these compounds indicated that the additional concentration may be from a less degraded TCE, that could be desorbed from the rock matrix due to the sudden concentration gradient change caused by the bioaugmentation.

Address of corresponding author: K. Révész: MS 431, Reston, VA 20192, USA
e-mail: krevesz@usgs.gov

Distribution and origin of organic matter in the Baltic sediments based on $\delta^{13}\text{C}$ profiles in sediment cores dated with ^{210}Pb and ^{137}Cs

Aleksandra Szczepanska, Anna Maciejewska, Karol Kulinski,
Janusz Pempkowiak
Institute of Oceanology, Sopot, Poland

Organic carbon in marine sediments is an important part of the global carbon cycle. Knowledge concerning the role of shelf seas (including the Baltic Sea) in the carbon cycle is inadequate. Accumulation of carbon in marine sediments, in general, and in the Baltic sediments, in particular, still requires clarification. The study demonstrates methods used and the obtained results for assessing organic carbon sedimentation rates and provenience in the Baltic contemporary sediments.

The experimental work is based on sediment cores covering sediment accumulation areas in the Baltic Sea. Mass sediment accumulation rates ($230\text{--}570\text{ gm}^{-2}\text{yr}^{-1}$) are based on ^{210}Pb method validated with ^{137}Cs measurements. The provenience of organic matter (autochthonous vs allochthonous) is assessed by $\delta^{13}\text{C}$ data (range from -23.2‰ to -26.4‰).

Marine (autochthonous) organic matter constitutes some 45% of the total in the surface (0–10 cm below sediment-water interface), and 30% in the subsurface (20–30 cm) sediment layers. The organic carbon accumulation rates in contemporary Baltic sediments ranging from 18 to $75\text{ g C m}^{-2}\text{yr}^{-1}$ were established.

The obtained results indicate that the Baltic Sea sediments are an important sink for organic carbon originating, mostly, from terrestrial areas.

Address of corresponding author: J. Pempkowiak: PO Box 197, Sopot, Poland
e-mail: pempa@iopan.gda.pl

Carbon and nitrogen isotopic analysis coupled with palynological data of PM10 dust in Wrocław city (SW Poland) – assessment of anthropogenic impact

Elzbieta Zwolińska, Maciej Górka
Dominika Lewicka-Szczebak
Mariusz-Orion Jędrysek
*Laboratory of Isotope Geology and Geochemistry,
Department Applied Geology and Geochemistry,
Institute of Geological Sciences,
University of Wrocław, Wrocław*

Malgorzata Malkiewicz
*Department of Paleobotany,
Institute of Geological Sciences,
University of Wrocław, Wrocław*

The purpose of this study was to assess the anthropogenic impact on the urban air quality in the city of Wrocław (SW Poland) based on carbon and nitrogen isotopic analyses and palynological analysis of PM10 samples. The 23 samples (about two per month) were chosen for isotopic analysis.

The PM10 concentrations vary from $10.5 \mu\text{g}/\text{m}^3$ (5th June 2007) to $98 \mu\text{g}/\text{m}^3$ (21st November 2007), showing higher values in heating season when compared to vegetative season. The $\delta^{13}\text{C}(\text{PM10})$ values vary from -26.9‰ (24th April 2007) to -25.1‰ (21st November 2007), with the average of -26.1‰ . The $\delta^{15}\text{N}(\text{PM10})$ values vary from 5.0‰ (9th September 2007) to 13.7‰ (5th June 2007), with the average of 9.9‰ . The palynological analysis determined eight taxons of pollen and six types of spores of mildew fungus. Furthermore, in the analyzed samples insect fragments, hair and plant tissues were noted.

The results obtained show that carbon isotopic delta values differ dependently on the season – the lower values are observed in the summer (vegetative season), and the higher in winter (heating season). During the heating season the main source of carbon in PM10 are products of coal combustion, while in the vegetative season, two generations of carbon in PM10 can be distinguished: (i) originating from the coal combustion, (ii) a mixture of organic molecules and pollution from transport. Seasonal variations in nitrogen isotopic values in PM10 were not clearly observed. However, it is possible to determine isotopic composition of the dominant nitrogen source, which is about 10‰ in summer and about 9‰ in winter. These values do not allow us to discriminate precisely between various sources of atmospheric dust.

Address of corresponding author: E. Zwolińska: Cybulskiego 30, 50-205 Wrocław, Poland
e-mail: elzbieta.zwolinska@ing.uni.wroc.pl:

GENERAL ISOTOPE GEOCHEMISTRY

Hydrogen isotope compositions in carbonado diamond: constraints on terrestrial formation

Attila Demény, Géza Nagy
Bernadett Bajnóczi, Tibor Németh
Institute for Geochemical Research
Hungarian Academy of Sciences, Budapest

József Garai
Department of Mechanical and
Materials Engineering
International University, Miami

Vadym Drozd
CeSMEC
Florida International University, Miami

Ernst Hegner
Dept. für Geo- und Umweltwissenschaften
Ludwig-Maximilians Universität, München

In this study we report the first hydrogen isotope composition analyses on carbonado diamond along with cathodoluminescence and scanning electron microscopic imaging, electron microprobe analyses, and stable (H and C) and radiogenic (Sr) isotope measurements. The hydrogen of bulk carbonado (consisting diamond and pore-filling minerals) yielded $\sim -4\%$, consistent with usual crustal or mantle-derived fluids. The diamond-related hydrogen component is about 70 ± 30 ppm and shows a D-depletion down to -200% . Determined H isotope values – together with C isotope compositions – overlap the ranges for mantle-derived hydrocarbons. Textural characteristics and Sr isotope ratios of pore-filling florencite indicate that the carbonado was formed in a fluid-rich environment, underwent a significant high-temperature influence and finally suffered thorough alteration. Based on these observations, a terrestrial formation during interaction of mantle rocks/melts or subducted crustal materials and reduced C-H fluids seems to be more plausible than an extraterrestrial origin.

Key words: carbonado, diamond, hydrogen isotope composition, carbon isotope composition, Sr isotope ratio, texture, cathodoluminescence microscopy

Introduction

Carbonado diamond, a special microcrystalline diamond variety that is found in placer deposits in Brazil and the Central African Republic (Trueb and

Addresses: A. Demény, G. Nagy, B. Bajnóczi, T. Németh: H-1112 Budapest, Budaörsi út 45, Hungary
e-mails: demeny@geochem.hu, gnagy@geochem.hu, bajnoczi@geochem.hu, ntibi@geochem.hu
J. Garai: Miami, FL 33199, USA, e-mail: jozsef.garai@fiu.edu
D. Vadym: Miami, FL 3319, USA, e-mail: vdrozdz@gmail.com
H. Ernst : Luisenstr. 37, D-80333 München, Germany, e-mail: hegner@lmu.de

Received: April 18, 2011; accepted: May 16, 2011

Butterman 1969), has a number of unique features that distinguish it from other diamond types (e.g., restricted to single time and locality, porphyroclastic and highly porous microstructure, narrow stable carbon isotope composition range of about $-27 \pm 3\%$) (see the comprehensive review by Heaney et al. 2005). Although the literature is extensive, there is no general consensus regarding the origin of carbonados. Genetical models are extremely varied: formation from organic matter due to subduction-related metamorphism (Robinson 1978) or extreme nuclear irradiation (Kaminsky 1987; Ozima et al. 1991; Ozima and Tatsumoto 1997), precipitation from carbonic fluids in the mantle (Kaminsky 1991; Nadolnny et al. 2003), or an impact origin either by transforming terrestrial organic matter into diamond (Smith and Dawson 1985) due to the impact shock or transporting extraterrestrial diamondiferous material (Haggerty 1996, 1999; Garai et al. 2006). The presence of hydrogen trapped in the diamond structure has recently been discovered in carbonado (Nadolnny et al. 2003; Garai et al. 2006; Kagi and Fukura 2008). Based on the resemblance of FTIR absorption spectra to those of presolar and CVD (chemical vapor deposition) diamonds, the hydrogen content was interpreted as an evidence for formation in a hydrogen-rich interstellar environment (Garai et al. 2006). An extraterrestrial origin has been suggested for carbonado on the base of those features which are distinct from terrestrial – especially mantle-derived – diamonds: close areal distribution, low carbon isotope composition, green and orange cathodoluminescence colour, high porosity, elevated concentrations of PAHs, occurrence of native metals, titanium and boron nitrides and planar-defect lamellae, lack of primary mantle mineral inclusions (Jones et al. 2003; Parthasarathy et al. 2005; Garai et al. 2006). Additionally, the carbonado grains have a smooth, glossy surface that has been interpreted as "fusion crust" formed during a bolide impact (Shelkov et al. 1997; Kletetschka et al. 2000). The arguments for extraterrestrial origin have been weakened by recent observations published in the last several years: osbornite (TiN) has been shown to form in deep subduction environment (Dobrzhinetskaya et al. 2007), deformation lamellae have been produced experimentally at mantle P-T conditions in carbonado diamond (De et al. 2004), green and yellow CL colours have been encountered in terrestrial diamonds (De Stefano et al. 2006), native metals have been described in kimberlite-hosted diamonds (Jacob et al. 2004 and references therein), diamonds with very low carbon isotope compositions (down to -41% relative to V-PDB, Cartigny et al. 2004; Cartigny 2007, 2008; De Stefano et al. 2009), low aggregation states (Cartigny 2007, 2008; Kagi and Fukura 2008) and elevated hydrogen contents (Hayman et al. 2005) have been reported from various types of mantle-derived diamonds. The latter observation is important as the hydrogen content of the carbonado diamond can provide new means to investigate its origin. Assuming an extraterrestrial origin, D/H ratios may be used to infer the ultimate origin of the H component, as it should either be strongly depleted in deuterium (solar hydrogen) or enriched in deuterium (interstellar organic matter from which the

diamond may have formed) (see reviews by Aléon and Robert 2004; Huss 2005). Until now, the major obstacle of such study has been the low hydrogen content of the carbonado, which itself is usually available only in very small quantities. Recent technical developments now makes it possible to analyse very small amounts of hydrogen extracted from minerals (Demény and Siklósy 2008).

The main aim of this study was to determine the amount and hydrogen isotope composition of the H compounds contained in carbonados, and the interpretation of these data in the light of carbonado origin, for which purpose five carbonado samples from Brazil and Central Africa were studied. However, as usual in stable isotope geochemistry, for the correct interpretation of hydrogen isotope data detailed investigations on sample characteristics are needed. This is especially true for the smooth surface, since the assumed fusion process (Shelkov et al. 1997; Kletetschka et al. 2000) cannot only provide arguments for an impact-related origin, but can also cause modifications in the original hydrogen content and isotope compositions by degassing. Carbon isotope analyses are also essential in order to demonstrate the typical carbonado nature of the selected samples. As mentioned above, carbonado is special among diamond classes for its mineral inclusion content. The volumetrically most important mineral within the diamond is florencite $[(\text{Ce,REE})\text{Al}_3(\text{PO}_4)_2(\text{OH})_6]$, whose presence indicate hydrothermal conditions (Trueb and de Wys 1971). Its coexistence with kaolinite suggest alteration (Trueb and de Wys 1971) from a precursor mineral (like monazite, also reported from carbonado, Trueb and de Wys 1971). The florencite is rather Sr-rich (up to 8.7 wt% SrO; De et al. 1998). Although the rare earth element (REE) compositions of Brazilian and African carbonado reflect crustal origin for the REE-bearing minerals, such high Sr content raises the possibility of partial preservation of the original strontium if the precursor mineral (e.g. monazite) was formed in a different environment (mantle or extraterrestrial). Thus, Sr isotope ratios were also determined in acid-leached fraction.

Based on these considerations, this paper presents a complex study on textural features, chemical and isotope compositions investigated by means of optical and cathodoluminescence (CL) microscopes, electron microprobe, and mass spectrometric (for H, C and Sr isotopes) analyses.

Samples and analytical techniques

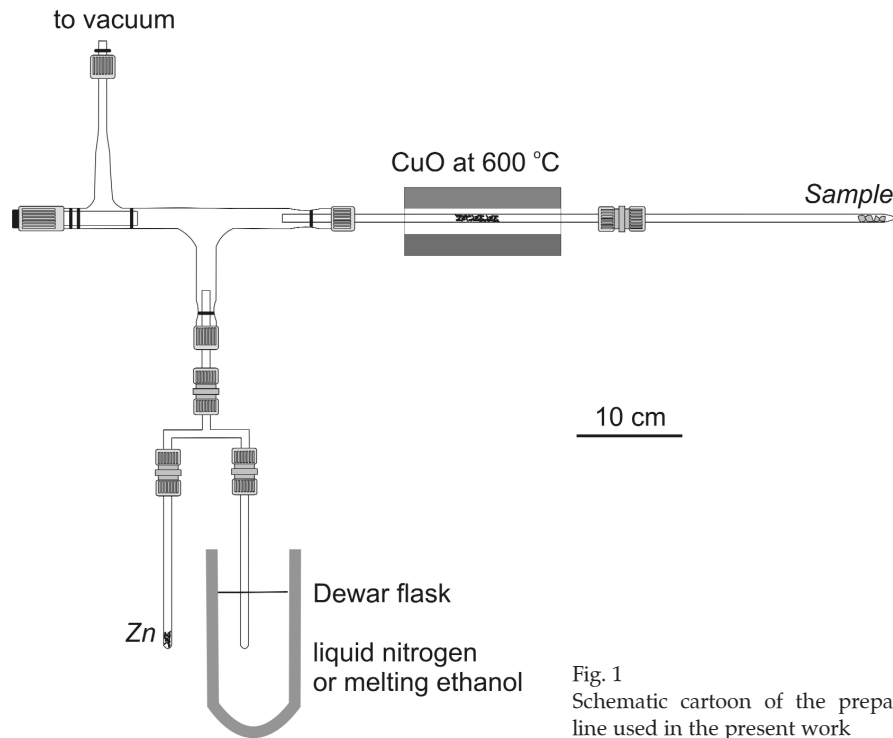
Five carbonado samples from Brazil (sample BR-H) and the Central African Republic (samples CAR-J2, CAR-J4, CAR-J5 and CAR-3), weighing about 200 mg each, were investigated. Measurement of more samples was precluded by the amount needed and the destructive nature of analyses. The samples were purchased and hence only approximate location coordinates can be given: E 15–25 and N 5–10 for the Central African Republic; W 37–47 and S 10–20 for Brazil. All analyses (excepting where stated otherwise) were conducted at the Institute for Geochemical Research, Budapest. Cathodoluminescence

microscopic characteristics were studied using Reliotron type cold-cathode equipment attached to a Nikon Eclipse E600 optical microscope equipped with a Nikon Coolpix 4500 digital camera. Major element compositions of pore-filling minerals were determined with a JEOL Superprobe 733 electron microprobe. Conditions used were: wavelength dispersive spectrometers, 15 kV accelerating voltage and 30 nA beam current. Raw data was corrected using the ZAF correction program provided by JEOL.

A Philips PW 1730 X-ray diffractometer controlled by PC-APD software was used for routine X-ray diffractometric analyses to identify mineral phases and to check the efficiency of acid treatment. In order to detect trace amounts of minerals, X-ray diffraction analyses were also conducted at B2 station of Cornell High Energy Synchrotron Source (CHESS), using synchrotron X-rays with a wavelength of $\lambda=0.4959$ Å and a Mar345 image plate detector. 2D diffraction patterns obtained were integrated using Fit2D software. The detection limit of minerals for usual XRD analysis is about 3 vol%, whereas the synchrotron-based XRD analysis has a much lower detection limit due to higher signal-to-noise ratio, below 1 vol%.

For carbon isotope analyses, about 2 mg of powdered (down to <0.1 mm grain size) and acid-treated (1:1 HCl) carbonado diamond samples were mixed with CuO and combusted at 1000 °C for 60 minutes, then the evolved CO₂ was purified by vacuum distillation and the carbon isotope compositions were determined using a dual inlet Finnigan MAT delta S type mass spectrometer. The results were calibrated using in-house standards and the CH-7 reference material supplied by the International Atomic Energy Agency.

For hydrogen isotope analyses different types of materials were prepared from 5 carbonado samples: 1) bulk, untreated carbonado, powdered or chips of 1–2 mm size; 2) powdered samples treated with HCl and HF acids; 3) powdered, but chemically untreated sample stepwise heated to 500, 1000 and >1500 °C. In order to remove silicate and phosphate minerals, powdered samples were dissolved in HCl for 1–3 days at 50 °C followed by washing with distilled water, then the remaining material was treated with HF for 3 days at 90–100 °C and washed again with distilled water. For bulk analyses samples weighing 30 to 50 mg were put into 6 mm silica tubes and attached to the vacuum preparation line modified after Demény and Siklósy (2008), by inserting a silica tube containing CuO between the sample and gas-collection cold fingers (see Fig. 1). The CuO was constantly held at 600 °C to produce an oxygen atmosphere of about 0.5 mbar in the vacuum line that allowed conversion of all hydrogen released to H₂O. After pumping to good vacuum (while the sample was held at 150 °C for 8 hours to get rid of surface-bound H₂O), the sample was slowly heated to 1500–1700 °C (elastic temperature of silica) using a gas-oxygen torch. The heating time was about 30 minutes. Very slow diffusion may partially retain hydrogen in the diamond structure resulting in incomplete yield, but graphitization and oxidation can effectively disrupt the crystal structure promoting H release (e.g. similarly to He,



Zashu and Hiyagon 1995). The agreement in H contents and isotope compositions for different analytical conditions supports complete hydrogen recovery. The gases evolved were collected at liquid nitrogen temperature in a 6 mm pyrex tube for another 15 minutes in order to convert all the released hydrogen to H₂O, then the temperature was raised to about -80 °C and the non-condensable gases were pumped away. The collected H₂O was transferred to another 6 mm pyrex tube containing zinc reagent (Indiana University, Bloomington), then the tube was flame-sealed and put into a muffle furnace to 480 °C to convert H₂O to H₂ gas (see Demény 1995; Demény and Siklósy 2008). The D/H ratios were analysed in the H₂ gas using a Thermo Finnigan delta XP mass spectrometer using a GASBENCH II equipment as a tube-cracker and inlet port (see Demény and Siklósy (2008) for the manual measurement protocol). As one of the reviewers kindly called our attention, hydrogen can diffuse through heated silica even at rather low temperature (<300 °C, Shang et al. 2009), contamination from the ambient atmosphere may occur especially at the high temperatures used in this study, thus, determination of blank level is important to assess the analyses' accuracy. Blank measurements were conducted twice during this study, yielding about 0.5 micromole H₂. For general sample weights

and H contents obtained for the carbonado samples this blank causes <10% contamination.

Hydrogen and carbon isotope compositions are reported in the conventional δ value given by the equation: $\delta = (R_{\text{sample}}/R_{\text{standard}} - 1) \cdot 1000$, where R_{sample} and R_{standard} are the $N(\text{D}) / N(\text{H})$ and $N(^{13}\text{C}) / N(^{12}\text{C})$ ratios of the sample and standard, respectively. The data are reported in ‰ relative to V-SMOW (δD values) and V-PDB ($\delta^{13}\text{C}$ values). Based on duplicate analyses on samples and standards the carbon isotope compositions are accurate within 0.2‰. The accuracy of hydrogen isotope analyses was determined as follows.

The H isotope composition of blank-derived hydrogen was also determined by collecting H_2O in the same vacuum line for 2 hours in order to get enough material for precise measurements. This procedure is periodically followed when H isotope analyses are conducted in the laboratory and using the preparation line, the long-term blank composition is $-100 \pm 10\%$. Using the amount and composition of blank-derived hydrogen, the data obtained on samples were corrected. The usual blank correction was 2–3 ‰ and rarely exceeded 5‰. The same procedure as for the diamond samples was followed for the NBS 30 biotite reference material. Amounts of 2.3 to 4.5 mg were weighed into the silica tubes in order to span the whole range of H_2O amounts recovered from the carbonado samples to reproduce the preparation conditions. A δD value of $-65.6 \pm 1.9\%$ and a water content of $3.35 \pm 0.35 \text{ wt}\%$ (2s, $n=4$) was obtained in the course of this study (theoretical compositions are $\delta\text{D} = -65.7\%$, $\text{H}_2\text{O} = 3.5 \text{ wt}\%$). As the NBS 30 analyses were conducted along with the sample preparations, the excellent agreement between measured and expected compositions verify the procedure. The sample amounts available precluded multiple analyses for most of the samples. However, enough sample material was available for sample CAR-3, for which two bulk analyses yielded -86.1 and -85.7% . Additionally, a third batch of sample CAR-3 was step-wise heated to 500 °C, 1000 °C and >1500 °C and the different H-fractions were collected separately. The material was just at the limit of measurement, yielding very small amounts of H_2 at the >1500 °C step that enhanced the effect of blank contamination and resulted in very large degrees of blank correction (up to 50‰). However, the bulk composition was also calculated for the step-wise combustion experiment on the base of hydrogen yields that gave -85.3% , in excellent agreement with the duplicate bulk analyses (-86.1 and -85.7%) in spite of the enormous blank correction. Based on these data, the analytical precision for δD analyses is better than $\pm 3\%$, as a conservative estimation. The precision of H content determination is about 10% for the biotite sample and about 20% for the carbonado.

For Sr isotope analyses the sample powders were dissolved in $\sim 0.5 \text{ N HCl}$ and Sr was separated by standard chromatographic methods. The Sr-isotope analyses were carried out at Ludwig-Maximilians Universität München, using standard procedures outlined by Hegner et al. (1995). Total procedure blanks are $\sim 200 \text{ ng}$ and not significant for the samples under investigation. $^{87}\text{Sr}/^{86}\text{Sr}$ ratios were measured in a dynamic double mass collection mode using a MAT 261 and

normalized to $^{86}\text{Sr}/^{88}\text{Sr} = 0.1194$. External precision for $^{87}\text{Sr}/^{86}\text{Sr}$ is $\sim 1.1 \times 10^{-5}$. The NIST 987 reference material yielded $^{87}\text{Sr}/^{86}\text{Sr} = 0.710229 \pm 6$ (N= 11).

Results

The most important textural observations made by optical and CL microscopic as well as electron microprobe investigations are the following: (1) the carbonados show angular shapes rounded to different degrees (Fig. 2); (2) a recrystallized zone of some 10s of microns is sometimes formed at the smooth,

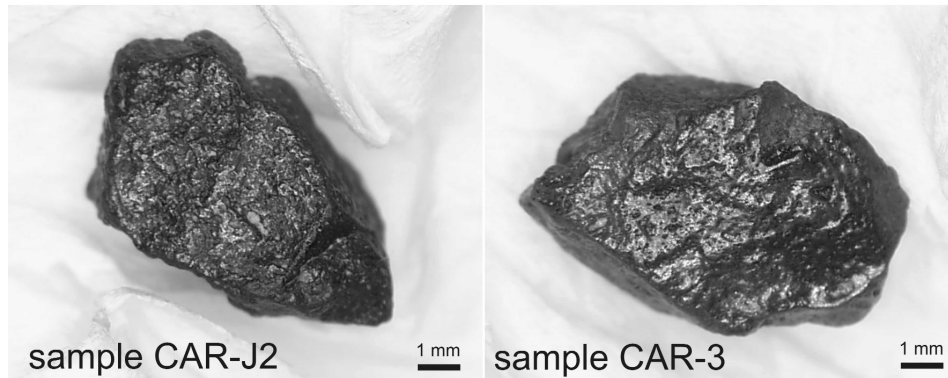


Fig. 2
Stereo microscopic pictures of carbonado samples. Note the angular shape, glossy surface and rounded edges

"glassy" looking surface (Fig. 3A); (3) the thickness of recrystallized zone changes at different sides of the carbonado; (4) the pores' structures and the florencite filling shows no change at the rim (Fig. 3B); (5) the carbonados show "flow" texture with pores concentrating in zones angular to the smooth surface (Fig. 3C); (6) the recrystallized rim contains no exotic mineral; (7) based on EDS spectra, the chemical composition of the florencite shows no change from the smooth surface to the inner parts with several wt% SrO contents (Table 1); (8) the smooth surface has a sharp edge to the pores and the inner surface of the pores is not smooth (Fig. 3D); (9) the different samples have different cathodoluminescence colour (Fig. 4) and (10) there is no change in cathodoluminescence properties in the recrystallized zone (Fig. 4A and C).

The carbonado samples had bulk $\delta^{13}\text{C}$ values of -32.0 to -24.3‰ , which compositions fall in the range of previous investigations (Vinogradov et al. 1966; Galimov et al. 1985; Ozima et al. 1991; Kamioka et al. 1996; Shelkov et al. 1997; De et al. 2001; Kagi et al. 2007; Yokochi et al. 2008), indicating that the studied samples are typical of carbonado. Amorphous carbon (Heaney et al. 2004) with different C isotope composition from the bulk might be present in carbonado. This possibility was tested by heating up few samples to 500 °C in oxygen

atmosphere which should oxidize the amorphous carbon. The experiment yielded no detectable amounts of carbon dioxide. Thus, the amount of amorphous carbon in the investigated samples is insignificant.

Sr isotope analyses of the HCl-soluble fraction of two samples (CAR-J2 and J4) yielded high Sr isotope compositions (~ 0.716 and ~ 0.717 , respectively, Table 1) that represent the Sr content of the pore-filling florencite.

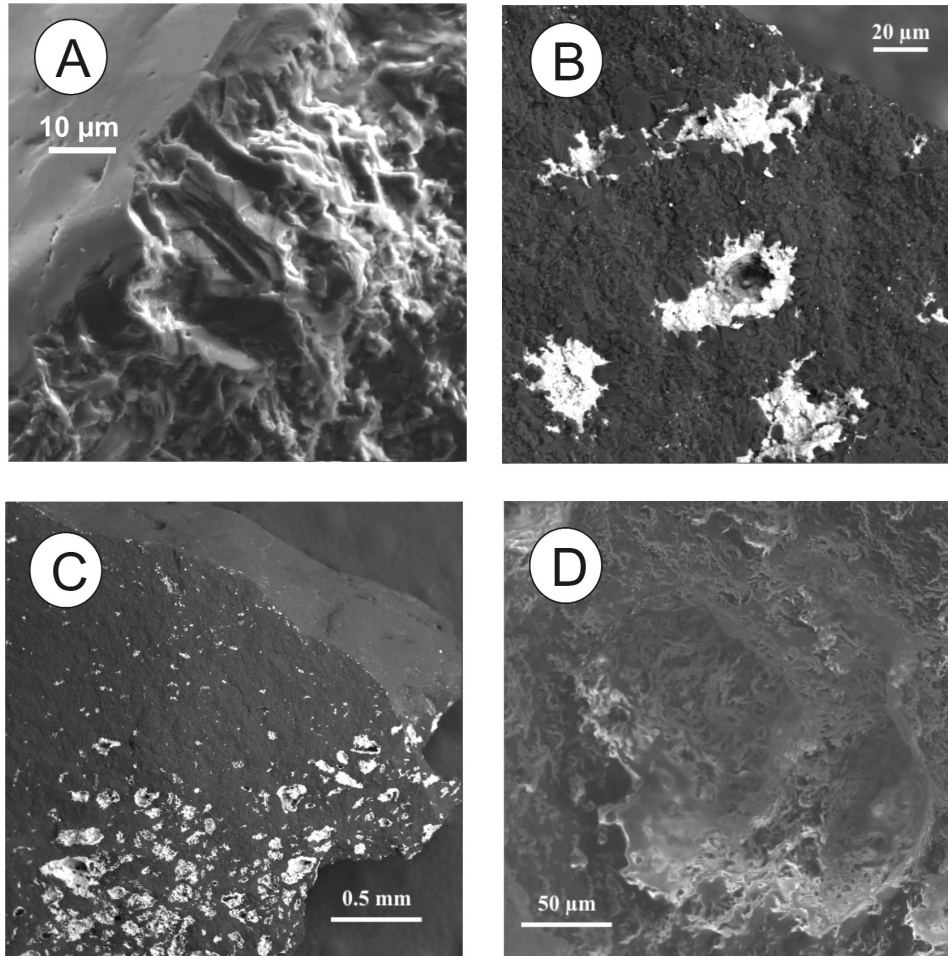


Fig. 3

Scanning electron microscope pictures of carbonado samples. (A) Sample CAR-J1, washed with distilled water, showing recrystallized margin. The upper left side is the smooth surface, the right side of the photo is a broken surface. At this part of the sample the diamond shows better crystallization at the margin than inside the grain. (B) Sample CAR-J1, washed with distilled water, showing no change in pore structure at the margin. (C) Sample BR-H, showing flow texture (see also Trueb and de Wys (1969), and Yokochi et al. (2008)) with pores concentrating in zones angular to the smooth surface. (D) Sample CAR-J2, HCl-treated. Note that the inner surface of the pore is not rounded and

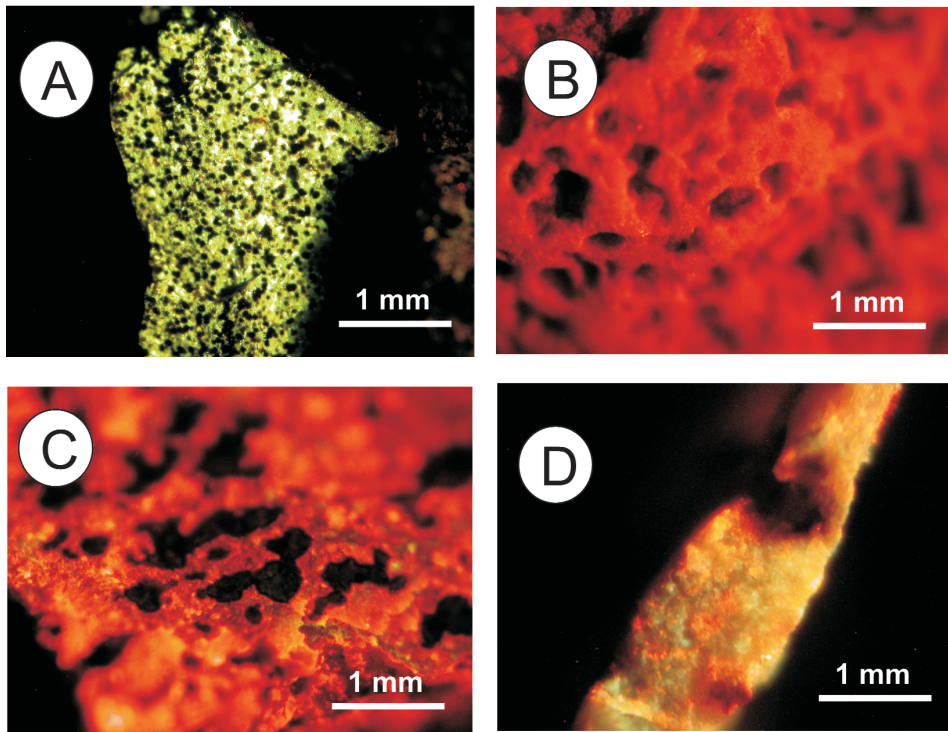


Fig. 4
Cathodoluminescence microscopic pictures of carbonado samples. (A) Sample BR-H, (B) sample CAR-J1, (C) sample CAR-J2, (D) sample CAR-J3. Note that the carbonado samples have very different cathodoluminescence colours that do not change at the grains' margins

Untreated – only crushed – carbonado samples yielded a bulk hydrogen isotope composition of $-84 \pm 11\%$, the average H content is 420 ± 90 ppm. The removal of the pore filling minerals by HCl and subsequent HF acid treatment resulted in significant decrease in the H content as well as in the δD values. The experimental values are listed in Table 1 and shown in Fig. 5. Neither the traditional X-ray diffraction (XRD) analyses nor the synchrotron-radiation XRD measurements detected any residual mineral in the chemically treated carbonado diamond samples. Thus, the detected H contents as well as the δD values are intrinsic of the carbonado-diamond. As we have no direct information on the site of hydrogen, different possibilities of trapped hydrogen (as H or OH in defects or H_2O in minute fluid inclusions, De et al. 1998; Kagi et al. 2010) will be treated as H trapped in the diamond structure.

In order to further constrain the hydrogen isotope compositions of carbonado-hosted hydrogen components, stepwise heating experiments were used. Three pyrolysis steps were conducted on sample CAR-3, at 550, 1000 and >1500 °C. The "low-temperature" component released at 550 °C had a δD value of -59% ,

Table 1

Chemical compositions of selected pore-filling minerals (in wt%), H contents (in ppm) and hydrogen isotope compositions (in ‰ relative to V-SMOW), stable carbon isotope compositions (in ‰ relative to V-PDB) and Sr isotope ratios in carbonado diamonds

Sample	Florencite	Kaolinite	Xenotime
Al ₂ O ₃	27.2	37.5	
SiO ₂		43.6	
P ₂ O ₅	26.6	3.7	32.8
CaO	2.5		
Fe ₂ O ₃		1.7	
CuO	1.0	1.4	0.1
SrO	4.6		
Y ₂ O ₃			38.3
La ₂ O ₃	8.9		
Ce ₂ O ₃	9.5	1.9	
Nd ₂ O ₃	3.7		
Gd ₂ O ₃			3.2
Dy ₂ O ₃			4.7
Er ₂ O ₃			2.6
PbO	2.9		
Total	86.8	89.7	81.7

Sample	H ppm	dD
CAR-J2 - untreated	319	-69
CAR-J2 - HCl treatment	306	-93
CAR-J2 - HF treatment	200	-121
CAR-J4- untreated	466	-85
CAR-J4 - HCl treatment	335	-66
CAR-J4 - HF treatment	122	-126
CAR-J5- untreated	481	-96
CAR-J5 - HCl treatment	312	-143
CAR-3- untreated	222	-85
CAR-3 - stepwise, 550 oC	174	-59
CAR-3 - stepwise, 1000 oC	40	-204
CAR-3 - stepwise, 1500 oC	2	38
CAR-3 - stepwise, bulk calculated	42	-195
BR-H- untreated	535	-112
BR-H - HF treatment	100	-196

Sample	δ ¹³ C	⁸⁷ Sr/ ⁸⁶ Sr
CAR-J2	-30.2	0.715977
CAR-J4	-24.3	0.717161
CAR-J5	-25.2	
CAR-3	-32.1	
BR-H	-32.0	

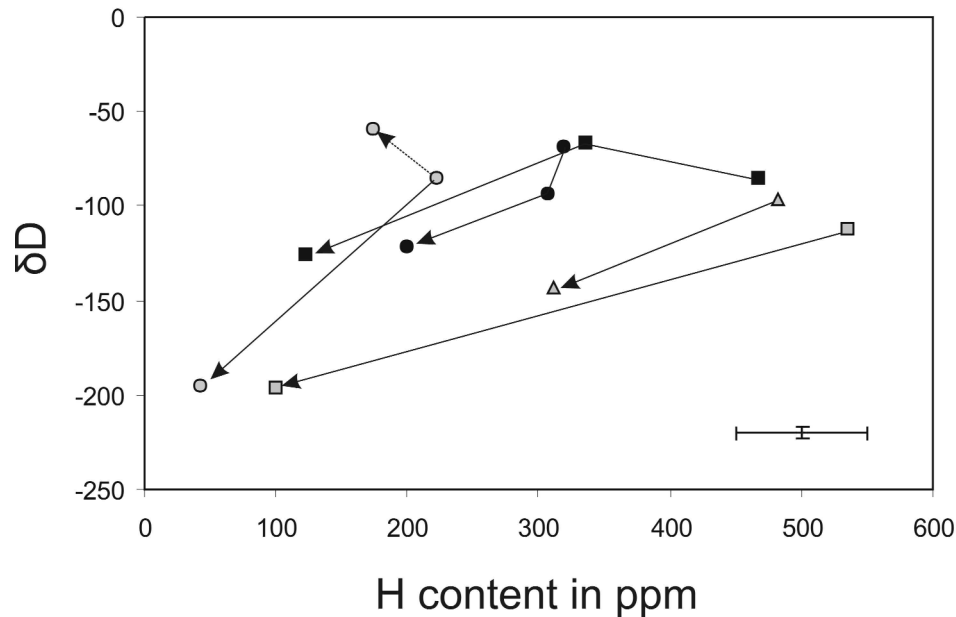


Fig. 5

H contents and stable hydrogen isotope compositions (in ‰ relative to V-SMOW) of carbonado samples. Tie-lines connect data obtained for the same sample using different treatments (untreated – HCl-treated – HCl&HF-treated, and stepwise combustion)

whereas the 1000 °C and the >1500 °C steps yielded $-204‰$ and $+38‰$, respectively. The δD difference in the two high-temperature steps can be attributed to the very slow hydrogen diffusion out of the diamond structure (Foreman et al. 1999) that would result in preferential escape of the light isotope and enrich the remaining material in the heavy isotope. Thus, the results of the two steps were combined on the base of H yields (see Table 1), obtaining a δD value of $-195‰$, in remarkable agreement with the low δD range observed for the HCl+HF-treated samples (Table 1).

Discussion

Formation of the carbonado textures and pore-filling minerals

Observations on textural features of carbonado grains can provide important information regarding formation processes (e.g. Petrovsky et al. 2010). The alignment of elongated pores and their concentration in zones within the carbonado grain (see Fig. 3C) is very similar to fluidized zones of vesicular basalts, and has been interpreted as a flow structure and sign of formation in a fluid-rich environment by Trueb and de Wys 1969; Yokochi et al. 2008). These zones bear no relation to the margins of the carbonado grain (Fig. 3B and C) so

their formation is not related to the process that induced surface smoothening. The pores were already filled with minerals (but not with florencite as this H₂O-rich mineral would be decomposed during the high-temperature influence at least at the margins), otherwise they would have been in contact with ambient environment (hot fluid and/or melt) and hence the inner surface of empty pores would have also been smoothened. The large variations in cathodoluminescence (CL) colour both within individual grains and between localities indicate changing formation environment. This compositional – and most probably formation condition – variability is reflected by the heterogeneous behaviour of carbon isotope composition and nitrogen content that show different relationships between samples and localities (De et al. 2001; Yokochi et al. 2008). Although these authors interpreted CL colour variations in carbonado as an indication of changing formation conditions, in this investigation the CL colour shows no significant change at the margins even where the recrystallized zone reaches 50 micrometer thickness. This observation suggests that the ambient environment during the "fusion" was not very much different from that of the diamond formation, otherwise the margin should show changes in nitrogen, hydrogen and trace element contents, thought to be responsible for CL characteristics (Taylor and Anand 2004). In case of low nitrogen and hydrogen fugacities, the diamond would release these trapped volatiles during the recrystallization, which should result in some CL colour change.

The presumed high-temperature influence (tentatively called "fusion") that caused recrystallization at the margin and surface smoothening did not affect the inner surface of the pores, suggesting that the pores were already filled with minerals during the fusion process. The pore-filling minerals could not be the present-day assemblage as the florencite and kaolinite are sensitive to the high temperature and would suffer breakdown. Thus, the florencite and kaolinite should have had precursor minerals, such as feldspars and monazite (whose alteration can produce florencite; Rasmussen and Muhling 2009), both reported from carbonado by Trueb and de Wys (1969; 1971). As the carbonado-hosted florencite contains several wt% Sr (Table 1, and see also De et al. 1998), it was suspected that a part of this high Sr content may be related to the precursor REE mineral, hereby providing clues to the origin of the initial pore-filling minerals. As a powerful tool for the determination of Sr origin, ⁸⁷Sr/⁸⁶Sr ratios were measured in the HCl-soluble fraction (related practically to the florencite). The ⁸⁷Sr/⁸⁶Sr ratios obtained are high compared to typical mantle compositions (<0.705) and consistent with a crustal origin. Taking the presence of hydrous minerals typically formed at low-temperatures (kaolinite) into account, the most plausible explanation is that the formation of pore-filling florencite and kaolinite is related to late-stage influx of crustal fluids and complete alteration of the original mineral assemblage. This observation would be in accordance with the rare earth element compositions characteristic for crustal rocks detected in some carbonados (Shibata et al. 1993), although other carbonado samples yielded

kimberlitic signatures (Kagi et al. 1994). This variation can be related to differences in the original mineral composition, or to the varying degree of alteration. The near-complete alteration of the original mineral assemblage even in the inner parts of carbonado grains requires interconnection of the pores. This was demonstrated by Dismukes et al. (1988) who were able to remove all the non-diamond minerals by one-week long sequential leaching, providing an analogue for the much longer natural alteration processes such as metamorphism or surficial alteration. Interestingly, native metal inclusions have been preserved in carbonado (Gorshkov et al. 1996; De et al. 1998) in spite of the late-stage alteration. Formation of native metals would indicate strongly reducing conditions, that would, however, not be unprecedented as native iron inclusions have also been encountered in kimberlitic diamonds from Siberia (Sobolev et al. 1981) and South Africa (Jacob et al. 2004).

Hydrogen isotope compositions: possible alteration effects and primary compositions

Bulk carbonado samples, which contains secondary, alteration-related minerals (florencite and kaolinite), yielded $-84 \pm 11\%$, which composition can be considered as typical for any terrestrial (mantle or crust) reservoir (Hoefs 1996). The diamond structure itself contains about 70 ± 30 ppm hydrogen and this diamond-related hydrogen has a δD range of -200 to -130% (Fig. 5). This composition is lower than usual mantle or crustal ranges, but it is still in the range of terrestrial organic matter and hydrocarbons (Hoefs 1996).

The obtained hydrogen isotope compositions is consistent with formation of carbonado in the mantle or in the crust. However, it should be investigated if the δD range can also be reconciled with impact or an extraterrestrial origin (see Introduction). As hydrogen isotope compositions of extraterrestrial materials can be extremely different from terrestrial values (see reviews by Aléon and Robert 2004; Huss 2005), strong effects should have influenced the carbonado in order to achieve the present compositions if starting from extraterrestrial values. The responsible processes should have either i) introduced hydrogen into the diamond structure, ii) caused exchange with terrestrial H reservoirs, or iii) should have resulted in partial hydrogen loss and large isotope fractionation. The recrystallization at the margins of carbonado grains ("fusion crust") and the thorough alteration of pore-filling mineral assemblages suggest interactions at different temperatures that may have induced degassing or isotope exchange. All of these processes require migration of hydrogen in the diamond structure, thus, the possibility of hydrogen diffusion at relevant temperatures should be explored.

Several estimations of hydrogen diffusion rate at various temperatures have been published, reporting D values from about $10^{-15} \text{ cm}^2\text{s}^{-1}$ (~ 500 °C, Teukam et al. 2003) to $2.4 \cdot 10^{-13} \text{ cm}^2\text{s}^{-1}$ (860 °C, Popovici et al. 1995), so a diffusion rate of 10^{-13} to $10^{-13} \text{ cm}^2\text{s}^{-1}$ can be roughly estimated for the temperature range of

1500–2000 °C. An energy barrier of 1.9 eV is given for H diffusion by Mehandru et al. (1992).

The pore-filling mineral assemblage of florencite and kaolinite suggests hydrothermal and metamorphic conditions followed by surficial weathering. Assuming a usual greenschist facies (see Smith and Dawson 1985; Martins-Neto 1996) metamorphic temperature up to 500 °C, the necessary time required to diffuse hydrogen at various lengths can be calculated using the well-known Arrhenius equation $D = D_0 \cdot e^{-E_a/RT}$, where E_a is the activation energy, D_0 is the diffusion coefficient, R is the gas constant, and T is temperature in K. Based on our calculations, about 1012 years would be needed to have hydrogen diffusion at a length of 10 microns (an average crystallite size in carbonado matrix, as the crystal size actually ranges from <1 to several 100 microns), while diffusion through a 100 micron distance would require about 10^{15} years, diffusion of hydrogen into the diamond structure or isotope exchange with the ambient fluids at hydrothermal-metamorphic temperatures can be excluded. This means that i) the low δD values could not have been caused by preferential migration of the light hydrogen isotope into the diamond, and ii) the diamond structure was closed to isotope exchange and any extraterrestrial composition (very low or very high δD) should have been preserved during the alteration process that produced the florencite-kaolinite assemblage.

Alternatively, a bolide impact would induce shock heating that can release trapped volatiles. Although there are a number of uncertainties concerning calculation of degassing effects (alteration temperature, duration, and fractionation between the escaping hydrogen and the remaining material), we can make some estimations. It is safe to assume that the hydrogen escapes as H_2 and not as H_2O , taking preferentially the light isotope, and thus, causing D-enrichment in the remaining carbonado. Consequently, the starting composition should be more D-depleted than the present-day composition, thus, in case of an initially deuterium-rich interstellar material dehydrogenation can in no way explain the observed δD range, as it must result in increasing δD values. If the initial composition of carbonado was around solar deuterium content of ~ 20 ppm ($\sim -900\text{‰}$; see Aléon and Robert 2004 and references therein), Rayleigh fractionation during degassing may cause a positive δD shift toward the observed compositions (from -200 to -130‰). However, this would require a significant amount of hydrogen to leave the diamond structure. Using the diffusion parameters discussed above, the necessary time required to have H migration through a 10 micron distance would be on the order of 10^2 to 10^4 years at a temperature of 1200 to 2000 °C that is again unlikely to maintain after the impact. These considerations suggest that the hydrogen isotope compositions observed in pure carbonado diamond (i.e. completely demineralized by acid treatment) represent primary compositions.

Terrestrial origin and possible relationships with other diamond types

The measured diamond-related hydrogen has a δD range from -200 to -130‰ which represents the hydrogen content trapped during the diamond formation. This composition is out of the range of extraterrestrial values, but similar to terrestrial hydrocarbons and organic matter. (Hoefs 1996). The additional constraint that a diamond with extraterrestrial origin should exhibit is its nitrogen isotope composition. For solar origin the $\delta^{15}N$ values should be down to -350‰ , while for interstellar matter the $\delta^{15}N$ values would range up to $+400\text{‰}$ (Aléon and Robert 2004). The $\delta^{15}N$ values reported for carbonado are in the range of -17 to $+8\text{‰}$ (Vicenzi and Heaney 2001; Heaney et al. 2005; Yokochi et al. 2008), which is practically equal with the mantle-derived peridotitic diamonds (Cartigny 2005). Diffusive alteration by terrestrial-like nitrogen isotope compositions can be excluded based on the very low diffusion rates in diamond.

Crustal organic matter have a wide range of $\delta^{13}C$ and δD values (Hoefs 1996), completely overlapping the diamond-related hydrogen isotope compositions obtained in this study. Methane formed biogenically or thermogenically during organic matter maturation has also similarly wide ranges, from which thermogenic methane compositions (Whiticar 1999) overlap the $\delta^{13}C$ - δD ranges of carbonado. Another possibility to explore is abiogenic hydrocarbons that may be formed in the deep Earth. Plotting the determined δD values against $\delta^{13}C$ and comparing to mantle-derived hydrocarbon determined from inclusion fluids of alkaline magmatic rocks and other terrestrial sources it can be seen that the carbonado data fit well to the compositions of these mantle-derived hydrocarbons (Fig. 6). The so-called "normal mantle range" (δD values around -80‰ ; Boettcher and O'Neil 1980; Kyser and O'Neil 1984; Kyser 1986; $\delta^{13}C$ values around -7 to -5‰ ; Keller and Hoefs 1995; Deines 2002) is not shown in Fig. 6, as it refers to hydrous minerals, oxidized forms of mantle-derived carbon (carbonatites, xenolith-hosted CO_2) and peridotitic diamonds which are certainly different from carbonado. It should be noted, however, that abiogenic methane and hydrocarbons from the Khibina alkaline complex have carbon and hydrogen isotope compositions close to the normal mantle compositions (similarly to the abiogenic methane compositions given by Whiticar 1999; Sherwood Lollar et al. 2002), with the higher hydrocarbons depleted in ^{13}C and 2H relative to CH_4 (Potter and Longstaffe 2007). These studies indicate that although mantle-derived hydrocarbons can be found with isotope values close to carbonado compositions, thermogenic methane would fit better to the observed $\delta^{13}C$ - δD ranges of carbonado. Either compared with mantle-derived C-H fluids, or crustal organic compounds, there is a significant overlap in carbon and hydrogen isotopic compositions, suggesting that carbonado may indeed have been formed from terrestrial carbon compounds.

Metasomatism by strongly reduced C-H fluids can explain the flow texture and the $\delta^{13}C$ - δD values of carbonado which is in accordance with earlier studies (Nadolinny et al. 2003; Kagi and Fukura 2008). This fluid may either have been

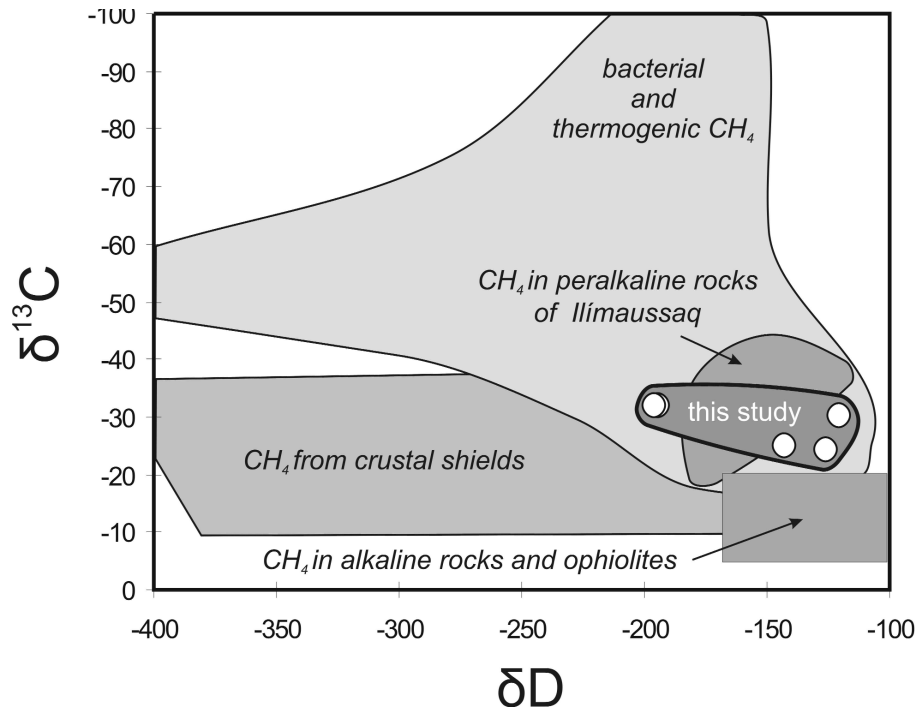


Fig. 6
Stable carbon and hydrogen isotope compositions (in ‰ relative to V-PDB and V-SMOW, respectively) of carbonado (this study) and different terrestrial CH_4 reservoirs (Graser et al. 2008)

mixed with REE-Sr-rich melt, resulting in an intermingled texture of diamond, REE- and silicate minerals, or a special rock type with REE-minerals and feldspar has to be assumed that was metasomatised. The former process would imply a carbonatitic melt (rich in REE and alkalis), analogous to the assumed formation of framesite diamond, whose low $\delta^{13}\text{C}$ values and trace element characteristics lead (Jacob et al. 2000; Maruoka et al. 2004) to suggest formation from a C-H fluid and carbonatite melt. It is important to note that the possibility of transitional position of framesites between carbonado and eclogitic diamonds has already been raised by Heaney et al. (2005) and the lower end of the $\delta^{13}\text{C}$ range of framesites overlaps with carbonado (Fig. 7), suggesting mixing of the very low $\delta^{13}\text{C}$ fluid with a relatively ^{13}C -enriched carbonatitic melt. The close relationship with framesites and the end-member characteristic of carbonado is also indicated by $\text{N}\%$ - $\delta^{15}\text{N}$ - ^{40}Ar results (Yokochi et al. 2008). A further analogue to carbonado is the komatiite-hosted diamond found in French Guyana (Capdevila et al. 1999) that show striking similarities (low $\delta^{13}\text{C}$ values, low N contents and aggregation states, Cartigny 2007; 2008) to carbonado raising the possibility of carbonado formation in the Earth's mantle.

The other possibility is subduction of REE-rich crustal rock that reacted with a C-H fluid. This process has been proposed as a mechanism for eclogitic diamond formation (e.g. Cartigny et al. 2004; Taylor and Anand 2004; De Stefano et al. 2009), thus, the observations presented in this paper are also compared to characteristics of eclogitic diamonds. The presence of K-feldspar may indicate genetic relationship with eclogitic diamonds as sanidine inclusions have been reported in this suite (e.g. Wang 1998; Sobolev et al. 1999; Taylor and Anand 2004). Further, carbon isotope compositions even lower than the carbonado range have been reported for eclogitic diamonds by Cartigny et al. (2004) and De Stefano et al. (2009) (Fig. 7). Green, orange and red cathodoluminescence colours unusual for mantle-derived diamonds but characteristic for carbonados have also been detected in calc-alkaline lamprophyre-related diamond populations (De Stefano et al. 2006) and orogenic microdiamonds (Yoshioka and Ogasawara 2005), both

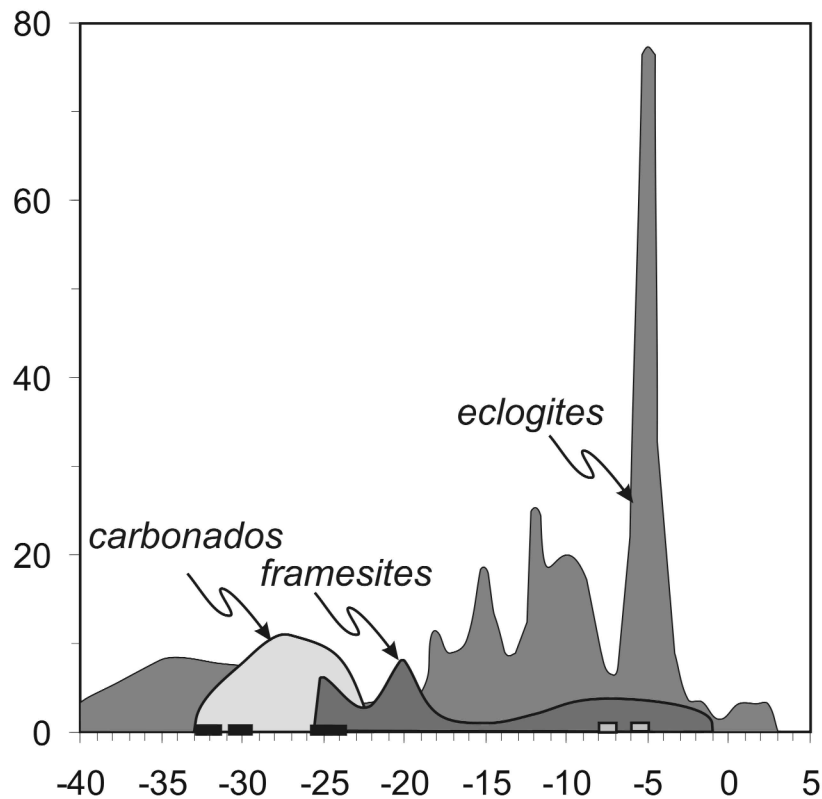


Fig. 7

Stable carbon isotope compositions (in ‰ relative to V-PDB) of eclogitic diamonds (De Stefano et al. 2009; Stachel et al. 2009), framesites and carbonados (Heaney et al. 2005). Carbonado compositions compiled by Heaney et al. (2005) are plotted within the light grey field and two outliers as light grey squares (see their Figure 1), whereas data obtained in this study are marked by solid squares

related to subduction processes. A further similarity with eclogitic diamonds is the low N content reported for carbonados. Figure 8 shows the $\delta^{13}\text{C}$ vs. N content distribution of eclogitic diamonds (after Cartigny et al. 2004) as well as data for carbonados reported by Shelkov et al. (1997). It is apparent that the carbonado compositions plot within the eclogitic diamond field, close to framesites' data. It is interesting to note that low $-\delta^{13}\text{C}$ zones in diamonds are also interpreted as formed from subducted crustal material by Schulze et al. (2004) (shown also in Fig. 8).

Either by mixing with mantle fluids/melts, or by interaction with subducted rocks, the low $\delta\text{D}-\delta^{13}\text{C}$ characteristics suggest the influence of a reduced C-H fluid. Microcrystalline diamond could be precipitated due to reaction between the reduced fluids and silicate magma, similarly to the mechanism proposed for metamorphic diamonds (Sobolev and Shatsky 1990). As CH_4 – and maybe higher hydrocarbons – are oxidized, metals are reduced to native form, and elemental carbon precipitates as diamond. Carbonado formation under mantle conditions

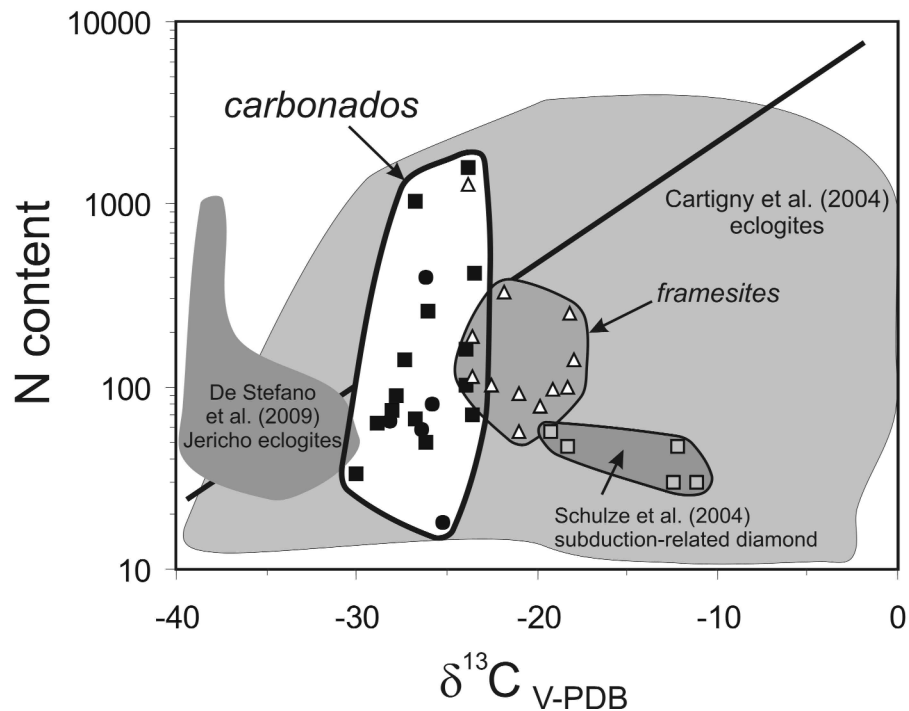


Fig. 8 Nitrogen content (in ppm) vs. carbon isotopic compositions (in ‰ relative to V-PDB) for eclogitic diamonds worldwide (Cartigny et al. 2004) and in Jericho Mine, Canada (De Stefano et al. 2009), diamond-zones related to subducted material (Schulze et al. 2004), framesites and carbonados (Shelkov et al. 1997; solid circles: Ubangui, solid squares: Brasil). Solid line shows the limit of the eclogite sector (Cartigny et al. 2001)

would also be supported by the presence of "large" (reaching several hundred micrometer size) octahedral crystals (Shelkov et al. 1997; De et al. 2001; Petrovsky et al. 2010), whose formation requires time.

The textural characteristics of carbonado suggest that the carbonado pieces suffered different degrees of recrystallization at their margins that may be related to a resorption effect by a high-temperature melt that transported the diamond pieces to the surface. Finally, after transportation to the surface by a magmatic pulse, weathering and deposition in placer deposits, metamorphism resulted in complete alteration of the original REE- and silicate minerals, producing the florencite and kaolinite mixture with small amounts of other crustal minerals like quartz and TiO_2 (anatase in our samples).

This model would be consistent with our textural observations and chemical and H-C-Sr isotope compositions. It would put the formation of carbonado, framesite and similar polycrystalline diamond varieties discovered in Russia and China (containing also florencite, Gorshkov et al. 1996; Seliverstov et al. 1996; Titkov et al. 2001) in a common framework in which carbonado is an end-member, while other polycrystalline diamonds are transitional between carbonado and regular kimberlitic diamonds. The process is rather special, diamond precipitation induced by mantle metasomatism by strongly reduced carbonic fluids and their mixing with REE-rich melts, or by interaction of hydrocarbons with subducted REE-rich rocks would be very occasional. Thus, it is no surprise that such diamonds are found rarely and their occurrences are confined to certain areas. However, recent investigations report more and more diamond features which are similar to those observed for carbonado. Green and orange CL colours and low $\delta^{13}\text{C}$ values are no more exclusively related to carbonado *sensu stricto*, and many new observations would be in agreement with a special formation process in the mantle.

Conclusions

This study presents the first hydrogen isotope composition analyses on carbonado diamond conducted in order to investigate the origin of hydrogen related to the diamond structure detected by earlier studies. The hydrogen of bulk carbonado (dominated by the H content of pore filling minerals) yielded $\sim -84\%$, consistent with an origin from either crustal or mantle-derived fluids. Textural characteristics and Sr isotope ratios indicate formation in a fluid-rich environment followed by a high temperature influence and finally by thorough alteration. The hydrogen component bound to the diamond shows a D-depletion down to -200 to -130% . Diffusion modelling of late stage alteration effects (either hydrogen incorporation during interaction with fluids or dehydrogenation during degassing) indicated that the diamond-related hydrogen most likely represent the original H content. The carbon and hydrogen isotope compositions of carbonado diamond overlap the δD and $\delta^{13}\text{C}$ ranges of terrestrial

organic compounds and abiogenic hydrocarbons. The H isotope data combined with textural evidence as well as with geochemical data of earlier studies are best explained with terrestrial formation, most probably by metasomatism of subducted crustal rocks or mantle rocks/melts by reduced C-H fluids.

Acknowledgments

The mass spectrometer facility at the Institute of Geochemical Research was financed by the National Office for Research and Technology (GVOP-3.2.1-2004-04-0235/3.0). JG is indebted to Professor Stephen Haggerty for numerous discussions and for donation of the Brazilian carbonado. We sincerely thank Nikolay Sobolev, Dorrit Jacob and Hiroyuki Kagi for their thorough reviews that greatly helped clarify our ideas.

References

- Aléon, J., F. Robert 2004: Interstellar chemistry recorded by nitrogen isotopes in Solar system organic matter. – *Icarus*, 167, pp. 424–430.
- Boettcher, A.L., J.R. O'Neil 1980: Stable isotope, chemical, and petrographic studies of high-pressure amphiboles and micas: evidence for metasomatism in the mantle source regions of alkali basalts and kimberlites. – *American Journal of Science*, 280-A, pp. 594–621.
- Capdevilla, R., N. Arndt, J. Letendre, J.F. Sanvage 1999: Diamonds in volcanoclastic komatite from French Guiana. – *Nature*, 399, pp. 456–458.
- Cartigny, P., T. Stachel, J. Harris, M. Javoy 2004: Constraining diamond metasomatic growth using C- and N-stable isotopes; examples from Namibia. – *Lithos*, 77, pp. 359–373.
- Cartigny, P. 2005: Stable isotopes and the origin of diamond. – *Elements*, 1, pp. 79–84.
- Cartigny, P. 2007: Mantle derived carbonados: insights from Dachine diamonds (French Guiana). – *Geochimica et Cosmochimica Acta*, 71-A, pp. 148.
- Cartigny, P. 2008: The formation of enigmatic carbonados from komatiite-related fluids: A model. – *Geochimica et Cosmochimica Acta*, 72-A, pp. 141.
- Cartigny, P., J.W. Harris, M. Javoy 2001: Diamond genesis, mantle fractionations and mantle nitrogen content: a study of $\delta^{13}\text{C}$ -N concentrations in diamonds. – *Earth and Planetary Science Letters*, 185, pp. 85–98.
- De, S., P.J. Heaney, R.B. Hargreaves, E.P. Vicenzi, P.T. Taylor 1998: Mineralogical observations of polycrystalline diamond – a contribution to the carbonado conundrum. – *Earth and Planetary Science Letters*, 164, pp. 421–433.
- De, S.R., P.J. Heaney, E.P. Vicenzi, J.H. Wang 2001: Chemical heterogeneity in carbonado, an enigmatic polycrystalline diamond. – *Earth and Planetary Science Letters*, 185, pp. 315–330.
- De, S., P.J. Heaney, Fei Yungwei, E.P. Vicenzi 2004: Microstructural study of synthetic sintered diamond, and comparison with carbonado, a natural polycrystalline diamond. – *American Mineralogist*, 89, pp. 438–446.
- De Stefano, A., N. Lefebvre, M. Kopylova 2006: Enigmatic diamonds in Archean calc-alkaline lamprophyres of Wawa, southern Ontario, Canada. – *Contributions to Mineralogy and Petrology*, 151, pp. 158–173.
- De Stefano, A., M.G. Kopylova, P. Cartigny, V. Afanasiev 2009: Diamonds and eclogites of the Jericho kimberlite (Northern Canada). – *Contributions to Mineralogy and Petrology*, 158, pp. 295–315.
- Deines, P. 2002: The carbon isotope geochemistry of mantle xenoliths. – *Earth-Science Reviews*, 58, pp. 247–278.

- Demény, A. 1995: H isotope fractionation due to hydrogen-zinc reactions and its implications on D/H analysis of water samples. – *Chemical Geology*, 121, pp. 19–25.
- Demény, A., Z. Siklósy 2008: Combination of off-line preparation and continuous flow mass spectrometry: D/H analyses of inclusion waters. – *Rapid Communications in Mass Spectrometry*, 22, pp. 1329–1334.
- Dismukes, J.P., P.R. Gaines, H. Witzke, D.P. Leta, B.H. Kear, S.K. Behal, S.B. Rice 1988: Demineralisation and microstructure of carbonado. – *Materials Science and Engineering*, A105/106, pp. 555–563.
- Dobrzhinetskaya, L., R. Wirth, J. Yang, I. Hutcheon, P. Weber, H.W. Green 2007: Osbornite (TiN) and boron nitride nanoinclusions in coesite from Tibet: a first record of nitrogen in a terrestrial ultrahigh pressure environment. – *American Geophysical Union, Fall Meeting, 2007*, abstract #V43E-04.
- Foreman, L.R., R.S. Barbero, D.W. Carroll, T. Archuleta, J. Baker, D. Devlin, J. Duke, D. Loemier, M. Trukla 1999: Diamond and Diamond-Like Materials as Hydrogen Isotope Barriers. – *DOE Scientific and Technical Information*, DOI 10.2172/759179.
- Galimov, E.M., F.V. Kaminskii, L.A. Kodina 1985: New data on isotopic composition of carbon in carbonado. – *Geokhimiya*, 5, pp. 723–726.
- Garai, J., S.E. Haggerty, S. Rekhi, M. Chance 2006: Infra-red absorption investigations confirm the extraterrestrial origin of carbonado diamonds. – *Astrophysical Journal*, 653, pp. L153–L156.
- Gorshkov, A.I., S.V. Titkov, A.M. Pleshakov, A.V. Sivtsov, L.V. Bershov 1996: Inclusions of native metals and other mineral phases into carbonado from the Ubangi region (Central Africa). – *Geology of Ore Deposits*, 38, pp. 114–119.
- Graser, G., J. Potter, J. Köhler, G. Markl 2008: Isotope, major, minor and trace element geochemistry of late-magmatic fluids in the peralkaline Ilímaussaq intrusion, South Greenland. – *Lithos*, 106, pp. 207–221.
- Haggerty, S.E. 1996: Diamond-carbonado models for a new meteorite class of circumstellar or solar system origin. – *EOS*, 77, pp. S143.
- Haggerty, S.E. 1999: A diamond trilogy: superplumes, supercontinents, and supernovae. – *Science*, 285, pp. 851–860.
- Hayman, P.C., M.G. Kopylova, F.V. Kaminsky 2005: Lower mantle diamonds from Rio Soriso (Juina area, Mato Grosso, Brazil). – *Contributions to Mineralogy and Petrology*, 149, pp. 430–445.
- Heaney, P.J., E.P. Vicenzi, E. Brevet 2004: The origin of porosity in carbonado diamond. – *Geochimica et Cosmochimica Acta*, 68, pp. A115.
- Heaney, P.J., E.P. Vicenzi, S. De 2005: Strange diamonds: the mysterious origins of carbonado and framesite. – *Elements*, 1, pp. 85–89.
- Hegner, E., H.J. Walter, M. Satir 1995: Pb-Sr-Nd isotopic compositions and trace element geochemistry of megacrysts and melilitites from the Tertiary Urach volcanic field: source composition of small volume melts under SW Germany. – *Contributions to Mineralogy and Petrology*, 122, pp. 322–335.
- Hoefs, J. 1996: *Stable isotope geochemistry*. – Springer-Verlag, 201 p.
- Huss, G.R. 2005: Meteoritic nanodiamonds: Messengers from the stars. – *Elements*, 1, pp. 97–100.
- Jacob, D.E., K.S. Viljoen, N. Grassineau, E. Jagoutz 2000: Remobilization in the cratonic lithosphere recorded in polycrystalline diamond. – *Science*, 289, pp. 1182–1185.
- Jacob, D.E., A. Kronz, K.S. Viljoen 2004: Cohenite, native iron and troilite inclusions in garnets from polycrystalline diamond aggregates. – *Contributions to Mineralogy and Petrology*, 146, pp. 566–576.
- Jones, A.P., A.D. Beard, J. Milledge, G. Cressey, C. Kirk, P. DeCarli 2003: New nitride minerals in carbonado diamond. – *Eighth International Kimberlite Conference Abstracts*, Victoria Canada, FLA 0167.
- Kagi, H. S. Fukura 2008: Infrared and Raman spectroscopic observations of Central African carbonado and implications for its origin. – *European Journal of Mineralogy*, 20, pp. 387–393.

- Kagi, H., K. Takahashi, H. Hidaka, A. Masuda 1994: Chemical properties of Central American carbonado and its implications. – *Geochimica et Cosmochimica Acta*, 58, pp. 2629–2638.
- Kagi, H., S. Sato, T. Akagi, H. Kanda 2007: Generation history of carbonado inferred from photoluminescence spectra, cathodoluminescence image and carbon isotopic composition. – *American Mineralogist*, 92, pp. 217–224.
- Kagi, H., H. Sakurai, H. Ishibashi, H. Ohfuji 2010: Finding primary fluid inclusions in carbonado diamond and its implication to the origin. – *Acta Mineralogica et Petrographica, Abstract Series, International Mineralogical Association 2010*, pp. 178.
- Kaminskiy, F.V. 1987: Genesis of carbonado-polycrystalline aggregates of diamond. – *Akademiya Nauk SSSR Doklady, Earth Sciences Section*, 294, pp. 439–440.
- Kaminskiy, F.V. 1991: Carbonado and yakutite: Properties and possible genesis. – *Proceedings of the International Kimberlite Conference*, 5, pp. 214–216.
- Kamioka, H., K. Shibata, I. Kajizuka, T. Ohta 1996: Rare-earth element patterns and carbon isotopic composition of carbonados: Implications for their crustal origin. – *Geochemical Journal*, 30, pp. 189–194.
- Keller, J., J. Hoefs 1995: Stable isotope characteristics of recent natrocarbonatites from Oldoinyo Lengai. – In: Bell, K., J. Keller (Eds): *Carbonatite Volcanism: Oldoinyo Lengai and the Petrogenesis of Natrocarbonatites*. Springer Verlag, Berlin, Heidelberg, New York, London, Paris, Tokyo, Hong Kong, Barcelona, Budapest, pp. 113–123.
- Kletetschka, G., P.T. Taylor, P.J. Wasilewski, H.G.M. Hill 2000: Magnetic properties of aggregate polycrystalline diamond: implications for carbonado history. – *Earth and Planetary Science Letters*, 181, pp. 279–290.
- Kyser, T.K. 1986: Stable isotope variations in the mantle. – In: Valley, J.W., H.P. Taylor, Jr., J.R. O'Neil (Eds): *Stable isotopes in high temperature geological processes*. Reviews in Mineralogy, Mineralogical Society of America, 16, pp. 141–164.
- Kyser, T.K., J.R. O'Neil 1984: Hydrogen isotope systematics of submarine basalts. – *Geochimica et Cosmochimica Acta*, 48, pp. 2123–2133.
- Martins-Neto, M.A. 1996: Lacustrine fan-deltaic sedimentation in a Proterozoic rift basin: the Sopa-Brumadinho Tectonosequence, southeastern Brazil. – *Sedimentary Geology*, 106, pp. 65–96.
- Maruoka, T., G. Kurat, G. Dobosi, C. Koeberl 2004: Isotopic composition of carbon in diamonds of diamondites: Record of mass fractionation in the upper mantle. – *Geochimica et Cosmochimica Acta*, 68, pp. 1635–1644.
- Mehandru, S.P., A.B. Anderson, J.C. Angus 1992: Hydrogen binding and diffusion in diamond. – *Journal of Materials Research*, 73, pp. 689–695.
- Nadolinny, V.A., V.S. Shatsky, N.V. Sobolev, D.J. Twitchen 2003: Observation and interpretation of paramagnetic defects on Brazilian and Central African carbonados. – *American Mineralogist*, 88, pp. 11–17.
- Ozima, M., M. Tatsumoto 1997: Radiation-induced diamond crystallization: Origin of carbonados at its implication on meteoritic nano-diamonds. – *Geochimica et Cosmochimica Acta*, 61, pp. 369–376.
- Ozima, M., S. Zashu, K. Tomura, Y. Matsuhisa 1991: Constraints from noble-gas contents on the origin of carbonado diamonds. – *Nature*, 351, pp. 472–474.
- Parthasarathy, G., S.E. Haggerty, A.C. Kunwar 2005: Nanocrystalline osbornite from carbonados: spectrographic studies. – *Geochimica et Cosmochimica Acta*, 69 Supplement, pp. 521.
- Petrovsky, V.A., A.A. Shiryayev, V.P. Lyutoev, A.E. Sukharev, M. Martins 2010: Morphology and defects of diamond grains in carbonado: clues to carbonado genesis. – *European Journal of Mineralogy*, 22, pp. 35–47.
- Popovici, G., R.G. Wilson, T. Sung, M.A. Prelas, S. Khasawinah 1995: Diffusion of boron, lithium, oxygen, hydrogen, and nitrogen in type IIa natural diamond. – *Journal of Applied Physics*, 77, pp. 5103–5106.
- Potter, J., E.J. Longstaffe 2007: A gas-chromatograph, continuous flow-isotope ratio mass-spectrometry method for $\delta^{13}\text{C}$ and δD measurement of complex fluid inclusion volatiles:

- Examples from the Khibina alkaline igneous complex, northwest Russia and the south Wales coalfields. – *Chemical Geology*, 244, pp. 186–201.
- Rasmussen, B., J.R. Muhling 2009: Reactions destroying detrital monazite in greenschist-facies sandstones from the Witwatersrand basin, South Africa. – *Chemical Geology*, 264, pp. 311–327.
- Robinson, D.N. 1978: The characteristics of natural diamond and their interpretation. – *Minerals Science*, 10, pp. 55–72.
- Schulze, D.J., B. Harte, J.W. Valley, D.M.D. Channer 2004: Evidence of subduction and crust-mantle mixing from a single diamond. – *Lithos*, 77, pp. 349–358.
- Seliverstov, V.A., A.I. Gorshkov, S.A. Shcheka, A.V. Sivtsov 1996: Diamonds and carbonado of the Primorskii Krai: Mineralogy, crystal chemistry, and genesis. – *Geology of Ore Deposits*, 38, pp. 429–441.
- Shang, L., I.-M. Chou, W. Lu, R.C. Burruss, Y. Zhang 2009: Determination of diffusion coefficients of hydrogen in fused silica between 296 and 523 K by Raman spectroscopy and application of fused silica capillaries in studying redox reactions. – *Geochimica et Cosmochimica Acta*, 73, pp. 5435–5443.
- Shelkov, D., A.B. Verchovsky, H.J. Milledge, C.T. Pillinger 1997: Carbonado: a comparison between Brazilian and Ubangui sources with other forms of microcrystalline diamond based on carbon and nitrogen isotopes. – *Russian Geology and Geophysics*, 38, 332–340.
- Sherwood Lollar, B., T.D. Westgate, J.A. Ward, G.F. Slater, G. Lacrampe-Couloume 2002: Abiogenic formation of alkanes in the Earth's crust as a minor source for global hydrocarbon reservoirs. – *Nature*, 6880, pp. 522–524.
- Shibata, K., H. Kamioka, F.V. Kaminsky, V.I. Koptil, D.P. Svisero 1993: Rare earth element patterns of carbonado and yakutite: evidence for their crustal origin. – *Mineralogical Magazine*, 57, pp. 607–611.
- Smith, J.V., J.B. Dawson 1985: Carbonado diamond aggregates from early impacts of crustal rocks. – *Geology*, 13, pp. 342–343.
- Sobolev, N.V., V.S. Shatsky 1990: Diamond inclusions in garnets from metamorphic rocks: a new environment for diamond formation. – *Nature*, 343, pp. 742–746.
- Sobolev, N.V., E.S. Efimova, L.N. Pospelova 1981: Native iron in diamonds of Yakutiya and its paragenesis. – *Geologiya i Geofizika*, 22, pp. 25–28.
- Sobolev, N.V., E.S. Efimova, V.I. Koptil 1999: Mineral inclusions in diamonds in the Northeast of the Yakutian diamondiferous province. – *Proceedings of the 7th Kimberlite Conference*, pp. 816–821.
- Stachel, T., J.W. Harris, K. Muehlenbachs 2009: Sources of carbon in inclusion bearing diamonds. – *Lithos*, 112S, pp. 625–637.
- Taylor, L.A., M. Anand 2004: Diamonds: time capsules from Siberian mantle. – *Chemie der Erde*, 64, pp. 1–74.
- Teukam, Z., D. Ballutaud, F. Jomard, J. Chevallier, M. Bernard, A. Deneuille 2003: Trap limited diffusion of hydrogen in boron-doped diamond. – *Diamond and Related Materials*, 12, pp. 647–651.
- Titkov, S.V., A.I. Gorshkov, S.F. Vinokurov, L.V. Bershov, D.I. Solodov, A.V. Sivtsov 2001: Geochemistry and genesis of carbonado for Yakutian diamond deposits. – *Geochemistry International*, 39, pp. 228–236.
- Trueb, L.F., W.C. Buttermann 1969: Carbonado, a microstructural study. – *American Mineralogist*, 54, pp. 412–425.
- Trueb, L.F., E.C. de Wys 1969: Carbonado: Natural polycrystalline diamond. – *Science*, 165, pp. 799–802.
- Trueb, L.C., E.C. de Wys 1971: Carbon from Ubangui. – *American Mineralogist*, 56, pp. 1252–1268.
- Vicenzi, E.P., P.J. Heaney 2001: The Carbon and Nitrogen Isotopic Composition of Carbonado Diamond: An In Situ Study. – *Eleventh Annual V. M. Goldschmidt Conference abstract*, pp. 3886.

- Vinogradov, A.P., O.I. Kropotova, Y.L. Orlov, V.A. Grinenko 1966: Isotopic composition of diamond and carbonado crystals. – *Geochemistry International*, 3, pp. 1123–1125.
- Wang, W. 1998: Formation of diamond with mineral inclusions of "mixed" eclogite and peridotite paragenesis. – *Earth and Planetary Science Letters*, 160, pp. 831–843.
- Whiticar, M.J. 1999: Carbon and hydrogen isotope systematics of bacterial formation and oxidation of methane. – *Chemical Geology*, 161, pp. 291–314.
- Yokochi, R., D. Ohnenstetter, Y. Sano 2008: Intragrain variation in $\delta^{13}\text{C}$ and nitrogen concentration associated with textural heterogeneities of carbonado. – *Canadian Mineralogist*, 46, pp. 1283–1296.
- Yoshioka, N., Y. Odasawara 2005: Cathodoluminescence of microdiamond in dolomite marble from the Kokchetav Massif – Additional evidence for two-stage growth of diamond. – *International Geology Review*, 47, pp. 703–715.
- Zashu, S., H. Hiyagon 1995: Degassing mechanisms of noble gases from carbonado diamonds. – *Geochimica et Cosmochimica Acta*, 59, pp. 1321–1328.

Carbon isotope study on Celtic graphite-tempered archaeological ceramics from the South Transdanubian region (Hungary)

Izabella Havancsák, József Fekete,
Bernadett Bajnóczi
*Institute for Geochemical Research,
Hungarian Academy of Sciences, Budapest*

The paper presents an application of carbon isotope analysis in the archaeometric research of graphite-tempered ceramics. Graphite separated from Celtic graphitic ceramics were analysed from Szűr, Szajk and Dunaszentgyörgy archaeological sites from the South Transdanubian region of Hungary. Variation in $\delta^{13}\text{C}$ values of graphite in the sampling sites is attributed to the characteristics of graphitic metamorphic rock used for tempering. The carbon isotope results will serve as basis for further provenance research on graphite.

Key words: graphite, Celtic graphitic ceramics, graphitic gneiss, temper, carbon isotope, $\delta^{13}\text{C}$

Introduction

The Celtic graphitic ceramic is a distinctive type of pottery tempered with graphite and known from most part of the Central European Celtic world. In the area of Hungary graphitic pots were produced in great numbers from the middle La Tène period (Szabó et al. 1999) until the decline of the Celtic dominion (1st cent. A.D.). Graphitic ceramics can be found in a wide geographical area, not only around the graphite sources, which suggests extended trade. Former results, based on the mineralogical and petrographic analyses carried out on graphitic ceramics from Hungary (Havancsák et al. 2009a, b), suggest that the studied ceramics were tempered with graphitic, medium- to high-grade metamorphic gneiss. This graphitic gneiss cannot be found in outcrops in the area of Hungary.

Addresses: I. Havancsák, J. Fekete, B. Bajnóczi: H-1112 Budapest, Budaörsi út 45, Hungary

Corresponding author: havancsaki@geochem.hu

Received: April 26, 2011; accepted: May 16, 2011

Our study is an example for utilizing carbon isotope analysis, a technique that is commonly used in geological research, on graphite temper of archaeological graphitic ceramics. The main aim of the overall work is to investigate the carbon isotope composition of graphite in the pottery and compare them with that of graphitic host rocks from the potential source regions. In this paper we present the first results of the carbon isotope analysis performed on graphitic ceramics from Hungary.

Sample description

The 32 graphitic ceramics were analysed from three archaeological sites: Dunaszentgyörgy (LT B2-C1, 11 sherds), Szűr (LT D, 14 sherds) and Szajk (LT B2-C1, 7 sherds), which are located in South Hungary on the flood plain of river Danube. The graphitic ceramics belong to situla-type sherds (thick wall, swollen rim). They were tempered with graphitic metamorphic rock. Graphite grains appear as opaque, individual fresh flakes and in lithoclasts with silicate minerals. The sherds show great variability in the amount and size of graphite from ~ 5 to 50% and between very fine and coarse grains (from few μm up to 5 mm), respectively. For their detailed archaeometric and petrographic description see Havancsák et al. (2009a, b).

Methods

The sherds chosen for isotope analysis were pulverized and treated with 10% acetic acid to remove carbonate. After being leached three times the samples were centrifuged and dried at 40 °C. The separated graphite samples were oxidized with copper oxide in evacuated quartz tubes closed with a Teflon valve at 950 °C based on the method of Sofer (1980). The evolved H_2O and CO_2 were separated online by cold traps using liquid nitrogen and ethyl alcohol cooled below -80 °C. The $^{13}\text{C}/^{12}\text{C}$ ratios were determined using a Finnigan MAT delta S type stable isotope ratio mass spectrometer. The results are given in the conventional δ value ($\delta = (R_{\text{sample}}/R_{\text{standard}} - 1) * 1000$, where R_{sample} and R_{standard} are the $^{13}\text{C}/^{12}\text{C}$ ratios in the sample and standard, respectively) relative to V-PDB in ‰. Based on sample reproducibility and differences in $\delta^{13}\text{C}$ values obtained for standards from their theoretical values, the accuracy is better than $\pm 0.1\text{‰}$ for $\delta^{13}\text{C}$.

Results and discussion

The $\delta^{13}\text{C}$ values of the samples range between -28.6 and -20.9‰ (Table 1). Figure 1 shows the distribution of $\delta^{13}\text{C}$ values in the archaeological sites.

Graphitic samples from Szűr show the largest variation in their $\delta^{13}\text{C}$ values, the ceramics from Szajk show a smaller variation, while the sherds from Dunaszentgyörgy show the smallest variation with $\delta^{13}\text{C}$ values ranging between

–26.0 and –24.1‰. In the sample sets three groups can be distinguished on the basis of $\delta^{13}\text{C}$ data (Fig. 1). Their separation is good at Szajk (from –28.6 to –27.9‰; from –26.2 to –25.6‰; –23.8‰) and Szür (from –28.5 to –27.0‰; from –25.6 to –22.7‰; from –21.2 to –20.9‰) and slightly weaker at Dunaszentgyörgy (from –26.0 to –25.8‰; from –25.4 to –24.9‰; –24.1‰). However, the separation of data groups may disappear if the number of analysed samples increases.

The observed variability in carbon isotope data was not detected in the petrographic or mineralogical characteristics of graphite. The wide range of $\delta^{13}\text{C}$ values may suggest that the graphitic raw material (graphitic rock) was not homogeneous in its carbon isotope composition or fractionation/isotope shift occurred during pottery making (firing) or after the burial (interaction with fluids). Based on the X-ray diffraction analyses the firing of the sherds was carried out in general at a maximum of about 850 °C in reducing atmosphere with short duration (Havancsák et al. 2009a). Graphite can suffer kinetic fractionation related to

partial oxidation during the firing process if it is not fully-ordered, which should occur at a temperature of around 500 °C (Landis 1971). It is presumable that the studied graphite is well-ordered based on the mineralogical assemblage of graphitic rock fragments in the ceramics: the used graphitic rock is a medium- to high-grade (amphibolite facies) metamorphic gneiss. Thus, kinetic fractionation effect can be neglected. However, isotope exchange may occur if carbonate is present. Argillic raw material mixed with the graphitic rock has usually up to 6 wt% CaO content (Havancsák et al. 2009a). The carbon isotope composition of graphite could change through exchange reactions with carbonate (e.g. Bottinga 1969). Contrarily, Chacko et al. (1991) report that an experiment run at 800 °C and 15 kbar for 170 hours produced essentially no isotope exchange between calcite and graphite. The firing process of the ceramics was probably shorter than the above-mentioned experimental time. In addition Wada and Suzuki (1983) suggest

Table 1
The $\delta^{13}\text{C}$ values of the studied graphitic ceramics

Sampling site	Sample	$\delta^{13}\text{C}$ (‰)
Szür	ö.2009.65.59.1.	–20.9
	ö.2009.65.64.309.	–20.9
	ö.2009.65.51.6.	–21.0
	ö.2009.65.11.26.	–21.2
	R.2009.65.28.14.	–22.7
	ö.2009.65.97.3.	–22.7
	ö.2009.65.56.51.	–23.5
	ö.2009.65.164.38.	–24.0
	ö.2009.65.56.87.	–24.7
	ö.2009.65.56.81.	–25.6
	ö.2009.65.166.77.	–27.0
	ö.2009.65.169.13.	–27.0
	R.2009.65.2.5	–27.9
	R.2009.65.2.3.	–28.5
	Szajk	ö.2006.73.53.38.
ö.2006.73.53.37.		–25.6
ö.2006.73.135.53.		–26.1
ö.2006.73.135.51.		–26.2
ö.2006.73.134.2.		–27.9
ö.2006.73.20.129.		–28.4
ö.2006.73.53.39.	–28.6	
Dunaszentgyörgy	GRDSZGY-14	–24.1
	GRDSZGY-3	–24.9
	GRDSZGY-20	–24.9
	GRDSZGY-19	–25.0
	GRDSZGY-6	–25.1
	GRDSZGY-2	–25.2
	GRDSZGY-12	–25.3
	GRDSZGY16	–25.4
	GRDSZGY-11	–25.8
	GRDSZGY-8	–25.9
GRDSZGY-4	–26.0	

that armouring of graphite by silicate minerals can hinder the isotope exchange between graphite and carbonate. Graphite grains in the texture of the studied ceramics are surrounded by silicate minerals, such as quartz, K-feldspar, mica, kyanite and sillimanite. Isotope exchange after the burial is not likely. Jüntgen and Karweil (1966) show that there is no isotope shift below temperatures of 100–150 °C, even if we disregard the above-mentioned "silicate armour effect" that blocks the isotope exchange.

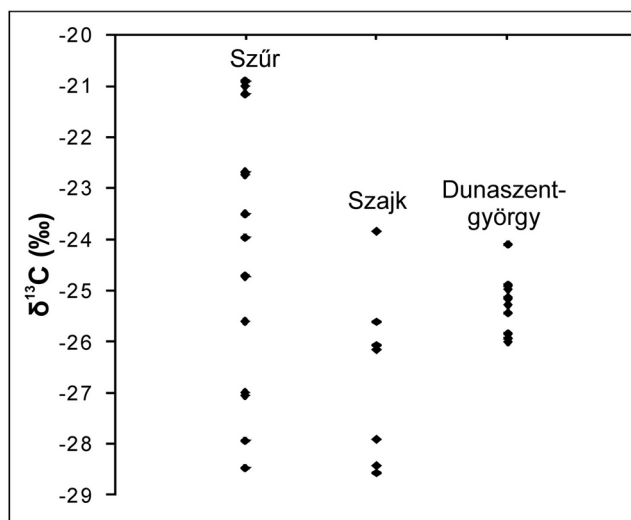


Fig. 1
The distribution of $\delta^{13}\text{C}$ values of graphite in each archaeological site

Isotope shifts during the pottery manufacturing process and after the burial can be excluded and we suggest that the measured carbon isotope composition of graphite is characteristic for the graphitic metamorphic gneiss.

The carbon isotope composition of graphite provides information about its genesis (e.g. Craig 1953; Galimov 1975). Based on the obtained values, the studied graphite temper is supposed to be syngenetic carbon material, i.e. formed through the metamorphic evolution of organic matter. The metamorphic origin of graphite is in good correspondence with the petrographic observations.

Conclusions

Carbon isotope analysis of graphite in Celtic ceramics revealed a wide range of $\delta^{13}\text{C}$ values. The observed variability suggests that the graphitic raw material used for tempering of pottery was not homogeneous in its carbon isotope composition. Kinetic fractionation effect and isotope exchange between graphite and carbonate in the pottery can be neglected. The measured $\delta^{13}\text{C}$ values are supposed to be characteristic for the metamorphic gneiss containing syngenetic (metamorphic) graphite.

The applicability of carbon isotope analysis for provenance determination of graphite temper in archaeological ceramics will be evaluated in the next stage of research.

References

- Bottinga, Y. 1969: Calculated fractionation factors for carbon and hydrogen isotope exchange in the system calcite-carbon dioxide-graphite-methane-hydrogen-water vapor. – *Geochimica et Cosmochimica Acta*, 33, pp. 49–64.
- Chacko, T., TK. Mayeda, R.N. Clayton, J.R. Goldsmith 1991: Oxygen and carbon isotope fractionation between CO₂ and calcite. – *Geochimica et Cosmochimica Acta*, 55, pp. 2867–2882.
- Craig, H. 1953: The geochemistry of the stable carbon isotopes. – *Geochimica et Cosmochimica Acta*, 3, pp. 53–92.
- Galimov, E.M. 1975: Carbon isotopes in oil and gas geology. NASA translation TTF-682, Washington.
- Havancsák, I., B. Bajnóczi, M. Tóth, A. Kreiter, Sz. Szöllösi 2009a: Kelta grafitos kerámia: elmélet és gyakorlat dunaszentgyörgyi kerámiák ásványtani, petrográfiai és geokémiai vizsgálatának tükrében (Celtic graphitic pottery: theory and practice in the light of mineralogical, petrographic and geochemical study of ceramics from Dunaszentgyörgy [S-Hungary]). – *Archeometriai Műhely*, VI/1, pp. 39–51. (In Hungarian.)
- Havancsák, I., B. Bajnóczi, Gy. Szakmány, A. Keiter, Sz. Szöllösi, Cs. Gáti 2009b: A petrográfiai vizsgálatok jelentősége a kelta kerámiák grafitos soványítóanyagának provenienciájának meghatározásában (Significance of petrographic investigations in the determination of provenance of graphitic temper in Celtic ceramics). – *Archeometriai Műhely*, VI/4, pp. 1–14. (In Hungarian.)
- Jüntgen, H., J. Karweil 1966: Gasbildung und Gasspeicherung in Steinkohlenflözen. I: Gasbildung. *Erdöl Kohle*, 19, pp. 251–258.
- Landis, C.A. 1971: Graphitization of dispersed carbonaceous material in metamorphic rocks. – *Contribution to Mineralogy and Petrology*, 30, pp. 34–35.
- Sofer, Z. 1980 Preparation of carbon dioxide for stable carbon isotope analysis of petroleum fractions. – *Analytical Chemistry*, 52, pp. 1389–1391.
- Szabó, M., JP. Guillaumet, B. Kriveczky 1999: Polgár-Király-érpart vaskori település a Kr .e. IV–III. évszázadban (Polgár-Király-érpart Iron Age settlement in the 4th-3rd cent. B.C.). – *A debreceni Déri Múzeum Évkönyve*, 1997/1998, pp. 177–181. (In Hungarian.)
- Wada, H., K. Suzuki 1983: Carbon isotope thermometry calibrated by dolomite-calcite solvus temperatures. – *Geochimica et Cosmochimica Acta*, 47, pp. 697–706.

Experimental study of D/H fractionation between water and hydrogen gas during the oxidation of Fe-bearing silicates at high temperatures (600 °C–1200 °C)

Laurent Simon, Christophe Lécuyer
François Martineau
Laboratoire de Géologie de Lyon, Lyon

François Robert
*Laboratoire de Minéralogie,
Muséum National d'Histoire Naturelle, Paris*

Hydrogen gas is produced during the oxidation of the FeO component of silicates by water. This redox reaction occurs during the high-temperature (400 °C–800 °C) hydrothermal alteration of oceanic crustal rocks, and is responsible for H₂ production at mid-ocean ridges. Samples of international reference biotite NBS30 ($\delta D = -65.7\text{‰}$) were reacted at high temperatures (600–1200 °C) in a high-vacuum line, releasing both structural water and hydrogen gas. An apparent fractionation factor α , derived from D/H measurements of water and hydrogen gas, is linearly dependent on T^{-2} following the equation $\alpha = 1.024 + 2477296 \cdot T^{-2}$ with a residual standard deviation $\sigma = 0.023$. The apparent D/H fractionation factors between water vapor and hydrogen gas during biotite oxidation show a dependency on T^{-2} that resembles those measured either by equilibration experiments or calculated from partition functions. Moreover, the apparent fractionation factors we measured are close to those determined at equilibrium in the same temperature range by Cerrai et al. (1954). This observation suggests that the D/H fractionation between H₂O and H₂ could be close to equilibrium during the reduction of water to hydrogen by the FeO component of silicates.

Key words: δD , oxido-reduction, high-temperature, isotopic fractionation, iron-bearing silicate, Archean ocean

Introduction

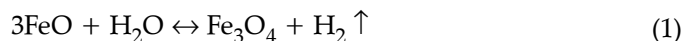
D/H ratios have been widely used to study the water evolution of terrestrial planet atmospheres. The D/H ratio of surficial water intimately depends on the evolution mode of the atmosphere and its interactions with inner envelopes of terrestrial planets. Water dissociation and hydrogen escape are responsible for high deuterium enrichment of Martian's and Venusian's atmospheres relative to

Address of corresponding author: C. Lécuyer: UMR CNRS 5276, Université Lyon 1 et Ecole Normale Supérieure de Lyon, 69622 Villeurbanne, France, e-mail: clecuyer@univ-lyon1.fr

Received: May 12, 2011; accepted: May 26, 2011

Earth's hydrosphere (Owen 1992; Donahue 1999). On Earth, the δD value of the oceans is mainly controlled by the isotopic exchange between mantle and seawater (Lécuyer et al. 1998) that occurs at mid-ocean ridges and the release of water to subduction zones. During the hydrothermal alteration of the oceanic crust, the D/H fractionation between hydrous silicates and seawater ($\alpha \sim 0.960$; Wenner and Taylor 1973; Suzuoki and Epstein 1976; Sakai and Tsutsumi 1978) leads to a deuterium enrichment of the hydrosphere while the outgassed mantle water $\delta D = -80\text{‰}$ to -30‰ ; Javoy 1980; Kyser and O'Neil 1984; Chaussidon et al. 1991; Deloule et al. 1991) contributes to decrease the D/H ratio of surficial waters.

During seawater-basalt interactions, the fayalite component of the basaltic rocks is oxidized to pyrite and magnetite by marine sulfates (Shanks et al. 1981). The oxidation of ferrous to ferric iron by sulfates results in a net flux of ferric iron to the mantle (Lécuyer and Ricard 1999). However, before the rise of O_2 in the Earth's atmosphere (2.4 to 2.2 Ga; Holland 1984; Rye and Holland 1998; Bau et al. 1999; Canfield et al. 2000; Farquhar et al. 2000), more reducing conditions prevailed in the oceans as witnessed by the occurrence of Banded Iron Formations (James and Trendall 1982; Kump and Holland 1992). Sulfur species in Precambrian seawater were both in reduced and oxidized states as suggested by the high variability of sulfur isotope ratios of both sulfides and sulfates in Precambrian rocks older than 2.4 Ga (Farquhar et al. 2000; Farquhar and Wing 2003; Ono et al. 2003). If marine sulfates were not the dominant oxidizing agent in seawater, the ferrous iron component of the oceanic crustal rocks could have been oxidized to Fe^{3+} by water during seawater-basalt interactions according to the reaction:



This reaction promotes the reduction of water to H_2 . On an O_2 -free planet, such as Mars and early Earth, the rate of hydrogen escape is proportional to the H_2 mixing ratio in the atmosphere (Hunten 1973). Thus, H_2 produced by reaction (1) may enhance hydrogen escape. Water reduction and hydrogen escape finally contribute to the evolution of the redox state of surficial planetary envelopes, potentially increasing the oxidation state of the atmosphere and surficial rocks.

Oxidation of silicates during seawater-basalt interactions is able to modify the D/H ratio of surficial water because of the high magnitude of D/H fractionation that occurs between water and H_2 , even at high temperatures (Suess 1949; Cerrai et al. 1954; Richet et al. 1977). For example, during on-axis mid-ocean ridge hydrothermal alteration (200 °C to 350 °C), the equilibrium fractionation factor $\alpha_{H_2O-H_2}$ between water and H_2 ranges from 1.567 to 1.962 (Richet et al. 1977). In order to quantify the effect of the oxidation of rocks by water on the hydrogen isotope composition of terrestrial atmospheres, experiments were performed to determine the isotopic fractionation between water and H_2 that accompanies silicate oxidation.

During heating and breakdown of biotite, water is released according to the following equation:



then a fraction of this water is partly reduced by Fe^{2+} into H_2 (Feldstein et al. 1996; Righter et al. 2002; Demény et al. 2006). These experimentally-determined apparent fractionation factors, most likely resulting from kinetic effects, are finally applied to mass balance calculations for estimating the D/H ratios of Earth's ocean and Mars' atmosphere through time.

Experimental methods

Experiments have been conducted in a high-vacuum extraction line. Selected material to promote the redox reaction is the biotite international reference standard NBS30 ($\delta\text{D} = -65.7\text{‰}$) which contains 4 wt.% of water. An amount of 30 mg to 60 mg of biotite was loaded into a quartz reactor and heated at 150 °C for 1 hour in vacuum to remove any atmospheric adsorbed water on the sample. Temperatures of reaction were selected between 600 °C and 1200 °C. At temperatures lower than 600 °C, we did not observe any production of hydrogen gas during sample heating. The vacuum extraction line made of Pyrex was maintained at a temperature of 80 °C over the complete manipulation to avoid water condensation on the inner sides of the experimental apparatus.

Biotite samples were instantaneously heated at the temperature of interest for 5 minutes when temperatures exceeded 900 °C, and up to 20 minutes when temperatures were lower than 700 °C. The amount of water released by the dehydration of biotite was qualitatively monitored using the pressure gauge. Water vapor was collected at liquid nitrogen temperature into a glass tube containing zinc metal. The residual gases, not condensable in liquid nitrogen, were mainly composed of H_2 produced by the oxidation of the FeO component of biotite by water. The hydrogen gas was quantitatively oxidized to water in a CuO furnace (500 °C), and the water was finally trapped in liquid nitrogen.

H_2 gas for isotopic measurement was obtained from both water samples following the off-line method of water reduction by hot zinc to produce hydrogen gas (Vennemann and O'Neil 1993). D/H isotopic analyses were then performed by using a dual-inlet MAT-Finnigan Delta E mass spectrometer. External reproducibility of D/H measurements was 3‰ relative to the SMOW-SLAP scale.

After expansion of H_2 into a constant volume of the mass spectrometer sample inlet, the amount of gas was estimated from the voltage of mass 2 collector (Vennemann and O'Neil 1993). We thus observed that during the experiments the H_2 production ranged between 3 and 8 μmol , at least one order of magnitude lower than the amount of water collected at the same time (20–70 μmol).

Statistical analyses were performed using JMP 7 software (SAS, Cary, NC, USA). Significance of all statistical tests was accepted at $\alpha < 0.05$.

Results

D/H ratio is expressed relative to SMOW and noted δD_{H_2O} for water and δD_{H_2} for hydrogen. The calibration of the procedure is achieved using SMOW and SLAP water aliquots (cf. Table 1). The isotopic fractionation factor $\alpha_{H_2O-H_2}$ is expressed as:

$$\alpha_{H_2O-H} = (1000 + \delta D_{H_2O}) / (1000 + \delta D_{H_2}) \quad (3)$$

The fractionation factors α between water and hydrogen gas have a linear dependence on $10^6 \cdot T^{-2}$ (Fig. 1), as follows:

$$\alpha = 1.024(\pm 0.022) + 0.247729(\pm 0.027705) \cdot 10^6 \cdot T^{-2}$$

with $r^2 = 0.83$, $P < 10^{-6}$ and the residual standard deviation of the linear regression $\sigma = 0.023$. This linearity of α vs. T^{-2} is accounted for by the property

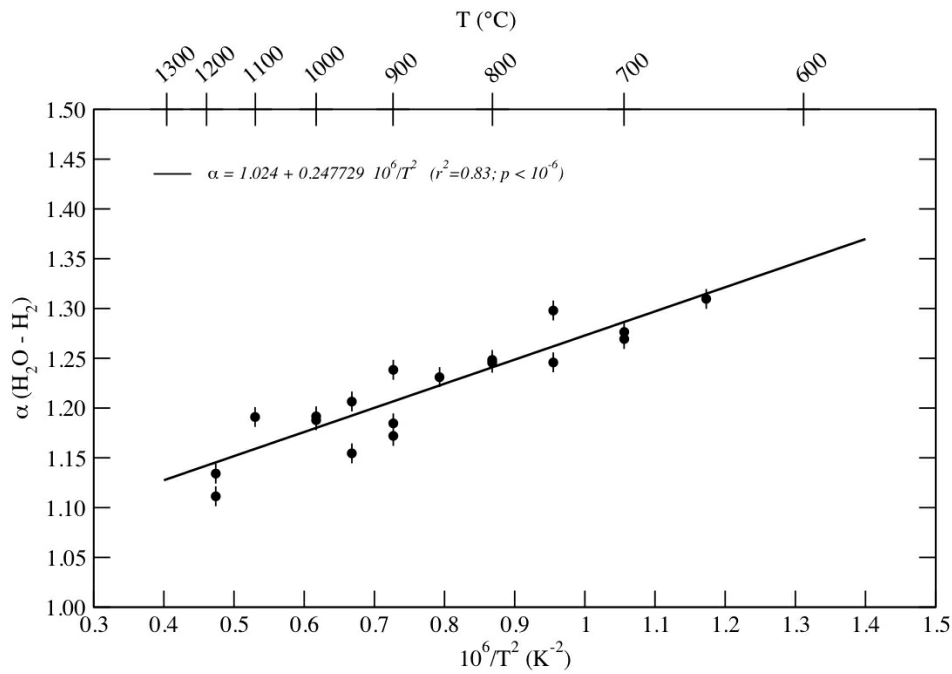


Fig. 1
Apparent fractionation factors $\alpha_{H_2O-H_2}$ reported as a function of $10^6 \cdot T^{-2}$

Table 1
D/H measurements of water and hydrogen gas released during the high-temperature oxidation of biotite NBS30. Apparent fractionation factors $\alpha_{\text{H}_2\text{O}-\text{H}_2}$ between H_2O and H_2 were determined in the temperature range 600–1200 °C. $\sigma = 3\text{‰}$ for the δD values

Experiment	T (K)		$\delta\text{D} (\text{H}_2\text{O})$	$\delta\text{D} (\text{H}_2)$	$\alpha_{\text{H}_2\text{O}-\text{H}_2}$
			(‰ SMOW)	(‰ SMOW)	
E – 23	923	±10	–49	–273	1.31
E – 05	973	±30	–42	–249	1.275
E – 08	973	±40	–51	–251	1.270
E – 16	1023	±10	–35	–256	1.297
E – 22	1023	±10	–47	–234	1.245
E – 01	1073	±10	–25	–218	1.247
E – 04	1073	±15	–42	–230	1.245
E – 17	1123	±25	–41	–220	1.230
E – 07	1173	±10	–50	–189	1.172
E – 15	1173	±10	–33	–184	1.185
E – 20	1173	±25	–27	–213	1.237
E – 21	1223	±20	–39	–167	1.154
E – 24	1223	±25	–35	–200	1.206
E – 19	1273	±40	–29	–182	1.187
E – 26	1273	±20	–25	–181	1.191
E – 18	1373	±30	–24	–179	1.190
E – 25	1453	±40	–36	–132	1.111
E – 27	1453	±45	–29	–143	1.133

of the partition functions of isotopically substituted H_2 and H_2O (Horibe and Craig 1995).

The slope of this apparent fractionation line is not significantly different from that obtained for the equilibrium fractionation factors between water and H_2 calculated by Richet et al. (1977) (Fig. 1; Analysis of Covariance, "Study" x "T" interaction effect, $P=0.358$). Nevertheless, these apparent fractionation factors are significantly higher than those deduced either from calculations (Bardo and Wolfsberg 1976; Richet et al. 1977, Analysis of Covariance, "Study" effect, $P<10^{-7}$)

or from equilibrium experiments between water vapor and hydrogen gas (Suess 1949). Our measured fractionation factors between water and hydrogen gas are, however, higher than those obtained by equilibrium experiments between H_2O and H_2 (Cerrai et al. 1954). Discrepancies between these experimental fractionation factors suggest that H_2 production during hydrothermal reactions are dominated by kinetic fractionation effects. Our results are also in agreement with those obtained by Kuroda et al. (1998) who have shown that at temperatures higher than 700°C , a small amount of water in minerals may react with ferrous iron to produce deuterium-depleted H_2 gas.

The results of our experiments can be compared to the isotopic compositions of high temperature hydrothermal gases. H_2 gas is produced by abiogenic processes in the high-temperature hydrothermal vents of the East Pacific Rise at 21°N (Welhan and Craig 1983). This H_2 gas has a mean δD value of about -395‰

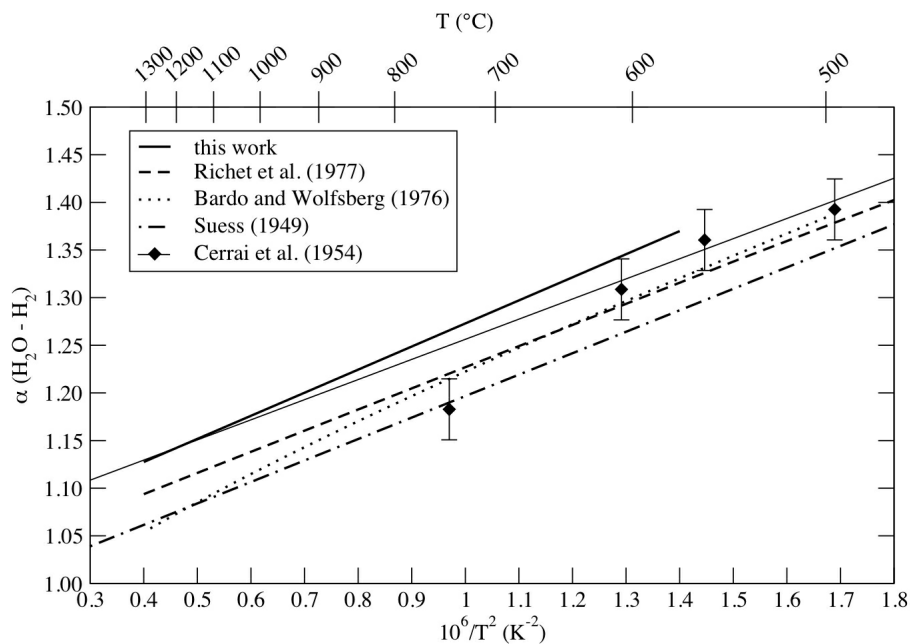


Fig. 2

Comparison of apparent fractionation factors $\alpha_{\text{H}_2\text{O}-\text{H}_2}$ between water and hydrogen gas released during our high-temperature oxidation experiments (plain line) with equilibrium fractionation factors determined from equilibrium experiments (dotted-dashed line: Suess 1949; thin line and diamonds: Cerrai et al. 1954) and theoretical considerations (dotted line: Bardo and Wolfsberg 1976; dashed line: Richet et al. 1977)

with a δD of the liquid water close to 0‰ (Welhan and Craig 1983; Horibe and Craig 1995). Using equation (3), the temperature calculated from the D/H ratio of H_2 is 350°C, matching well the measured regional base temperature of the vent field (Welhan and Craig 1983).

Implications on the D/H ratio of Early Earth and Mars volatile envelopes

D/H evolution of the Early Earth

D/H fractionation between water and hydrogen is expected to be associated with the hydrothermal reaction between basaltic rocks and water. A corresponding flux of water lost during silicate oxidation equals $1.3 \cdot 10^3 \text{ kg} \cdot \text{s}^{-1}$ (equivalent to $10^{10} \text{ atom H} \cdot \text{cm}^{-2} \cdot \text{s}^{-1}$) according to reaction (1) and also based on the net flux of Fe^{3+} subducted into the mantle ($12 \cdot 10^3 \text{ kg} \cdot \text{s}^{-1}$) proposed by Lécuyer and Ricard (1999). Integrating this flux over 4 Gy provides a maximum water mass of $1.6 \cdot 10^{20} \text{ kg}$, corresponding to about 10% of the present-day oceanic masses which would have escaped from Earth's atmosphere as hydrogen. Such a rate of water escape is two orders of magnitude higher than the present-day escape H_2 flux in the upper atmosphere which equals about $2 \cdot 10^8 \text{ atom H} \cdot \text{cm}^{-2} \cdot \text{s}^{-1}$, corresponding to a water flux of $8 \cdot 10^8 \text{ kg} \cdot \text{a}^{-1}$ (Hunten and McElroy 1974). Two reasons could be invoked to explain this difference: (i) the present-day Earth's atmosphere contains oxygen gas which rapidly oxidizes H_2 to water during atmospheric reactions and (ii) most of the Fe^{3+} in the subducted oceanic crust results from the oxidation of basaltic rocks by marine sulfates. As far as (i) is concerned, the absence of oxygen gas in the Precambrian atmosphere (before 2 Ga) prevents any atmospheric oxidation of H_2 , hence enhancing the escape flux of H_2 . The flux of ferric iron (ii) that entered the mantle remains still impossible to quantify because of the lack of available $Fe^{3+}/\Sigma Fe$ data for Precambrian hydrothermally-altered oceanic rocks. Nevertheless, the net flux of Fe^{3+} subducted to the mantle, calculated by Lécuyer and Ricard (1999), could be used for the Precambrian if we consider two counterbalancing processes that are (i) a lower sulphate concentration less than 200 μM (Habicht et al. 2002) in seawater and (ii) a higher rate of oceanic crust production from 6 to 10 times the present-day value of $3 \text{ km}^2 \cdot \text{y}^{-1}$ (Kröner 1985; Hargraves 1986; Catling et al. 2001). The resulting net flux of hydrogen escape from the atmosphere of $10^{10} \text{ atom H} \cdot \text{cm}^{-2} \cdot \text{s}^{-1}$ is bracketed by the two boundary values ($1.9 \cdot 10^9$ – $1.9 \cdot 10^{10} \text{ atom H} \cdot \text{cm}^{-2} \cdot \text{s}^{-1}$) of hydrogen fluxes released by the volcanic activity into the early atmosphere (Holland 1984). According to the relationship that links the escape flux to the total mixing ratio of hydrogen in an oxygen-free atmosphere (Walker 1977; Holland 1984), a total hydrogen mixing ratio of $4 \cdot 10^{-4}$ is calculated and is compatible with a negligible content of O_2 in the lower atmosphere (Kasting and Walker 1981; Holland 1984).

The change of the D/H ratio of the hydrosphere caused by the oxidation of the mantle rocks can be modeled by a Rayleigh-type distillation in which H_2 is

instantaneously removed after its production from water reduction. The isotopic evolution of the residual water is:

$$d \ln(D/H)_{H_2O} = (\alpha_{H_2O-H_2} - 1) d \ln f \quad (4)$$

where f is the fraction of water remaining, $(D/H)_{H_2O}$ is the D/H isotope ratio of water, and $\alpha_{H_2O-H_2}$ the fractionation factor between hydrogen gas and water. Considering again the calculated hydrogen flux of 10^{10} atom $H.cm^{-2}.s^{-1}$ escaping from Earth's atmosphere as a consequence of hydrothermal reactions, calculated δD values of the remaining ocean mass vary between +17‰ (assuming a mean temperature of hydrothermal reaction of 400 °C and $f = 0.95$, i.e. 5% of the hydrosphere was lost) and +55‰ (for $T=200$ °C and $f=0.9$). In combination to the hydrogen isotope fractionation that takes place between water and OH-bearing minerals during the alteration of the oceanic crust ($-15‰ < \delta D$ seawater $< 10‰$; Lécuyer et al. 1998), the primordial ocean was deuterium-depleted relative to SMOW, possibly down to $-70‰$.

D/H evolution of the Martian atmosphere

The D/H ratio of Martian atmospheric water vapor is $8.1 \pm 0.3 \cdot 10^{-4}$ (Owen et al. 1988), a value 5.4 times greater than the D/H terrestrial ratio. Without any strong supporting evidence, the pristine D/H ratio of Mars water could be assumed to be close to the terrestrial ratio (e.g. Donahue 1995; Krasnopolsky 2000; Boctor et al. 2003). D/H ratios of apatite grains from Martian meteorites (Leshin 2000) suggest that the initial D/H value could have been about 1.9 times the terrestrial value. The dynamical simulations of Mars accretion performed by Lunine et al. (2003) suggest a primitive D/H ~ 1.2 to 1.6 times the Earth's D/H ratio. Analyses of Martian meteorite NWA817 reveal that a primitive component of Martian surface water with a low δD value of $-170‰$ could have been recorded by alteration products (Gillet et al. 2002). Present-day estimates of the amount of surficial water mainly trapped in ice caps would represent a 30 m-thick layer of water covering totally the Martian surface. The physical properties of the Martian regolith suggest that it could contain an amount of water equivalent to a homogeneous layer comprised between 50 and 450 m (Carr 1986; Clifford 1993; Jankovski and Squyres 1993; Mangold et al. 2002; Boyce et al. 2005). Taking into account the presence of a large amount of ice stored near the Martian surface combined to a volcanic activity documented during nearly all Mars' history (Hartmann et al. 1999; McEwen et al. 1999), hydrothermal systems should have been active on Mars (Soderblom and Wenner 1978; Mouginiis-Mark 1985; Squyres et al. 1987). They could be responsible for a storage of about 30 m of water in hydrous minerals (Griffith and Shock 1997).

The Deuterium-enrichment of SNC meteorites may be related to high-temperature isotope exchange with Martian atmospheric water that was strongly

isotopically fractionated during the mechanism of hydrogen escape (Bjoraker et al. 1989). Demény et al. (2006) have shown, however, that dehydrogenation and dehydration of hydrous silicates such as amphiboles can account for the δD values that were measured in Martian meteorites.

If hydrothermal systems have existed on Mars, crustal oxidation by water could have changed the D/H of residual water circulating in the crust. Because the atmosphere of Mars is oxygen-free, H_2 produced from water reduction can escape to space. The maximum ability of Martian crust to oxidize, hence to change its water D/H ratio, can be tested by using the Rayleigh distillation equation (eq. 4). The D/H ratio of residual water is calculated as a function of the fraction of remaining water for mean temperatures of hydrothermal reactions ranging from 100 to 400 °C (Fig. 3). A 5.4-fold increase of D/H ratio is achieved by a loss of water of about 93% (100°C) to more than 99% (400 °C). If the present-day Martian D/H ratio is the result of a 4-fold enrichment, a 89–98.5% range of water loss is then required (Fig. 3). Considering the mechanism of hydrogen escape, comparable fractions of water losses (80–90%) have been proposed to explain the present-day D/H ratio of the Martian's atmosphere (Carr 1996). Consequently, the

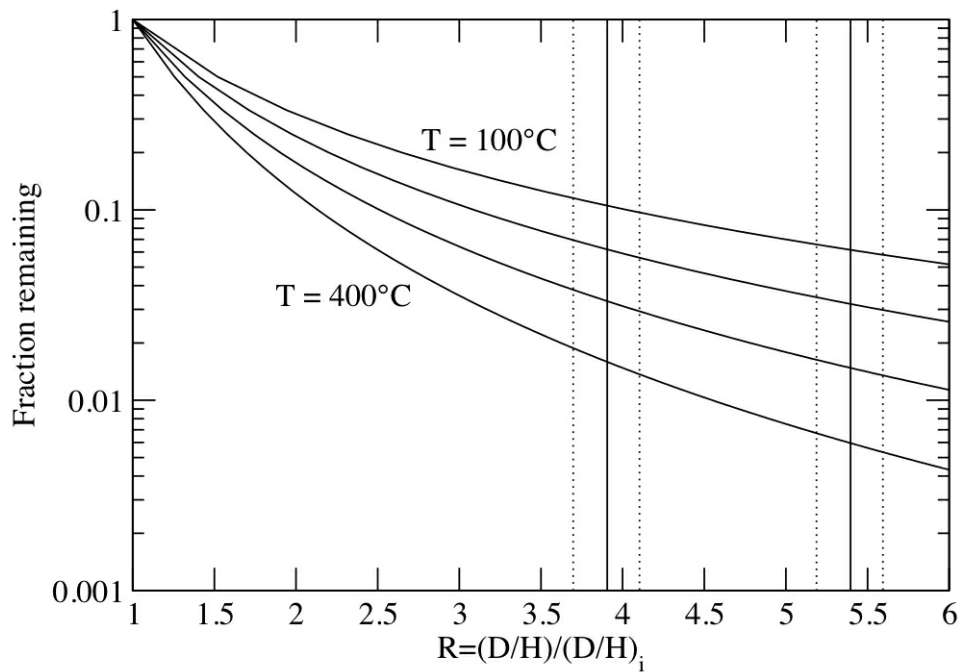


Fig. 3 Influence of water loss by silicate oxidation in hydrothermal conditions on the D/H ratio of Martian atmosphere. The fraction of original water remaining is reported as a function of the D/H enrichment for temperatures ranging from 100 °C to 400 °C (curves each 100 °C). Vertical lines represent enrichments of 3.9 ± 0.2 and 5.4 ± 0.2 , corresponding to a primitive D/H ratio of 210×10^{-6} (~ 1.4 SMOW) and 150×10^{-6} (\sim SMOW), respectively

reduction of water to hydrogen by iron-bearing silicates during hydrothermal activity could have significantly contributed to the D/H increase of the Martian's atmosphere, especially if the mean temperature of crust alteration was low enough. Estimates of primordial amounts of water that are based on the present-day D/H ratio of atmospheric water vapor could have been overestimated if Mars has undergone an extensive hydrothermal activity.

Concluding remarks

At high temperatures, oxidation of the FeO component of biotite by water results in a production of H₂. The hydrogen isotope apparent fractionation factor α between H₂O and H₂ was measured in the temperature range 600–1200 °C. The linear dependency of α vs. T⁻² resembles both experimental and theoretical fractionation lines that were determined for equilibrium hydrogen isotope exchange between water and hydrogen gas. This result suggests that H₂O and H₂ could be in isotopic equilibrium during the dehydration reaction. If we admit the net flux of Fe³⁺ toward the mantle as a plausible estimate during the Archean (Lécuyer and Ricard 1999), a flux of hydrogen escape of 10¹⁰ atom H.cm⁻².s⁻¹ in an oxygen-free atmosphere may produce a δ D increase of Earth's oceans up to 50‰. In a similar way, if Mars has undergone an extensive hydrothermal activity, water loss by oxidation of iron-bearing silicates could also have contributed to the present-day high D/H ratio of Martian's atmosphere.

Acknowledgment

This work was supported by grants from the "Programme National de Planétologie" INSU-CNRS program.

References

- Bardo, R.D., M. Wolfsberg 1976: A theoretical calculation of the equilibrium constant for the isotopic exchange reaction between H₂O and HD. – *The Journal of Physical Chemistry*, 80, pp. 1068–1071.
- Bau, M., R.L. Romer, V. Lödgers, N.J. Beukes 1999: Pb, O, and C isotopes in silicified Mooidraai dolomite (Transvaal Supergroup, South Africa): implications for the composition of Paleoproterozoic seawater and 'dating' the increase of oxygen in the Precambrian atmosphere. – *Earth and Planetary Science Letters*, 174, pp. 43–57.
- Bjoraker, G.L., M.J. Mumma, H.P. Larson 1989: Isotopic abundance ratios for hydrogen and oxygen in the martian atmosphere. – *Bulletin of the American Astronomical Society*, 21, pp. 991.
- Boctor, N.Z., C.M.O'D. Alexander, J. Wang, E. Hauri 2003: The Sources of water in Martian meteorites: clues from hydrogen isotopes. – *Geochimica et Cosmochimica Acta*, 67, pp. 3971–3989.
- Boyce, J.M., P. Mouginis-Mark, H. Garbeil 2005: Ancient oceans in the northern lowlands of Mars: evidence from impact crater depth/diameter relationships. – *Journal of Geophysical Research Planets*, 110, E03008.

- Canfield, D.E., K.S. Habicht, B. Thamdrup 2000: The Archean sulfur cycle and the early history of atmospheric oxygen. – *Science*, 288, pp. 658–661.
- Carr, M.H. 1986: Mars: a water-rich planet. – *Icarus*, 68, pp. 187–216.
- Carr, M.H. 1996: *Water on Mars*. – Oxford University Press, Oxford.
- Catling, D.C., K.J. Zahnle, C.P. McKay 2001: Biogenic methane, hydrogen escape, and the irreversible oxidation of early Earth. – *Science*, 293, pp. 839–843.
- Cerrai, E., R. Marchetti, R. Renzoni, L. Roseo, M. Silvestri, S. Villani 1954: A thermal method for concentrating heavy water. – *Chemical Engineering Progress Symposium Series*, 50, pp. 271–280.
- Chaussidon, M., S.M.F. Sheppard, A. Michard 1991: Hydrogen, sulphur and neodymium isotope variations in the mantle beneath the EPR at 12°50'N. – In: Taylor, H.P., Jr., J.R. O'Neil, I.R. Kaplan (Eds): *Stable isotope geochemistry: A tribute to Samuel Epstein*. Geochemical Society Special Publications, 3, pp. 325–337.
- Clifford, S.M. 1993: A model for the hydrologic and climatic behavior of water on Mars. – *Journal of Geophysical Research*, 98, pp. 10973–11016.
- Deloule, E., F. Albarede, E. S.M.F. Sheppard 1991: Hydrogen isotope heterogeneities in the mantle from ion probe analysis of amphiboles from ultramafic rocks. – *Earth and Planetary Science Letters*, 105, pp. 543–553.
- Demény, A., T.W. Vennemann, S. Harangi, Z. Homonnay, I. Fórizs 2006 : H₂O- D-FeIII relations of dehydrogenation and dehydration processes in magmatic amphiboles. – *Rapid Communications in Mass Spectrometry*, 20, pp. 919–925.
- Donahue, T.M. 1995: Evolution of water reservoirs on Mars from D/H ratios in the atmosphere and crust. – *Nature*, 374, pp. 432–434.
- Donahue, T.M. 1999: New analysis of hydrogen and deuterium escape from Venus. – *Icarus*, 141, pp. 226–235.
- Farquhar, J., H. Bao, M. Thiemens 2000: Atmospheric influence of Earth's earliest sulfur cycle. – *Science*, 289, pp. 756–758.
- Farquhar, J., B.A. Wing 2003: Multiple sulfur isotopes and the evolution of the atmosphere. – *Earth and Planetary Science Letters*, 213, pp. 1–13.
- Feldstein, S., R.A. Lange, T. Vennemann, J.R. O'Neil 1996: Ferric-ferrous ratios, H₂O contents and D/H ratios of phlogopite and biotite from lavas of different tectonic regimes. – *Contributions to Mineralogy and Petrology*, 126, pp. 51–66.
- Gillet, Ph., J.A. Barrat, E. Deloule, M. Wadhwa, A. Jambon, V. Sautter, B. Devouard, D. Neuville, K. Benzerara, M. Lesourd 2002: Aqueous alteration in the Northwest Africa 817 (NWA 817) Martian meteorite. – *Earth and Planetary Science Letters*, 203, pp. 431–444.
- Griffith, L.L., E.L. Shock 1997: Hydrothermal hydration of Martian crust: illustration via geochemical model calculations. – *Journal of Geophysical Research*, 102, 9135–9143.
- Habicht, K.S., M. Gade, B. Thamdrup, P. Berg, D.E. Canfield 2002: Calibration of sulfate levels in the Archean ocean. – *Science* 298, pp. 2372–2374.
- Hargraves, R.B. 1986: Faster spreading or greater ridge length in the Archean? – *Geology* 14, pp. 750–752.
- Hartmann, W.K., M. Malin, A. McEwen, M. Carr, L. Soderblom, P. Thomas, E. Danielson, P. James, J. Veverka 1999: Evidence for recent volcanism on Mars from crater counts. – *Nature*, 397, pp. 586–589.
- Holland, H.D. 1984: *The chemical evolution of the atmosphere and oceans*. Princeton University Press, New York.
- Horibe, Y., H. Craig 1995: D/H fractionation in the system methane-hydrogen-water. – *Geochimica et Cosmochimica Acta*, 59, pp. 5209–5217.
- Hunten, D.M. 1973: The escape of light gases from planetary atmospheres. – *Journal of the Atmospheric Sciences*, 30, pp. 1481–1494.
- Hunten, D.M., M.B. McElroy 1974: Production and escape of terrestrial hydrogen. – *Journal of the Atmospheric Sciences*, 31, pp. 305–317.

- James, H.L., A.F. Trendall 1982: Banded iron formation: Distribution in time and paleoenvironmental significance. – In: Holland H.D., M. Schidlowski (Eds): Mineral deposits and the evolution of the biosphere. Springer-Verlag, Berlin, pp. 199–217.
- Jankowski D.G., S.W. Squyres 1993: Softened impact craters on Mars: Implications for ground ice and the structure of the martian megaregolith. – *Icarus*, 106, pp. 365–379.
- Javoy, M. 1980: $^{18}\text{O}/^{16}\text{O}$ and D/H ratios in high temperatures peridotites. – Centre National de la Recherche Scientifique Colloque International, 272, pp. 279–287.
- Kasting, J.F., J.C.G. Walker 1981: Limits on oxygen concentration in the prebiological atmosphere and the rate of abiotic fixation of nitrogen. – *Journal of Geophysical Research*, 86, pp. 1147–1158.
- Krasnopolsky, V. 2000: On the deuterium abundance on Mars and some related problems. – *Icarus*, 148, pp. 597–602.
- Kröner, A. 1985: Evolution of the Archean continental crust. – *Annual Review of Earth and Planetary Sciences*, 13, pp. 49–74.
- Kump, L.R., H.D. Holland 1992: Iron in Precambrian rocks: Implications for the global oxygen budget of the ancient Earth. – *Geochimica et Cosmochimica Acta*, 56, pp. 3217–3223.
- Kuroda, Y., S. Matsuo, T. Yamada 1988: D/H fractionation during dehydration of hornblende, mica and volcanic glass. – *Journal of Mineralogy, Petrology and Economical Geology*, 83, pp. 85–94.
- Kyser, T.K., J.R. O'Neil 1984: Hydrogen isotope systematics of submarine basalts. – *Geochimica et Cosmochimica Acta*, 48, pp. 2123–2133.
- Lécuyer, C., P. Gillet, F. Robert 1998: The hydrogen isotope composition of seawater and the global water cycle. – *Chemical Geology*, 145, pp. 249–261.
- Lécuyer, C., Y. Ricard 1999: Long-term fluxes and budget of ferric iron; implication for the redox states of the Earth's mantle and atmosphere. – *Earth and Planetary Science Letters*, 165, pp. 197–211.
- Leshin, L.A. 2000: Insights into martian water reservoirs from analyses of martian meteorite QUE94201. – *Geophysical Research Letters*, 27, pp. 2017–2020.
- Lunine J.I., J. Chambers, A. Morbidelli, L.A. Leshin 2003: The origin of water on Mars. – *Icarus*, 165, pp. 1–8.
- Mangold, N., P. Allemand, P. Duval, Y. Géraud, P. Thomas 2002: Experimental and theoretical deformation of ice-rock mixtures: implications on rheology and ice content of Martian permafrost. – *Planetary and Space Science*, 50, pp. 385–401.
- McEwen, A.S., M.C. Malin, M.H. Carr, W.K. Hartmann 1999: Voluminous volcanism on early Mars revealed in Valles Marineris. – *Nature*, 397, pp. 584–586.
- Mouginis-Mark, P.J. 1985: Volcano/ground ice interactions in Elysium Planitia, Mars. – *Icarus*, 64, pp. 265–284.
- Ono, S., J.L. Eigenbrode, A.A. Pavlov, P. Kharecha, D. Rumble III, J.F. Kasting, K.H. Freeman 2003: New insights into Archean sulfur cycle from mass-independent sulfur isotope records from the Hamersley Basin, Australia. – *Earth and Planetary Science Letters*, 213, pp. 15–30.
- Owen, T., J.P. Maillard, C. deBergh, B.L. Lutz 1998: Deuterium on Mars: the abundance of HDO and the value of DH. – *Science*, 240, pp. 1767–1770.
- Owen, T. 1992: Composition and early history of the atmosphere. – In: Kieffer, H.H., B.M. Jakosky, C.W. Snyder, M.S. Matthews (Eds): Mars. Arizona University Press, Tucson, pp. 818–834.
- Richet, P., Y. Bottinga, M. Javoy 1977: A review of hydrogen, carbon, nitrogen, oxygen, sulphur, and chlorine stable isotope fractionation among gaseous molecules. – *Annual Review of Earth and Planetary Sciences*, 5, pp. 65–110.
- Righter K., M.D. Dyar, J.S. Delaney, T.W. Vennemann, R.L. Hervig, P.L. King 2002: Correlations of octahedral cations with OH-, O2-, Cl- and F- in biotite from volcanic rocks and xenoliths. – *American Mineralogist*, 87, pp. 142–154
- Rye, R., H.D. Holland 1998: Paleosols and the evolution of atmospheric oxygen: a critical review. – *American Journal of Science*, 298, pp. 621–672.

- Sakai, H., M. Tsutsumi 1978: D/H fractionation factors between serpentine and water at 100°C to 500°C and 2000 bar water pressure, and the D/H ratios of natural serpentines. – *Earth and Planetary Science Letters*, 40, pp. 231–242.
- Shanks, W.C., J.L. Bischoff, R.J. Rosenbauer 1981: Seawater sulfate reduction and sulfur isotope fractionation in basaltic systems: interaction of seawater with fayalite and magnetite at 200–350°C. – *Geochimica et Cosmochimica Acta*, 45, pp. 1977–1995.
- Soderblom, L.A., D.A. Wenner 1978: Possible fossil H₂O liquid water interfaces in the Martian crust. – *Icarus*, 34, pp. 622–637.
- Squyres, S.W., D.E. Wilhelms, A.C. Moosman 1987: Large-scale volcano-ground ice interactions on Mars. – *Icarus*, 70, pp. 385–408.
- Suess, H.E. 1949: Das Gleichgewicht $H_2 + HDO = HD + H_2O$ und die weiteren Austauschgleichgewichte im System H_2 , D₂ und H₂O. – *Zeitschrift für Naturforschung A*, 4, pp. 328–332.
- Suzuoki, T., S. Epstein 1976: Hydrogen isotope fractionation between OH-bearing minerals and water. – *Geochimica et Cosmochimica Acta*, 40, pp. 1229–1240.
- Vennemann, T.W., J.R. O'Neil 1993: A simple and inexpensive method of hydrogen isotope and water analyses of minerals and rocks based on zinc reagent. – *Chemical Geology*, 103, pp. 227–234.
- Walker, J.C.G. 1977: *Evolution of the Atmosphere*. MacMillan, New York, 318 pp.
- Wenner D.B., H.P. Jr., Taylor 1973: Oxygen and hydrogen isotope studies of the serpentinization of ultramafic rocks in oceanic environments and continental ophiolite complexes. – *American Journal of Science*, 273, pp. 207–239.
- Welhan, J.A., H. Craig 1983: Methane, hydrogen and helium in hydrothermal fluids at 21°N on the East Pacific Rise. – In: Rona, P.A. (Ed): *Hydrothermal Processes at Seafloor Spreading Centers*, Plenum Publishers, pp. 391–409.

$\delta^2\text{H}$ and $\delta^{13}\text{C}$ of methane in lignite fermentation

Michał Bucha, Łukasz Pleśniak
*Department of Applied Geology and Geochemistry,
Institute of Geological Sciences,
University of Wrocław, Wrocław*

Katarzyna Kubiak, Mieczysław Błaszczak
*Department of Microbial Biology, Faculty of
Agriculture and Biology, The Warsaw University of
Life Sciences, Warsaw*

Mariusz-Orion Jędrysek
*Department of Applied Geology and Geochemistry,
Institute of Geological Sciences,
University of Wrocław, Wrocław*

The aim of these analyses was to determine isotopic composition of carbon and hydrogen from methane to indicate fermentation pathways of lignite. The lignite samples were collected from the "Kazimierz Północ" Konin Mine deposit. Those with a grain size of <1 mm were placed in 500 ml glass bottles with M9 medium (microbial nutrient) with various mineral additives and bacterial inoculum. The duration of the fermentation experiment was 3 months at 20 °C, with every 2 weeks sampling. Nine experimental variants involving different mineral additives and two control variants without inoculum were carried out. Results of two of them, i.e. inoculated IVA and IXB, are reported here (6 and 8 samples, respectively). The gas samples were analyzed by means of gas chromatography and isotope ratio mass spectrometry.

As a result of lignite fermentation in IVA and IXB variant of experiments, the total volume of gas were 839 ml and 1929 ml, respectively. In both variants methane appeared in the third day of the experiment and was present during each gas collection till the end of observations reported. The $\delta^{13}\text{C}_{\text{CH}_4}$ ranged from -66.34‰ to -25.77‰ in the IVA and from -71.40 to -34.12‰ in the IXB. The $\delta^2\text{H}_{\text{CH}_4}$ ranged from -361.9 to -249.4‰ and from -370.0 to -293.3‰ , respectively. No correlation between $\delta^{13}\text{C}$ and $\delta^2\text{H}$ in the methane has been observed. Likewise both isotopic values show chaotic variation during the experiment. Gas production varied with time, but the higher value was accompanied by higher $\delta^2\text{H}_{\text{CH}_4}$ value ($R^2=0.46$ in the IVA) and lower $\delta^{13}\text{C}_{\text{CH}_4}$ value ($R^2=0.37$ in the IVA and $R^2=0.33$ in the IXB). This may evidence that variation in amount of methane production during lignite fermentation varied with time and probably depended on methanogenic pathways. The thesis on suspected gradual increase of the role of CO_2 reduction and simultaneous decrease of acetic fermentation pathways, will be discussed during presentation. Alternatively, some carbon compounds contained in nutrients might influence the $\delta^{13}\text{C}_{\text{CH}_4}$ value.

Address of corresponding author: M. Bucha: Max Born pl. 9, 50-205 Wrocław, Poland
e-mail: michal.bucha@ing.uni.wroc.pl

Calculation of chlorine and bromine isotope fractionation factors in aqua-gas system

Maciej Czarnacki, Stanislaw Halas, Andrzej Pelc
*Mass Spectrometry Laboratory, Institute of Physics,
Marie Curie-Skłodowska University, Lublin*

We report calculated values of isotope fractionation factors between chlorine and bromine hydrated anions and gaseous compounds HCl, Cl₂, HBr and Br₂, respectively. For calculation of reduced partition function ratios of hydrated Cl⁻ and Br⁻ anions we used simple model of [Cl/Br(H₂O)_n]- cluster (n = 14) based on electrostatic interaction between ion and water molecules treated as electric dipoles. Reduced partition function ratios for hydrogen chloride, hydrogen bromide and molecular chlorine and bromine were already calculated from vibrational frequencies, reported by earlier studies.

At temperatures 50–80 °C the equilibrium isotope fractionation between hydrated chlorine anion and hydrogen chloride attains 1.55–1.68‰ (this work) which is in good agreement with existing experimental data (1.4–1.8‰). The predicted isotope fractionations between HBr and Br₂ gases and hydrated bromine ion are very small, 1000lnα do not exceed 0.8‰, thus the expected natural variations of bromine isotope composition in aqua-gas system will require enhanced precision for their detection.

This research was supported by the Polish Ministry of Science and Higher Education (Grant No. N N307 062136).

Address of corresponding author: M. Czarnacki: 20-031 Lublin, Poland
e-mail: maciej.czarnacki@gmail.com

Dissolving halite for H, C and S isotopic analysis of fluid inclusions

Wojciech Drzewicki
*Laboratory of Isotope Geology and Geoecology,
The University of Wrocław, Wrocław*

Stanisław Burliga
*Department of Structural Geology and Tectonic
The University of Wrocław, Wrocław*

Janusz Krajniak, Łukasz Pleśniak, Mariusz-Orion Jędrysek
*Laboratory of Isotope Geology and Geoecology
The University of Wrocław, Wrocław*

Among large knowledge on salt formation research, little is known on the origin and especially migration of methane and hydrogen sulphide within salt structures. Therefore, we report hereby on stable isotopic composition of these gases contained in fluid inclusions in the salt, what presumably could allow us to conclude on migration (directions), and identify factors controlling variations in concentration of methane and hydrogen sulphide. To obtain isotopic results, first it was necessary to quantitatively release gases enclosed in inclusions in salt – the proposed method allowed us to obtain the material to determine both chemical and isotopic data. Namely we have carried out decrepitation of fluid inclusions due to dissolving of salt samples in aqueous solution using home-made vacuum line. Standard CH_4 oxidation and H_2S precipitation (cadmium sulphide) and oxidation, have been used for further C and S isotopic ratios analyses (CO_2 and SO_2).

All salt samples used for isotopic analyses of methane and hydrogen sulphide from inclusions, came from salt mine Klodawa (central Poland). Preliminary results showed that inclusions contain (neglecting CO_2): CH_4 (from 0.84 to 2.13%), N_2 (from 66.58 to 71.22%), O_2 (from 23.71 to 30.73%) and Ar (from 1.87 to 2.41%), He (from 0.02 to 0.13%) and H_2S (amount H_2S of the inclusions of salt from 0.7 to 11.1 mol.). The $\delta^{13}\text{C}_{\text{CH}_4}$ value varied from -47.1‰ to -29.7‰ , $\delta\text{D}_{\text{CH}_4}$ value varied from -128.6‰ to -147.6‰ and the $\delta^{34}\text{S}_{\text{H}_2\text{S}}$ value varied from -6.28‰ to 3.20‰ . We will discuss on potential factors controlling isotopic ratios during our presentation.

Address of corresponding author: W. Drzewicki: Cybulskiego 30, 50-205 Wrocław, Poland
e-mail: wojciech.drzewicki@ing.uni.wroc.pl

Origin of Precambrian carbonate rocks of the Ukrainian Shield by geological-structural peculiarities and isotopic signatures

Vasyl' Guliy

Ukrainian State Geological Research Institute, Kyiv

Vasyl' Zagnitko, Ruslana Bochevar

Kyiv Taras Shevchenko National University, Kyiv

Carbonate rocks are widespread within the Precambrian metamorphic complexes of the Ukrainian Shield. The rocks comprise of a number of genetic types, including primary sedimentary and geologically later varieties (calc-silicate rocks, carbonatites, carbonate veins, etc.), whose geneses are connected to igneous and metasomatic processes. The discovery of kimberlites and lamproites related rocks carbonate rocks at the Azov Block of the Shield has demonstrated that the carbonate rocks of the Shield are even more diverse and stimulated vivid discussions on their origin.

To divide these families of the carbonate rocks we used system of geological-structural indicators and isotopic (C, O, Sr) signatures of carbonates and some coexisting minerals.

Taking into consideration the obtained data, we determined origin of different kinds of carbonates from objects with more complicated geological history. For example, we examined rocks of the Kapitanivsky ore field (Golovanivska zone of the Shield), where 15 large serpentine (primary dunites and pyroxenites) massives with different metamorphic and metasomatic rocks are present. We identified at least three groups of carbonate rocks here. 1. Primary sedimentary with $\delta^{13}\text{C} = 1 \pm 2\text{‰}$, $\delta^{18}\text{O} = 20 \pm 2\text{‰}$. 2. Metasomatic carbonates with $\delta^{13}\text{C} = -3.2 \pm 2\text{‰}$, $\delta^{18}\text{O} = 16 \pm 2\text{‰}$. 3. Late carbonate veins as a result of intensive alterations of low $\delta^{13}\text{C}$ values (less then -8.0‰). Similar values of the $\delta^{13}\text{C}$ we obtained for late carbonates related to the kimberlites.

Address of corresponding author: V. Guliy: 78 Avtozavods'ka str., Kyiv 04114, Ukraine
e-mail: vgul@ukr.net

Anomalous $\delta^{18}\text{O}$ isotope composition of minerals from North Karelia (Russia)

Aleksandr V. Ignatiev,
Sergey V. Vysotskiy
Far East Geological Institute, Vladivostok

Viktor I. Levitskiy
A.P. Vinogradov Institute of Geochemistry, Irkutsk

Sergey Yu. Budnitskiy, Tatiana A. Velivetskaya
Far East Geological Institute, Vladivostok

The Earth's rocks and minerals commonly have positive $\delta^{18}\text{O}$ values, being enriched in isotope ^{18}O relative to the sea water. Most of silicate rocks are characterized by $\delta^{18}\text{O}_{\text{smow}}$ from +0 to +15‰. The recent findings in Karelian rocks, i.e. anomalously poor in heavy oxygen isotope, suggest very specific conditions of their formation and cause interest to further researches. The corundum-bearing rocks of the northern Karelia composed of few major mineral varieties are characterized by a high diversity of textures and structures, among which zoning is widely presented. Garnet, amphibole and plagioclase of different generations mix with each other in different proportions and form both early corroded relics and late mineral phases, indicating development of paragenetic sequences in a wide range of temperature and pressure.

Oxygen isotope ratios in garnet, corundum, amphibole and plagioclase were analysed. Most of them are anomalously low (from -15.5 to -26‰) that were not known until recently. We believe that minerals may retain the extremely low $\delta^{18}\text{O}$ values, which resulted from interaction of glacial water with their protolith, after metamorphic transformations. The Svecofennian high-alumina corundum-bearing plagioclase was probably formed after the hydrothermally altered Paleoproterozoic rocks formed in the shallow zone of fumarole field under a glacier. Both sufficiently large volume of water with light oxygen isotope composition and long duration of the water-rock interaction were necessary to provide such a deep alteration. The metasomatic processes took place probably in the oldest Huronian glaciation period, which maximum occurred 2.3 billion years ago. Later, these rocks suffered the high-pressure Svecofennian (1.9–1.8 billion years) metamorphism.

We are grateful to the Russian Foundation for Basic Research (No. 10-05-00371-a) for funding our investigation.

Address of corresponding author: A. V. Ignatiev: FEGI, FEB RAS, pr. Stoletiya Vladivostoka 159, Vladivostok, 690022 Russia, e-mail: ignatiev@fegi.ru

INERT GAS AND RADIOGENIC ISOTOPES

Noble gases in mantle derived xenoliths from Eastern Australia and their implications for the tectonic evolution: Summary

György Czuppon
Institute for Geochemical Research, Budapest

Takuya Matsumoto
IAEA

Jun-ichi Matsuda
*Dep. of Earth and Space Science,
Osaka University, Osaka*

Monica R. Handler
*School of Geography, Victoria University of
Wellington, Wellington*

John Everard
Tasmanian Mineral Resources, Tasmania

Lin Sutherland
Australian Museum, Sydney

Noble gas elemental and isotopic compositions of mantle derived xenoliths have been measured from different localities along eastern margin of Australia. The observed noble gas composition of xenoliths samples from northernmost locality (Mt. Quincan, North Queensland) seems to be very homogeneous, and it is very similar to those reported from mid-ocean ridge basalts (MORBs). The studied xenoliths from Tasmania indicate more heterogeneous noble gas isotopic compositions with the presents of MORB-like and radiogenic components. The contributions of MORB-like noble gas component to the xenoliths from both regions indicate a large-scale occurrence of this component in subcontinental lithospheric mantle (SCLM) beneath eastern Australia. This MORB-like fluid addition is likely linked with rifting tectonic settings when asthenospheric fluid (and magma) could rise into the subcontinental lithospheric mantle. Eastern margin of Australia has been controlled by rifting tectonic setting during Mesozoic and Cenozoic when opening of Tasman Sea and subsequent extension phase took place. The MORB-like component found xenoliths might reflect these tectonic events. The presence of radiogenic component in xenoliths from Tasmania might reflect subduction events when the mantle wedge and SCLM could be metasomatised by U, Th rich fluids. Subduction processes have played important role in the evolution of Eastern Australia during the Paleozoic; the radiogenic component likely associated with this event. Although this Paleozoic subduction was extend from Tasmania to Northeastern Australia, the samples from North Queensland do not indicate contribution of subduction related (i.e. radiogenic) noble gas component showing pure MORB-like noble gas composition. Thus, the fluid-entrapment responsible for this MORB-like signature likely overwrites any pre-existing signatures or even replaces it with "MORB"-like mantle by physical removal of previously metasomatised lithospheric mantle (i.e. delamination).

Address of corresponding author: Gy. Czuppon: H-1112 Budapest, Budaörsi út 45, Hungary
e-mail: czuppon@geochem.hu

Helium isotopes distribution in NW Iberian peninsula: evidences of a local neotectonic activity

Fausto Grassa, Giorgio Capasso
*Istituto Nazionale di Geofisica Vulcanologia,
Sezione di Palermo, Palermo*

Paula M. Carreira
Instituto Tecnológico e Nuclear, Sacavém

Maria R. Carvalho
*Universidade de Lisboa, Faculdade Ciências,
Dpt. Geologia, Lisboa*

Jose M. Marques
Instituto Superior Técnico, Lisboa

Manuel Antunes da Silva
UNICER Bebidas, S.A. S. Mamede de Infesta

In this work we report new data on He abundances and isotope ratios ($^3\text{He}/^4\text{He}$) from gas associated to some thermal and CO_2 -rich mineral waters in N-Portugal. Collected gas samples are mainly CO_2 -dominant except two sites where gas is N_2 -rich. All the sampling sites are characterized by exceptionally high helium contents with $^3\text{He}/^4\text{He}$ ratios, corrected for air contamination, varying considerably from 0.09 to 2.68 Ra. In all sites, the $^3\text{He}/^4\text{He}$ ratios are higher than that typical for stable continental areas thus indicating a variable but not-negligible (up to 30%) contribution of mantle-derived primordial He. In all the CO_2 -rich waters, $\text{CO}_2/^3\text{He}$ ratios and $\delta^{13}\text{C}_{\text{CO}_2}$ are comparable with mantle values, thus suggesting a magmatic origin also for CO_2 . On the contrary, in the N_2 -rich waters He is mainly radiogenic, and CO_2 is organic in origin. Since no recent volcanic activity is observed in NW Iberia, high $^3\text{He}/^4\text{He}$ values could be due, at least, to three processes:

a) releasing of gas from the local upper mantle through deep extensional fault systems; b) releasing of magmatic volatiles from crustal reservoir(s) formed during past volcanic activity; c) degassing of a subsurface emplaced magma body.

Mantle He flux in N-Portugal has been estimated to be up to 3 orders of magnitude higher than that typical for stable continental areas, thus suggesting, in this area, the presence of a tensional tectonic regime. This implies that mantle gases could migrate upward probably through inherited tectonic structures reactivated by neotectonic activity. The third possible scenario seems to be less plausible since seismic surveys carried out in NW Iberian did not find any significant evidence of mantle intrusion in the crust. The observed spatial variability in mantle-derived contribution could reflect the geometry of the granitic plutons in this area, thus supporting the hypotheses of an upper mantle degassing. Alternatively, it could be the result of a lateral migration of magmatic volatiles stored in a crustal reservoir.

Address of corresponding author: F. Grassa: Via Ugo La Malfa 153, 90146 Palermo, Italy
e-mail: grassa@pa.ingv.it

Deep groundwater age dating with noble gases (He) and chlorine-36: The Continental Intercalaire aquifer from the Sahara basin

Abdelhamid Guendouz
*Engineering and Science Faculty, Blida University,
Blida-Algeria*

Adnane Souffi Moulla
*Dating and Isotope Tracing Dept.
Algiers Nuclear Research Centre, Algiers*

Jean-Luc Michelot
Paris-Sud University, Orsay

In the northern part of the Sahara desert, is located a very large aquifer system, the deep "Continental Intercalaire" (C.I.), extending over an area of approximately 1,000,000 km². This arid zone vital resource is considered as being "fossil", i.e. mainly inherited from previous climatic conditions, that were more humid than at present.

Sampled groundwaters show a quite wide range of ³⁶Cl contents, ranging from 8 to 99 10⁻¹⁵ at-at⁻¹, expressed as ³⁶Cl/Cl atomic ratio. The space distribution of ³⁶Cl contents fits fairly well with what is known about the piezometric contours of the aquifer: a decrease is observed from recharge to discharge zones. If this decrease is result of radioactive decay, it can be interpreted in terms of groundwaters transit time. Maximum time intervals of about 3 half-lives (900 Ka) may be computed using ³⁶Cl specific activities (at.l⁻¹).

In order to evaluate the epigene production, measurements were performed on chloride extracted by leaching from a soil profile. The results are the same order of magnitude (10⁻¹⁵ at-at⁻¹) as for groundwater chloride sampled near recharge areas and could reflect the true value of initial ³⁶Cl input.

The residence times determined on the main flow line where the radio decay is observed are expressed in terms of minimum ages (16 to 500 Ka) and maximum ages (25–1200 Ka).

Noble gas data are presented to improve the palaeoclimatic and residence time interpretation for the Continental Intercalaire aquifer system. The groundwater recharge temperatures (RT) were estimated from the averaged amounts of noble gases (Ne, Kr, Xe) corrected for the excess air effect. The RTs for most groundwaters are generally lower than the present day recharge temperatures. Along the main flow direction (south-east from the Atlas mountains), the CI Paleowaters (ages 20 to 40 ka BP) have an average RT of 16.9 °C which is some 5 °C cooler than at the present day. Recharge temperatures calculated in four samples from the CT aquifer (30–150 m depth) average 19.7 °C, close to the present day mean annual temperature of 21 °C.

Address of corresponding author: A. Guendouz: PO Box. 270. Route de Soumâa Blida 09000
Algeria, e-mail: ah_guendouz@hotmail.com

Study of the behavior of radon isotope in Pál-völgy show cave (Budapest, Hungary)

Hedvig Éva Nagy

Lithosphere Fluid Research Lab, Department of Petrology and Geochemistry, Eötvös University, Budapest

Department of Atomic Physics, Eötvös University, Budapest

Ákos Horváth

Department of Atomic Physics, Eötvös University, Budapest

Csaba Szabó

Lithosphere Fluid Research Lab, Department of Petrology and Geochemistry, Eötvös University, Budapest

Attila Kiss

Danube-İpoly National Park Directorate Pál-völgy show cave, Budapest

We have been doing radon measurements in Pál-völgy cave (Budapest, Hungary) for one and a half year. The cave is situated in the Buda Hills, which is the NE part of the Transdanubian Central Range. The wall rock of the cave is dominantly Eocene Szépvölgy Limestone Formation. Above the limestone Eocene Buda Marl and Oligocene Tard Clay are deposited. The main aim of this study is to determine the time dependent radon concentration and the sources of the radon in the cave.

The radon concentration in the cave air has been measured continuously by AlphaGUARD radon monitor and outside the cave meteorological parameters were collected simultaneously. The radon concentration of the air in the cave varies between 104–7776 Bq/m³ during the measurements, the average value is 1920 Bq/m³. These data strongly depend on the outside air temperature. If the temperature outside is higher than inside (11 °C) the radon concentration increases. The correlation coefficient between the radon concentration of the air in the cave and the outside air temperature is 0.75. The spatial distribution of radon concentration in the cave air was measured simultaneously by active radon detectors, which shows values as high as 1000 Bq/m³ where Buda Marl is the surrounding rock, and 500 Bq/m³ where Szépvölgy Limestone is the wall rock.

To define the source of radon, besides the wall rock limestone and marl, clayish cave sediments have been collected. The radioactive isotope (²²⁶Ra, ²³²Th, ⁴⁰K) content of clayish cave sediments shows results typical for soils: 26–37 Bq/kg ²²⁶Ra, 21–31 Bq/kg ²³²Th, 265–386 Bq/kg ⁴⁰K. However, the radon and thoron exhalation rates of these samples, 2–12 Bq/kg for ²²²Rn and 1–12 Bq/kg for ²²⁰Rn, are higher than expected based on the ²²⁶Ra content. These results can be related to high percentage of fine grain size fraction corresponding to high specific surface which provides high possibility of exhalation. Our results suggest that the most likely radon source is the Buda Marl.

Address of corresponding author: H. É. Nagy: 1117 Budapest, Pázmány P sétány 1/C, Hungary
e-mail: jadzsa@gmail.com

Uranium, radium and ^{222}Rn isotopes in thermal waters from Podhale Trough (Polish Inner Carpathians)

Chau Dinh Nguyen, Jakub Nowak, Pawel Jodlowski

AGH University of Science and Technology, Faculty of Physics and Applied Computer Science, Kraków

The Podhale Trough belongs to Polish Inner Carpathians; it is situated between the Tatras in the south and the Pieniny Klippen Belt in the north. The Trough is the most important geothermal water system in Poland. Thermal water has been reported in over a dozen boreholes, but only nine of them are exploited. Currently the water is used for heating and for recreational purposes.

From all exploited boreholes, water samples were collected. For each sample ^{238}U , ^{234}U , ^{226}Ra , ^{228}Ra and ^{222}Rn activity concentrations were determined. Uranium isotopes were measured by α -spectrometer after separation of them by adequate procedure. The radium isotopes were separated from the water sample as sulfate compounds and measured with α/β liquid scintillation spectrometer (LSC). The ^{222}Rn activity concentrations were determined by LSC method. The chemical composition of water sample was measured using an ICP-AES spectrometer.

The obtained results show that the activity concentrations of ^{234}U and ^{238}U vary from 4.1 mBq/L to 303 mBq/L and from 2.8 mBq/L to 324 mBq/L, respectively. Radium isotopes activity concentrations vary from 29 mBq/L to 590 mBq/L for ^{226}Ra and from 17 mBq/L to 360 mBq/L for ^{228}Ra . The ^{222}Rn concentrations of the samples range from <0.2 Bq/L to about 80 Bq/L. The highest activity concentrations of uranium and radon isotopes were found in the water sample from the Szymoszkowa GT-1 borehole. The highest activities of radium isotopes were observed in the water sample from the Bukowina Tatrzańska PIC/PGNIG borehole. The maximum activities of radium and uranium isotopes contained in the mineral waters of the similar mineralization from the Outer Carpathians are significantly lower and amount to 170 mBq/L and 56 mBq/L respectively. Such a high level of natural radioactivity in the thermal waters from the investigated region could be resulted by the interaction of water with the crystalline, igneous and metamorphic rocks of the Tatra Mts. as the thermal waters likely have strong leachability.

This work was supported by the "Doctus - Malopolska Scholarship for PhD" co-funded by the European Union (Project No MCPZS.4110-29.1/2009).

Address of corresponding author: J. Nowak: Al. Mickiewicza 30, 30-059 Kraków, Poland
e-mail: jnowak@novell.ftj.agh.edu.pl

^{222}Rn concentration measurements of soil gas in Hungary

Katalin Zsuzsanna Szabó

Lithosphere Fluid Research Lab, Department of Petrology and Geochemistry, Eötvös University, Budapest

Ákos Horváth

Department of Atomic Physics, Eötvös University, Budapest

Csaba Szabó

Lithosphere Fluid Research Lab, Department of Petrology and Geochemistry, Eötvös University, Budapest

^{238}U is one of those terrestrial radioisotopes that can be found on Earth since its formation. The ^{222}Rn radioactive noble gas is a daughter product of uranium decay chain. Its parent isotope is ^{226}Ra , which is present in the rocks and soils. Alpha decay of ^{226}Ra provides the ^{222}Rn which emanate out from rock or soil mineral to the pore space by diffusion or alpha recoil. Exhalation coefficient shows that how many percent of radon got to the soil gas or the surface. Because radon is an inert gas and has half life of 3.8 days it can migrate in subsurface and soil environment getting into the indoor air. It can be accumulated in high concentrations in rooms and can cause lung cancer. Soil gas radon concentration is the main source of indoor radon. Geogenic radon risk can be determined from soil gas radon values taking into account the permeability of soil.

We studied the radon exhalation rate in the upper 150 cm of soils for better understanding of the importance of depth from radon point of view in Pest County. Five–five soil samples of 11 soil profiles (down to depth of 150 cm) were examined by gamma spectroscopy to have radium content. We also measured the radon exhalation of soil samples and then the radon exhalation coefficient was calculated. *In situ* soil gas radon and soil permeability measurements were made at 47 sites in 80 cm depth to assess the geogenic radon risk.

Results show that the average of exhalation coefficient is 0.15 (min. and max. values are 0.03 and 0.62, respectively) in the upper 90–100 cm and the deeper layer has 10 times lower values (average is 0.01, min. and max. values are 0.003 and 0.03, respectively). The reason of this decrease is the increase of compactness with depth where the radon cannot escape easily. This indicates the relevant depth for radon is the upper 90–100 cm in general case where there are no special geological features (e.g. uranium deposit). This depth (90–100 cm) also means the measurements depth for soil gas radon measurements.

Radon risk of the 47 sample sites of Pest County was determined from *in situ* soil gas radon and permeability measurements. It shows that 2 sites have high, 16 sites have medium and 29 sites have low radon risk in the study area.

Address of corresponding author: K. Zs. Szabó: H-1117 Budapest, Pázmány P. sétány 1/C, Hungary
e-mail: sz_k_zs@yahoo.de

Testing of fast ^{222}Rn and ^{220}Rn exhalation measurements of high number of Hungarian adobe building material samples

Zsuzsanna Szabó, Csaba Szabó
*Lithosphere Fluid Research Lab, Department of
Petrology and Geochemistry, Eötvös University,
Budapest*

Ákos Horváth
*Department of Atomic Physics, Eötvös University,
Budapest*

^{222}Rn and ^{220}Rn are responsible for 52% of the total annual effective dose to humans, therefore it is important to know the exhalation properties of different building materials. The main aim of this work is to test a ^{222}Rn exhalation rate measurement technique and to study ^{222}Rn and ^{220}Rn exhalation rates of Hungarian adobe considering that this is a common building material at certain parts of the country and a potential source of ^{220}Rn .

Adobe samples were taken from settlements in three areas: Békés County (SE-Hungary), Sajó and Hernád Rivers Valleys (NE-Hungary) and E-Mecsek Mts (S-Hungary).

^{222}Rn exhalation rates were estimated in laboratory by two different techniques, both using Al-accumulation chambers and RAD7 detectors. One technique is based on measuring the growth curve of ^{222}Rn concentration in the chamber for ten days, and the other on measuring for four hours the ^{222}Rn equilibrium concentration after three weeks (about $5(T_{1/2})$) closing. The latter one is faster for high number of samples. For ^{220}Rn only the equilibrium concentrations can be used ($5(T_{1/2}) \approx 5$ min).

The second method shows less ^{222}Rn exhalation rates but correlation ($R=0.85$) is found between the ratio of results and the degree of leakage. It is shown that when leakage is below $\alpha \approx 0.006 \text{ h}^{-1}$, based on the growth curve, the two methods give the closest results. Accepted as correct results of ^{222}Rn and ^{220}Rn exhalation rates are similar (average values are 8 ± 2 , $7 \pm 2 \text{ s}^{-1} \text{ kg}^{-1}$, respectively), Hungarian adobe building materials can exhale short half-lived ^{220}Rn almost in the same amount as ^{222}Rn .

It can be concluded that a tightly gas proof circuit is required for the best estimation of both of the methods; however, measurements for high number of samples can be made faster. Hungarian adobe is a potential ^{220}Rn exhaling building material; therefore indoor measurements are necessary to evaluate its effect.

Address of corresponding author: Zs. Szabó: H-1117 Budapest, Pázmány P. s. 1/C, Hungary
e-mail: zsszabo86@gmail.com

Isotopic constraints on genesis of the multistacked CO₂-CH₄-N₂ Répcelak gas field (Pannonian Basin System, W Hungary)

István Vető
Consultant geochemist, Budapest

László Palcsu
Nuclear Research Institute, Debrecen

István Futó, Gergely Vodila, László Papp, Zoltán Major
Nuclear Research Institute, Debrecen

Several multistacked CO₂-CH₄-N₂ gas fields have been found in different parts of the Neogene-Quaternary Pannonian Basin System. These fields are characterised by drastic upward decrease of CO₂ content and very low CH₄/N₂ ratio (< 4).

The 22 reservoirs (mostly sandy) of the multistacked Répcelak gas field (W-Hungary) are developed between 1300 to 800 m depth below sea level (BSL). In this depth interval the CO₂ content gradually decreases upward from 95 to 1–2%. This gradual but drastic change in gas composition is the result of mixing of CO₂ with a CH₄-N₂ fluid that probably arrived later.

Here results of an stable and noble gas isotope study of five reservoirs among the deeper ones (1300–1000 m BSL) of the Répcelak field are presented and discussed.

³He/⁴He ratios prove the predominantly mantle origin of the helium and suggest the same origin for CO₂. The most likely source of these two gases is a basic magmatic body intruding the basement during the late Neogene. The rather high N₂/noble gas (Ne, Ar) ratios confirm that the N₂ cannot be of atmospheric origin. The very low CH₄/N₂ ratios (<3) suggest late thermogenic origin of the CH₄ and N₂. Anchimetamorphic Paleozoic shales of the basement are the most likely source of the CH₄-N₂ fluid.

Within the 1300–1000 m depth interval CO₂ content decreases from 94 to 72.5%, this decrease is accompanied by a moderate increase of δ¹³C_{CO2} (from –3.28 to –2.61‰).

In four of the five reservoirs CH₄/N₂ ratio shows upward increase from 1.16 to 2.65, while δ¹³C_{CH4} and δD_{CH4} show upward decreases from –41.9 to –49‰ and from –181 to –214.5‰, respectively. These depth related changes in composition and isotopic compositions of the CH₄-N₂ fluid likely reflect a moderate and upward increasing contribution of isotopically light (bacterial?) CH₄.

Address of corresponding author: I. Vető: H-1026 Budapest, Balogh Á. u. 18/c, Hungary
e-mail: vetoie3840@gmail.com

Examination of radiogenic isotopes and chemical composition of coal slag and fly ash bearing building materials

Péter Völgyesi, Hedvig Éva Nagy, Csaba Szabó

Lithosphere Fluid Research Lab, Department of Petrology and Geochemistry, Eötvös University, Budapest

Building materials or additives of building materials can contain relatively high levels of natural radionuclides, which increases the indoor radiation exposure of residents. By residential request we made *in situ* radiometric measurements in 14 houses in the central region of Hungary and we analyzed the building materials (gas silicate, containing fly ash; slag concrete and slag samples) from the studied houses using physical and chemical methods. It is important to know the background of the coal's radioactivity which the coal slag and fly ash was formed of. Laboratory studies have shown that coal can contain primarily uranium and a small amount of thorium. In Hungary the uranium content of coals varies in a wide range (~10 g/t–1 kg/t). The usage of such large U-bearing by-products as building material can cause serious risk to the health of residents, mainly due to radon exhalation. Based on the microscopic, scanning electron microscopic and X-ray diffraction analysis on coal slag, slag concrete and gas silicate samples, the most frequently identified mineralogical phases are quartz, calcite, metallic phases that have iron as their primary constituent, Ca-Mg-rich aluminosilicates and gypsum. Also, 2–3 μm uranium-bearing grains in the coal slag sample were identified in large number by scanning electron microscope. The indoor radon concentration was measured by using active detector (short-term measurements) (40–226 Bq/m³) and we also measured the radon concentration (by using track-etched detectors) and the equilibrium factor on a long term scale (3–6 months). The gamma dose rate was measured with FH 40G L10 detector. The results show values between 70–1000 nSv/h in the 14 studied houses. The ²²⁶Ra, ²³²Th and ⁴⁰K content of the samples was determined by HPGe Gamma-spectrometry. These results were used to classify with indices the building materials studied. Radium equivalents (Ra_{eq}) vary between 33–2812 Bq/kg and activity concentration indices (I) vary between 0.1–9.4. The calculated radon exhalations (RE) vary between 0.3 and 61.3 Bq/kg. The results show that the fly ash containing building materials (Ra_{eq} : 63–128 Bq/kg; I: 0.2–0.5; RE: 0.4–4.8 Bq/kg) do not have any risk, however in some cases the slag containing materials can achieve or significantly exceed the threshold values (Ra_{eq} : 33–2812 Bq/kg; I: 0.1–9.4; RE: 0.3–61.4). Our study draws the attention to the need of complex physical and chemical methods.

Address of corresponding author: P. Völgyesi: H-1117 Budapest, Pázmány P. s. 1/c, Hungary
e-mail: petervolgyesi11@gmail.com

ISOTOPE HYDROLOGY

Comparison of the isotope hydrogeological features of thermal and cold karstic waters in the Denizli Basin (Turkey) and Buda Thermal Karst (Hungary)

István Fórizs
*Institute for Geochemical Research,
Hungarian Academy of Sciences, Budapest*

Ali Gökgöz
*Department of Geological Engineering,
Pamukkale University, Denizli*

Sándor Kele
*Institute for Geochemical Research,
Hungarian Academy of Sciences, Budapest*

Mehmet Özkul
*Department of Geological Engineering,
Pamukkale University, Denizli*

József Deák
GWIS Ltd, Dunakeszi

Mehmet Oruç Baykara,
Mehmet Cihat Alçiçek
*Department of Geological Engineering,
Pamukkale University, Denizli*

The isotopic compositions of the Hungarian warm and cold water samples are spread in a wide range along the Global Meteoric Water Line (GMWL), which is a result of the significant change in the climate (mainly temperature) during infiltration (Last Glaciation and Holocene) and of the mixing process along the fault zone. The thermal karst water is isotopically lighter as it was infiltrated in a 7 to 9 °C cooler climate in the Ice Age. However, in the Denizli Basin isotopic composition of all of the thermal, lukewarm and cold waters varies in a relatively narrow range, with the exception of some warm waters whose d18O values have been shifted as a result of water-rock interaction.

Isotope data prove that all the waters in the Denizli Basin infiltrated in the Holocene under more or less the same climate, so these waters are young indicating much shorter transit time from the recharge to the discharge areas because of faster flow under the surface or shorter path of the subsurface flow.

Key words: thermal water, stable oxygen and hydrogen isotopes, water age, water-rock interaction

Introduction

The importance of researches focussed on the sustainability of thermal water systems worldwide has increased recently. In the framework of a Turkish–Hungarian scientific cooperation several thermal and cold karst springs and wells and their carbonate deposits (travertines) have been studied both in the Denizli Basin (SW-Turkey) and in the Buda Thermal Karst system (Budapest, Hungary). Stable isotope and chemical methods have been applied beside the standard sedimentological, petrographical methods (optical microscope, SEM, XRD, etc.). This paper is restricted to the presentation and compar-

Address of corresponding author: I. Fórizs: H-1112 Budapest, Budaörsi út 45, Hungary
e-mail: forizs@geochem.hu

Received: May 24, 2011; accepted: June 6, 2011

ison of the stable hydrogen- and oxygen isotopic composition of water samples from the two study areas located under different climatic and tectonic conditions.

The Denizli Basin is a 70 km long and 50 km wide fault bounded Neogene–Quaternary depression located in the Western Anatolian Extensional Province, which is one of the most seismically active and rapidly extending regions (30–40 mm/year) in the world (Westaway 1993; Bozkurt 2001; Alçiçek et al. 2007; Alçiçek 2010) (Fig. 1B). The climate in the Denizli Basin is not uniform and mostly terrestrial with hot and dry summers and mild and rainy winters. The outflow temperature of the cold and thermal karst waters varies from 15 °C to 70 °C. The annual precipitation is 560 mm.

The Buda Thermal Karst system (Hungary) is located at the boundary of uplifted carbonates and a sedimentary basin and serves as a discharge zone of the regional fluid flows.

Within this fault zone in the vicinity of the Danube more than 100 thermal springs are arising yielding totally about 40 000 m³ per day of warm and lukewarm mineral water. Ascending thermal water (along faults) mix with cooler meteoric water producing the thermal springs and spas along the Danube with varying temperature. The climate in the Buda Hills area is continental with annual precipitation of 600–700 mm. The outflow temperature of the cold and thermal karstic waters varies from 10 °C to 77 °C.

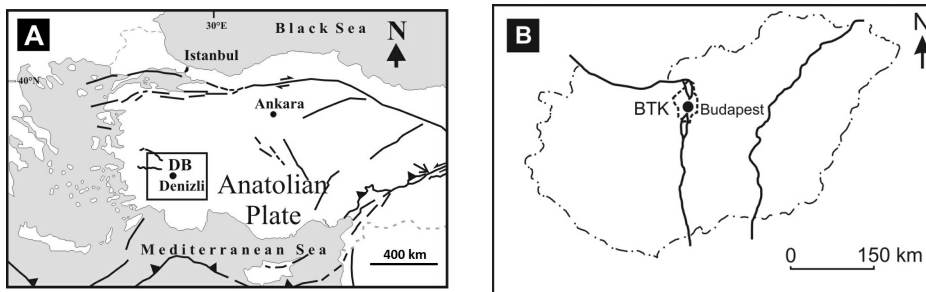


Fig. 1
Location of the study areas. A: Denizli Basin DB in Turkey modified after Uysal et al. 2009; B: Buda Thermal Karst BTK (Hungary)

Results and discussion

In Hungary, the study of thermal waters focussed on the Buda Hills (Buda Thermal Karst system), whereas in the Denizli Basin (SW-Turkey) on hot to lukewarm thermal waters and in both areas cold karstic waters were also investigated. These studies provided new and important information on the origin of waters and on the distribution of the water circulation systems in both investigated areas.

Thermal waters (>50 °C) of Budapest and its neighbouring areas are isotopically significantly lighter than those of the cold karst waters (Fig. 2) and

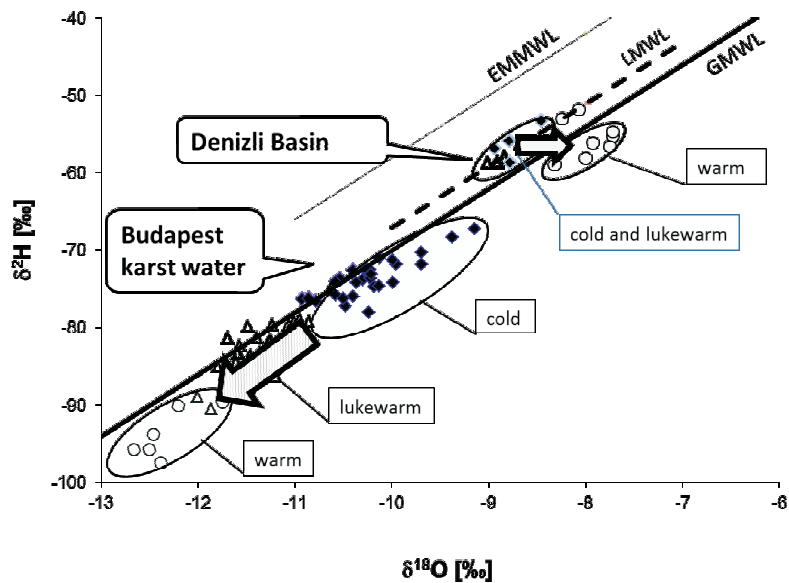


Fig. 2
Stable oxygen and hydrogen isotopic composition of the thermal and cold karst waters in the Denizli Basin (Turkey) and in the Budapest Thermal Karst Water system (Hungary). GMWL = Global Meteoric Water Line, LMWL = Local Meteoric Water Line of Denizli Basin (this work), EMMWL = Eastern Mediterranean Meteoric Water Line (Gat and Carmi 1970)

local precipitation of $\delta^{18}\text{O} = -9.5\text{‰}$ and $\delta^2\text{H} = -65\text{‰}$ (Deák 1979). "Altitude effect" can be excluded because the recharge area has only 300 to 500 m elevation so the possible reason of the lower $\delta^{18}\text{O}$ and $\delta^2\text{H}$ values should be a 7 to 9 °C colder climate at the time of infiltration than recent. These results refer to the Ice Age infiltration of warm water and are in good agreement with corrected ^{14}C ages of thermal waters as 15 to 25 ka (Deák 1980). Following the flow path from the recharge to the discharge areas, karst water is continually becoming lighter reflecting the significant change in the mean annual air temperature during the infiltration period (from Holocene back to Ice Age). Additionally, later, on the discharge area (at the fault zone along the Danube River) the "old" warm waters are mixed up with younger (and colder) waters infiltrated during the last centuries. Accordingly, the isotopic compositions of subsurface waters of the Budapest karst system are spread in a wide range along the Global Meteoric Water Line following the direction of the arrow in Fig. 2 from cold to warm water.

However, in the Denizli Basin the isotopic composition of all karst water samples varies in a relatively narrow range (Fig. 2). Deuterium (^2H) contents of cold, lukewarm and warm waters are similar, suggesting that all the waters in the

Denizli Basin infiltrated under more or less the same climate, probably during the Holocene. For some lukewarm and hot waters, what we have also studied in the Pamukkale and Karahayit areas, Simsek (2003) reported tritium contents around 4 TU, which indicates a very young, namely modern component infiltrated after the first thermonuclear bomb tests of 1952. These waters are certainly mixtures of hot, older component and a cold, (tritium-bearing) modern component, where the old component is younger than 10 ka indicated by the stable isotopic composition. The small variations in $\delta^2\text{H}$ are caused mostly by the elevation effect, i.e. different flow systems have their recharge area located at different heights above sea level. Accepting these results, thermal waters are young (infiltrated in the last 10 ka) by stable isotope data, indicating much shorter transit time because of either faster flow or shorter path of the subsurface flow.

Some Turkish warm water samples fall below the GMWL (Fig. 2) because their $\delta^{18}\text{O}$ values are shifted to more positive values. Usually this kind of $\delta^{18}\text{O}$ shift is characteristic for hot waters, where during the rock-water interaction the $\delta^{18}\text{O}$ value is changed to positive direction, but the $\delta^2\text{H}$ value remained unaltered. Direction of this shift is presented by the arrow in Fig. 2.

The cold and lukewarm water samples of the Denizli Basin – comprising the majority of the studied waters in Fig. 2 – are above the GMWL and below the Eastern Mediterranean Meteoric Water Line (EMMWL, Gat and Carmi 1970), closer to the GMWL. This observation suggests a Local Meteoric Water Line for the Denizli Basin as $\delta^2\text{H} = 8 \cdot \delta^{18}\text{O} + 13$, although in the future more data has to be used to refine this equation.

The Budapest samples plot just below the GMWL, which is characteristic for the present precipitation in the Carpathian Basin and nearby areas (Vodila et al. 2011; Vreca et al. 2006; Deák 2006). While the cold and tepid Turkish waters plot over the GMWL which is characteristic for the Eastern Mediterranean territories. Gat and Carmi (1970) reported $\delta^2\text{H} = 8 \cdot \delta^{18}\text{O} + 22\text{‰}$ as the Eastern Mediterranean Meteoric Water Line (EMMWL). The very high intercept of 22‰ in the above equation is caused by the component of evaporation from the Mediterranean Sea, because the relative humidity over this sea is less than global average (85%). In the case of Denizli Basin this intercept is around 13‰ indicating smaller effect of the Mediterranean Sea here than in the Levant.

Acknowledgements

This study was performed in the frame of a Turkish–Hungarian joint project supported by The Scientific and Technical Research Council of Turkey (TÜBİTAK, Project Number: 106 Y 207) and the National Office for Research and Technology (NTKH, Hungary, project number: TR-10/2006). The sampling in the area of Budapest and the related stable isotope analyses have been financed by the Hungarian Scientific Research Fund (project OTKA K 60921).

References

- Alçiçek, H. 2010: Stratigraphic correlation of the Neogene basins in southwestern Anatolia: regional palaeogeographical, palaeoclimatic and tectonic implications. – *Palaeogeography, Palaeoclimatology, Palaeoecology*, 291, pp. 297–318.
- Alçiçek, H., B. Varol, M. Özkul 2007: Sedimentary facies, depositional environments and palaeogeographic evolution of the Neogen Denizli Basin, SW Anatolia, Turkey. – *Sedimentary Geology*, 202, pp. 596–637.
- Bozkurt, E. 2001: Neotectonics of Turkey – a synthesis. – *Geodinamica Acta*, 14, pp. 3–30.
- Deák, J. 1979: Environmental isotopes and water chemical studies for groundwater research in Hungary. – *Isotope Hydrology*, 1978, pp. 221–249., IAEA, Vienna.
- Deák, J. 1980: Radiocarbon dating of the thermal waters in the Budapest area. – *Zentralinstitut für Isotopen, Mitteilungen*, 30, pp. 257–266, Leipzig.
- Deák, J. 2006: A Duna–Tisza köze rétegvíz áramlási rendszerének izotóp hidrológiai vizsgálat (Isotope hydrological study of the groundwater flow regime of Danube–Tisza region). – PhD thesis Eötvös Loránd University, Budapest, 112 p. (In Hungarian.)
- Gat, J.R., I. Carmi 1970: Evolution in the isotopic composition of atmospheric waters in the Mediterranean Sea area. – *Journal of Geophysical Research*, 75, pp. 3039–3048.
- Simsek, S. 2003: Hydrogeological and isotopic survey of geothermal fields in the Büyük Menderes graben, Turkey. – *Geothermics*, 32, pp. 669–678.
- Uysal, T., Y. Feng, J. Zhao, V. Isik, P. Nuriel, S.D. Golding 2009: Hydrothermal CO₂ degassing in seismically active zones during the late Quaternary. – *Chemical Geology*, 265, pp. 442–454.
- Vodila, G., L. Palcsu, I. Futó, Zs. Szántó 2011: A 9-year record of stable isotope ratios of precipitation in Eastern Hungary: Implications on isotope hydrology and regional palaeoclimatology. – *Journal of Hydrology*, 400/1–2, pp. 144–153.
- Vreca, P., I. Krajcar-Bronic, N. Horvatincic, J. Barešic 2006: Isotopic characteristics of precipitation in Slovenia and Croatia: Comparison of continental and maritime stations. – *Journal of Hydrology*, 330/3–4, pp. 457–469.
- Westaway, R. 1993: Neogene evolution of the Denizli region of western Turkey. – *Journal of Structural Geology*, 15, pp. 37–53.

Study of the bank filtered groundwater system of the Sava River at Zagreb (Croatia) using isotope analyses

Nada Horvatinčić, Jadranka Barešić,
Ines Krajcar Bronić
Rudjer Boškovic Institute, Zagreb

Krisztina Kármán, István Fórizs
Institute for Geochemical Research,
Hungarian Academy of Sciences, Budapest

Bogomil Obelić
Rudjer Boškovic Institute, Zagreb

Radioactive isotope tritium (^3H) and stable isotopes of hydrogen ($^2\text{H}/^1\text{H}$) and oxygen ($^{18}\text{O}/^{16}\text{O}$) were measured during 2010 in the Sava River, precipitation and groundwater at 3 monitoring wells and 1 production well of the Petruševac aquifer, close to the Sava River in the Zagreb area. Significant increase of ^3H activity in the Sava River was observed in June, (200 ± 20) TU, and in groundwater of all wells with damped response (maximum 60 TU) and with delay of 3–5 months related to the Sava River. This increase was explained by release of tritiated water from the Krško Nuclear Power Plant, 30 km upstream from Zagreb in the beginning of June 2010. Stable isotope analyses showed similar range of $\delta^2\text{H}$ and $\delta^{18}\text{O}$ values for the Sava River and groundwater samples with higher variations in surface water. Differences in monthly variations of $\delta^{18}\text{O}$ values between particular monitoring wells, together with ^3H values, indicated different infiltration times of surface water of the Sava River to different wells of the Petruševac aquifer.

Key words: tritium ^3H , stable isotopes ^2H and ^{18}O , Sava River, Petruševac aquifer

Introduction

Measurements of radioactive isotope tritium (^3H) and stable isotopes of hydrogen ($^2\text{H}/^1\text{H}$) and oxygen ($^{18}\text{O}/^{16}\text{O}$) can give useful information in hydrogeological studies of (i) mixing of surface and groundwaters, (ii) water circulation in nature, especially in karst areas, and (iii) mean residence time of water in aquifers. Increased ^3H activities in natural waters may indicate some contamination, such as global contamination of atmosphere with ^3H due to

Addresses: N. Horvatinčić, J. Barešić, I. Krajcar Bronić, B. Obelić: Bijenička 54, 10000 Zagreb, Croatia, e-mail: nada.horvatincic@ibr.hr
K. Kármán, I. Fórizs: H-1112 Budapest, Budaörsi út 45, Hungary

Received: May 11, 2011; accepted: May 6, 2011

atmospheric thermonuclear bomb tests (Rozanski et al. 1991), or local contamination due to release of tritiated waters from various nuclear facilities.

^3H and stable isotope $^2\text{H}/^1\text{H}$ and $^{18}\text{O}/^{16}\text{O}$ ratios in monthly precipitation of the Zagreb area have been measured since 1979, and the results have been included into the GNIP (Global Network of Isotopes in Precipitation) database (IAEA/WMO, 2011) of the International Atomic Energy Agency (IAEA). The investigation of the Petruševac aquifer in the Zagreb area is included in the *Regional IAEA Project RER/8/016 Using Environmental Isotopes for Evaluation of Streamwater/Groundwater Interactions in Selected Aquifers in the Danube Basin* with the aim to determine the influence of surface stream of the Sava River on the groundwater of aquifer used for water exploitation.

Sampling and measurement

^3H , $^2\text{H}/^1\text{H}$ and $^{18}\text{O}/^{16}\text{O}$ were measured during 2010 in the Sava River, precipitation and groundwater at 3 monitoring wells (piezometers) and 1 production well of the Petruševac aquifer, close to the Sava River in Zagreb area. Groundwater samples were collected monthly and the Sava River weekly for stable isotopes. Details of the sampling sites are given in Table 1.

Measurements of ^3H activities in waters were performed by the liquid scintillation counter Quantulus 1220 (Barešič et al. 2011). All samples were electrolytically enriched prior to LSC measurements. The system for electrolytic enrichment consists of 20 cells, the initial volume of water is 500 mL and the final

Table 1
Sampling data

Location	Distance from the Save R. (m)	Depth (m)	Analysis and sampling frequency
Sava R., Zagreb, below the bridge "Domovinski most"			^3H – monthly $^2\text{H}/^1\text{H}$, $^{18}\text{O}/^{16}\text{O}$ – weekly
Precipitation, Zagreb Meteorological station Grič			^3H , $^2\text{H}/^1\text{H}$, $^{18}\text{O}/^{16}\text{O}$ – monthly integrated sample
Well B-5A, Petruševac	400	38.0	^3H , $^2\text{H}/^1\text{H}$, $^{18}\text{O}/^{16}\text{O}$ – monthly
Piezometer PP-23/5, Petruševac	200	16.4	^3H , $^2\text{H}/^1\text{H}$, $^{18}\text{O}/^{16}\text{O}$ – monthly
Piezometer PP-18/30, Petruševac	500	32.0	^3H , $^2\text{H}/^1\text{H}$, $^{18}\text{O}/^{16}\text{O}$ – monthly
Piezometer PP-19, Petruševac	500	41.6	^3H , $^2\text{H}/^1\text{H}$, $^{18}\text{O}/^{16}\text{O}$ – monthly

volume is 19 ± 1 mL resulting in the mean enrichment factor of 22.5 ± 0.5 . The limit of detection is 0.3 TU (TU – Tritium unit, 1 TU = 0.118 Bq/L).

The oxygen and hydrogen isotopic composition was analysed with a Liquid Water Isotope Analyser (LWIA-24d) by Los Gatos Research. The initial water sample volumes of 1 ml have been analyzed twice, with <10 microliter injected

into the instrument during each measurement. The uncertainty of the measurements is $\pm 0.2\text{‰}$ for $\delta^{18}\text{O}$ and $\pm 0.6\text{‰}$ for $\delta^2\text{H}$.

Results and discussion

^3H activity (Fig. 1) in precipitation showed slight seasonal fluctuation between 4 TU and 14 TU, with higher values in summer. ^3H activity of the Sava River and groundwater of the Petruševac aquifer followed ^3H of precipitation till May 2010. Significant increase of ^3H activity in the Sava River, (200 ± 20) TU, was observed in June and in the next month it fell down to 6 TU. This increase was explained by release of tritiated water from the Krško Nuclear Power Plant, 30 km upstream from Zagreb in the beginning of June 2010 (Stepišnik et al. 2011). Increase of ^3H was also observed in groundwater of all monitoring wells and the production well with damped response and a delay of several months in relation to the Sava River. The maximum ^3H activity (~ 60 TU) was observed in monitoring wells PP-23/5 and PP-18/30 with the delay of 3 and 5 months, respectively. The second peak activity in piezometer PP-23/5 in November could be resulted by the extremely high level of Sava River in September 2010. In the deepest groundwater of well B-5A and in piezometer PP-19 (Table 1) the rate of increase of ^3H activity was slower and the maximum value was lower (30 TU).

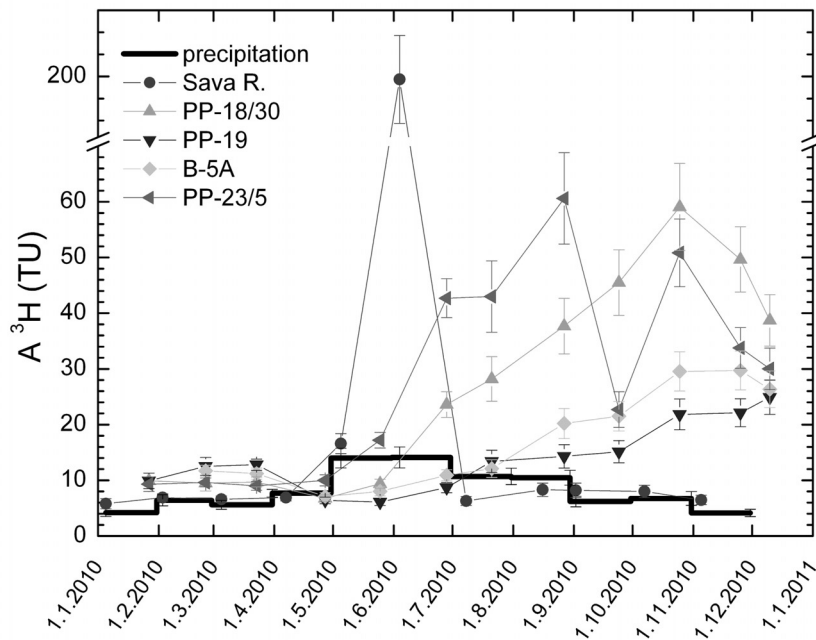


Fig. 1 ^3H activities in monthly precipitation and in the Sava River and groundwaters from the Petruševac aquifer (piezometers PP-23/5, PP-18/30, PP-19, well B-5A) during 2010

Stable isotope analyses of precipitation (Fig. 2) showed seasonal variations of $\delta^2\text{H}$ and $\delta^{18}\text{O}$ values typical for continental precipitation. The relation of $\delta^2\text{H}$ vs. $\delta^{18}\text{O}$ for Zagreb precipitation in 2010 (Fig. 3) is $\delta^2\text{H} = (7.7 \pm 0.3) \delta^{18}\text{O} + (6.1 \pm 3.2)$, $n = 12$, $R = 0.992$, and it is in agreement with the long-term (1980–2003) Local Meteoric Water Line (LMWL) for Zagreb: $\delta^2\text{H} = (7.8 \pm 0.1) \delta^{18}\text{O} + (5.7 \pm 0.8)$, $n = 271$, $R = 0.98$ (Vreča et al. 2006).

The range of $\delta^2\text{H}$ and $\delta^{18}\text{O}$ values (Table 2) for the Sava River and groundwater samples was similar with higher variations in surface water. The regression line

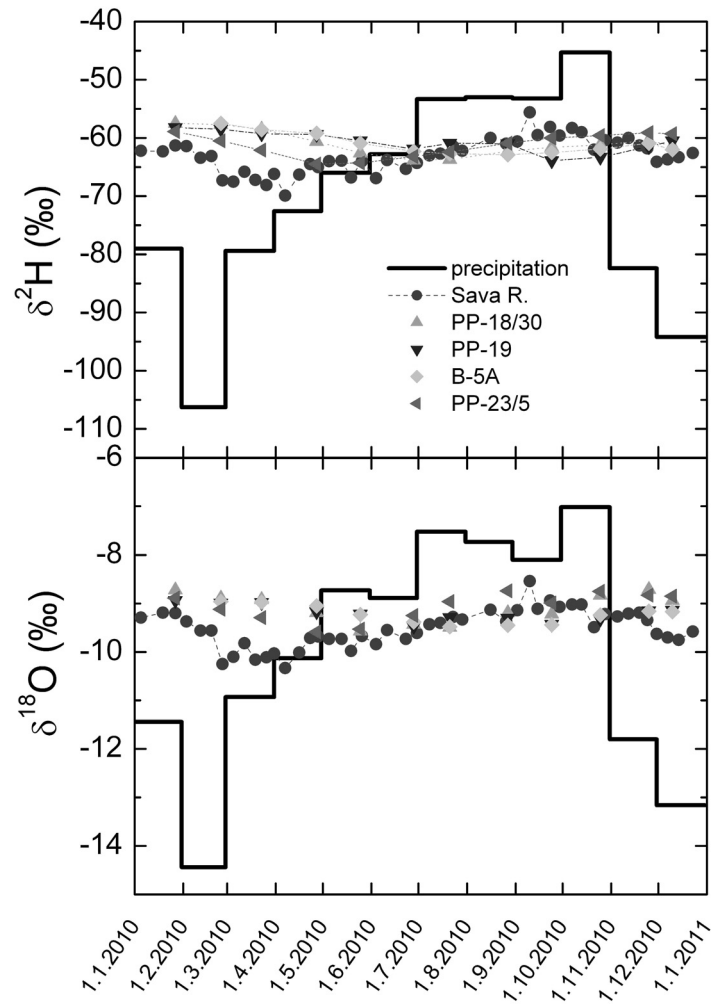


Fig. 2
 $\delta^2\text{H}$ and $\delta^{18}\text{O}$ in monthly precipitation and in the Sava River and groundwaters from the Petruševac aquifer during 2010

Table 2
 $\delta^{18}\text{O}$ mean values with standard deviation and the minimum and maximum $\delta^{18}\text{O}$ values in the Sava River and groundwater of the Petruševac aquifer during 2010

Location	^{18}O (‰)		
	mean \pm	minimum	maximum
Sava River	-9.5 ± 0.4	-10.33	-8.54
Well B-5A	-9.2 ± 0.2	-9.48	-8.96
Piezometer PP-23/5	-9.1 ± 0.3	-9.59	-8.74
Piezometer PP-18/30	-9.1 ± 0.3	-9.57	-8.71
Piezometer PP-19	-9.2 ± 0.2	-9.47	-8.94

$\delta^2\text{H}$ vs. $\delta^{18}\text{O}$ in the Sava River and all groundwaters laid above the LMWL for Zagreb precipitation from 2010 (Fig. 3) and was described as $\delta^2\text{H} = (7.5 \pm 0.3) \delta^{18}\text{O} + (8.2 \pm 2.6)$, $n = 47$, $R = 0.972$. This relation could be compared with the long-term (1981–2006) LMWL for precipitation in Ljubljana, Slovenia: $\delta^2\text{H} = (8.1 \pm 0.1) \delta^{18}\text{O} + (9.8 \pm 0.7)$, $n = 290$, $R = 0.99$ (Vreca et al. 2008). Ljubljana is geographically much closer to the springs of the Sava River than Zagreb and

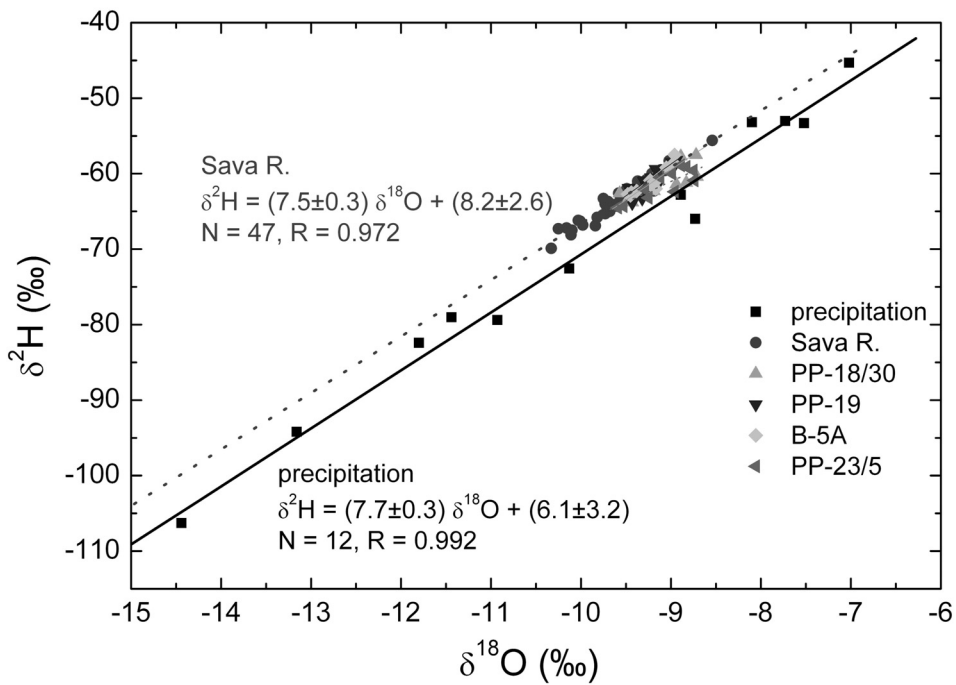


Fig. 3
 Relation between $\delta^{18}\text{O}$ and $\delta^2\text{H}$ in the Sava River and in groundwaters of the Petruševac aquifer during 2010

therefore the LMWL for Ljubljana precipitation better describes the stable isotopic composition of the Sava River recharge area. All groundwater values laid very close to the correlation line of the Sava River (Fig. 3) showing direct influence of the Sava River on the groundwater of the Petruševac aquifer. Differences in monthly variations of $\delta^{18}\text{O}$ values between particular wells (Table 2), together with ^3H activities, indicated different infiltration times of surface water of the Sava River to different wells of the Petruševac aquifer: the wells B-5A and PP-19, which showed the slowest response to the changes in ^3H in the Sava River, had also the smallest standard deviations and narrow range of the $\delta^{18}\text{O}$ values.

Conclusions

Results of measurements of ^3H and stable isotopes $^2\text{H}/^1\text{H}$ and $^{18}\text{O}/^{16}\text{O}$ in precipitation, the Sava River and groundwaters from the Petruševac aquifer in the Zagreb area showed the following:

The isotopic water line ($\delta^2\text{H}$ vs. $\delta^{18}\text{O}$ relation) of the Sava River was closer to the Local Meteoric Water Line for Ljubljana precipitation than that for Zagreb precipitation indicating the source of river water. The time series of stable isotope composition of groundwater followed that of the Sava River showing a direct influence of the river on the groundwater of the Petruševac aquifer.

Significantly higher ^3H activity of the Sava River in June 2010 indicated the influence of the release of tritiated water from the Nuclear Power Plant Krško. Maximal ^3H activity was detected 1–2 days after the release.

Increase in ^3H activities in groundwater of the Petruševac aquifer was less pronounced and showed different time delay of 3 to 5 months for different wells. Intensity and time delay of the response could be correlated to the depth of the wells and the distance from the Sava River. This observation pointed to some differences in the infiltration time of the water from the Sava River to individual wells.

In this case ^3H has been proven to be a good environmental tracer for determination of the transit time of the river water to the aquifer. The results of ^3H and stable isotopes $^2\text{H}/^1\text{H}$ and $^{18}\text{O}/^{16}\text{O}$ will be used for modelling the transit time of the Sava River water to the groundwater reservoirs/aquifers.

Acknowledgements

We thank dipl.ing. Branka Jakuš, Mira Mihovec Grdic and Mladen Klemar, from water supply company "Vodoopskrba i odvodnja", Zagreb, for help in water sampling of aquifer Petruševac and for data about the aquifer. This work was performed as a part of the IAEA Project RER/8/016 and the Project 098-0982709-2741 from the Ministry of Science, Education and Sport.

References

- Barešić, J, N. Horvatinčić, I. Krajcar Broić, B. Obelić, J. Kozar-Logar 2011: Tritium activity measurement of water samples using liquid scintillation counter and electrolytical enrichment. – Proceedings of the 8th Symposium of Croatian Radiation Protection Association, Krk, Croatia, 13–15 April, 2011. HDZZ, Zagreb, 2011. pp. 461–467.
- IAEA/WMO, 2011. Global Network of Isotopes in Precipitation. The GNIP database. Accessible at: <http://isohis.iaea.org> and <http://nds121.iaea.org/wiser/index.php> (9 May 2011)
- Rozanski, K., R. Gonfiantini, L. Araguas-Araguas 1991: Tritium in the global atmosphere: distribution patterns and recent trends. – *J Phys G: Nucl Part Phys* 17, pp. 523–536.
- Stepišnik, M. 2011: Sava. – In: Stepišnik, M., B. Zorko (Eds): Assessment of the influence of radioactivity in the environment of the Nuclear Power Plant Krško on the public. Jozef Stefan Institute, Ljubljana, Slovenia 2011, pp. 1–18. (In Slovene.)
- Vreča, P., I. Krajcar Bronić, N. Horvatinčić, J. Barešić 2006: Isotopic characteristics of precipitation in Slovenia and Croatia: Comparison of continental and maritima stations. – *J. Hydrology*, 330, pp. 457–469.
- Vreča, P., I. Krajcar Bronić, A. Leis, M. Brencić 2008: Isotopic composition of precipitation in Ljubljana (Slovenia). – *Geologija*, (Ljubljana) 51/2, pp. 169–182.

Isotopic study of nitrates and bicarbonates in mineral waters of the Southeast Poland

Anna Baran

*The Institute of Technical Engineering, Father Bronislaw
Markiewicz Vocational State University, Jaroslaw*

The territory of Southeast Poland, and especially its southern part, is rich in various mineral and therapeutic waters of high quality. The balneological resources of the region and in particular its mineral and therapeutic waters of Iwonicz Spa, Lubatówka and Horyniec Spa are exceptionally precious.

Isotope studies of $\delta^{13}\text{C}$ in bicarbonate ions were conducted, and they were used to prove the hypothesis about the origin of the Iwonicz Spa and Lubatówka water. The observed variation of $\delta^{13}\text{C}$ in bicarbonate ion ranges from -5.0 to $+24.0$ per mill PDB.

On the other hand, isotope methods with double markers, $\delta^{15}\text{N}$ and $\delta^{18}\text{O}$ in NO_3^- ions were used to identify the origin of nitrates in Iwonicz Spa and Horyniec Spa waters. Because nitrates from different sources have different isotope compositions, it is possible to test the quality of water and identify alteration processes of nitrate compounds in the aquifer. For these purposes the studies of nitrates isotope composition were conducted for the first time in the selected waters of the investigated region. $\delta^{15}\text{N}$ and $\delta^{18}\text{O}$ in the NO_3^- ions prove that these nitrates are derived from soil organic compounds. It is not possible to estimate the advancement of the alteration processes of nitrogen compounds (mainly nitrification) at this stage of studies.

The author has also identified reducing-oxidizing conditions in the aquifer because they influence hydro-geochemical processes and migration of elements.

Address: A. Baran: 37-500 Jaroslaw, Poland, e-mail: annabaran1212@o2.pl

Error in variables regression model for meteoric water line determination

Mihael Brenčič

*Department of Geology & Department of Hydrogeology,
Faculty of Natural Sciences and Engineering,
University of Ljubljana, Ljubljana
Geological Survey of Slovenia, Ljubljana*

Since the very beginning of the stable isotope investigations it was established that $\delta^2\text{H}$ and $\delta^{18}\text{O}$ are interrelated and their relation reflects certain processes which can help to track the history of water path through the hydrological cycle. It was Craig (1961) who first discovered a global relation between $\delta^2\text{H}$ and $\delta^{18}\text{O}$ and illustrated its relative stability. This relation can be described as the global meteoritic water line with relation $\delta^2\text{H} = 8 \delta^{18}\text{O} + 10$. Several authors have studied distribution of local characteristics of $\delta^2\text{H}$ and $\delta^{18}\text{O}$ in precipitation as well as in various water bodies. It was determined that relation between $\delta^2\text{H}$ and $\delta^{18}\text{O}$ can depend on locality and these relations are defined as local meteoritic water lines.

In isotope hydrology the relation between $\delta^2\text{H}$ and $\delta^{18}\text{O}$ variables is usually estimated by orthogonal regression. The application of this regression analysis is a mutual agreement among isotope hydrologists. However, detailed inspection of statistical principles of the regression analyses when both variables in the model are subject to error, as it is the case of $\delta^2\text{H}$ and $\delta^{18}\text{O}$ variables, shows that orthogonal regression can be questionable.

The paper discusses determination and illustrates the application of error in variables regression model in relation to the meteoritic water line. Errors in variables regression model are mathematically and statistically more correct than other regression models, however it poses several problems in its application to stable isotope hydrology. The model is compared and discussed in comparison with other "unsuitable" regression models frequently applied in the isotope hydrology literature.

Address : M. Brenčič: Privoz 11, SI-1000 Ljubljana, e-mail: mihael.brencic@ntf.uni-lj.si

Stable isotope feature of groundwaters from Graciosa volcanic Island (Azores) – preliminary results

Paula M. Carreira
Instituto Tecnológico e Nuclear, Sacavém, Portugal

José Manuel Marques
Instituto Superior Técnico, Lisboa, Portugal

Maria do Rosário Carvalho
Faculdade de Ciências de Lisboa, Lisboa, Portugal

Fausto Grassa, Giorgio Capasso
*Instituto Nazionale di Geofisica e Vulcanologia
Sezione di Palermo, Palermo, Italy*

Dina Nunes
Instituto Tecnológico e Nuclear, Sacavém, Portugal

Joao Carlos Nunes
*Universidade dos Açores & INOVA Institute,
S. Miguel, Azores, Portugal*

The Azores archipelago is made of nine islands all of volcanic origin and a few islets located in the North Atlantic Ocean, about 1800 km west of Portuguese mainland at the triple junction of the Eurasian, North American and Nubian plates (Azores Triple Junction = ATJ). Graciosa Island is part of the Central Group of Azores archipelago and is located on the Terceira Rift, a major tectonic feature of the ATJ. The main hydrothermal manifestations at Graciosa Island occur in the Caldeira volcano (SE part of the island), and particularly inside the huge (150 m wide, 80 m high) Furna do Enxofre lava cave located in the Caldeira, where a bubbling mud pool releases steam and gases, leading to the accumulation of CO₂ at the bottom of the cave, filled by a coldwater subterranean lake. Three field work campaigns were carried out at Graciosa Island and 14 water samples have been collected, from boreholes, springs and the subterranean lake for isotopic (¹⁸O, ²H and ³H) and chemical analysis. The groundwater samples were plotted along the GMWL, and two water groups were identified in the δ¹⁸O vs. δ²H diagram. The splitting up of the samples is even more visible when the O-18 content is plotted as a function of the temperature or as a function of the electrical conductivity. Besides the differences in mineralization and temperature observed in the groundwater samples from Graciosa Island, an isotopic shift towards more enriched values is also observed. The salinity and isotopic content seems to indicate not a simple mixture between two end-members, i.e. seawater – fresh water: another process of mineralization and isotope enrichment must be considered in this active volcanic environment. A hypothesis to be formulated is that the source of salts could be associated to mixing with boiling seawater, that by evaporation will be able to: i) increase groundwater salinity, ii) strongly change the ²H content to more enriched values, and iii) absent or limited variation in δ¹⁸O content.

Address of corresponding author: P.M. Carreira: Estrada Nacional no 10, 2686-953 Sacavém, Portugal, e-mail: carreira@itn.pt

Determining forest turbulent transport and evapotranspiration partition with the help of a new soil water isotope model

Matthias Cuntz

*UFZ – Helmholtz Centre for Environmental Research,
Leipzig*

Vanessa Haverd

*CSIRO Marine and Atmospheric Research,
Canberra*

David W Griffith

University of Wollongong, Wollongong

Claudia Keitel

University of Sydney, Sydney

Carol Tadros, John Twining

*Australian Nuclear Science and Technology
Organisation (ANSTO), Menai*

We determine the profile of turbulent transport and evapotranspiration ET partition in an Eucalypt forest for a two-week period. We therefore optimise agreement between modelled and measured vertical profiles of temperature T , water vapour H_2O , carbon dioxide CO_2 , and deuterium content of water vapour HDO . Modelling was done by a Soil Vegetation Atmosphere Transfer (SVAT) model, enhanced by a new scheme for coupled transport of heat, water and stable isotopes in soil and litter.

We first present the new water isotope model Soil-Litter-Iso. Deuterium contents (δD) of soil evaporation and vertically-resolved transpiration are then derived using the SVAT model as prior estimates for the optimisation. An advection-diffusion description is used in the SVAT model for the isotopic composition of transpiration, and Soil-Litter-Iso is used for isotopes in soil evaporate.

Predictions of δD in soil evaporate were validated using soil chamber measurements, while the transpirates were validated using isotopic analyses of leaf and xylem water, combined with leaf-level gas exchange measurements. Hence, modelled energy, water and trace gas concentration profiles are generated using Lagrangian dispersion theory combined with source/sink coming from the SVAT model. Optimisation of turbulent transport and ET partition was then performed twice, once with and once without profiles of δD of water vapour. The modelled concentration profiles resulting from inclusion of δD demonstrate our ability to make consistent estimates of both the source distributions and δD of the water vapour sources. However, introducing measurements of δD in water vapour does not significantly alter resulting estimates of turbulent transport and the ET partition, suggesting that the additional data and modelling required to use deuterium are not warranted for the purpose of partitioning ET using the framework presented here.

Address of corresponding author: M. Cuntz: Permoserstr. 15, 04318 Leipzig, Germany
e-mail: matthias.cuntz@ufz.de

Stable isotope composition of carbon dioxide and TDIC reservoir associated with mineral waters of the Polish Flysch Carpathians

Marek Dulinski

*Faculty of Physics and Applied Computer Science,
AGH University of Science and Technology, Kraków*

Lucyna Rajchel, Jacek Rajchel

*Faculty of Geology, Geophysics and Environmental
Protection, AGH University of Science and
Technology, Kraków*

Mineral waters widely occurring in the Polish Flysch Carpathians owe their high mineralization to the presence of geogenic carbon dioxide. For several decades origin of gaseous CO₂ in this area has been a subject of many controversies. Early hypotheses pointed to mantle origin of CO₂. Results of ³He-²⁰Ne analyses performed at the end of the last century suggest that the mantle component in the total geogenic flux of CO₂ is in the order of several per cent. Between 1997 and 2004, 20 samples of TDIC and 41 samples of gaseous CO₂ from 36 sources representing boreholes, springs and "dry exhalations" have been analysed. Measured δ¹³C values of gaseous carbon dioxide are within the range between -5.8 to -1.0‰, pointing to thermal decomposition of crustal carbonate rocks as the primary source. The carbon isotope composition of TDIC reservoirs (δ¹³C) calculated from molalities of individual carbon species in waters are out of isotopic equilibrium with gaseous CO₂ present in the area. Oxygen isotope composition of gaseous CO₂ is also out of equilibrium with mineral waters at the measured temperatures, although distinct trend towards equilibrium is observed for number of waters with different isotopic composition.

Address of corresponding author: M. Dulinski: al. Mickiewicza 30, 30-059 Kraków, Poland
e-mail: dulinski@novell.ftj.agh.edu.pl

Assessing the impacts of anthropogenic activities on groundwater quality using nitrogen isotopes – Alter do Chão-Monforte (Portugal)

Paula Galego Fernandes, Maria Rosário Carvalho, Catarina Silva
Centro Geologia, Faculdade de Ciências da Universidade de Lisboa, Lisboa

The Alter do Chão-Monforte aquifer is composed by Cambrian carbonate formations and Pre-Variscan basic igneous complex. The groundwater flow in the Alter do Chão-Monforte aquifer (Alentejo, Portugal) is quite influenced by the lithology and structural features. The aquifers are unconfined with a mixed karstic-fissured circulation. Direct recharge is important and natural discharge is from springs located in the contact of limestones with the fissured rocks. This aquifer system represents one of the main water resources of this region, located in an area of intensive agriculture and cattle breeding, generating growing nitrate pollution problems.

The use of isotope techniques is an important tool to evaluate aquifers contamination origin, so 14 groundwater samples were collected from wells, drilled wells and springs for chemical and isotopic analysis ($\delta^{18}\text{O}$ and $\delta^{15}\text{N}$ of NO_3 and $\delta^2\text{H}$ and $\delta^{18}\text{O}$ of H_2O).

The major sources of nitrate, responsible for the water resources degradation present isotopically distinct $\delta^{15}\text{N}$ values. Using these features, stable nitrogen isotopes can offer a direct way of source identification. The relative contribution of the different sources to groundwater or surface water can be estimated by mass balance. However, in some situations, such as soil-derived nitrate and fertilizer, nitrate shows overlapping $\delta^{15}\text{N}$ values, preventing their separation using $\delta^{15}\text{N}$ alone. Thus, the analysis of $\delta^{18}\text{O}$ of nitrate in conjunction with $\delta^{15}\text{N}$ is fundamental to improve the ability to trace nitrate origins. From the dual isotope study of groundwater nitrate conducted in Alter do Chão-Monforte region, proved to be useful in source identification allowing for establishing the manure and septic waste and N soil as the main nitrate sources in the analysed waters. The samples with nitrates derived from manure and septic waste are mainly located near cattle breeding activities. This study allowed identifying nitrogen sources and assessing agriculture, cattle breeding, urban and industrial contributions to nitrogen cycle in Alter do Chão-Monforte groundwater ecosystem, based on the fact that the main sources of nitrate in the area have distinct $\delta^{15}\text{N}$ and $\delta^{18}\text{O}$ values.

Address of corresponding author: P. G. Fernandes: Bloco C6 - 3 Piso, Campo Grande,
1749-016 Lisboa, Portugal, e-mail: ppfernandes@fc.ul.pt

$\delta^{18}\text{O}$ spatial distribution of precipitation in Croatia

Tamara Hunjak, Diana Mance
*Stable Isotope Laboratory, Medical Faculty,
Rijeka University, Rijeka*

Hans O. Lutz
*A Stable Isotope Laboratory, Medical Faculty,
Rijeka University, Rijeka*

Physics Faculty, Bielefeld University, Bielefeld

Zvezdana Roller-Lutz
*Stable Isotope Laboratory, Medical Faculty,
Rijeka University, Rijeka*

The precipitation as the input into the water system and its stable isotope composition is a basic part whose knowledge is required for proper use and management of water resources. The geomorphology of Croatia (e.g. high mountains next to the sea) can cause specific local conditions. We have monitored the stable isotopic composition ($\delta^{18}\text{O}$ and $\delta^2\text{H}$) of precipitation in more than 25 stations in various locations at different altitudes. For the work reported here, only those data sets are used that span at least one year, altogether 22 stations. The $\delta^{18}\text{O}$, $\delta^2\text{H}$ and d-excess altitude effects have been extracted from the measured data base of precipitation isotope ratios. This data base has been used to produce a gridded map of $\delta^{18}\text{O}$ for Croatia.

Address of corresponding author: T. Hunjak: Brace Branchetta 20, Rijeka, Croatia
e-mail: thunjak@medri.hr

The effect of the mutual interaction between climate change and the land-use pattern on the hydrologic regime under dry-land conditions

Joel R. Gat

*Department of Environmental Sciences
and Energy Research; Weizmann Institute
of Science, Rehovot*

Under a given land-use pattern the response of the hydrological regime to climate change, and in particular to changes in precipitation and temperature, is well documented for different climate regions and can be monitored by the response of the ITF (the Isotope Transfer Function) to the transition from precipitation to either surface runoff or groundwater recharge.

Changes in the land-use pattern (be it deforestation, agricultural activity or urbanization) similarly affect the hydrological regime and its isotopic signature, in particular the partitioning of the incoming precipitation into evapotranspiration, surface runoff or groundwater recharge fluxes, respectively. An additional anthropogenic factor of great relevance under dry-land conditions is provided by the introduction of extraneous water resources via irrigation practices, canalization or the use of recycled or desalinized water sources, thus profoundly affecting the isotopic signature of the water resources.

The inter-dependence between the changes in land-use pattern and the climate regime has also to be recognized when considering the isotopic response of the hydrologic systems. The most dramatic effect is to be expected under semi-arid conditions as these can then be converted to more moist or dry-land conditions, respectively, as a result of changes of the climate pattern.

Address of corresponding author: J. R. Gat: 76100 Rehovot, Israel, e-mail: joel.gat@weizmann.ac.il

Hydrogeochemistry of Alpine springs from North Slovenia: insights from stable isotopes

Tjaša Kanduč
*Department of Environmental Science,
Jožef Stefan Institute, Ljubljana*

Nataša Mori
*Department of Freshwater and Terrestrial
Ecosystems research, National Institute of Biology,
Ljubljana*

David Kocmanan, Vekoslava Stibilj
*Department of Environmental Science,
Jožef Stefan Institute, Ljubljana*

Fausto Grassa
*Istituto Nazionale di Geofisica e Vulcanologia
Sezione di Palermo, Palermo*

Hydrochemistry and stable isotope compositions of karst spring waters provide critical information regarding sources of groundwater recharge and water-rock interaction along flow paths.

The investigated Alpine springs in Slovenia represent waters strongly influenced by chemical weathering of Mesozoic limestone and dolomite, only one spring was located in Permo-Carbonian shales. The carbon isotopic composition of dissolved inorganic carbon (DIC) and suspended organic carbon (POC) as well as major solute concentrations yielded insights into the origin of carbon in Alpine spring waters. The major solute composition was dominated by carbonic acid dissolution of calcite. Waters were generally close to saturation with respect to calcite, and dissolved CO₂ was up to fortyfold supersaturated relative to the atmosphere. The $\delta^{13}\text{C}$ of DIC ranged from -15.8‰ to -1.5‰ and indicated less and more vulnerable aquifers. Mass balances for spring waters draining carbonate rocks suggest that carbonate dissolution contributes from about 49% to 86% and degradation of organic matter from 13.7% to 51.4%, depending on spring and its relation with geological composition. Isotopic composition of oxygen ($\delta^{18}\text{O}_{\text{H}_2\text{O}}$), and tritium values range from -12.2 to -9.3‰ , and from 6.4 to 9.8 TU, indicate recharge from precipitation. Residence time and age of spring water are related to distance of flow path of groundwater and mixing with older water retained in Alpine slopes from recharge to emerge.

Address of corresponding author: T. Kanduč: Jamova cesta 39, Ljubljana 1000, Slovenia
e-mail: tjasa.kanduc@ijs.si

Estimation of groundwater transit time by lumped parameter model using $\delta^{18}\text{O}$ on Szentendre Island, Hungary

Krisztina Kármán
*Institute for Geochemical Research,
Hungarian Academy of Sciences, Budapest*

Piotr Maloszewski
*Helmholtz Zentrum München, Institut für
Grundwasserökologie, Ingolstädter*

ELTE TTK, Lithosphere Fluid Research Lab., Budapest

István Fórizs
*Institute for Geochemical Research,
Hungarian Academy of Sciences, Budapest*

József Deák
GWIS Kft., Dunakeszi

Csaba Szabó
ELTE TTK, Lithosphere Fluid Research Lab., Budapest

The drinking water of Budapest is mainly supplied from the good quality riverbank filtration system of the Szentendre Island. It is important to know the transit time and dispersion of the water from the Danube to the production wells and the dilution of a potential pollution for the safe operation of the system.

In this paper we examined a multiple collector well on the Szentendre Island. Water samples were taken from the collector well as well as the Danube River (near the well) 4–5 times a week between 24 February and 31 May 2011 for oxygen isotopic measurements. We also measured the background water of the island which could mix to the water of the collector well. The measured $\delta^{18}\text{O}$ value of the well was compared with the expected composition of the well by a lumped parameter model. The lumped parameter model is the most widely used method for the interpretation of stable isotopic data.

Although in the sampled period the oxygen isotopic composition of the Danube water (between -10.40‰ and -11.1‰) and the background water (-10.40‰) were close to each other, certainly the portion of the Danube water was dominant ($> 93\%$) in the collector well. The oxygen isotopic composition of the collector well water changed between -10.48‰ and -10.93‰ . The transit time of the water from the Danube to the collector well is 17–18 days by the lumped parameter model, which is realistic, considering other case studies. The dispersion of the geological settings is $P_D=0.8$. The water level of the Danube was stagnant in the measured period. Refining the results it would be important to use other input parameters (tritium, chemistry, temperature, etc.) and compare the results with other models.

The authors would like to say thanks to the RER/8/016 project at International Atomic Energy Agency.

Address of corresponding author: K. Kármán: H-1112 Budapest, Budaörsi út 45, Hungary
e-mail: karman@geochem.hu

Isotopic investigations on some mineral waters from Corund, Harghita County, Romania

Boglárka Mercedesz Kis
*Faculty of Environmental Science and Engineering,
Babes-Bolyai University, Cluj-Napoca*

Krisztina Kármán
*Institute for Geochemical Research, Hungarian
Academy of Sciences, Budapest*

Calin Baciú
*Faculty of Environmental Science and Engineering,
Babes-Bolyai University, Cluj-Napoca*

Corund village is located on the eastern side of the Transylvanian Basin, southwest of the volcanic plateau of Gurghiu Mts., in the catchment of Corund River, at an elevation of 590 m. From a geological point of view, the study area consists of three major types of rocks: Middle Miocene (Badenian) salt deposits of the Transylvanian Basin, Pannonian sediments mainly represented by marls, salty and carbonated clays and sandstones, and the products of the Neogene volcanic activity of the Gurghiu Mts. aged 9.4–5.4 Ma. Along the valleys, Quaternary alluvial deposits are also present. At the southern part of the area, mineral water springs are carbonated-ferrous and fizzy with mineralizations between 379–1800 mg/l. On the northern part, the springs are carbonated-salty and fizzy with high mineralizations (134,000–142,000 mg/l). Significant CO₂ contents can be measured at each source (704–1,760 mg/l), with pH ranging between slightly acidic to neutral (5.2–6.8) values.

We sampled the Corund River and 8 springs on 11 March 2011. The oxygen vs. hydrogen isotopic compositions of the Corund River and the Dióvápai spring, Árcsó spring-1, Árcsó spring-2 and Cseredombi spring were lying on the GMWL. The $\delta^{18}\text{O}$ and δD values varied from -10.6 to -9.2‰ , and from -76 to -67‰ , respectively. It means that the river and these springs originate from local precipitation. The high conductivity could be due to the leakage through the volcanic tuffs and subordinately limestones. These springs are on the southern part of the area. Szőlő-máli spring is a large open hole, thus its isotopic composition indicates evaporation effect. The stable isotopic compositions of the Unnamed Spring, Csigadomb spring and Salty fountain are very peculiar: their $\delta^{18}\text{O}$ values vary from $+7.4$ to $+8.6\text{‰}$, while their δD values are the same (cca. -21‰) within the analytical uncertainty. These springs may have been affected by fractionation during the dissolution of salt, largely changing the isotopic composition, or alternatively, these springs may be fossil evaporated seawater. These springs are on the northern part of the area.

Address of corresponding author: B. M. Kis: Mihail Kogălniceanu 1 Street, 400084 Cluj-Napoca, Romania; e-mail: hawki@yahoo.com

Quantitative assessment of lake water balance components: new calculation approach

Dominika Lewicka-Szczebak, Mariusz-Orion Jędrysek
*Laboratory of Isotope Geology and Geoecology, Institute of Geological Sciences,
University of Wrocław, Wrocław*

The study aimed at the application of oxygen and hydrogen stable isotopic analyses of lake waters, groundwaters and precipitation waters to quantitatively assess the magnitude of lake water balance components, i.e. amount of water supply, evaporation and outflow to groundwater aquifers. The field studies were carried out within the mining area of Lignite Mine Konin and on the neighbouring Powidzkie Lakes, central Poland, from October 2007 to April 2009. $\delta^2\text{H}$ and $\delta^{18}\text{O}$ values of precipitation waters vary from -140 to $+13\text{‰}$ and from -19.3 to 7.6‰ , for lake waters from -44 to -21‰ and from -5.2‰ to -1.7‰ , and for groundwaters from -10.2 to -6.5‰ and from -75 to -42‰ , respectively.

The isotopic data obtained have been applied to calculate the lakes' water balance using the Craig-Gordon model and isotopic mass balance. The equations of isotopic mass balance have been modified to construct an original calculating method, based on the coupled usage of $\delta^2\text{H}$ and $\delta^{18}\text{O}$ values. Applying this new calculating approach allowed to obtain more precise and lake-specific water balance components, when compared to the commonly used calculation approach based on separate usage of 2 equations (distinct for H and O isotopes). Moreover, the proposed method enable the simultaneous calculation of 3 unknown lake water balance components (i.e. evaporation, input and outflow amount) based entirely on isotopic signatures of lake waters and precipitation. The isotopic signature of groundwaters reinforced the conclusions driven from lake water balance calculations concerning the amount of lake waters outflow (from the particular lake) to groundwater aquifers.

Address of corresponding author: D. Lewicka-Szczebak: Cybulskiego 30, 50-205 Wrocław, Poland
e-mail: dominika.lewicka@ing.uni.wroc.pl

Strontium isotopic ($^{87}\text{Sr}/^{86}\text{Sr}$) and geochemical signatures of CO_2 -rich thermal and mineral waters (N-Portugal)

José Manuel Marques
*Centro de Petrologia e Geoquímica,
Instituto Superior Técnico, Lisboa*

Paula Mimo Carreira
Instituto Tecnológico e Nuclear, Sacavém

Hermanus Gerardus Maria Eggenkamp
*Centro de Petrologia e Geoquímica
Instituto Superior Técnico, Lisboa*

Manuel Antunes da Silva
Unicer Bebidas, S.A., S. Mamede de Infesta

Luís Aires-Barros
Centro de Petrologia e Geoquímica Instituto Superior Técnico, Lisboa

The main objective of this study was to use Sr isotopic and geochemical signatures to improve knowledge on the relation between hot (Chaves – 76 °C) and cold (Vilarelho da Raia, Vidago and Pedras Salgadas – 17 °C) CO_2 -rich mineral waters discharging at the northern part of Portuguese mainland. The regional geology is dominated by Hercynian granites (syn-tectonic–310 Ma and post-tectonic–290 Ma) and Silurian metasediments (quartzites, phyllites and carbonaceous slates). The thermomineral waters have $^{87}\text{Sr}/^{86}\text{Sr}$ isotopic ratios between 0.716713 and 0.728035. The plot of $^{87}\text{Sr}/^{86}\text{Sr}$ vs. $1/\text{Sr}$ for the hot and cold mineral waters shows a decrease in the $^{87}\text{Sr}/^{86}\text{Sr}$ values from the north to the south due to the interaction with young granitic rocks having lower $^{87}\text{Sr}/^{86}\text{Sr}$ ratios. In such diagrams, the scattering of the Sr data can be understood through the existence of three end-members (Vilarelho da Raia/Chaves, Vidago and Pedras Salgadas) of a concentration trend, from the rain waters towards the CO_2 -rich thermal and mineral waters, suggesting different underground flow paths. In fact, the plot of $^{87}\text{Sr}/^{86}\text{Sr}$ vs. $(\text{Ca}+\text{Mg})/\text{HCO}_3$ shows the same three end-members, being the Vidago and Pedras Salgadas CO_2 -rich mineral waters characterized by higher $(\text{Ca}+\text{Mg})/\text{HCO}_3$ ratios and lower $^{87}\text{Sr}/^{86}\text{Sr}$ values. This trend could be ascribed to: i) the fact that in CO_2 -rich hydromineral systems, low temperatures enhance water-rock interaction (with a special emphasis on Ca and Mg increasing in waters), and ii) the fact that in the case of Vidago and Pedras Salgadas CO_2 -rich mineral waters, the recharge areas are characterised by the presence of highly fractured quartzites with $^{87}\text{Sr}/^{86}\text{Sr}$ ratios around 0.726642, while in Vilarelho da Raia / Chaves the recharge areas are within granitic rocks with much higher $^{87}\text{Sr}/^{86}\text{Sr}$ ratios (from 0.743689 up to 0.789683). These values also indicate that no equilibrium was reached between the CO_2 -rich thermal and mineral waters and the granitic rocks. In fact, the mean Sr isotopic ratio of the thermal and mineral waters ($^{87}\text{Sr}/^{86}\text{Sr}_{\text{mean}} = 0.722419$) is similar to the Sr isotopic ratios of the plagioclases of the granitic rocks (from 0.71261 to 0.72087).

Address of corresponding author: J. M. Marques: Av. Rovisco Pais, 1049-001 Lisboa, Portugal
e-mail: jose.marques@ist.utl.pt

Application of isotopes for assessment of pollution probability of drinking water resources in Georgia

George I. Melikadze
*Institute Geophysics Ivane Javakishvili
Tbilisi State University, Tbilisi*

The Tbilisi-Baku-Ceyhan crude oil pipeline has been laid over several groundwater recharge areas in Georgia. Since the time of planning, and even after its opening, there are intensive discussions on the possibility of ecological catastrophe in the case of its damage (spilling) at some areas. One of such most complicated and extremely responsible sections lies within the geomorphologically dangerous Borjomi area, where the problem is connected to possible pollution of drinking groundwater source from lava layer at Bakuriani-Tsikhisjvari area by oil-products. In order to study the possibility of spoiling of drinking water in Borjomi area a conceptual model of water flows has been developed with special focus on 1) the interactions of the rivers and mineral springs with the surrounding aquifers; 2) use of nuclear techniques (natural isotopes) and geophysical prospecting in selected areas for investigation of the recharge and discharge areas of the groundwater and possible propagation directions of pollution; 3) compile numerical hydrogeological model of catchment and organize the control system against possible drinking water pollution.

Address: G.I. Melikadze: 1, Aleksidze Str., 0171, Tbilisi, Georgia
e-mail: g.melikadze@seismo.ge

Relationship between atmospheric circulation and stable isotope composition of Belgrade daily precipitation

Nada Miljević, Ana Pešić,
*Jaroslav Černi Institute for Development
Water Resources, Belgrade*

Dušan Golobocanin
Vinča Institute for Nuclear Sciences, Belgrade

Zoran Gršić
Nuclear Facilities of Serbia, Belgrade

Miroslava Unkašević, Ivana Tošić
*Institute of Meteorology, Faculty of Physics,
University of Belgrade, Belgrade*

Factors that control stable isotopic compositions ($\delta^2\text{H}$ and $\delta^{18}\text{O}$) of meteoric precipitation involve fractionation processes associated with the evaporation and condensation history of the precipitating water vapour.

Daily precipitation were collected in the period from May to December 2010 as well as the corresponding meteorological data (air temperature, humidity, amount of precipitation) in Vinča Institute of Nuclear Sciences (44°45'33" N, 20°35'57" E), Belgrade, Serbia. Our goal was to collect the sample representing the precipitation that had fallen over the previous 24-hour in the order to understand the relationship between atmospheric circulation and stable isotope content of individual precipitation events. However, during weekends and holidays precipitation was collected as a composite sample. The highest daily $\delta^{18}\text{O}$ and ^2H values were measured on 9 December (-1.3‰ and -8.7‰), respectively, whereas the lowest values were measured on 28 December (-143.2‰ and -19.3‰), respectively. Circulation back trajectories, weather maps, and $\delta^2\text{H}$ and $\delta^{18}\text{O}$ values for 69 precipitation samples were examined to determine the circulation type for each event.

Address of corresponding author: N. Miljevic: Jaroslava Černog 80, 11226 Belgrade, Serbia
e-mail: emiljevi@vinca.rs

Hydrogeochemical and isotopic assessment of seawater intrusion into alluvial aquifers in the Western Algiers coastal area (Tipasa, Algeria)

Adnane S. Moulla
*Dating & Isotope Tracing Dept.,
Algiers Nuclear Research Centre, Algiers*

Abdelhamid Guendouz
*Blida University, Engineering and Science Faculty,
Blida*

Mouloud Belaidi, Hayet Maamar
National Agency for Water Resource, Blida

SidAli Ouarezki
*Dating & Isotope Tracing Dept.,
Algiers Nuclear Research Centre, Algiers*

Western Algiers coastal region that extends up to the city of Tipasa is known for both tourists and agricultural vocations. It is composed of three alluvial valleys, namely Wadi El-Hachem, Wadi Mazafran and Wadi Nador. These three small catchments being exorheic, the alluvial aquifers that they host are thus very likely to be subjected to a saline hazard through seawater encroachment. Besides industrial and agricultural developments, unrestrained demographic growth has induced important needs for freshwater. Unfavourable climatic conditions causing long period droughts have predictably led to a contamination of coastal groundwaters along the Mediterranean by ingressive seawater. Intensive pumping practices in use for the sake of securing water allocation for both populations and agriculture have drastically affected the groundwater reserves through overexploitation of the resource creating a consequent drawdown in the water table. During the dry season, the mobile fresh/sea water interface moves forward farther inland contaminating wells and boreholes. Two out of the three valleys that are present in the investigated sector were targeted by the present study. Two approaches making use of both hydrochemical and isotopic tools were applied to assess the extent of seawater intrusion. For Wadi Nador, the Br vs. Cl plot showed that the points align in a parallel way to seawater dilution line confirming thus a marine origin for those elements. Na/Cl ratio vs. Cl plot brings to the fore two poles of points: one composed of shallow unaffected groundwater and a second one composed of deeper boreholes and wells for which seawater is present to different extents. This is further confirmed by isotopes which exhibited a wide range of values mirroring the affected and unaffected areas as well as those points submitted to intermingling between different end-members.

Address of corresponding author: A. S. Moulla: PO Box 399, Alger-RP, Algiers, 16000, Algeria
e-mail: asmoulla@gmail.com

Isotopic composition of sulphates dissolved in waters of deep aquifers associated with copper ore deposits: implications for sulphate source and water-rock interaction

Adam Porowski, Jan Dowgiallo
Institute of Geological Sciences PAS, Warsaw

Stanislaw Halas
*Mass Spectrometry Laboratory, Faculty of Physics,
Lublin*

Roman Becker
Polish Copper Consortium KGHM PM S.A., Lublin

In Europe the largest resources of copper ore occur in SW Poland in the area of Foresudetic Monocline. The main copper-rich sediments constitute the lowermost part of the Zechstein sedimentary formation of Permian age. As much as seven water-bearing horizons are drained in the mines. They constitute multiaquifer systems of Paleogene-Neogene, Triassic and Permian (Rotliegend and Zechstein). Geochemical studies of drainage waters shows that water-bearing horizons remain in hydraulic connections. Sulphur and oxygen isotope analyses of dissolved sulphates were used to determine the sources of sulphate mineralization and processes affecting the distribution of sulphate concentration in drainage waters. Chemical and isotopic (O and H) composition of drainage waters revealed that all of them form two distinct groups. Brackish waters of $\text{SO}_4\text{-HCO}_3\text{-Ca-Na}$ and $\text{SO}_4\text{-Cl-Ca-Na}$ type and isotopic composition very close to the water of modern hydrological cycle form the first group. $\delta^{34}\text{S}$ and $\delta^{18}\text{O}$ values of dissolved sulphates are in the range of 12.05–15.94‰ and 11.07–16.57‰, respectively, are almost identical with S and O isotopic composition of Zechstein anhydrites indicating that their dissolution is the main source of sulphates. Saline waters and brines (TDS in the range 57.9–262.2 g/dm³) of Na-Cl type form the second group of drainage waters. Their ^{18}O and ^2H content locates them in the upper parts of GMWL strongly suggesting their palaeo-infiltration origin. $\delta^{34}\text{S}$ and $\delta^{18}\text{O}$ values of dissolved sulphates show large variability, from 3.34 to 13.03‰ and from 5.87 to 15.29‰, respectively. This suggests multiple origin of sulphates mineralization. Some of the brines studied gained their sulphate mineralization from dissolution of anhydrites or gypsum. The presence of recrystallization processes connected with dissolution of anhydrites and secondary precipitation of gypsum are also likely. Much lower $\delta^{34}\text{S}$ and $\delta^{18}\text{O}$ values of sulphates in some brine with respect to that of anhydrites suggest that such waters associate with zones of sulphide (mainly pyrite) oxidation.

Address of corresponding author: A. Porowski: Twarda 51/55, 00-818 Warsaw, Poland
e-mail: adamp@twarda.pan.pl

Badenian salinity crisis in Carpathian foredeep: new insights from stable isotope composition of fluid inclusions in halite deposits of Wieliczka and Bochnia, southern Poland

Kazimierz Różanski, Marek Dulinski
*AGH University of Science and Technology, Faculty
of Physics and Applied Computer Science, Kraków*

Krzysztof Bukowski
*AGH University of Science and Technology, Faculty
of Geology, Geophysics and Environmental
Protection, Kraków*

Halite deposits located in the southern Poland, near Kraków, are famous mostly due to presence of medieval salt mine located in Wieliczka. They were deposited ca. 15 Ma ago and form distinct beds, extending from west to east, on the area of ca. 10 km², with several types of salt identified. Stable isotope composition of fluid inclusions trapped in halite crystals originating from Wieliczka and Bochnia salt mines was investigated. Three distinct groups of samples were analysed: (i) samples derived from so-called "green salt" beds forming extensive horizontal structures, (ii) samples derived from so-called zuber-type salt, and (iii) large monocrystals of halite collected in two crystal caves existing in the mine. The stable isotope data of fluid inclusions form two distinct clusters in the $\delta^2\text{H}$ - $\delta^{18}\text{O}$ space, representing crystal caves and green- and zuber-type salts, respectively. The cluster representing green- and zuber-type salt deposit is shifted to the right-hand side of the Local Meteoric Water Line (LMWL), towards more positive $\delta^2\text{H}$ and $\delta^{18}\text{O}$ values, pointing to evaporative conditions during formation of these deposits. The modelling of isotope data suggest that the green- and zuber-type salt deposits might have been formed in a lagoon-type environment, from mixture of sea water and water of continental origin. Although the evaporation trajectories for the Miocene sea water suggest that fluid inclusions might represent remnants of original solution, this notion has to be excluded due to the fact that only halite is present in the deposits. Other salts are present locally only in trace amounts. The data points representing monocrystals of halite collected in the crystal caves lie close to the LMWL and cover the range of $\delta^2\text{H}$ and $\delta^{18}\text{O}$ values typical for glacial/interglacial infiltration waters. This provide the proof that large monocrystals of halite in the crystal caves are of secondary origin and were formed with participation of infiltration water, most probably during the Quaternary.

Address of corresponding author: K. Różanski: al. Mickiewicza 30, 30-059 Kraków, Poland
e-mail: rozanski@novell.ftj.agh.edu.pl

Oxygen isotope variations in shallow lake water and bivalve shells: application of the isotope mass balance model

Gabriella Schöll-Barna, Attila Demény
*Institute for Geochemical Research,
Hungarian Academy of Sciences, Budapest*

Tibor Cserny
Hungarian Academy of Science, Budapest

István Fórizs
*Institute for Geochemical Research,
Hungarian Academy of Sciences, Budapest*

Pál Sümegi
*Department of Geology and Paleontology, University
of Szeged, Szeged*

Stable oxygen isotope compositions of accretionary biogenic carbonates (e.g. bivalve $\delta^{18}\text{O}_{\text{shell}}$) can potentially record environmental variability of shallow lakes; therefore have been extensively used to evaluate climate and environmental conditions. As $\delta^{18}\text{O}_{\text{shell}}$ reflects the water temperature and the oxygen isotope composition of host water ($\delta^{18}\text{O}_{\text{L}}$), it is required to interpret which climatic parameters and how influence $\delta^{18}\text{O}_{\text{L}}$. Using the known isotope mass balance model ($\delta_2 = [D_1\delta_1 + P\delta_p + I\delta_i - E\delta_e] / D_2$), we tested the hypothesis that $\delta^{18}\text{O}_{\text{L}}$ variability of lake Balaton (Hungary) can be described as a result of combined effects of three climatic parameters such as river runoff, precipitation and evaporation. We calculated $\delta^{18}\text{O}_{\text{L}}$ time series for the period 1998–2008 for whole water body at Siófok (eastern part of Lake Balaton) based on measured precipitation, inflow and evaporation amount and measured precipitation, inflow and calculated vapor $\delta^{18}\text{O}$ data.

Based on the comparison of modelled (for whole water body) and measured surface $\delta^{18}\text{O}_{\text{L}}$ data, the results showed that Balaton is highly sensitive for variation of climatic parameters at the surface, while the whole water body is less sensitive, assuming different stable isotope hydrologic conditions.

High-resolution sampling was made in two *Unio* shells from Siófok covering the period of 2001–2008 and the carbonate samples were analyzed for oxygen isotope composition. On the other hand, $\delta^{18}\text{O}_{\text{shell}}$ values were calculated on the base of model (for whole water body) and measured (surface) $\delta^{18}\text{O}_{\text{L}}$ data using water temperature data, and both predictions were compared to measured shell $\delta^{18}\text{O}$ records.

The prediction based on model data for whole water body fits better the measured shell $\delta^{18}\text{O}$ values, assuming that the whole water body describes the isotope variability of shell more accurately. In addition, we presented the effect of precipitation and evaporation on the $\delta^{18}\text{O}_{\text{shell}}$ values. The relationship between intra-shell amplitude and precipitation/evaporation ratio were determined in order to precisely quantify the meteorological parameters affecting $\delta^{18}\text{O}_{\text{shell}}$ values.

Address of corresponding author: G. Schöll-Barna: H-1112 Budapest, Budaörsi út 45, Hungary
e-mail: gbarna@geochem.hu

Sulphate reduction in deep groundwater

Gerhard Strauch

*Helmholtz Centre for Environmental Research –
UFZ, Department Hydrogeology, Leipzig*

Khalid Al-Mashaikhi

*Ministry of Regional Municipality and Water
Resources, Salalah*

Kay Knöller

Helmholtz Centre for Environmental Research – UFZ, Department Catchment Hydrology, Halle/Saale

Groundwater in arid to semi-arid regions is mostly recharged hundreds and thousands of years ago. Its abstraction is otherwise managed for agricultural, urban and industrial purposes because of a vital source for social welfare in arid countries. The Dhofar region in the south of Oman is a plain area along the Arabian Sea, but most of the region is covered by a desert landscape, called Najd. Here, extended Tertiary limestone and gypsum/clayish layers form four main aquifer systems A to D which are the source of paleo-groundwater, but also are filled by recent recharge processes.

The water quality is controlled by the aquifer matrices, dissolution and reaction processes. Water type is characterized by Ca-Mg-SO₄-Cl to Na-Ca-Cl-SO₄-HCO₃ composition. Organic rich inclusions are detected in the aquifers B to D.

$\delta^{18}\text{O}$ and $\delta^2\text{H}$ cover a range between -8‰ to $+2\text{‰}$ and -50‰ to $+7\text{‰}$ (vs. VSMOW), respectively. However, the linear relationship detected between the water isotopes is close to the GMWL. No obvious evaporation processes are detected, but the annual monsoon is a clear signal for recent precipitation.

Strong enrichment in ^{34}S and ^{18}O was observed in different parts of the aquifer systems. The $\delta^{34}\text{S}$ and $\delta^{18}\text{O}$ ranges from $+10\text{‰}$ up to $+101\text{‰}$, and from $+2\text{‰}$ to $+18\text{‰}$ respectively. A strong enrichment in ^{34}S due to sulphate reduction processes is not unusual for groundwater. However, the $\delta^{34}\text{S}$ range detected in the Najd groundwater points to bacterial sulphate reduction (BSR) under compound limiting conditions. The sulphate reduction follows different steps depending on the sulphate concentration and the exchange with groundwater. These steps are observed in the groundwater of the Najd. Moreover, sulphate reduction also influences the dissolved organic/inorganic carbon system and affects thus the ^{14}C age dating of the groundwater. Insofar, the knowledge of the occurrence and extension of BSR is important for the evaluation of the groundwater quality, its origin, and dating.

Address of corresponding author: G. Strauch: Permoserstrasse 15, 04318 Leipzig, Germany
e-mail: gerhard.strauch@ufz.de

Radiocarbon age study of Slovenian–Hungarian transboundary groundwater

Teodóra Szócs
Geological Institute of Hungary, Budapest

Nina Rman
Geological Survey of Slovenia, Ljubljana

Miklós Süveges
Hydrosys Labor Kft, Budapest

A hydrogeochemical evaluation of thermal and cold groundwaters was carried out within the framework of the T-JAM project under a Slovenian–Hungarian Operational Programme. The survey, based on common methodologies by the Geological Institute of Hungary and the Geological Survey of Slovenia, was carried out in SW Hungary and NE Slovenia in the Mura–Zala basin. A uniform hydrogeochemical methodology could be applied for the identification and evaluation of the potential transboundary geothermal aquifers.

Chemical and isotope analyses of 24 cold and thermal groundwater samples were performed.

Main component and trace element analyses confirm the vertical stratification of geothermal aquifers, already suggested in previous studies, and also indicate the presence of transboundary flow systems. Hydrogeological connections are proposed, and groundwater ages are calculated, based on stable ($\delta^{18}\text{O}$, δD , $\delta^{13}\text{C}$) and radioactive isotope (^{14}C), and noble gas analyses.

Radiocarbon groundwater age determinations are common in hydrogeology, but the interpretations raise many questions. Different age calculation methods (simple carbon-14 decay, carbon-13 correction, chemical correction with CO_2 content) were made in this study. When the $\delta^{13}\text{C}$ values are shifted significantly towards very positive values they cannot be used for radiocarbon age corrections. Age calculations using the ^{14}C decay or using chemical correction with CO_2 content gave very similar results. The radiocarbon ages vary from fresh water up to 33 500 years.

Address of corresponding author: T. Szócs: H-1143 Budapest, Stefánia út 14 Hungary;
e-mail: szocst@mafi.hu

Preliminary geochemical and isotope results in a hydrogeologic complex volcanic system aquifer in Tumbaco – Cumbayá region (Ecuador)

Jean-Denis Taupin, Carla Manciatì
*IRD, Institut de Recherche pour le Développement,
HydroSciences, Montpellier*

Teresa Munoz, Nelson Arias,
Oscar Larrea, Rafael Alulema
*EMAAP-Q, Av. Mariana de Jesús entre
Alemania e Italia, Quito*

Christian Leduc
IRD, Institut de Recherche pour le Développement, UMR G-Eau, Montpellier

The study zone is located 15 km from Quito (2200 m) including Ilaló, an active volcano in the southern part. The hydrogeologic system is complex, from top to bottom; an aquitard (Cangahua Formation, composed of ashes – max. 60 m thickness) overhanging two volcanic sedimentary series, Chiche (max 120 m depth) and Guayllabamba, which present high hydraulic capacities (for instance there is no hydrogeological information about the Guayabamba series). Another local aquifer (Ilaló) is situated on the side of volcano, composed of volcanic material and overhanging down side the Chiche formation. The aquifer zone is limited by natural barriers, in the North, East and West with rivers San Pedro, Machangara and Chiche. In the southern part we can suppose a hydraulic continuity on either side of Ilaló volcano. Some chemical and isotope results were obtained in the 1980s in the southern part of the aquifer system, and completed in the northern part in 2010. Hydrothermal and overpressured waters are locally present in Ilaló aquifer. The chemical results show no differences between the Ilaló and Chiche aquifers ($\text{HCO}_3\text{-Na}$ to $\text{HCO}_3\text{-Mg}$) but the conductivity range is moderate for Chiche ($400\text{--}600 \mu\text{S}\cdot\text{cm}^{-1}$) and higher ($1000\text{--}3000 \mu\text{S}\cdot\text{cm}^{-1}$) for Ilaló aquifer. Water stable isotopes also show different behaviours for the two aquifers, with an altitudinal recharge zone lower in Chiche (local recharge) despite the Cangahua formation assumed as impermeable. Finally tritium and Carbon-14 show different residence times (actual to 5000 years – Chiche, and older – Ilaló). These first results have allowed improving the knowledge on the hydrodynamic and chemical evolution processes in this complex system (recharge zone, flux direction; residence time, chemical evolution) and the relationship between the two aquifers.

Address of corresponding author: J.-D. Taupin: 300 av. Jeanbrau, Montpellier, France
e-mail: taupin@msem.univ-montp2.fr

Tritium level in several European surface waters

Carmen Varlam, Ioan Stefanescu,
Amalia Soare, Ionut Faurescu
*National Institute of Cryogenics and Isotopic
Technologies – ICSI Rm. Valcea*

Tritium isotope (radioactive hydrogen) is produced in the upper layer of the atmosphere by the interaction of cosmic rays with the atmospheric nitrogen. It finds its way to environment especially as HTO, entering in hydrological cycle. The atmospheric testing of nuclear weapons increased the inventory of tritium on the Earth's surface, in the early '60s, with more than two orders of magnitude. Since then, the ^3H content in precipitation has decreased continuously, approximating natural levels in our days. Other tritium sources, apart from the natural production, are the anthropogenic activities as: nuclear power plants, watch industry, consumer products and medical wastes.

A review of tritium level and its evolution in surface water from France, Germany, Suisse, Great Britain, Belgium, and Romania has been given in this paper. The values of tritium concentration are studied comparatively for two periods 1993–1994 and 2007–2008, these values being obtained from different monitoring reports of environmental radioactivity.

Applying the "Global Network of Isotope in Precipitation" model, International Atomic Energy Agency developed the "Global Network of Isotopes in Rivers", where one of the monitored isotopes is tritium. The recorded values over 39 years in Vienna location decrease from 544.3 \pm 5 TU (mean of 1966) to 15.8 \pm 2.2 TU (mean of 2005). The nuclear activity developed along the Danube is present in the recorded values by the maximum values of 66.7 \pm 0.5 TU (December 2002), or 129 \pm 0.5 TU (July 2004). Tritium concentration in the Danube water has decreased in the latest years despite numerous nuclear power plants settled on its basin.

Most cases of environmental ^3H contamination are harmless, from the standpoint of radiation protection. The measured concentrations are far below the permissible value of 100 Bq/l (= 840 TU) tritium concentration for drinking water. However, the contamination does cause an increase in environmental ^3H concentrations, which are several orders of magnitude more than normal values, and which must be considered in isotopes hydrology.

Address of corresponding author: C. Varlam: Uzinei Street, no.4, PO Raureni, Box 7, Rm. Valcea, 240050, Romania, e-mail: cvarlam@icsi.ro

A 9-year record of stable isotope ratios of precipitation in Eastern Hungary: implications on isotope hydrology and regional palaeoclimatology

Gergely Vodila, László Palcsu,
István Futó

*Hertelendi Laboratory of Environmental Studies of the
Institute of Nuclear Research of the Hungarian
Academy of Sciences, Debrecen*

Zsuzsanna Szántó

University of Debrecen, Debrecen

The stable isotopic composition of hydrogen and oxygen of precipitation from Debrecen, Eastern Hungary was analysed in event based samples collected from the beginning of 2001 to the end of 2009.

During the monitoring period, the $\delta^{18}\text{O}$ values varied between -22.3‰ and 6.64‰ and the δD values between -176.8‰ and 10.7‰ . The LMWL for the monthly based data ($\delta^2\text{H} = (6.55 \pm 0.22)\delta^{18}\text{O} - 7.74 \pm 1.97$) is close to the GMWL, but shows the effect of secondary evaporation of falling raindrops with lower intercept and slope. LMWL of each year shows highly different parameters due to differences in precipitation amount and summer temperatures, especially in the extreme years of 2002 and 2003. On the basis of our data, deuterium-excess is considered to be the best parameter to reveal the extremities of dry and warm periods. Deuterium excess also proved to be a useful tool to show the different formation histories of certain precipitation events. Good correlation of $\delta^{18}\text{O}$ with temperature was obtained for the samples. The slope of the $\delta^{18}\text{O} - T$ functions for the whole sampling period was $0.32 \pm 0.03\text{‰}/^\circ\text{C}$ for the monthly samples; however, a slope of $0.37 \pm 0.03\text{‰}/^\circ\text{C}$ was obtained if monthly mean temperatures were replaced with the monthly mean temperatures of the rainy days. Considering the temperature dependency of the $\delta^{18}\text{O}$ values in the past, it can be concluded that $\Delta\delta^{18}\text{O}/\Delta T$ relationship using monthly mean temperatures of the rainy days might be a better approach than monthly mean temperatures.

The article with the same title was published in the *Journal of Hydrology* 400 (2011) 144–153.

Address of corresponding author: G. Vodila: H-4026 Debrecen, Bem tér 18/C, Hungary,
e-mail: gvodila@atomki.hu

Detailed isotopic mapping of the karstic Savica River, NW Slovenia

Polona Vreca
Jožef Stefan Institute, Ljubljana

Mihael Brencic
*Department of Geology & Department of
Hydrogeology, Faculty of Natural Sciences and
Engineering, University of Ljubljana
Geological Survey of Slovenia, Ljubljana*

Savica River is a natural phenomenon with wide spectrum of different high Alpine karstic features in the recharge area interesting for thorough and precise hydrogeological and geochemical study. It flows out from a 300 m long flooded cave, represents one of the largest Slovenian karstic springs and is the main tributary to the biggest Slovene natural lake, Lake Bohinj. The discharge of Savica River is in the interval between 0.03 m³/s to 132 m³/s. The discharge of Savica River is typical of snow-rain regime. The hydrograph consist of two parts, the first part belongs to long spring thawing period that lasts up to 4 months, and the other part is typical for the drainage of karstic aquifer with fast rainfall infiltration rate. High Q_{\max}/Q_{\min} ratio indicates highly developed karstic channel network inside of the Dachstein carbonate rocks. In the major part of recharge area average annual precipitation is up to 3200 mm/year with evapotranspiration well below 550 mm/year. Average annual number of days with the air temperature below frost point is estimated between 70 to 100 days and average fresh snow thickness for the period between 1961 and 1990 was over 4.2 m. In the Savica River hinterland typical weather situation is represented by incoming wet and relatively warm southwest air masses.

However, despite its importance, Savica River was studied only occasionally by chemical and isotopic tracers until now. Therefore, a detailed mapping was performed in August 2010 and February 2011. Approximately every 100 m along the river temperature and conductivity were measured, and discharge was estimated. In addition, samples for isotopic composition of oxygen were collected. The results will enable to 1) investigate the homogeneity of the water body along the Savica River, 2) determine the spatial and temporal trends in isotopic composition along the Savica River, and 3) determine the recharge area.

Address of corresponding author: P. Vreca: Jamova 39, 1000 Ljubljana, Slovenia
e-mail: polona.vreca@ijs.si

PALEOCLIMATE

Calculation of temperature and $\delta^{18}\text{O}$ of depositing water by measured $\delta^{18}\text{O}$ of recent travertines deposited from the Budapest thermal karst water

József Deák
GWIS Ltd, Dunakeszi

Sándor Kele, István Fórizs,
Attila Demény
Institute for Geochemical Research, Hungarian
Academy of Sciences, Budapest

Gyula Scheuer
Budapest

Linear correlation between the temperature and measured $\delta^{18}\text{O}_{\text{water}}$ of Budapest thermal karst water system presents an opportunity to estimate both the temperature and $\delta^{18}\text{O}$ of the depositing water if only the $\delta^{18}\text{O}_{\text{travertine}}$ is known.

Our observations on several Hungarian groundwaters and travertines deposited recently from them resulted that $\delta^{18}\text{O}$ data of travertines originating from cold karst water and thermal water of porous aquifer are close to the "experimental" curve presented by Friedman and O'Neil (1977). Conversely, the calculated fractionation factors of thermal karst waters significantly deviate from the experimental curve following an "empirical-curve" ($R^2 = 0.99$) as: $1000 \cdot \ln \alpha = (2.76 \cdot 10^6)/T^2 - 1.31$.

The empirical equations calculated by this "empirical-curve" as $T_{\text{water}} = (25 - \delta^{18}\text{O}_{\text{trav}})/0.22$ and $\delta^{18}\text{O}_{\text{water}} = 0.186 \cdot \delta^{18}\text{O}_{\text{trav}} - 14.22$ are usable only for the Budapest thermal karst regime and only for recent travertines. Extrapolation of these equations to the past and use them to estimate the deposition temperature of paleo-travertines needs detailed information of the paleoclimate and age of travertine.

Key words: oxygen isotope fractionation, travertine, thermal karst water, empirical equation

Introduction

Studies of climate variations in the geological past can significantly contribute to reliable estimations of expected future climate trends. Valuable paleoclimate records for continental areas are provided by non-marine carbonates, including lacustrine sediments, travertines, freshwater tufa deposits and speleothems.

Addresses: J. Deák: H-2120 Dunakeszi, Alkotmány u. 45, Hungary
e-mail: deak47jozsef@gmail.com

S. Kele, I. Fórizs, A. Demény: H-1112, Budapest, Budaörsi u. 45, Hungary

Gy. Scheuer: H-1126 Budapest, Szendrő u. 6, Hungary

Received: May 9, 2011; accepted: May 23, 2011

Their formation temperatures can be calculated using various methods, and among them conventional carbonate-water paleothermometry (McCrea 1950; Epstein et al. 1953; Kim and O'Neil 1997) is one of the most frequently used one. The disadvantage of this method is that it requires knowledge or estimation of the oxygen isotope composition of the water from which the carbonate was precipitated.

Final prospecting goal of our investigations is to develop a combined method for paleoclimate and water temperature estimations from $\delta^{18}\text{O}$ and $\delta^{13}\text{C}$ data of paleo-travertines. Our paper presents the results of the first steps of this investigation as development of a method for calculation of both temperature and $\delta^{18}\text{O}$ of parent water in the Budapest thermal karst water system using only measured $\delta^{18}\text{O}$ of recent travertines deposited at the orifice of thermal springs/wells. Further steps will need additional hydrogeological, geothermal and dating studies, too.

Method of calculations

In case of calcite-water isotopic equilibrium stable oxygen isotope composition of travertines ($\delta^{18}\text{O}_{\text{trav}}$) is controlled by the temperature (T) of deposition and by the $\delta^{18}\text{O}$ of the travertine-depositing thermal water ($\delta^{18}\text{O}_{\text{water}}$). $\delta^{18}\text{O}$ fractionation factor between travertine and water ($1000 \cdot \ln \alpha$) depends on the temperature and can be calculated using the equation of Friedman and O'Neil (1977) as:

$$1000 \cdot \ln \alpha = 1000 \cdot \ln [(1000 + \delta^{18}\text{O}_{\text{trav}})/(1000 + \delta^{18}\text{O}_{\text{water}})] = (2.78 \cdot 10^6)/T^2 - 2.89 \quad (1)$$

The fractionation factor values calculated by Equation 1 as a function of $10^6/T^2$ (where T is given as °K) are presented in Fig. 1 ("experimental curve"). The validity of this curve was tested by measuring temperatures and oxygen isotope compositions of waters and recently precipitated carbonates in Hungary. These "empirical" values (points in Fig. 1) were compared with the experimental ones calculated by the known temperature of deposition. In optimal case these two values should be the same, i.e. the points should fit to the "experimental-curve".

Origin of groundwater and recent travertine data

Detailed studies of stable oxygen and carbon isotope compositions of travertines have been accomplished in the Institute for Geochemical Research, Hungarian Academy of Sciences (Budapest) (Kele et al. 2008, 2011; Demény et al. 2010). Additional travertine $\delta^{18}\text{O}$ and $\delta^{13}\text{C}$ data were provided by the ATOMKI (Institute of Nuclear Physics, Debrecen) (Szöőr et al. 1991; Hertelendi and Svingor 1996) and by the measurements of Deák (1986) at the Institute for Environmental Physics in Heidelberg.

Groundwater isotope data (Fórizs et al. 2007; Deák et al. 2010) were used to determine the isotope-hydrogeological features of the Budapest thermal karstwater system. The other groundwater isotope data were collected from archive publications (Deák 1979; Hertelendi 1995).

Evaluation of data

Recent Hungarian travertines were divided into three groups by the type of depositing water as:

- karst thermal waters (K/thermal) with temperature $>20\text{ }^{\circ}\text{C}$
- cold karst waters (K/cold) with temperature $<20\text{ }^{\circ}\text{C}$
- thermal waters of the porous Pannonian aquifer on the Great Hungarian Plain.

Figure 1 presents that in case of Pannonian thermal waters and cold karst waters the experimental and the empirical fractionation ($1000\cdot\ln\alpha$ values are similar to each other.

Conversely, the empirical fractionation factors of thermal karst waters (20 to 95 $^{\circ}\text{C}$) significantly deviate from the experimental curve following the equation ($R^2 = 0.99$):

$$1000\cdot\ln\alpha = (2.76\cdot 10^6)/T^2 - 1.13 \quad (2)$$

Equation 2 presents that the coefficient of T^{-2} ($2.76\cdot 10^6$) is similar to the experimental value ($2.78\cdot 10^6$) so the two curves are parallel to each other. This fact suggests that the deviation is less dependent on temperature than the additional constant as -1.13‰ and -2.89‰ , respectively. This difference of 1.76‰ ($= 2.89-1.13$) means about $8\text{ }^{\circ}\text{C}$ higher measured temperature of deposition as the "experimental" value calculated by Eq. 1 as it was also shown by Kele et al. (2008, 2011) in case of recently forming travertines in Egerszalók (Hungary) and Pamukkale (Turkey). Using the experimental curve of Kim and O'Neil (1997) as $1000\cdot\ln\alpha = 18030/T - 32.42$ (dashed line in Fig. 1) the difference will be even higher between the calculated and empirical fractionation factors.

International comparison

The validity of the empirical oxygen isotope fractionation curve established for the Hungarian thermal karst waters was investigated using available data set from other karst areas abroad (Table 1). Values of travertines deposited at the nearest place to the orifice were selected ruling the disturbing effect of secondary fractionation out (Kele et al. 2008, 2011).

The method of calculation was the same as in the case of recent Hungarian travertines. The differences of the calculated and experimental $1000\cdot\ln$ data (Fig. 2) were found in other areas to be similar to the Hungarian thermal karst travertines. Two points out of 13 (No. 11 and 12 in Table 1, from Colorado and

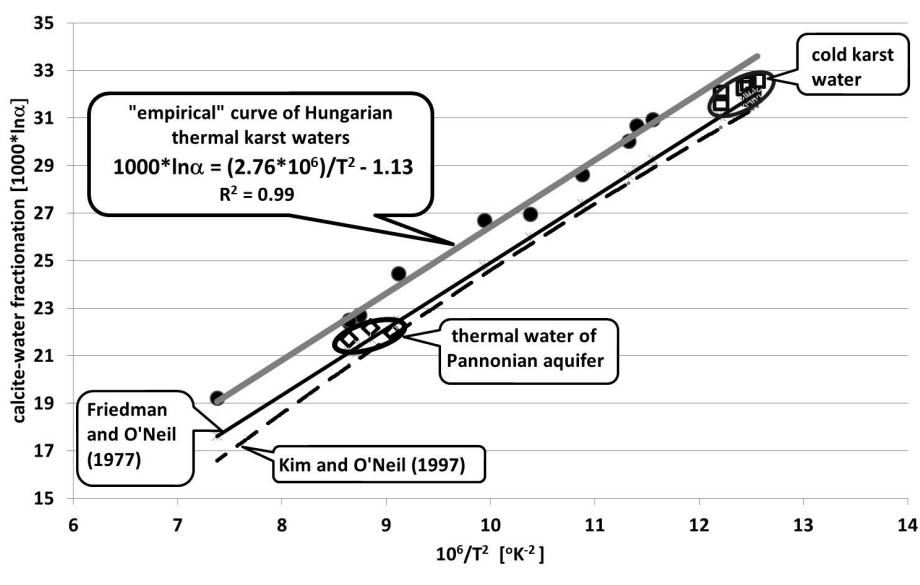


Fig. 1
 "Empirical-curve" by detected calcite-water oxygen isotope fractionations of recent travertines in Hungary compared to "experimental-curves" of Friedman and O'Neil (1977) and Kim and O'Neil (1997)

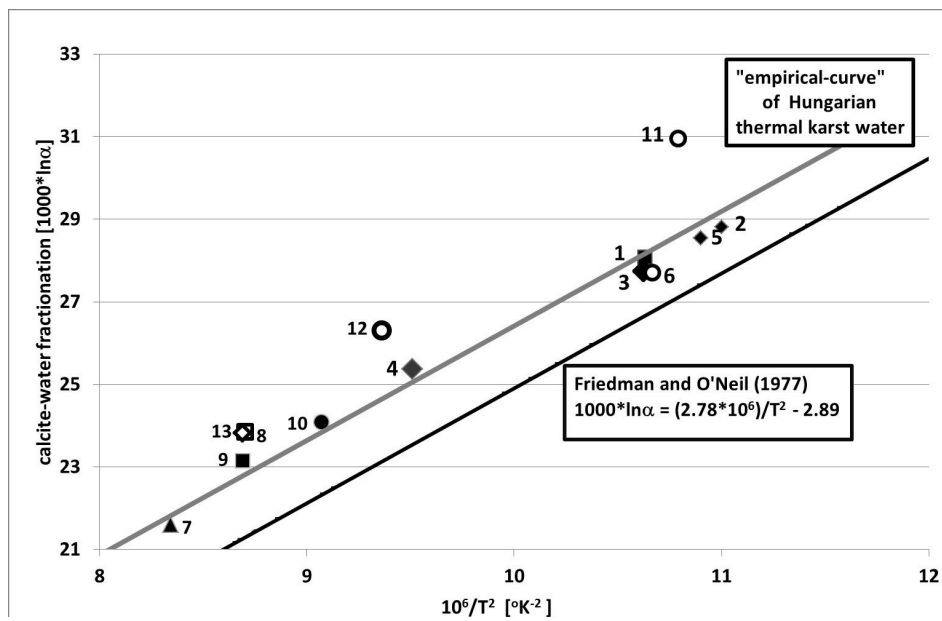


Fig. 2
 Comparison of fractionation factors established in Hungary with data of other karst areas. No. of points are listed in Table 1

Table 1
Foreign data of recent travertines and their parent thermal karst waters

Area	Local name	Source of data	Number on Fig 2	Water temperature		$\delta^{18}\text{O}_{\text{water}}$ (measured) [%] _{SMOW}	$\delta^{18}\text{O}_{\text{trav}}$ (measured) [%] _{SMOW}	1000* $\ln\alpha$ (travertine/water)	
				[°C]				Calculated by measured $\delta^{18}\text{O}$	Friedman and O'Neil (1977)
Nevada	Devils Hole	Coplen 2007	1	33.7		-13.5	14.6	28.1	26.7
Tenerife	Los angeles	Demény et al. 2010	2	28.5		-8.1	20.9	28.8	27.7
Tenerife	Madre del Agua	Demény et al. 2010	3	33.8		-8.1	19.8	27.7	26.6
Karahayit	Kirmizi Su spring	Kele et al. 2011	4	51.3		-7.8	17.7	25.4	23.5
Pamukkale	Jandarma spring	Kele et al. 2011	5	30.1		-8.8	19.9	28.5	27.1
Pamukkale	Beltes 2 spring	Kele et al. 2011	6	33.2		-8.5	19.3	27.7	26.8
Yellowstone Park	Angel Terrace Spring	Fouke et al. 2000	7	73.2		-18.3	4.0	22.5	20.3
Yellowstone Park	Narrow Gauge 3	Chafetz and Lawrence 1994	8	66.0		-18.3	5.4	23.9	21.3
Yellowstone Park	Narrow Gauge 5	Chafetz and Lawrence 1994	9	66.2		-17.9	5.1	23.1	21.3
Viterbo	Le Zitelle	Chafetz and Lawrence 1994	10	59.0		-6.7	17.5	24.1	22.3
Colorado	Durango	Chafetz and Lawrence 1994	11	31.4		-14.2	16.8	31.0	27.1
California	Pagosa Spring	Chafetz and Lawrence 1994	12	53.8		-12.7	13.6	26.3	23.1
California	Bridgeport	Chafetz and Lawrence 1994	13	66.2		-16.7	7.0	23.8	21.3

California) are lying far from the "empirical-curve" presenting even higher deviations from the "experimental-curve".

Estimation of temperature and $\delta^{18}\text{O}$ of depositing water by $\delta^{18}\text{O}$ of recent travertines in the Budapest thermal karst water system

The "empirical-curve" (Eq. 2) can serve as an excellent tool to estimate the $\delta^{18}\text{O}$ of recent travertines being deposited from thermal karst waters in Hungary, but the inverse problem (i.e. estimation of temperature of deposition and $\delta^{18}\text{O}$ of water from the measured $\delta^{18}\text{O}$ of travertine) needs additional information about the hydrogeological system.

Such information is available in the Budapest thermal karst water system. Linear correlation between the temperature and measured $\delta^{18}\text{O}$ of water (Fig. 3)

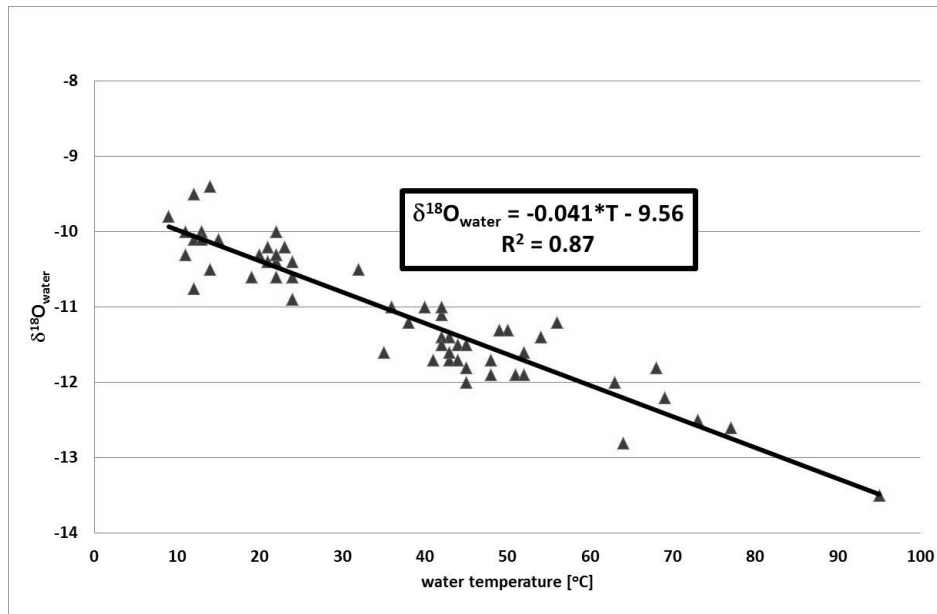


Fig. 3
Correlation between the temperature and $\delta^{18}\text{O}$ of the Budapest thermal karst water system

presents an opportunity to estimate both temperature and $\delta^{18}\text{O}$ of water from $\delta^{18}\text{O}$ of recent travertines.

First step: $\delta^{18}\text{O}$ values of possibly deposited travertines were calculated by the measured $\delta^{18}\text{O}$ and temperature data of water of Budapest thermal karst system, using the "empirical" fractionation curve (Eq. 2) for the Hungarian thermal karst waters (Fig. 4). The seven travertines to be measured (triangles in Figure 4) are – of course – close to the curve.

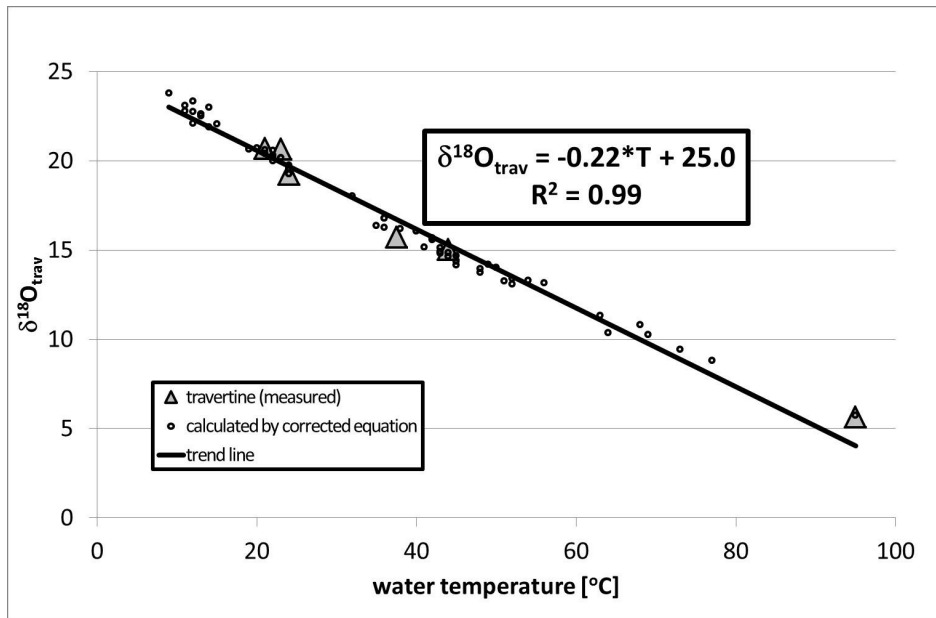


Fig. 4
Estimated and measured $\delta^{18}\text{O}$ of recent travertines in the Budapest thermal karst water system

The temperature of depositing karst water can be calculated from the $\delta^{18}\text{O}$ of travertine by arranging the equation of regression line in Figure 4 as:

$$T_{\text{water}} [\text{°C}] = (25 - \delta^{18}\text{O}_{\text{trav}})/0.22 [\text{‰}] \quad (3)$$

Combining the Eq. 3 with equation of Figure 3, the stable oxygen isotope ratio of depositing water can be calculated as:

$$\delta^{18}\text{O}_{\text{water}} = 0.186 * \delta^{18}\text{O}_{\text{trav}} - 14.22 \quad (4)$$

These empirical relations are usable only for the Budapest thermal karst regime and only for the recent travertines. Extrapolation of these equations to the past and their use to estimate the deposition temperature of paleo-travertines needs detailed information on the paleo-hydrogeology, paleoclimate and age of travertine.

Conclusion

The linear correlation between temperature and measured $\delta^{18}\text{O}_{\text{water}}$ of the Budapest thermal karst water system provides an opportunity to estimate both the temperature and $\delta^{18}\text{O}$ of the depositing water if the $\delta^{18}\text{O}$ of travertine is known. Studies on recent Hungarian travertine deposits and their parent waters

were used to calibrate the experimentally determined fractionation curve of Friedman and O'Neil (1977). The calculated oxygen isotope fractionation factors between travertine and water of recent travertine deposited from Hungarian thermal karst waters deviate significantly from the "experimental curve" following an "empirical-curve" ($R^2 = 0.99$) as $1000 \cdot \ln \alpha = (2.76 \cdot 10^6)/T^2 - 1.13$. The empirical equations calculated by this "empirical-curve" as $T_{\text{water}} = (25 - \delta^{18}\text{O}_{\text{trav}})/0.22$ and $\delta^{18}\text{O}_{\text{water}} = 0.186 \cdot \delta^{18}\text{O}_{\text{trav}} - 14.22$ are usable only for the Budapest thermal karst regime and only for the recent travertines. Extrapolation of these equations to the past and their use to estimate the deposition temperature of paleo-travertines needs detailed information on the paleo-hydrogeological conditions, paleoclimate and age of travertine.

Acknowledgements

Part of this study, dealing with the Budapest thermal karst system, has been financed by the Hungarian Scientific Research Fund (OTKA K 60921).

References

- Chafetz, H.S., J.R. Lawrence 1994: Stable isotopic variability within modern travertines. – *Géographie physique et Quaternaire*, 48, pp. 257–273.
- Coplen, T.B. 2007: Calibration of the calcite-water oxygen-isotope geothermometer at Devils Hole, Nevada, a natural laboratory. – *Geochimica et Cosmochimica Acta*, 71/16, pp. 3948–3957.
- Deák, J. 1979: Environmental isotopes and water chemical studies for groundwater research in Hungary. – In: *Isotope Hydrology 1978*, v. I., IAEA-SM-228/13, IAEA, Vienna, 1979, pp. 221–249.
- Deák, J. 1986: Paleoklíma vizsgálatok stabil izotóp elemzésekkel (Paleoclimatic studies using stable isotope analyzes) – VITUKI Final Research Report, Budapest. (In Hungarian.)
- Deák, J., I. Főrizs, Á. Lorberer, Gy. Tóth 2010: Verification of conceptual model of the Budapest karstwater regime by environmental isotopes. – *Proceedings of XXXVIIIth IAH Congress*, Krakow, pp. 1777–1778
- Demény, A., S. Kele, Z. Siklósy 2010: Empirical equations for the temperature dependence of calcite-water oxygen isotope fractionation from 10 to 70 °C. – *Rapid Communications in Mass Spectrometry*, 24, pp. 3521–3526.
- Epstein, S., R. Buchsbaum, H. Lowenstam, H.C. Urey. 1953: Revised carbonate-water isotopic temperature scale. – *Bull. Geol. Soc. Amer.*, 64, pp. 1315–1325.
- Fouke, B.W., J.D. Farmer, D.J. Des Marais, L. Pratt, N.C. Sturchio, P.C. Burns, M.K. Discipulo 2000: Depositional facies and aqueous-solid geochemistry of travertine depositing hot springs (Angel Terrace, Mammoth Hot Springs, Yellowstone National Park, U.S.A.). – *Journal of Sedimentary Research*, 70, pp. 565–585.
- Főrizs, I., J. Deák, Gy. Tóth, Á. Lorberer 2007: Origin of groundwater in the Budapest thermal karst regime by preliminary environmental isotope data. – *Studia Universitatis Babeş-Bolyai*, 52/1, pp. 92–93.
- Friedman, I., J.R. O'Neil 1977: Compilation of stable isotope fractionation factors of geochemical interest. – In: *Data of Geochemistry 6th*, Geol. Surv. Prof. Paper 440-KK, p. 61.
- Hertelendi, E., É. Svingor 1996: Carbon and oxygen isotope ratios in carbonates deposited from hot water emerged from a well Demjén No. 42. – *ESIR VII Isotope Workshop*, Budapest, Hungary. *Acta Geologica Hungarica (Suppl. 39)*, p. 71.

- Hertelendi, E., M. Veres, L. Mikó, I. Futó, L. Lénárt, J. Hakl, É. Svingor 1994: Environmental isotope study of karst systems. – In: Hertelendi, E., L. Lénárt, É. Svingor (Eds): ISOKARST '94, University of Miskolc, Miskolc, pp. 36–180.
- Kele, S., A. Demény, Z. Siklósy, T. Németh, M. Tóth, M.B. Kovács 2008: Chemical and stable isotope compositions of recent hot-water travertines and associated thermal waters, from Egerszalók, Hungary: depositional facies and non-equilibrium fractionations. – *Sedimentary Geology*, 211, pp. 53–72.
- Kele, S., Ö. Mehmet, I. Fórizs, A. Gökgöz, M.C. Baykara, M.C. Alçiçek, T. Németh 2011: Stable isotope geochemical and facies study of Pamukkale travertines: New evidences of low-temperature non-equilibrium calcite-water fractionation. – *Sedimentary Geology*, 238, pp. 191–212.
- Kim, S.-T., O'Neil, J.R. 1997: Equilibrium and nonequilibrium oxygen isotope effects in synthetic carbonates. – *Geochimica et Cosmochimica Acta*, 61/16, pp. 3461–3475.
- McCrea, J.M. 1950: On the isotopic chemistry of carbonates and a paleotemperature scale. – *Journal of Chemical Physics*, 18, pp. 849–857.
- Scheuer, Gy., Gy. Szőőr, P. Sümegy, É. Balázs, E. Hertelendi, F. Schweitzer 1993: A magyarországi quarter és neogén édesvízi mészkövek termoanalitikai és izotópgeokémiai elemzése fácies és rétegtani értékeléssel (Thermoanalytical and isotopegeochemical study of quaternary and neogene travertines of Hungary with facies and stratigraphical evaluation). – *Hidrológiai Közöny*, 73/5, pp. 298–306. (In Hungarian.)
- Szőőr, Gy., É. Balázs, P. Sümegy, Gy. Scheuer, F. Schweitzer, E. Hertelendi 1992: A magyarországi édesvízi mészkövek termoanalitikai és izotópgeokémiai elemzése fáciestani és rétegtani értékeléssel. – In: Szőőr, Gy. (Ed.): *Fáciésanalitikai, paleobiogeokémiai és paleoökológiai kutatások*, Debrecen, pp. 93–107. (In Hungarian.)

Sedimentary changes vs. climate signals in bivalve shell and bulk rock compositions in a Late Pleistocene to Early Holocene fluvial section at Körösladány, SE-Hungary

Attila Demény
Gabriella Schöll-Barna
Institute for Geochemical Research,
Hungarian Academy of Sciences, Budapest

Pál Sümegi
Department of Geology and Paleontology
University of Szeged, Szeged

Péter Sipos, Brigitta Réka Balázs
Institute for Geochemical Research, Hungarian Academy of Sciences, Budapest

In this paper we present sedimentological and geochemical data for a section of fluvial deposits from SE Hungary covering the period of 25 to 5 ky BP. Major and trace element geochemistry of bulk sediments as well as stable C and O isotope compositions of the carbonate content indicate significant changes in depositional facies and/or sediment provenance. Correlations of mineralogical and geochemical compositions were used to determine the stable isotope compositions of authigenic calcite component. Additionally, C and O isotope compositions of *Unio crassus* shell fragments were analysed that show a good agreement with climate change. Major climate change events within the studied time period were detected both in the shells and the authigenic calcite's compositions.

Key words: Pleistocene-Holocene transition, stable isotopes, geochemistry, fluvial sediments,
Unio crassus

An about 5 m thick fluvial section was studied in this work to detect climate signals during the latest Pleistocene and early Holocene. Based on three conventional ^{14}C age dates the section covers the period of ~25 to 5 ky BP and was formed at constant deposition rate. The 5.2 meter sediment profile was cleaned and collected for palaeontological, geological and geochemical analyses in the clay quarry which is located at the edge of the village of Körösladány in SE part of the Great Hungarian Plain (Hungary). According to the sedimentological, geomorphologic and geofaciological investigations the analysed profile consists of the sediment series of a filled up point bar channel which formed during the last phase of the Ice Age.

Address of corresponding author: A. Demény: H-1112 Budapest, Budaörsi út 45, Hungary
e-mail: demeny@geochem.hu

The bottom of the profile (5.2–4.5 m) yielded medium sandy fine sands with a significant fraction of coarse-grained sands implying a deposition from high-energy fluvial waters. These sediments correspond to the active point bar channel deposits of a former meandering river. In this sandy layer there is a mass of shells of the mussel *Unio crassus*, preferring moving water habitats corroborated our first conception of the prevailing palaeoenvironmental conditions. The structure of this sand-rich layer was cross-bedding. The deposition of very fine-fine sands continued in the section between the depths of 4.5–2.5 m with the intercalation of minor silty seams and layers providing some *Unio* mussels suitable for analyses. The differential deposition of the sedimentary layers containing alternatively more sand or silt in the active riverbed must have been linked to the fluctuations of the water level in the channel. All these sediment layers show a fine wavy laminated structure. The relative high coarse silt sediment content show a possible deposition within Late Pleniglacial dust accumulation process.

At about 2.5 meters, the clay content increases in the sediment profile and the sand content decreases drastically parallel with this change, then at about 2.0 meters the organic matter content increase suddenly. The sedimentological changes suggest that the depositional environment and the climate might change strongly when this part of the analysed profile accumulated. According to the increasing clay and organic material content the temperature and weathering degree increased. Some fragments of *Unio mussel* can be found in this very fine parallel laminated clayey silt layer. From 2 meters up to the surface the content of the organic matter and clay increase gradually. The sediment structure and content suggest that the terminal phase of the filling process developed in this phase and alluvial sedimentation started around the analysed profile. Sporadic mussel shells can be found in this organic and clay-rich alluvial sediment. Some terrestrial warmth-loving molluscs, such as *Cepaea vindobonensis*, *Chondrula tridens*, *Granaria frumentum* suggest that this alluvial sedimentation developed already in the postglacial phase, during the Early Holocene.

Bulk sediments were analysed by means of XRF technique in order to determine major and trace element concentrations. Mineralogical compositions were determined by conventional semiquantitative XRD analyses. Stable C and O isotope analyses were conducted on the carbonate fraction of the bulk sediment using conventional off-line preparation and dual inlet mass spectrometer. Fragments (usually 2–3 cm in size) of *Unio crassus* shells were collected from the sediments at 20–25 cm increments, then the preservation of their original aragonite structure was checked by cathodoluminescence microscopy. The fragments were sampled by at drilling three spots, the C and O isotope compositions of carbonate powders were determined using a continuous flow mass spectrometer equipped with an automated Gasbench device, then the results were averaged for each shell.

As usual for fluvial deposits, the studied sediments are dominated by quartz (54–68 wt%) and plagioclase (8–20 wt%), while phyllosilicates, feldspars, chlorite and carbonates are generally below 10 wt%. The calcite content rises between 300 and 375 cm to 10–13 wt% with a concomitant increase of dolomite (5–9 wt%). The samples contained no aragonite. This is partly due to the collection of large shell fragments from the sediment samples. Below 400 cm, the carbonate amount is low with a relatively elevated calcite/dolomite ratio. The dolomite content suddenly increases at 375 cm, and then it shows a constant decrease along with the calcite/dolomite ratio. The SiO_2 content is slightly elevated below 400 cm (57 to 69 wt%) compared to the upper section part (52 to 62 wt%). The MgO concentration is low below 400 cm (1.7 to 1.9 wt%), suddenly increases to 3.4 wt% at 375 cm, then it decreases gradually to about 2.4 wt% in the uppermost part, with a significant positive MgO-dolomite correlation ($R^2=0.67$). The MnO content shows again a difference between the lower (=400 cm) and the upper part of the section (0.18–0.38 and 0.10–0.17 wt%, respectively). The Sr concentration of the bulk sediment is 160 to 180 ppm below 400 cm, then it decreases to about 120 ppm up-section (Fig. 1A). The oxygen isotope composition of bulk sediment carbonate negatively correlates with the Sr content ($R^2=0.85$)

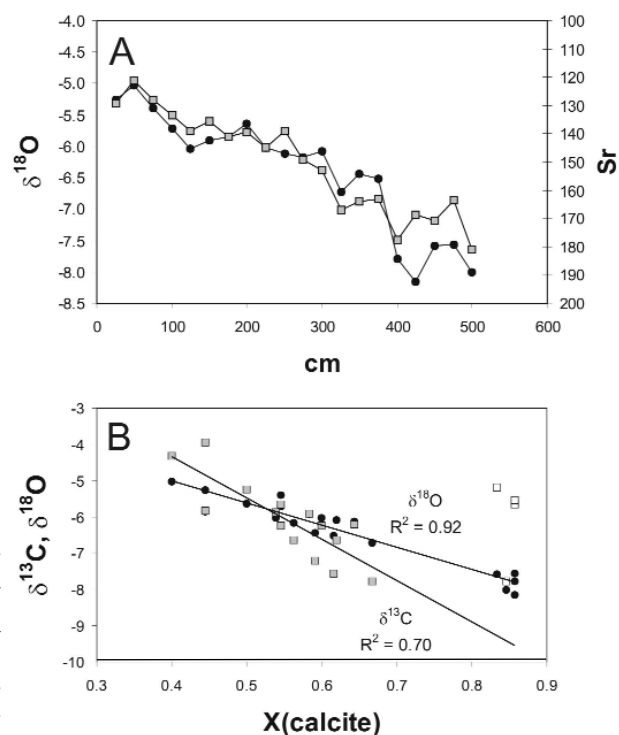


Fig. 1
A. Stable oxygen isotope compositions of bulk carbonate (in ‰ relative to V-PDB; filled circles) and Sr contents (in ppm; grey filled squares) of bulk sediment. B. Stable carbon and oxygen isotope compositions (in ‰ relative to V-PDB) as a function of calcite content of bulk carbonate

and shows a perfect negative correlation ($R^2=0.92$) with the X_{calcite} value (calcite/(calcite+dolomite)) (Fig. 1B). The bulk carbonate's carbon isotope compositions are negatively correlated with the carbonate content ($R^2=0.60$), whereas the correlation with the Sr content is not that straightforward ($R^2=0.28$). The carbon isotope - X_{calcite} negative correlation is significant only if the samples below 400 cm are excluded ($R^2=0.70$) (Fig. 1B). The concentrations of other mineral components and elements show either random or rather complex patterns.

The carbon isotope compositions of bivalve shells are fluctuating between -14 and -10‰ , whereas the oxygen isotope values show a distinct pattern with $<-10\text{‰}$ below 150 cm and a sudden increase to -8.3‰ at 150 cm.

Although it is well known that a major climate change with significant fluctuations occurred in the last 25 ky, the variations in mineralogical and chemical compositions indicate changes in deposition environment or denudation source as well. This is supported by the observation that the bulk carbonate's isotopic compositions (that may depend on the amount and origin of detrital carbonate) show no agreements with the shell data (that may depend more on climate).

Between 20 and 25 ky the composition of the sediment was different from that of the subsequent period with higher amount of quartz, lower amount of dolomite and a calcite domination in the bulk carbonate. The good relationships between the bulk carbonate's isotopic compositions and the mineralogical and chemical compositions suggest mixing of different components. These relationships show that the denudation was dominated by limestones before 20 ky then a dolomitic terrain started to be eroded afterwards with some calcitic components in the sediments.

Opposite to the bulk carbonate compositions, the shells' oxygen isotope values show a clear relationship with climate. Although the fluctuations between 12 and 25 ky do not significantly appear in the isotope values, the Pleistocene-Holocene transition is well displayed (Fig. 2A). This indicates that the bivalve shell data can reflect climate conditions in this fluvial environment.

Using the correlations with X_{calcite} values, the isotopic compositions of the calcite component in the bulk carbonate can be calculated. Apart from the lower part of the section (= 20 ky) that shows relatively high $\delta^{13}\text{C}$ values (Fig. 2B), the C and O isotope compositions of the calcite component resemble those of the shell fragments. Interestingly, the calculated compositions seem to reflect climate variations, correlating with the shell compositions (Fig. 2A–B).

Based on these data we can conclude that the stable isotope compositions of bulk sediment carbonate and bivalve shell data can be used as proxies of climate conditions, but facies and sediment source changes should also be taken into account before drawing a conclusion.

This study was financially supported by the Hungarian Scientific Research Fund (OTKA K-68343).

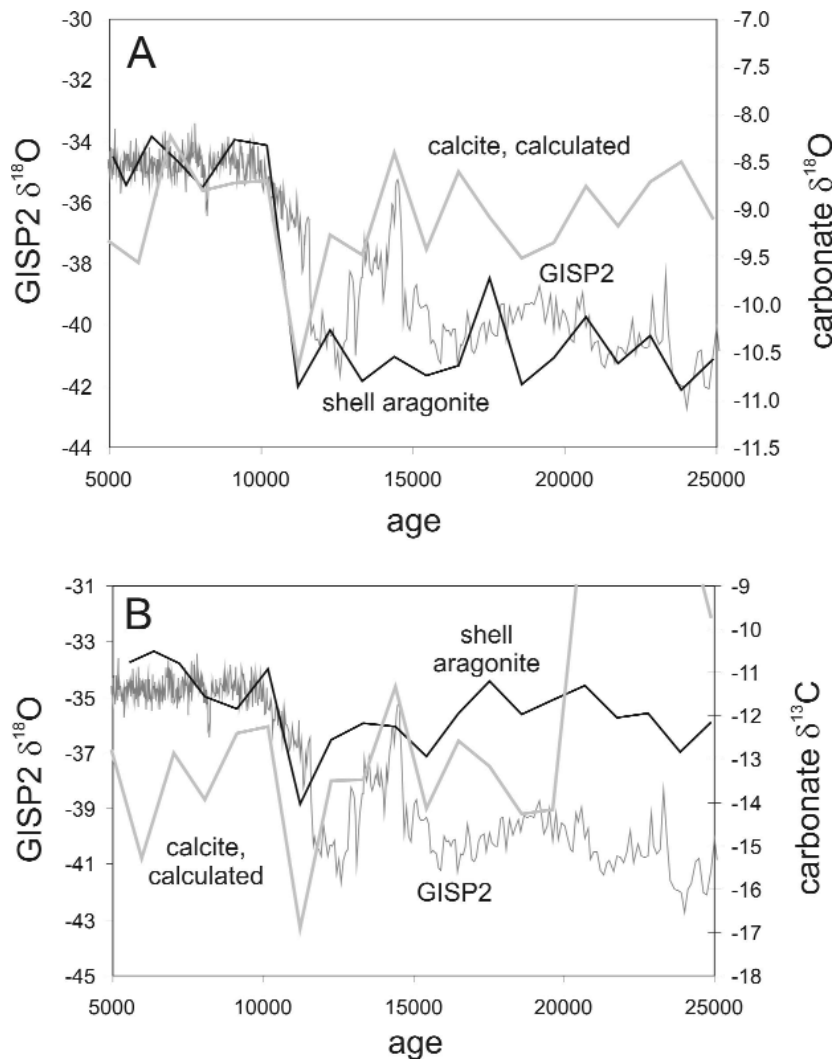


Fig. 2
 Stable oxygen isotope compositions (in ‰ relative to V-SMOW) of the GISP2 ice core (source: <ftp://ftp.ncdc.noaa.gov>) and stable oxygen (A) and carbon (B) isotope compositions of carbonates (aragonitic shells and calculated authigenic calcite component)

Stable isotope studies of secondary carbonates of the Süttő loess-paleosoil sequence, Hungary

Gabriella Barta
*Department of Physical Geography,
Eötvös Loránd University, Budapest*

Paul Koeniger
Leibniz Institute for Applied Geophysics, Hannover

Erzsébet Horváth
*Department of Physical Geography,
Eötvös Loránd University, Budapest*

Manfred Frechen
Leibniz Institute for Applied Geophysics, Hannover

Bernadett Bajnóczi
*Institute for Geochemical Research,
Hungarian Academy of Sciences, Budapest*

Research on secondary carbonates in loess-paleosoil sequences is of great importance because it provides detailed paleoenvironmental information, and might serve as proxies for climate. Different secondary carbonate subtypes (e.g. calcified root cells, hypocoatings) reflect detailed signals on the extension and intensity of leaching processes.

In the formation of secondary (authigenic) carbonates different processes take part, like the flow of the bicarbonate soil solutions and biomineralization. During dust accumulation the soil development remains mostly continuous, but can be inhibited by higher sedimentation rates, whereas secondary carbonates remain in the deposits. Secondary carbonate subtypes and their distribution help to recognize and characterize environmental and pedosedimentary processes.

Multidisciplinary investigations have been carried out recently on the loess-paleosoil sequence at Süttő (e.g. luminescence dating, granulometry and malacology). For a combined (micro)morphological and stable isotope study, samples were taken in 10 cm vertical resolution from the approximately 15 m thick sequence. Secondary carbonates were separated by using wet sieving and stereomicroscopy prior to stable isotope analysis.

Carbon and oxygen isotope composition of calcified root cells shows mean values of -21.6‰ for $\delta^{13}\text{C}$ and -13.7‰ for $\delta^{18}\text{O}$, respectively. For hypocoatings mean values of -6.7‰ and -6.6‰ , for carbonate-coatings -7.3‰ and -7.5‰ , and for calcite crystal aggregates -12.1‰ and -6.7‰ were measured for $\delta^{13}\text{C}$ and $\delta^{18}\text{O}$, respectively.

Stable isotope clusters will help to describe genetic processes of secondary carbonates and vertical patterns in the loess sequence might serve as more reliable environmental indicators than stable isotope compositions of bulk samples.

Address of corresponding author: G. Barta: H-1117 Budapest, Pázmány Péter sétány 1/C, Hungary
e-mail: gabriellabarta86@googlemail.com

Calcite carbon and oxygen stable isotopes in riverine tufas as paleoclimatic records of Interglacials: the sequence of Condat-sur-Vézère (MIS 5, South-western France)

Julie Dabkowski

Département de Préhistoire du Muséum National d'Histoire Naturelle, UMR 7194, Paris

Nicole Limondin-Lozouet, Pierre Antoine

Laboratoire de Géographie Physique, CNRS UMR, 8591 Meudon

Laboratoire de Géographie Physique, CNRS, UMR, 8591 Meudon

Alina Marca-Bell, Julian Andrews, Paul Dennis

School of Environmental Sciences, University of East Anglia, Norwich

Calcareous tufas result from calcite precipitation under open-air conditions in streams, rivers and lakes. In Europe, they are characteristic of Interglacials and common in almost any area with carbonate bedrock where mean annual air temperature is above 5 °C. Their composition (95% of CaCO₃) makes them suitable for oxygen and carbon stable isotopes ($\delta^{18}\text{O}$ and $\delta^{13}\text{C}$) investigations. These parameters have been shown to be important palaeoclimatic proxies in Holocene tufas. At decadal-scale sampling resolution, in modern and Holocene tufas, $\delta^{18}\text{O}$ of calcite records variations in $\delta^{18}\text{O}$ of regional rainfall. Thus, it reflects mainly air temperature variations, as source or amount effects (particularly continentality), depending on locality, should not change at a given site. $\delta^{13}\text{C}$ of tufa calcite indicates rainfall intensity and moisture availability (linked to biomass type/abundance).

We have recently investigated the suitability of $\delta^{18}\text{O}$ and $\delta^{13}\text{C}$ as palaeoclimatic proxies in Pleistocene tufas. The 'Condat tufa' (commune of Condat-sur-Vézère, South-Western France) was first attributed to the Last Glacial Maximum by radiocarbon dates. This attribution was refuted in the 1980s as its molluscan and ostracod faunas show clear temperate attributes. Two new dates by U/Th-TIMS around 100–110 ky now clearly assigned the Condat tufa to MIS 5 although not to the full interglacial Eemian (MIS 5e, from c. 130 to c. 115 ky). Tufa was sampled continuously at 5 cm resolution along the 6 m high Condat profile. Neither $\delta^{18}\text{O}$ nor $\delta^{13}\text{C}$ show important climatic variations in temperature or rainfall intensity, except at the bottom of the sequence where a relative cooler and drier episode is recorded. In the upper 5 m, $\delta^{18}\text{O}$ indicates a constant low warming whereas stable humidity is recorded by $\delta^{13}\text{C}$. No wet and warm climatic optimum is identified. This climatic reconstruction is coherent with the U/Th dates that attribute the 'Condat tufa' to an advanced phase of the MIS 5, younger than the Eemian.

Address of corresponding author: J. Dabkowski: 1. Rue René Panhard 75013 Paris, France
e-mail: dabkowski@mnhn.fr

Isotope hydrological and geophysical studies on the perennial cave ice deposit of Saarahalle (Mammuthöhle, Dachstein Mts, Austria)

Zoltán Kern

Department of Paleontology, Eötvös University, Budapest

István Fórizs

Institute for Geochemical Research, Hungarian Academy of Sciences, Budapest

László Palcsu

Institute of Nuclear Research of the Hungarian Academy of Sciences, Debrecen

Michael Behm, Helmut Hausmann

Institute of Geodesy and Geophysics, Vienna University of Technology, Vienna

Rudolf Pavuza

Department of Karst and Cave Science at the Museum of Natural History, Vienna

The largest perennial ice deposit of the Mammuthöhle cave system is located in the "Saarahalle" chamber. Its extension is 40 m by 15 m and the maximum ice depth is 6 m. The cave system can be classified as a dynamic cave, but within this large dynamic system Saarahalle can be regarded as a static chamber. The ground penetrating radar data show that the base of the ice in Saarahalle is dominated by large boulders, and that the ice is stratified. A multitude of reflection bands is visible down to depths of 4–6 m. These reflection signatures are interpreted as thin layers of sediments and might help to understand the ice formation by representing isochrones. A 5.28 m long ice core was extracted from the Saarahalle ice block and sectioned into 105 samples. Tritium activity, $\delta^{18}\text{O}$ and δD compositions were analysed. Tritium activities of 12 non-neighbouring samples distributed along the upper 1.65 m were measured by ^3H – ^3He ingrowth method applying the ^4He spike technique. The pattern of tritium activities along the studied profile suggests that an "old" and a "modern" water are mixing. The stable isotope composition of the ice core samples showed relative enrichment and d-excess values were characteristically lower compared to the potential sources (local precipitation, karstwater) indicating the fractionation effect of the freezing process. However the cave ice water line provided a slope coefficient of 8.13. These isotopic characteristics reflect a mixed-component open-system freezing model. Our previous opinion about the age of the uppermost cave ice layers needs revision as the tritium activities provided by the more sensitive ^3H – ^3He ingrowth method clearly indicate contribution of modern water at least down to 1.21 m depth. GPR data show layering parallel with subsurface topography. Major shifts in stable isotope values show some correspondence to reflector zones observed in the GPR profile. Both tritium activities and stable isotopic characteristics suggest that cave ice has been formed from more than one water source.

Acknowledgements: TÁMOP 4.2.1./B-09/KMR-2010-0003 and OTKA K67583.

Address of corresponding author: Z. Kern: H-1117 Budapest, Pázmány P. s. 1/c, Hungary
e-mail: zoltan.kern@gmail.com; kern@geochem.hu

Stable O-isotope record of Holocene freshwater tufa in Lake Valgejärve, Estonia – an interpretation of postglacial climate changes

Liina Laumets, Volli Kalm
University of Tartu, Tartu

High-resolution stable oxygen isotope data from 3.1 m long freshwater tufa section in Lake Valgejärve, northwestern Estonia reveals changes in palaeoclimate and -hydrological conditions between ca. 10 500 and 2 000 cal yr BP. $\delta^{18}\text{O}$ values fluctuate in a 3.17‰ (V-PDB) wide interval and reflect several warming and cooling episodes throughout the time of lake marl precipitation. Gradual increase in $\delta^{18}\text{O}$ in the tufa deposited between 10 500 and 9000 cal yr BP is caused by postglacial rapid warming and the $\delta^{18}\text{O}$ values reach their first maximum at around 9000 cal yr BP. Since then onwards the $\delta^{18}\text{O}$ values decrease (with several fluctuations) by 1‰ until 4800 cal yr BP. This trend includes small peak of relatively negative $\delta^{18}\text{O}$ values at ca. 8200 cal yr BP. In tufa deposited between 4800 and 2200 cal yr BP there is another clear increase in $\delta^{18}\text{O}$ values of ca. 2.5‰. The youngest analysed tufa sequence, representing 2200–2000 cal yr BP, shows once again a decrease in $\delta^{18}\text{O}$ values. However, in general the recorded fluctuations in $\delta^{18}\text{O}$ values do not directly correlate to up to now known changes in temperature and lake water levels in the region. For example, if the recorded $\delta^{18}\text{O}$ values attribute only to temperature changes, then the TMJJA varies approximately 10 °C, being highest between 6500–4000 cal yr BP.

Address of corresponding author: L. Laumets: Ravila 14a, Tartu, 50411, Estonia
e-mail: Liina.Laumets@ut.ee

The isotopic memory of fossils

Christophe Lécuyer

Laboratoire de Géologie de Lyon, Université Lyon, Villeurbanne

Invited speaker

Oxygen isotope compositions of invertebrate (carbonate) and vertebrate (phosphate) skeletons are able to record both temperature of mineralization and isotopic composition of the aqueous solution. In the case of 'cold-blooded' vertebrates, temperature is close to that of their environment (air, water) whilst in the case of 'warm-blooded' vertebrates, temperature is close to that of their body. The oxygen isotope composition of body water can match that of ambient water (invertebrates, fish) or it can be ^{18}O -enriched by several ‰ (e.g. 4–5‰ in Human Beings). The amplitude of body water ^{18}O -enrichment relative to ambient water depends on the mass balance between input (diet) and output (sweat, breathing, faeces) fluxes in relationship to the residence time of body water.

Isotopic fractionation equations may be experimentally determined. Oxygen isotope compositions of structural carbonate in apatite are commonly used to track climate changes in the continental environment, however, the knowledge of a temperature-dependent isotopic fractionation between carbonate and water is needed to quantify paleotemperatures. The oxygen isotope fractionation between the structural carbonate of inorganically-precipitated hydroxyapatite and water was determined in the range 10 °C–37 °C. Values of $1000\ln\alpha(\text{CO}_3^{2-}\text{-H}_2\text{O})$ are linearly correlated to the inverse of the temperature (K) according to the following equation: $1000\ln\alpha(\text{CO}_3^{2-}\text{-H}_2\text{O}) = 25.19 (\pm 0.53) \cdot 10^3 \cdot \text{T}^{-1} - 56.47 (\pm 1.81)$ ($R^2 = 0.998$). This fractionation equation has a slightly steeper slope than those already established between calcite and water even though measured fractionations are of comparable amplitude in the temperature range of these experimental studies. It is consequently observed that the oxygen isotope fractionation between apatite carbonate and phosphate increases from about 7.5‰ up to 9.1‰ with decreasing temperature from 37 °C to 10 °C. A compilation of $\delta^{18}\text{O}$ values of both phosphate and carbonate from

Address: CNRS UMR 5276, Université Lyon 1, Institut Universitaire de France, 69622, Villeurbanne, France, e-mail: christophe.lecuyer@univ-lyon1.fr

modern mammal teeth and bones confirms that both variables are linearly correlated, despite a significant scattering up to 3.5‰, with a slope close to 1 and an intercept corresponding to a $1000\ln\alpha(\text{CO}_3^{2-}-\text{PO}_4^{3-})$ value of 8.1‰. This apparent fractionation factor is slightly higher or close to the fractionation factor expected to be in the range 7–8‰ at the body temperature of mammals.

Two case studies are also presented to illustrate how continental seasonal changes in past air temperatures and the metabolic status of extinct marine vertebrates may be inferred from the oxygen isotope composition of tooth enamel phosphate:

– Continuous tooth growth and absence of enamel remodeling in bovid teeth ensures a reliable record of the intra-annual variability of air temperature through an incremental $\delta^{18}\text{O}$ analysis from apex to cervix. This method has been applied to *Bison priscus* dental remains of Late Middle Pleistocene from the fossiliferous level of a cave at Coudoulous I in South-Western France. The stacked oxygen isotope signal obtained by combining nine bison teeth shows sinusoidal variations (15.0‰ to 19.1‰ V-SMOW) of seasonal origin over 2.5 years. The corresponding computed mean annual temperature of 9 ± 3 °C is about 4 °C lower than at present. Seasons appear more contrasted in Coudoulous I during level 4 deposition with summers as warm as present ones (19 ± 3 °C) and significantly colder winters about 0 ± 3 °C compared to 6 ± 1 °C at present.

– Thermoregulation and body temperature of extinct vertebrates are central questions for understanding their ecology and evolution. The thermophysiological status of the great marine reptiles is still unknown, even though some studies suggested that thermoregulation may have contributed to their exceptional evolutionary success as apex predators of Mesozoic aquatic ecosystems. We have tested the thermal status of ichthyosaurs, plesiosaurs and mosasaurs by comparing their oxygen isotope compositions of tooth phosphate to those of co-existing fish. Data distribution reveals that these large marine reptiles were able to maintain a constant and high body temperature from tropical to cold temperate oceanic environments. Their estimated body temperatures, in the range 35 ± 2 °C– 39 ± 2 °C, suggest high metabolic rates required for predation and fast swimming over large distances offshore.

Oxygen isotope compositions of vertebrate apatite are considered to represent valuable proxies of past climate changes including the determination of mean annual air temperatures, sea surface temperatures, seasonal changes in air or water temperature, and latitudinal thermal gradients. The study of faunal assemblages also opens possibilities to decipher the metabolic status of extinct vertebrates such as the Mesozoic great marine reptiles and the contemporaneous dinosaurs.

Semi-continuous online isotope and elemental ratio measurements of high time resolution on Greenland ice cores for temperature reconstruction

Markus Leuenberger

Invited speaker

Philippe Kindler, Christof Huber

Climate and Environmental Physics, Physics Institute and Oeschger Centre for Climate Change Research, University of Bern, Bern

Greenland temperature variations on millennial time scales were characteristic for the last ice age. Abrupt warmings, known as Dansgaard-Oeschger (DO) events, can be traced in $\delta^{18}\text{O}_{\text{ice}}$ records of Greenland ice cores. However, it has been shown that $\delta^{18}\text{O}_{\text{ice}}$ is not only influenced by temperature but also by seasonal precipitation changes. Therefore, independent temperature estimates are requested. Measurements of the isotopic composition of gases trapped in the ice, namely $\delta^{15}\text{N}$, $\delta^{17}\text{O}$, $\delta^{18}\text{O}$ and $\delta^{40}\text{Ar}$ can be used to calibrate the paleothermometer. Since atmospheric nitrogen and argon isotopes are stable over very long time periods, corresponding changes are solely due to separation processes occurring within the firn column – the uppermost part of an ice sheet. The firn column can be classified into three parts, (i) the convective zone, (ii) the diffusive zone and (iii) the non-diffusive zone. The height of the latter zone is given by the depth difference of the lock in depth (LID) and the close-off depth (COD). Whereas at the LID diffusion stops the air is closed off and conserved in bubbles at the COD. The convective zone is mainly governed by wind-driven convection but it is generally limited to only a few meters. The diffusive zone, though, is the dominating part of the firn column and leads to changes in the isotope and elemental ratios due to gravitational settling and thermal diffusion separation. Additionally, an already existing gradient within the firn column that originates from a temporal evolution of any concentration in the atmosphere leads to a diffusive flux. For nitrogen and argon isotopes this is not the case and the observed values can be interpreted as combined signal from gravitational enrichment and thermal diffusion effect. The combination of nitrogen and argon isotopes allows a separation of these two processes, this has been applied in a number of study up to now. For the atmospheric oxygen isotope ratios ($\delta^{17}\text{O}$ and $\delta^{18}\text{O}$) the situation is different since they change as a function of time representing on the one hand an isotope signal of sea-water (mainly through ice

Address of corresponding author: M. Leuenberger: Sidlerstrasse 5, 3012 Bern, Switzerland
e-mail: leuenberger@climate.unibe.ch

buildup or ice melting) or on the other hand a varying exchange of atmospheric oxygen with the biosphere (terrestrial as well as oceanic) associated with respiration fractionations. Both oxygen isotope ratios are believed to change rather smoothly with time due to the large reservoir of atmospheric oxygen. These allow us to disentangle the gravitational and thermal diffusion effects from the atmospheric signals with a triple isotope approach, namely the use of $\delta^{15}\text{N}$, $\delta^{17}\text{O}$ and $\delta^{18}\text{O}$. A record for the last 100 kyrs will be shown measured on the NorthGRIP ice core. Temperature shifts in the range of 8 to 12 degree Celsius are common for DO events, but values as high as 16°C were estimated.

This powerful tool of short-term temperature reconstruction has been discovered about two decades ago and will be discussed in detail based on different published examples. Its potential, limitations and implications will be presented. Particularly, the influence of the measurement uncertainty onto the temperature estimate will be discussed. Conclusions based on obtained temperature estimates during rapid climate change events involving hydrology and biogeochemical cycles are drawn. In addition, the influence of thermal diffusion effect over a transition phase glacial-interglacial, exhibiting a strong temperature gradient over an extended time period, will be discussed.

Carbon and oxygen isotopes in Baltic Early Palaeozoic geology: some results and trends

Tonu Martma, Dimitri Kaljo
Institute of Geology, Tallinn University of Technology, Tallinn

Carbon and oxygen isotopes were introduced into Baltic early Palaeozoic geology by Brenchley and co-workers in 1994. The Institute of Geology, Tallinn University of Technology, has played a decisive role in the following progress in that field. More than 3000 whole rock analyses from Estonia, Latvia, Lithuania, Russia (St. Petersburg and Far East areas), Ukraine (Podolia), Norway (Oslo area, Farsund) and Sweden (Dalarna) have been made, mostly from the Ordovician-Silurian, but a few also from the Devonian. Recently new equipment was purchased, allowing further developments.

The quality of whole rock analyses compared to those of brachiopod shell calcite has been discussed repeatedly. Baltic sedimentary rocks are, as a rule, weakly altered diagenetically and the results of analyses are therefore trustworthy, but show slightly lower values compared to brachiopod shell calcite.

Carbon isotopes are mainly used in chemostratigraphy, but together with oxygen (brach.) isotopes also applied for interpretations in palaeoenvironmental and biodiversity studies.

Recently Ainsaar et al. established a standard curve for most of the Ordovician section with a series of $\delta^{13}\text{C}$ excursions. Medium-sized excursions (from the bottom) are Mid-Darriwilian, Guttenberg (GICE), Rakvere, Saunja, Moe and Paroveja. Detailed studies in the uppermost Ordovician, displaying a major carbon isotope excursion (Hirnantian) triggered by global climate change, have revealed causal links between cooling and glaciation with sea level changes and a severe mass extinction of biota. The succession of excursions indicates differences in carbon cycling in pre- and post-GICE time.

The Silurian carbon isotope trend is in general lines similar to that in the Ordovician. The first half of the period shows rather weak perturbations (only two medium excursions in the Llandovery), the second half (beginning with the early Wenlock) four major $\delta^{13}\text{C}$ excursions. The 3rd of the latter, in the late Ludlow, is among the strongest in the whole Phanerozoic. The suggested glacial origin of those excursions remains disputable.

Address of corresponding author: T. Martma: Ehitajate tee 5, Tallinn 19086, Estonia
e-mail: martma@gi.ee

Stable isotopes of rainfall and dripwater at Ursilor Cave (Romania): the path to reliable speleothems paleoclimate reconstructions

Bogdan P. Onac

*Department of Geology, University of South Florida,
Tampa*

Tudor Tămaș, Iuliana Vișan

*Department of Geology, Babes-Bolyai University,
Cluj, & "Emil Racovita" Institute of Speleology, Cluj,*

Department of Geology, Babes-Bolyai University, Cluj, & "Emil Racovita" Institute of Speleology, Cluj

The Ursilor (Bears) Cave is located on the western edge of the Bihor Mountains (NW Romania) at 482 m asl and is highly decorated with a variety of speleothems, making it the most important show cave in Romania. The cave's main passage develops ~150 m beneath the surface. The mean annual temperature in the cave area is 9.7 °C, whereas in the cave temperature is constant year around (9.8 °C). The overall climate conditions are mild and humid (~950 mm/year). Paleoclimate reconstructions based on speleothems from this cave have already produced some interesting results. However, it is crucial to understand the long-term relationship between the isotopic composition of modern precipitation and the key climatic parameters (temperature, precipitation amount, source of precipitation etc.). Equally important is to decipher how the isotopic signal is altered while the meteoric water is stored or travels thorough the soil and epikarst above the cave. A two-year monitoring study (here we report results of the first 9 months) that implies collection of precipitations (on weekly basis) and cave drip water sampling at 4-day intervals was initiated in July 2010. The surface meteorological station (within one km from the cave) is also recording the amount of rainfall, air temperature, and relative humidity. In-cave water collection device is located at the far end of the touristic path. Data loggers at the cave water collection site measure the cave temperature, relative humidity, and drip rates at one-hour interval. The local meteoric water line (LMWL) obtained from 15 values of $\delta^2\text{H}$ and $\delta^{18}\text{O}$ of rainwater samples collected nearby Ursilor Cave has a slope of 7.95 ($\delta^2\text{H} = 7.952 \cdot \delta^{18}\text{O} + 8.46$; $R^2 = 0.986$), which is very close to the global meteoric water line (GMWL; $\delta^2\text{H} = 8 \cdot \delta^{18}\text{O} + 10$). By contrast, the $\delta^2\text{H}$ in cave drip water reflects a narrow range (average = -10.60‰ ; $n = 34$), indicating an attenuation of the seasonal rainfall isotopic variation due to mixing between the water in the soil/epikarst storage and recharge water from different rain events. This phenomenon is not expressed in such a well-visible way in the $\delta^2\text{H}$ values. However, the limited data set (mid-July to early March 2010) precludes us in explaining such differences.

From our current data, the mean *d*-excess value for the first 9 months is 8.85‰ in rain water and 10.20‰ in cave drip water, both values being typical of Atlantic air masses.

Address of corresponding author: B. P. Onac: 4202 E. Fowler Ave., SCA 528, Tampa, USA
e-mail: bonac@usf.edu

Modelling the effects of melting and refreezing on the original isotopic signal in cave ice

Aurel Perşoiu

Department of Geography, "Ştefan cel Mare" University, Suceava

A series of recent studies have targeted oxygen and hydrogen stable isotopes in cave ice as proxies for past air temperatures, but the results are far from being as straightforward as they are in high latitude and altitude glaciers and ice caps. The main problems emerging from these studies are related to the mechanisms of cave ice formation (i.e. freezing of water) and post-formation processes (melting and refreezing), which both alter the original isotopic signal in water. Different methods have been put forward to solve these issues, and a fair understanding of the present-day link between stable isotopes in precipitation and cave ice exists now. However, the main issues still lays unsolved: 1) is it possible to extend this link to older ice and thus reconstruct past changes in air temperature?; 2) to what extent are ice dynamics processes modifying the original climatic signal and 3) what is the best method to be used in extracting a climatic signal from stable isotopes in cave ice?

To respond to these questions, we have conducted a modelling experiment, in which a theoretical cave ice stable isotope record was constructed using present-day observations on stable isotope behaviour in cave ice and ice dynamics, and different methods (presently used for both polar and cave glaciers), were used to reconstruct the original, known, isotopic values. Our results show that it is possible to remove the effects of ice melting and refreezing on stable isotope composition of cave ice, and thus reconstruct the original isotopic signal, and further the climatic one.

Address: A. Perşoiu: Universitatii 13, Suceava, 720229, Romania, e-mail: apersoiu@mail.usf.edu

Correlating $\delta^{18}\text{O}$ values of Barbary sheep tooth enamel and environmental waters: Implications for North African palaeoclimate reconstructions

Hazel Reade, Graeme Barker, Tony Legge,
Tamsin O'Connell, Rhiannon Stevens
Department of Archaeology, University of Cambridge, Cambridge

The climate of North Africa is known to have been highly variable during the most recent 100,000 years. Over the same time period archaeological sites show significant changes in human behaviour, leading to suggestions that climate change was a driving force behind human behavioural developments. However, a direct link between climate and humans remains to be established, in part due to a lack of directly comparable archaeological and climatological records. The isotopic analysis of mammalian remains, which accumulate through human hunting and butchery practices, provides a means to address this problem.

The $\delta^{18}\text{O}$ of mammalian tooth enamel can be correlated with the $\delta^{18}\text{O}$ of local meteoric water because 1) teeth mineralise in isotopic equilibrium with body water, and 2) the diet and drinking water of an animal determines the $\delta^{18}\text{O}$ of its body water. This relationship allows the $\delta^{18}\text{O}$ of tooth enamel to be used as a palaeoclimatic proxy. Furthermore, quantitative palaeoclimatic reconstructions are possible if a numerical relationship between modern species and modern climate can be established, and applied to the fossil record. As the isotopic enamel-climate relationship varies between species a species-specific relationship must be derived.

This paper presents data from modern Barbary sheep populations, demonstrating a link between the $\delta^{18}\text{O}$ of the species tooth enamel and the $\delta^{18}\text{O}$ of local environmental waters. These results are then applied to Barbary sheep teeth from archaeological contexts in the Gebel Akhdar of northeast Libya. Results show patterns of climate change over the last 100 ka that can be correlated to the archaeological record, providing the means to assess the impact of such changes on human populations.

Address of corresponding author: H. Reade: Downing Street, Cambridge, CB2 3DZ, United Kingdom, e-mail: hr296@cam.ac.uk

Recent achievements and future prospects of ice core science

Rein Vaikmäe

Institute of Geology at Tallinn University of Technology, Tallinn

Since the early 1960s the ice core community has produced a wealth of scientific results from a still relatively limited number of deep drilling sites in Greenland and Antarctica with the longest record extending back to the last interglacial in Greenland and covering eight glacial-interglacial cycles in Antarctica. Although measurements performed on the first ice cores, Camp Century and Byrd, largely focused on the isotopic composition of the ice as an indicator of climate change, the number of studied parameters has steadily increased encompassing numerous measurements performed on the entrapped air bubbles, on various impurities as well as on the ice itself. The climatic information provided by these various paleodata is extremely rich. The relationships between forcing factors and climate, about the importance of carbon cycle feedbacks, about the occurrence of abrupt climate variability, and about the interplay between polar climate, ice sheet dynamics, and sea-level variations are examples that are highly relevant to future climate change.

With the completion of major projects in Greenland and Antarctica over the last 15 years, the international ice coring community is planning for the next several decades. The costs and scope of future work create the need for coordinated international collaboration. Developing this international collaboration is the charge of IPICS, International Partnerships in Ice Core Sciences, a planning group currently composed of ice coring scientists, engineers, and drillers from 19 nations. By now the discussions have led to an ambitious four-element framework that both extends the ice core record in time and enhances spatial resolution.

The four projects were defined as:

- 1) A deep ice coring program in Antarctica that extends through the mid-Pleistocene transition, a time period where Earth's climate shifted from 40,000 year to 100,000 year cycles.
- 2) A deep ice core in Greenland recovering an intact record of the last interglacial period.
- 3) A bipolar network of ice core records spanning approximately the last 40,000 years.
- 4) A global network of ice core records spanning the last 2,000 years.

Address: ReinVaikmäe: Ehitajate tee 5, 19086 Tallinn, Estonia, e-mail: Rein.vaikmae@ttu.ee

Pleistocene seasonal temperature reconstructions from $\delta^{18}\text{O}$ of bison teeth, Ural Russia

Tatiana A. Velivetskaya
Far East Geological Institute, FEB Russian Academy of Sciences, Vladivostok

Nikolay G. Smirnov
Institute of Plant and Animal Ecology, Ural Centre Academy of Sciences, Yekaterinburg

Sergey I. Kiyashko
Institute of Marine Biology, FEB Russian Academy of Sciences, Vladivostok

Alexandr V. Ignatiev
Far East Geological Institute, FEB Russian Academy of Sciences, Vladivostok

Alexandr I. Ulitko
Institute of Plant and Animal Ecology, Ural Centre Academy of Sciences, Yekaterinburg

The aim of present study is the reconstruction of seasonal temperature variations during the late Pleistocene in Nether-Polar Urals, Russia. For this purpose, we analysed the $\delta^{18}\text{O}$ values of the carbonate component in enamel of tooth from fossil bison (*Bison priscus* Boj.). The lower jaw with fully preserved tooth sequences and fragments of cranium from adult bison have been collected from a grot located in the Urals, Russia (56°23'N, 57°37'W). The age of remains is estimated by a time interval from 17 to 23 thousand years according to radiocarbon datings of bones from upper and lower covered layers.

Oxygen isotope composition of the carbonate component in tooth enamel was analysed from five teeth (M1, M2, M3, P3 and P4). Enamel samples were collected by drilling of grooves from the cervix to the apex of tooth crown. Sample preparation for $\delta^{18}\text{O}$ analysis was performed using 105% phosphoric acid at 95 °C. The evolved CO_2 was cryogenically purified. The oxygen isotope ratio of CO_2 was measured with a Finnigan MAT 253 mass spectrometer in a continuous flow mode with He as the carrier gas. Standard deviation of the $\delta^{18}\text{O}$ analysis is $\pm 0.15\text{‰}$.

The intra-tooth $\delta^{18}\text{O}_{\text{V-SMOW}}$ values of enamel displayed variations: M1 (from 16.6 to 18.0)‰; M2 (from 16.8 to 20.5)‰; M3 (from 16.2 to 20.7)‰; P3 (from 15.5 to 17.9)‰; P4 (from 16.9 to 20.9)‰. The temporal record of $\delta^{18}\text{O}$ variations over 2.5 yr obtained by connection of individual intra-tooth $\delta^{18}\text{O}$ variations on a time scale. The connection was performed according the eruption sequence of M1, M2, M3, P3, P4 tooth. The temporal $\delta^{18}\text{O}$ record reproduces the seasonal $\delta^{18}\text{O}$ variations with amplitude from 15.5‰ to 20.9‰. Adjusted for dampened $\delta^{18}\text{O}$ values due to the mineralization process, the seasonal $\delta^{18}\text{O}$ values ranged from 13.7‰ to 23.1‰. This data has allowed us to estimate the $\delta^{18}\text{O}$ values of environmental waters in range from -10.0‰ to -23.4‰. Winter and summer temperatures were estimated to be respectively -25°C and +10°C. Pleistocene winter temperature was about 9 °C lower then at present and summer temperature was about 7 °C lower then at present.

Address of corresponding author: T. A. Velivetskaya: 100-let Vladivostoku 159, Vladivostok, 690022, Russia, e-mail: velivetskaya@mail.ru

TECHNICAL DEVELOPMENTS

Reduced partition function ratios for isotopes of hydrated alkali and alkaline earth ions calculated by a simple electrostatic model

Maciej Czarnacki, Stanislaw Halas
Mass Spectrometry Laboratory, Institute of Physics,
Marie Curie-Skłodowska University, Lublin

We describe a simple electrostatic model of hydrated ions $[M(H_2O)_n]^+$ ($n = 3-18$, $M = Li, Mg, Ca, K$) which enables to calculate ion vibration frequency of the ground state. In this model the considered ion with a reduced mass vibrates in quasispherical well formed by the ion-dipole attractive potential and repulsive valence potential, these simplifications allowed to solve one dimensional Schrödinger equation, whilst the calculated ground state was considered as one of triply degenerated state of the three dimensional motion of the ion vs. hydration shell. The reduced partition function ratios were calculated from the vibration frequencies using Urey's (1947) harmonic approximation formula.

The results obtained in this way are in good agreement with those obtained by much more laborious ab initio molecular orbital methods, like SCF Hartree-Fock, DFT, MP2, etc. Moreover, we were able to extend calculations to hydrated Li and K ions surrounded with two shells of water molecules. These results are the first estimations of the upper limit of isotope fractionation in water solutions, which are 99.3‰ for Li and only 2.5‰ for K isotopes.

Key words: hydration, ion radii, isotope effects, Li, Mg, Ca, K, vibration frequencies, β factors

Introduction

For more than a decade precise analytical methods (TIMS and ICPMS) for the study of natural variations of lithium isotopes have been developed (Tomascak 2004 and references therein). These studies recognized that natural variation of $^7Li/^6Li$ isotope ratios exceeds 60‰. In contrast the variation of the $^{41}K/^{39}K$ ratio in terrestrial materials is at the 0.5‰ level (Humayun and Clayton 1995), which is surprising for a mass dependent isotope effect at the relative mass differences of

Addresses: M. Czarnacki, S. Halas: Marie Curie-Skłodowska University, 20-031 Lublin, Poland
e-mails: maciej.czarnacki@gmail.com, halas@tytan.umcs.lublin.pl

Received: April 4, 2011; accepted: June 8, 2011

$(7-6)/6=0.16$ and $(41-39)/39=0.05$, respectively. The answer to this puzzle relates to the hydration of these elements.

Lithium has the smallest cation radius, but the largest radius of the hydration sphere. For this reason the electric interaction of Li^+ with the inner shell of dipoles of water molecules is particularly strong and it leads to such a great isotope fractionation. In this paper we will compare the hydration effect in the case of Li, K, Mg and Ca cations. We have extended calculation of reduced partition function ratios to these of Mg and Ca cations in order to test our model by comparison with the results obtained by more sophisticated ab initio methods (Rustad et al. 2010).

The first calculation of equilibrium constant for isotope exchange reaction between lithium hydrides (LiH and LiD) and lithium vapour for a broad temperature range was reported by Urey (1947): at 298.1 K the equilibrium constants attain 1.025 and 1.029, respectively. Lithium isotope exchange reaction between solid Li and dissolved LiCl was experimentally determined by Singer and Rock (1972). However, their equilibrium constant ($K = 1.046 \pm 0.013$) was determined electrochemically with low precision and for one temperature (298.6K) only. They also tried to calculate this equilibrium constant from statistical thermodynamics, but their value was evidently too large (1.29–1.33). Theoretical estimation of lithium isotopic reduced partition function ratio for lithium ions in aqueous solution were made by Yamaji et al. (2001), who report their ab initio results for only one temperature (298 K): their maximum value of lithium isotope fractionation factor between hydrated ion and " Li^+ exchanger" is 1.07.

Model

We will consider a metal ion electrically interacting with surrounding electric dipoles of water molecules. Such electrostatic approach is fully justified because the ion motion is much slower in comparison to the electronic motion in both water molecule and ion. Geometry of the electrostatic model used in calculations is shown in Fig. 1. Numerical values for the water molecule were taken from Malenkov (1962).

Let p denote dipole moment of the water molecule, then the electric potential at distance r from its center (for $r \gg$ distance between negative, $-q$, and positive, $+q$, charge making up this dipole) in polar coordinates is

$$V(r, \varphi) = \frac{p}{4\pi\epsilon_0} \frac{\cos\varphi}{r^2} \quad (1)$$

where φ is the angle between vector $(-q, +q)$ and the vector r , and ϵ_0 is the electric constant.

Formula (1) may be rewritten in Cartesian coordinates, taking into account that for any plane (x,y) passing along the vector $(-q, +q)$ we have $r^2 = x^2 + y^2$, and $\cos \varphi = x/r$

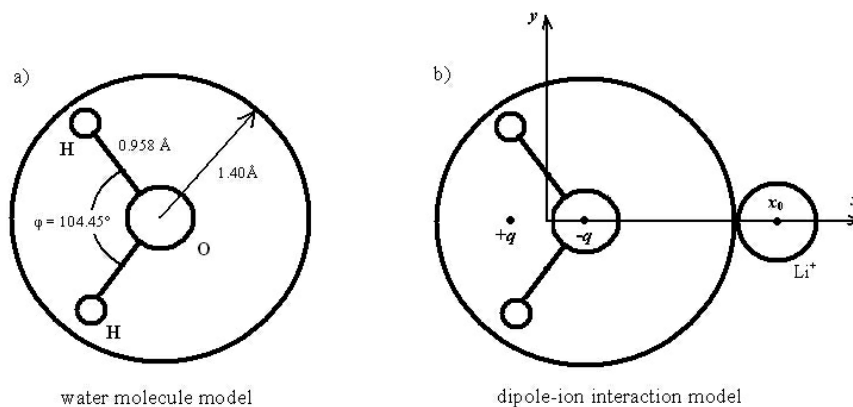


Fig. 1
Geometry of the electrostatic model used in calculations

Hence

$$V(x, y) = \frac{p}{4\pi\epsilon_0} \frac{x}{(y^2 + x^2)^{3/2}} \tag{2}$$

In our model x will be fixed to an x_0 value at which the ion sphere touches that of oxygen atom in H_2O molecule, thereby the stationary (time independent) states of the ion motion can be found from the Schödinger equation

$$\hat{H}(y)\psi(y) = E\psi(y) \tag{3}$$

Where $\hat{H}(y)$ is the Hamiltonian and E is the energy of the state represented by the wave function $\psi(y)$

In order to account for the total energy from interaction of the ion with k dipoles in the first shell (at the distance x_0) and l dipoles in the second shell (at a larger distance x_1) the potential energy of the Hamiltonian was extended as follows:

$$\hat{H}(y) = \frac{h^2}{2\mu} \nabla^2 - \frac{ekp}{4\pi\epsilon_0} \frac{x_0}{(y^2 + x_0^2)^{3/2}} - \frac{elp}{4\pi\epsilon_0} \frac{x_1}{(y^2 + x_1^2)^{3/2}} \tag{4}$$

where μ is the reduced mass of the ion surrounded by k water molecules in the first shell of the hydration sphere and it was expressed by the mass of ion and mass of oxygen of the adjacent k water molecules:

$$\mu = \frac{m_M \cdot km_O}{m_M + km_O} \tag{5}$$

The x_0 values given in Table 1 are defined as the distances between the considered cation center and dipole center of water molecules from the first shell, note that the last center differs from the water molecule center treated as a ball of radius given in Table 1. In similar manner are defined distances x_1 , though not shown in Fig. 1. In calculations of the distances x_0 and x_1 , we anticipated that water dipoles are uniformly distributed in the space around a considered metal ion due to their mutual repulsion. In calculations of the reduced mass (Table 2), only the first shell of dipoles was taken into account, because the second one has a weak interaction and is more elastically bounded to the ion.

The Schrödinger equation (3) with the Hamiltonian (4) was solved in order to calculate the ground state, i.e. zero point energy (ZPE) level. The lowest state may be considered as that of quantum oscillator state, because the resulting potential energy of the considered metal ion surrounded by one or two shells of water dipoles has a parabolic character, see plots in Fig. 2.

For the ZPE calculation we used the computer program MARRS (Salejda et al. 2002), the algorithm of which was based on the finite elements method with 5 points approximation of the second derivative. Calculations of the wave functions, ψ , and the energy states were made on grids composed of 64000 elements. The parameters used in this model are listed in Table 1, the reduced masses are listed in Table 2, whereas in Table 3 are given the calculated vibrational frequencies (in cm^{-1} units) of the central ion of each considered cluster (for heavy and light isotope, respectively).

Table 1
Values of parameters used in ion-water dipole interaction model calculations

Parameter	H ₂ O	Li ⁺	Mg ²⁺	Ca ²⁺	K ⁺
Radius [Å]	1.4	0.38 ³	0.66 ²	0.99 ²	1.33 ²
Charge [e]	0	+1	+2	+2	+1
x_0 [Å]	-	2.08	2.35	2.68	3.02
x_1 [Å]	-	3.41	3.43	3.47	3.59
Dipole moment [D]	1.8546 ¹	-	-	-	-

¹ Clough et al. 1973, ² Weast 1980, ³ Halas and Mackiewicz 2003

Table 2
Reduced mass of cations used in our calculations expressed in atomic mass units

k	⁶ Li ⁺	⁷ Li ⁺	²⁴ Mg ²⁺	²⁶ Mg ²⁺	⁴⁰ Ca ²⁺	⁴⁴ Ca ²⁺	³⁹ K ⁺	⁴¹ K ⁺
3	5.33	6.11	-	-	-	-	-	-
4	5.48	6.31	-	-	-	-	-	-
5	5.33	6.11	-	-	-	-	-	-
6	5.64	6.52	19.20	20.46	28.23	30.17	27.73	28.73

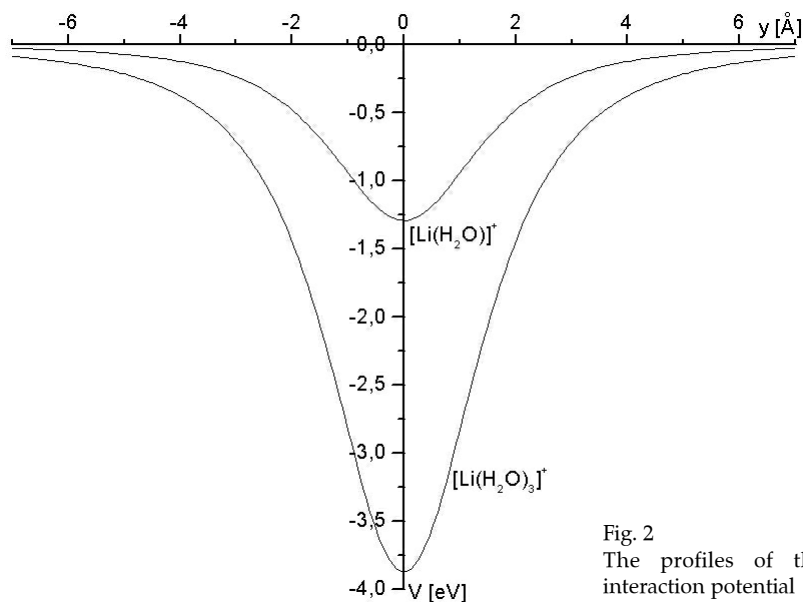


Fig. 2
The profiles of the dipole-ion interaction potential

Calculation of β factors for hydrated ions

Having calculated ZPE levels of the vibration motion of the ion, we can calculate the β factors, i.e. reduced partition function ratios, which are fundamental in calculation of the isotope effects at thermodynamic equilibrium. The β factor is defined as follows:

$$\beta = \frac{Q_{tr}^H Q_{rot}^H Q_{vib}^H}{Q_{tr}^L Q_{rot}^L Q_{vib}^L} \tag{6}$$

where the upper subscripts, H and L, refer to the appropriate partition function, Q, of the isotopically substituted hydrated ion by heavy and light isotope, respectively, whereas the lower subscripts denote translational, rotational and vibration degree of freedoms. In the harmonic approximation the formula (6) can be converted to the following (Urey 1947, O'Neil 1986, Chacko et al 2001):

$$\beta = \prod_i \frac{u_i^H}{u_i^L} \frac{\exp\left(-\frac{u_i^H}{2}\right) (1 - \exp(-u_i^L))}{(1 - \exp(-u_i^H)) \exp\left(-\frac{u_i^L}{2}\right)} \tag{7}$$

where $uj = 2 \cdot E_j / (k_B T)$, E_j is the ZPE value of the j -th vibration mode, k_B is the Boltzmann constant and T is absolute temperature.

The product in equation (7) is extended over all vibration modes. It should be noted that this product is reduced to the three vibration states of the hydrated ion only, because the remaining vibrations in the considered system are insensitive to isotope substitution of the central ion. In the case of highly symmetric system, which is the case for high hydration degree, we may safely assume that all the three vibrational modes (the motion proceeds in the 3-dimensional space) are identical. This assumption is equivalent to triple degeneration of the energy states of the full 3-dimensional Schrödinger equation, which should be solved instead of equation (3).

Results

The β factors for the following isotopically substituted systems of $[\text{Li}(\text{H}_2\text{O})_n]^+$, $[\text{Mg}(\text{H}_2\text{O})_n]^{2+}$, $[\text{Ca}(\text{H}_2\text{O})_n]^{2+}$ and $[\text{K}(\text{H}_2\text{O})_n]^+$ were calculated by the method presented above and compared with those existing literature data (Yamaji et al. 2001, Rustad et al. 2010).

In Table 3 β factors calculated for temperature 273.15 K are shown for $[\text{M}(\text{H}_2\text{O})_n]^+$ clusters with different number of water molecules, $n = k + l$, distributed in two shells. In frame-work of the electrostatic model we could straightforward consider the influence of water dipoles from the second shell of the hydrated ion. It should be noted that for hydrated ion of potassium, $[\text{K}(\text{H}_2\text{O})_n]^+$, no evaluations of β factors were published by far.

The comparison of calculated reduced partition function ratios with literature data is shown in Table 4. It is seen that our values for lithium isotopes are close to the first set of results calculated by Yamaji et al. (2001) or fall between their two sets. The same refers to β factors for magnesium and calcium isotopes, which are compared with results of Rustad et al. (2010). The calculated $1000 \cdot \ln(\beta)$ values as a function of temperature are listed in Table 5 and plotted in Fig. 3.

Discussion

The calculations made in this paper refer to highly symmetric systems of the hydrated ions of alkali and alkaline earth metals. These systems within electrostatic approximation attain nearly spherical symmetry due to dominant electrostatic interactions between H_2O dipoles and considered spherical ions having closed electron shells.

Below we will discuss the influence of the parameters used in our model (Tables 1 and 2) on the final result. We will allow varying the most important parameters (ion radius, reduced mass, and dipole moment of water molecule) in calculation of β factor for lithium, which is the most sensitive cation to hydration isotope effects. These calculations have been made for $[\text{Li}(\text{H}_2\text{O})_n]^+$, where $n = 6$

Table 3

Values of the reduced partition function ratio, β , at 273.15 K for $[M(H_2O)_n]^+$ clusters. k is the number of water molecules in the first hydration shell and l is the number of water molecules in the second shell, ν^H and ν^L are triply degenerated vibrational frequencies of the central ion (of heavy and light isotope, respectively) in each considered cluster

Cluster type	k	l	ν^H [cm ⁻¹]	ν^L [cm ⁻¹]	β
$[Li(H_2O)_n]^+$	3	0	347.64	371.91	1.059
	4	0	395.29	423.77	1.078
	5	0	403.28	431.43	1.079
	6	0	397.46	427.03	1.082
	6	8	437.32	469.80	1.098
	6	12	454.81	488.56	1.104
$[Mg(H_2O)_n]^{2+}$	6	0	300.16	309.69	1.020
	6	8	333.15	343.67	1.024
	6	12	346.34	357.28	1.026
$[Ca(H_2O)_n]^{2+}$	6	0	190.30	196.61	1.008
	6	8	221.89	229.20	1.011
	6	12	234.85	242.56	1.013
$[K(H_2O)_n]^+$	6	0	108.27	110.17	1.0014
	6	8	133.88	136.22	1.0022
	6	12	143.23	145.74	1.0025

+ 12. For $r_{Li} = 0.68 \text{ \AA}$, at the remaining parameters conserved, one obtains $\beta = 1.091$, which is considerably lower than result 1.104 presented in Table 3, but still it looks sensible. However we have intentionally used the revised value of 0.382 \AA from Halas and Mackiewicz (2003) as the most reliable, because it is consistent with other ionic radii for two electron systems: H^- , He , Li^+ , Be^{2+} , B^{3+} ... Another independent estimation of Li^+ radius follows from consideration of the length of nearly pure ionic bonding in the $LiCl$ molecule, which is $2.01\text{--}2.03 \text{ \AA}$ (Pauling 1960, Boldyrev and Simson 1993). Calculating the length of ionic bonding in $LiCl$ molecule with Li^+ radius taken from CRC Handbook one obtains 2.49 \AA , whereas with that of Halas and Mackiewicz (2003) one obtains a more

Table 4

Comparison of calculated reduced partition function ratios with literature data. N is total number of water molecules in the considered cluster

N	This work		Literature	
	Li ⁺ T = 298 °K			
3	1.050	1.059 ¹	1.067 ¹	1.067 ¹
4	1.066	1.067 ¹	1.070 ¹	1.070 ¹
5	1.066	1.074 ¹	1.056 ¹	1.056 ¹
6	1.069	1.081 ¹	1.041 ¹	1.041 ¹
Mg ²⁺ T = 273.15 °K				
14	1.024	-	-	-
18	1.026	1.027 ²	1.028 ²	1.028 ²
Ca ²⁺ T = 273.15 °K				
14	1.011	-	-	-
18	1.013	1.016 ²	1.017 ²	1.017 ²
21	-	1.013 ²	1.014 ²	1.014 ²

¹ Yamaji et al. 2001, ² Rustad et al. 2010.

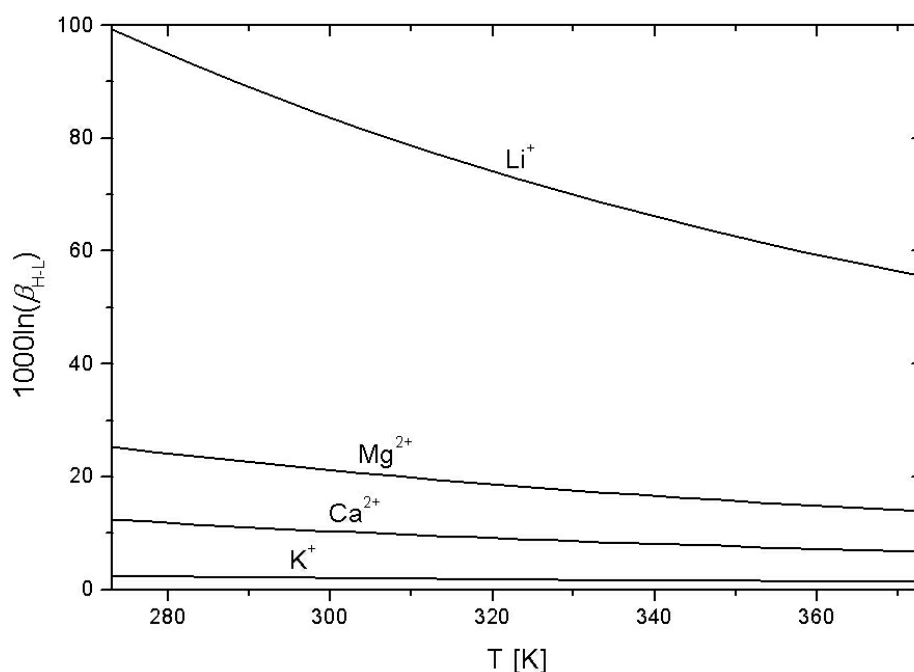


Fig. 3
Permil fractionation between hydrated ion and respective metal vapor as a function of temperature

reliable value of 2.19 Å. Similar consideration for ionic bonding in the LiF molecule yields 1.71 Å with Li⁺ radius taken from Halas and Mackiewicz (2003) and 2.01 Å with Li⁺ radius taken from CRC Handbook, whilst Boldyrev and Simson (1993) report 1.59 Å (ab initio calculation) and 1.56 Å (experimental result). These two examples of ionic bonding support the revised value for Li⁺ radius.

The next parameter, μ , was calculated assuming that only oxygen in H₂O is moving during ion vibration, which seems sensible. However with mass of the whole water molecule, we obtain for μ values 5.68 and 6.57 a.u., respectively, and identical $\beta = 1.104$ as in Table 3. Finally we have considered the uncertainty of dipole moment of H₂O molecule. Assuming $p = 3$ D for liquid water instead 1.85 D one obtains obviously too large $\beta = 1.165$; such high value for p was calculated by Silvestrelli and Parrinello (1999), however it has not been determined experimentally.

The advantages and drawbacks of our approach in comparison with ab initio methods may be summarized as follows. The new method is highly effective for fast evaluation of the reduced partition function ratios for hydrated ions. The results obtained by this method are in good agreement with those obtained by

Table 5
Calculated $1000 \cdot \ln(\beta)$ values as a function of temperature for all the considered hydrated ions

T [°C]	1000·ln(β), n = 18			
	[Li(H ₂ O) _n] ⁺	[Mg(H ₂ O) _n] ²⁺	[Ca(H ₂ O) _n] ²⁺	[K(H ₂ O) _n] ⁺
0	99.3	25.3	12.4	2.48
10	93.0	23.6	11.6	2.31
20	87.2	22.1	10.8	2.16
25	84.5	21.4	10.5	2.08
30	81.9	20.7	10.1	2.02
40	77.2	19.5	9.5	1.89
50	72.8	18.3	8.9	1.78
60	68.7	17.3	8.4	1.67
70	65.0	16.3	7.9	1.58
80	61.6	15.4	7.5	1.49
90	58.4	14.6	7.1	1.41
100	55.5	13.9	6.7	1.33

much more laborious ab initio molecular orbital methods, like SCF Hartree-Fock, DFT, MP2, etc. Another advantage is a lesser number of assumptions than in the case of ab initio methods. Only well known fundamental parameters like ion radii, size of water molecule and its dipole moment was used in the electrostatic model. There is no need to apply a scaling factor to the experimental data in this model. Also small computers of class PC are sufficient for calculation by this model.

However, the electrostatic model could give no answers regarding precise cluster structure of hydrated ions, because water-water interactions are not included into calculations.

The model assumed that water dipoles are uniformly distributed around the ion, due to their mutual repulsions.

In summary, we present a new simple and effective model for calculation of the reduced partition function ratios for hydrated ions and the results of $1000 \cdot \ln \beta$ calculation for Li, K, Mg and Ca hydrated cations in temperature range from 0 to 100 °C. The same model can be also applied to other hydrated ions (spherically symmetric) like Cl⁻ and Br⁻, and S²⁻, but not to Fe²⁺, Fe³⁺, Cu²⁺ etc., which do not have closed electronic shells alike in noble gas atoms.

Conclusions

Inasmuch as β factors obtained here for Mg and Ca are in good agreement with those obtained by more sophisticated ab initio methods (Rustad et al. 2010), our electrostatic model may be considered as an alternative tool which allows to

estimate quickly the isotope fractionation range for a number of elements which exist in ionic form (with closed electronic shells) in water solutions.

Our model of hydrated ions was for the first time applied to such broad range of temperature and cation species including the second hydration shell in Li^+ and K^+ ions. So far the calculated $1000 \cdot \ln \beta$ for potassium is the first estimation of the upper limit for this element in the Earth. At temperature of 273 K these values are 99.3‰ for $[\text{Li}(\text{H}_2\text{O})_n]^+$, and only 2.5‰ for $[\text{K}(\text{H}_2\text{O})_n]^+$. These limits for divalent metals, Mg and Ca, fall between these two extremes (see Table 5 and Fig. 3).

References

- Boldyrev A.I., J. Simson, P von R. Schleyer 1993: Ab initio study of the electronic structures of lithium containing diatomic molecules and ions. – *J. Chem. Phys.*, 99., pp. 8793-8804.
- Chacko T., D. Cole., J Horita 2001: Equilibrium oxygen, hydrogen and carbon isotope fractionation factors applicable to geologic systems. – *Rev. in Mineralogy & Geochemistry*, 43, pp. 1-81.
- Clough S.A., Y. Beers, G.P Klein, .S. L Rothman 1973: Dipole moment of water from Stark measurements of H_2O , HDO, and D_2O . – *J. Chem. Phys.*, 59, pp. 2254-2259.
- Halas, S., P Mackiewicz 2003: Radii of di-electron systems: H, He, Li^+ , Be^+ , B^{3+} , C^{4+} . a revision of the ionic radius for lithium. – *Ann. Pol. Chem. Soc.* 2, pp. 909-913.
- Humayun, M., R.N. Clayton 1995: Precise determination of the isotopic composition of potassium: Application to terrestrial rocks and lunar soils. – *Geochim. Cosmochim. Acta*, 59, pp. 2115-2130.
- Malenkov, G.G. 1962: Geometry of structures consisting of water molecules in hydrated crystals. – *J. Struct. Chem.*, 3, pp. 206-226.
- O'Neil, J.R. 1986: Theoretical and experimental aspects of isotope fractionation. – *Rev. in Mineralogy*, 16, pp. 1-40.
- Pauling, L. 1960: *The Nature of the Chemical Bond*. – Cornell Univ. Press, Ithaca, New York.
- Rustad, J.R., W.H. Casey, Q-Z. Yin E.J. Bylaska, A.R. Felmy, S.A. Bogatko, V.E. Jackson, D.A. Dixon 2010: Isotopic fractionation of $\text{Mg}^{2+}(\text{aq})$, $\text{Ca}^{2+}(\text{aq})$, and $\text{Fe}^{2+}(\text{aq})$ with carbonate minerals. – *Geochim. Cosmochim. Acta*, 74, pp. 6301-6323.
- Salejda, W, M.H. Tyc, M. Just 2002: Algebraic methods for resolving of the Schrödinger equation. – Polish Scientific Publishers PWN, Warsaw. (In Polish.)
- Silvestrelli, P.L., M. Parrinello 1999: Water molecule dipole in gas and in the liquid phase. – *Phys. Rev. Lett.*, 82, pp. 3308-3311.
- Singer, G., P.A. Rock 1972: Thermodynamics of lithium exchange reactions. III. Electrochemical studies of exchange between isotopic metals and aqueous ions. – *J. Chem. Phys.*, 12, pp. 5556-5561.
- Tomascak, P.B. 2004: Development in the understanding and application of lithium isotopes in the earth and planetary systems. – *Rev. in Mineralogy & Geochemistry*, 55, pp. 153-195.
- Weast, R.C. Ed. 1980: *CRC handbook of chemistry and physics*, 61st ed. – CRC Press Inc. 1980-1981.
- Urey, H.C. 1947: *The thermodynamic properties of isotopic substances*. – *J. Chem. Soc.*, 1947 (London), pp. 562- 581.
- Yamaji K., Y. Makita H. Watanabe, H. Sonoda, H. Kanoh, T. Hirotsu, Ooi Kenta 2001: Theoretical estimation of lithium isotopic reduced partition function ratio for lithium ions in aqueous solution. – *J. Phys. Chem., A* 105, pp. 602- 613.

Ab initio calculations of sulfur isotope fractionation factor for H₂S in aqua-gas system

Maciej Czarnacki, Stanislaw Halas
Mass Spectrometry Laboratory, Institute of Physics,
Marie Curie-Skłodowska University, Lublin

High level *ab initio* calculations have been performed for hydrogen sulfide in aqua-gas system. Based on B3LYP density functional method with two Pople basis sets, 6–31G(d) and 6–311+ +G(d,p), we have obtained the minimum energy structures of H₂S molecule and H₂S–nH₂O hydrogen bonded molecular clusters (where n = 1–5). For these structures the internal and intermolecular harmonic vibrational frequencies were calculated. No scaling factor was used.

Using the Bigeleisen-Mayer formula we have evaluated the reduced partition functions ratios for the clusters and respective sulfur equilibrium isotope fractionation factor as a function of temperature. The highest sulfur isotope fractionation of 1.16‰ (at 20 °C) for hydrogen sulfide in aqua-gas system obtained from our calculations is in good agreement with experimental data published so far (0.85‰ and 1.52‰). This is the first theoretical estimation of sulfur isotope fractionation between gaseous and hydrated hydrogen sulfide (dissolved H₂S).

Address of corresponding author: M. Czarnacki: 20-031 Lublin, Poland
e-mail: maciej.czarnacki@gmail.com

Rapid ^2H analysis of small H_2O samples by CF-IRMS

Eric M. Galimov, Vyacheslav S. Sevastyanov
*Vernadsky Institute of Geochemistry and Analytical
Chemistry, Moscow*

Nataliya E. Babulevich
NRC Kurchatov Institute, Moscow

Alexander A. Arzhannikov
*Vernadsky Institute of Geochemistry and Analytical
Chemistry, Moscow*

In the past few years, an increase in interest in oxygen-conducting solid electrolyte electrochemical devices has been observed. The basic principles of operation of devices based on the solid electrolyte are (1) the oxidation of organic compounds followed by formation of simple gases CO_2 , H_2O , NO_x or (2) the reduction of water and organic compounds followed by formation of H_2 . These principles we have used for IRMS analysis of water. The present study is devoted to development of the high-temperature solid electrolyte reactor (SER) based on yttria-stabilized zirconia for decomposition of water. The device proposed is coupled on-line to Delta Plus XP stable isotope mass spectrometer (Thermo Fisher Scientific).

A solid electrolyte possesses the oxygen ions related conductivity at high temperatures (800–1000 °C). This reactor is made of tubular, thin-walled zirconia ceramics with inner diameter of 1 mm and of 10 cm total length. The solid-electrolyte reactor is connected in three-electrode circuit supported by the Elins PS8 Potentiostat. The inner electrode of the reactor served as the working electrode. Reference electrode is on the outer side.

The H_2O is decomposed on the triple-phase interface of the SER. Oxygen is turned into ions which under electrical voltage (1.2V) are moved through solid electrolyte wall outward. The flow of a He carrier gas swept hydrogen to isotope ratio mass spectrometer.

During several seconds compounds passed through the SER. To introduce 0.2 μL of water into He flow at ~ 1 mL/min a split mode (split ratio 500:1) was used. The injector temperature is held at 250 °C. The solid electrolyte reactor was set to a temperature of 950 °C. Full time of analysis was 100-150 sec.

We measured δD values of water standards: VSMOW, SLAP, OH-1, OH-2, OH-3, OH-4 and obtained precision of 1–2‰. Our reduction SER can also be used for rapid ^2H analysis of organic materials.

New reactor has a very small size, provides rapid measurements of small water sample in the wide range of δD values, and has a good reliability.

Address of corresponding author: V. S. Sevastyanov: ul. Kosygin 19, Moscow 119991, Russia
e-mail: vsev@geokhi.ru

Innovations in technical developments of stable isotope analyses

Stanislaw Halas

*Mass Spectrometry Laboratory, Institute of Physics,
Maria Curie-Skłodowska University, Lublin*

I will start my lecture by recalling the memory of Roy Krouse, the great ESIR member, who passed away in March 2, 2010. I will mention his developments in stable isotope analysis of sulphur, e.g. use of Paar bomb and Kiba reagent for sulphur preparation in early 80's. At that time he already used GC separation of gaseous components in hydrocarbon gas combined with IRMS to study samples for exploration of fuels. His developments have been recalled in a special issue of *Chemical Geology* by Mayer and Hutcheon (2004) starting from Roy's pioneering study of selenium isotopes.

Then I will review briefly the new developments in the Lublin laboratory. Particularly I will present the latest achievements in highly reproductive oxygen extraction method from phosphates. This method enabled us to calibrate 3 new Ag_3PO_4 standards in cooperation with two internationally well-known laboratories abroad. By the application of this new method, we have studied the oxygen isotopes of shark teeth phosphates from Eocene deposits in Mangyshlak peninsula, Kazakhstan, where we estimated seawater paleotemperatures.

Another important development is the start of a new IRMS for precision chlorine isotope measurement. The achieved precision is better than 0.01‰. Details will be presented in the lecture by A. Pelc during this session.

Finally I would present $^7\text{Li}/^6\text{Li}$ technique and our first results. We have used the TIMS technique with double filaments in the ion source. We have tried to apply lithium isotope data to explain relatively high concentration of Li (17 mg/L) in the most famous mineral water named "Zuber" from Krynica Spa in Polish Carpathians.

Address: S. Halas: PL 20-31 Lublin, Poland, e-mail: stanislaw.halas@umcs.lublin.pl

UV laser ablation microanalysis of $\delta^{34}\text{S}$

Aleksandr V. Ignatiev, Tatiana A. Velivetskaya
Far East Geological Institute, FEB RAS, Vladivostok

Sulphur isotopes have been widely used in the study of igneous, sedimentary, hydrothermal, and biologic processes on the Earth. The development of *in situ* IR laser techniques enables high spatial resolution for sulphur isotope analysis. Laser ablation is becoming a dominant technology for direct solid sampling in geochemistry. UV laser ablation refers to the process in which an intense burst of energy delivered by a short laser pulse is used to remove a portion of sample material. The high photon-energy, short UV wavelength penetrates the plasma more efficiently and directly initiates bond breaking in the sample. These two conditions lead to a larger ablation rate and less fractionation.

We have developed a technique for determination of $^{34}\text{S}/^{32}\text{S}$ isotope ratios ($\delta^{34}\text{S}$) in sulphur-bearing minerals using UV laser ablation. A laser microprobe system has been constructed for high-accuracy (0.2‰), high-precision sulphur isotope analysis (0.1‰) with improved spatial resolution (50–100 μm). The system uses laser for *in situ* spot analysis by ultraviolet (UV) photoablation with 213 nm (Laser UP-213, New Wave Research). Our equipment consists of small volume stainless steel chamber, a capillary quartz reactor with quartz wool and six ports Valco valve with a trap for SO_2 . Helium (flow 40 cm^2/min) with 5% impurity of oxygen passes through the chamber. At a photoablation of the sample SO_2 and an aerosol are formed. SO_2 and the aerosol pass through the quartz reactor in a stream of helium. The aerosol is oxidized by oxygen to SO_2 at temperature 1000 °C. Total SO_2 is condensed to a trap with liquid nitrogen. The trap is slowly defrozen and cryogenically purified SO_2 enters through the open split in the ion source. Measuring the ratios of sulphur isotopes are carried out on a MAT-253 mass spectrometer. Reference SO_2 with known isotopic composition was used for standardization. Additionally, the camera (chamber?) is loaded with standards IAEA-S1, IAEA-S2, and IAEA-S3. In our system to obtain the amplitude of 1 Volt signal (for pyrite) 150 laser pulses is sufficient at a resolution of 100 μm and the radiation power of about 6 J/cm^2 . For all other cases 300 pulses are required at the same power. The high precision is documented by comparing *in situ* laser data with conventional analyses of sulphides. No dependence of $\delta^{34}\text{S}_{\text{V-CDT}}$ values on UV laser energy flux has been observed. Mineral-specific fractionation of sulphur isotopes in analysing pyrite, sphalerite, galena, has not been observed with a UV laser (213 nm)

Address of corresponding author: A. V. Ignatiev: FEGI, FEB RAS, pr. Stoletiya Vladivostoka 159, Vladivostok, 690022 Russia, e-mail: inatiev@fegi.ru

Noble gas measurements from 1 μL of water: fluid inclusions of speleothems

László Palcsu, László Papp, Zoltán Major
Institute of Nuclear Research of the Hungarian Academy of Sciences, Debrecen

We show that noble gases from fluid inclusions can be extracted and measured by a noble gas mass spectrometer. The water amount is measured via its vapour pressure in a certain volume. The accuracy of such a water determination is less than 1% in the case of 1 μl of liquid water, which allows us to determine accurate noble gas concentrations. The overall mass spectrometric measurement process is calibrated by means of well-known air aliquots in the range of $2.5 \cdot 10^{-5}$ to $1.0 \cdot 10^{-6}$ ccSTP. The reproducibility of ^{40}Ar measurements is better than 0.6%, while those of krypton and xenon isotopes are 0.9–2.2% and 0.8–2.0%, respectively. Theoretically, these precisions for noble gas concentrations obtained from sample measurements allow us to determine noble gas temperatures with an uncertainty of less than 1 °C. To verify the reliability of the measurement, noble gases of air equilibrated water (AEW) samples have been measured. In this measurement run we have performed numerous measurements. Some of these AEW samples show excess noble gases mainly in the heavier ones. Pre-treatment of the capillaries by helium flushing and heating improved the AEW sample preparation: although the measurement of two samples might have failed, the measurements of other two AEW samples gave reasonable noble gas concentrations very close to the expected ones. Noble gas concentrations obtained from soda straw stalactites showed extra excesses mainly for the heavier noble gases that can be attributed to an artefact from sample preparation, although noble gases of few samples sustain the potential of the method based on temperature dependent solubility concentration to be a useful palaeoclimate proxy.

Address of corresponding author: L. Palcsu: H-4026 Debrecen, Bem tér 18/c, Hungary
e-mail: palcsu@atomki.hu

Chlorine stable isotope ratio analysis by the negative surface ionization of chloromethane

Andrzej Pelc, Stanislaw Halas, Maciej Czarnacki
*Mass Spectrometry Laboratory, Institute of Physics,
Marie Curie-Skłodowska University, Lublin*

The most common method used in chlorine isotope ratio analysis employs the conversion of a chlorine sample to chloromethane (CH_3Cl) prior to the mass spectrometric analysis. Chloromethane is very convenient for mass spectrometry as it has no memory effect in vacuum systems and could be easily obtained from a chlorine sample and transferred from the preparation line to the inlet system of mass spectrometer (MS) since its melting point is -97.7°C .

In almost all chlorine isotope ratio studies the chloromethane gas is admitted to an electron impact ion source of an MS, where as many as 14 various type of positive ions are formed. Two of the ion species generated at m/z of 50 and 52, attributed to $\text{CH}_3^{35}\text{Cl}^+$ and $\text{CH}_3^{37}\text{Cl}^+$, are used for the isotope ratio measurements. The possible ions interference has got a considerable impact on the measured isotope ratios.

To eliminate disadvantages of the electron impact ionization and to increase the accuracy and efficiency of chlorine isotope ratio studies a new mass spectrometer with the negative ion source has been constructed. The novel part of this MS is the chlorine ion source which involves negative surface ionization of the chloromethane, whilst the remaining constituents are typical of dual inlet and dual collector MS. The negative ions are generated by the electron attachment to the Cl atoms followed by the CH_3Cl molecule dissociation. Using the invented ion source the only Cl^- anions ($m/z = 35$ and 37) are generated with efficiency dependent on the filament material and its temperature.

Moreover, enormous yield of the ion beam intensities leads to enhanced precision of the measurements. The standard uncertainty of single determination of $\delta^{37}\text{Cl}$ as small as 0.005‰ was obtained. In terms of the sample size the new method is more sensitive than IRMS, but less than TIMS and it requires at least 1 mg Cl. The method can also be applied for bromine isotope analysis on CH_3Br gas without instrumental modifications because Br has electron affinity (3.364 eV) close to that of Cl (3.615 eV).

This research was supported by Polish Ministry of Science and High Education (grant No. N N307 062136).

Address of corresponding author: A. Pelc: M. Curie-Skłodowskiej 1, 20-031, Poland,
e-mail: Andrzej.Pelc@poczta.umcs.lublin.pl

Isotope Ratio Mass Spectrometry for tracing the origin of cyanide for forensic investigation

Illa Tea, Ingrid Antheaum, Ben-Li Zhang

*Chimie et Interdisciplinarité, Synthèse, Analyse, Modélisation (CEISAM)
CNRS-Université de Nantes, Nantes*

Cyanide is often the poison of choice in murders because it is easily available at chemical and photographic supply house. In cases of an offender who has used cyanide, forensic investigation could reveal the source of cyanide and identify the supplier. Traditional forensic techniques are based on anionic impurities analysis for matching cyanide salts back to their source. Nevertheless, this analysis technique may be perturbed by sample contamination.

Our objective was to examine the possibility of distinguishing a set of commercial cyanide through $\delta^{13}\text{C}$ and $\delta^{15}\text{N}$ values and to develop a protocol for the $\delta^{13}\text{C}$ and $\delta^{15}\text{N}$ analysis of cyanide extracted from several food and medicine matrices.

Thirteen KCN and 9 NaCN stocks originating from different suppliers, batches and purities were analysed by Elemental Analyser coupled to Isotope Ratio Mass Spectrometry (EA-IRMS). In order to evaluate the ^{13}C and ^{15}N isotope fractionation and its influence during the isolation of cyanide from complex matrices, several methods of cyanide derivatization were tested on two different sources of cyanide solutions and in 3 matrices: orange juice, yogurt drinking and medicine.

The isotopic signature of each commercial cyanide varied from -51.96 to -25.77‰ for $\delta^{13}\text{C}$ and from -4.51 to $+3.81\text{‰}$ for $\delta^{15}\text{N}$, highlighting the potential of EA-IRMS technique to differentiate cyanide collected from different suppliers and batches. The comparison of isotope analysis results with different derivatives, revealed that $\text{Cu}_2[\text{Fe}(\text{CN})_6]$ was a most appropriate derivative compared to $\text{Fe}_4[\text{Fe}(\text{CN})_6]_3$ and AgCN derivatives. Indeed, the $\delta^{13}\text{C}$ and $\delta^{15}\text{N}$ values of $\text{Cu}_2[\text{Fe}(\text{CN})_6]$ were identical to those obtained from pure cyanide (KCN and NaCN), suggesting there was no isotope fractionation. The isotopic results obtained for the extracted and isolated cyanide from the 3 matrices showed a good reproducibility of the method and a weak matrix effect on isotope values.

These obtained results show that the developed method for determining N and C isotope in cyanide by EA-IRMS is a good tool for forensic investigations to compare cyanide from crime product with it from supplier.

Address of corresponding author: I. Tea: rue de la Houssiniere, BP 92208, F-44322 Nantes, France
e-mail: illa.tea@univ-nantes.fr

Simultaneous measurements of carbon and oxygen isotopologues of carbon dioxide using a mid-IR laser based platform

Eric Wapelhorst
Thermo Fisher Scientific, Bremen

Hans-Jürg Jost, James J. Scherer,
Joshua B. Paul
Thermo Fisher Scientific, Redwood City, CA

We are leveraging the strong absorption lines in the mid-infrared to simultaneously measure both isotopologues $\delta^{18}\text{O}$ and $\delta^{13}\text{C}$ of carbon dioxide at atmospheric concentration. For many applications, such as ecosystem fluxes or atmospheric monitoring, precision and accuracy required is less than $<0.1\%$. In the mid-infrared, CO_2 has very strong transitions that are particularly suited to achieve this goal using a robust multi-pass absorption cell. We will present results from laboratory tests of sensitivity and precision of a sensor currently under development.

Address of corresponding author: E. Wapelhorst: Hanna-Kunath Str. 11, D-28199 Bremen, Germany, e-mail: eric.wapelhorst@thermofisher.com

Index of authors

- Aires-Barros, L. 141
Alçıçek, M. C. 115
Al-Mashaikhi, K. 148
Alulema, R. 150
Alvarrão, F. 17
Andrews, J. 174
Antheaum, I. 205
Antoine, P. 174
Apostolopoulou, M.-V. 35
Arias, N. 150
Arzhannikov, A. A. 200
Babulevich, N. E. 200
Baciu, C. 139
Badeck, F. W. 16
Bajnóczy, B. 51, 75, 173
Balázs, B. R. 167
Baran, A. 129
Barešić, J. 121
Barker, G. 184
Barta, G. 173
Bathellier, C. 16
Baykara, M. O. 115
Becker, R. 145
Bedaso, Z. 22
Behm, M. 175
Belaid, M. 144
Benčić, M. 130, 153
Berkényi, T. 23
Biega, B. 43
Blaszczyk, M. 95
Blessing, M. 15
Bochevar, R. 98
Bojar, A.-V. 36
Bojar, H.-P. 36
Bronić, I. K. 121
Bucha, M. 20, 95
Budnitskiy, S. Yu. 99
Bukowski, K. 146
Burliga, S. 97
Busenberg, E. 45
Capasso, G. 104, 131
Carreira, P. M. 104, 131, 141
Carvalho, M. R. 104, 131, 134
Chmura, L. 38
Cieřka, M. 37
Costa, F. 17
Cuntz, M. 132
Czarnacki, M. 96, 189, 199, 204
Czuppon, Gy. 103
Cserny, T. 147
da Silva, M. A. 104, 141
Dabkowski, J. 174
Deák, J. 115, 138, 157
Dehairs, F. 35
Demény, A. 1, 51, 147, 157, 167
Dennis, P. 174
Dowgiallo, J. 145
Drozd, V. 51
Drzewicki, W. 97
Dulinski, M. 133, 146
Eggenkamp, H. G. M. 141
Everard, J. 103
Faurescu, I. 151
Fekete, J. 5, 75
Ferencz, I. 22
Fórizs, I. 1, 115, 121, 138, 147, 157, 175
Frechen, M. 173
Futó, I. 110, 152
Galego Fernandes, P. 134
Galimov, E. M. 200
Galkowski, M. 38
Garai, J. 51
Gat, J. R. 136
Ghashghaie, J. 16
Golobocanin, D. 143
Goode, D. J. 45
Gorczyca, Z. 38
Górka, M. 37, 38, 47
Gökgöz, A. 115
Grassa, F. 104, 131, 137
Griffith, D. W. 132
Gršić, Z. 143
Guendouz, A. 105, 144
Guliy, V. 98
Guller, I. 23
Gyöngyi, Z. 23

- Halas, S. 39, 96, 145, 189, 199, 201, 204
 Hamer, B. 18
 Handler, M. R. 103
 Hausmann, H. 175
 Havancsák, I. 75
 Haverd, V. 132
 Hegner, E. 51
 Henriques, B. 17
 Hofmann, M. E. G. 40
 Horváth, Á. 106, 108, 109
 Horváth, B. 40
 Horváth, E. 173
 Horvatinčić, N. 121
 Huber, C. 179
 Hunjak, T. 135
 Ignatiev, A. V. 99, 186, 202
 Imbrigiotta, T. E. 45
 Janeiro, A. I. 17
 Jasek, A. 38
 Jędrysek, M.-O. 21, 37, 39, 43, 47, 95, 97, 140
 Jelen, D. 38
 Jezierski, P. 25, 41
 Jodlowski, P. 107
 Jost, H.-J. 206
 Kaljo, D. 181
 Kalm, V. 176
 Kanduč, T. 18, 19, 20, 42, 137
 Kármán, K. 121, 138, 139
 Keitel, C. 132
 Kele, S. 115, 157
 Kern, Z. 175
 Kindler, P. 179
 Kirshtein, J. 45
 Kis, B. M. 139
 Kiss, A. 106
 Kiyashko, S. I. 186
 Knöller, K. 148
 Kocman, D. 19, 137
 Koeniger, P. 173
 Kosmas, P. 35
 Kovács, A. 23
 Krajcar Bronić, I. 26
 Krajniak, J. 97
 Krempels, K. 23
 Kubiak, K. 95
 Kuc, T. 38
 Kufka, D. 39, 43
 Kulinski, K. 46
 Larrea, O. 150
 Laumets, L. 176
 Lécuyer, C. 81, 177
 Leduc, C. 150
 Legge, T. 184
 Leuenberger, M. 179
 Levitskiy, V. I. 99
 Lewicka-Szczebak, D. 47, 140
 Limondin-Lozouet, N. 174
 Lojen, S. 29
 Lutz, H. O. 135
 Maamar, H. 144
 Maciejewska, A. 46
 Major, Z. 110, 203
 Malkiewicz, M. 47
 Maloszewski, P. 138
 Mance, D. 135
 Manciat, C. 150
 Marca-Bell, A. 174
 Markić, M. 42
 Marques, J. M. 104, 131, 141
 Martineau, F. 81
 Martma, T. 44, 181
 Marzecova, A. 44
 Matsuda, J. 103
 Matsumoto, T. 103
 McIntosh, J. C. 19, 42
 Medaković, D. 18
 Melikadze, G. I. 142
 Michelot, J.-L. 105
 Mikomägi, A. 44
 Miljević, N. 143
 Modelska, M. 37
 Molnár, M. 23
 Mori, N. 137
 Moulla, A. S. 105, 144
 Munoz, T. 150
 Nagy, G. 51
 Nagy, H. É. 106, 111
 Necki, J. 38
 Németh, T. 51
 Nguyen, C. D. 107
 Nowak, J. 107
 Nunes, D. 131
 Nunes, J. C. 131
 Obelić, B. 121
 O'Connell, T. 184

- Onac, B. P. 182
 Ouarezki, S. 144
 Özkul, M. 115
 Pack, A. 40
 Palcsu, L. 110, 152, 175, 203
 Papp, L. 110, 203
 Paul, J. B. 206
 Pavuza, R. 175
 Pelc, A. 96, 204
 Pempkowiak, J. 46
 Persoiu, A. 183
 Pešić, A. 143
 Pezdić, J. 20, 29
 Pintar, M. 29
 Pleśniak, L. 21, 95, 97
 Porowski, A. 145
 Proust, E. 15
 Puscas, C. M. 22
 Rajchel, J. 133
 Ramalho, L. 17
 Reade, H. 184
 Révész, K. 45
 Rman, N. 149
 Robert, F. 81
 Roller-Lutz, Z. 135
 Roman, C. 22
 Roose, P. 35
 Rózanski, K. 38, 146
 Sajgó, Cs. 5
 Santos, L. 17
 Scherer, J. J. 206
 Scheuer, Gy. 157
 Schöll-Barna, G. 147
 Sevastyanov, V. S. 200
 Shapiro, A. M. 45
 Sherwood Lollar, B. 45
 Silva, C. 134
 Simon, L. 81
 Sipos, P. 167
 Skowronek, A. 25, 41
 Smirnov, N. G. 186
 Soare, A. 151
 Somlyai, G. 23
 Somlyai, I. 23
 Sonninen, E. 24
 Stacko, S. 37
 Stefanescu, I. 151
 Stevens, R. 184
 Stibilj, V. 137
 Strapoc, D. 39
 Strauch, G. 148
 Stremtan, C. C. 22
 Šturm, M. 19, 26
 Sutherland, L. 103
 Sümegi, P. 147, 167
 Süveges, M. 149
 Szabó, Cs. 106, 108, 109, 111, 138
 Szabó, K. Zs. 108
 Szabó, M. 23
 Szabó, Zs. 109
 Szántó, Zs. 152
 Szczepanska, A. 46
 Szócs, T. 149
 Tádros, C. 132
 Tâmaş, T. 182
 Taupin, J.-D. 150
 Tcherkez, G. 16
 Tea, I. 205
 Teixeira, A. J. R. 17
 Tiedeman, C. R. 45
 Tošić, I. 143
 Trojanowska, A. 25, 41
 Tufar, W. 36
 Twining, J. 132
 Uhan, J. 29
 Ulitko, A. I. 186
 Unkašević, M. 143
 Vaikmäe, R. 185
 Varlam, C. 151
 Velivetskaya, T. A. 99, 186, 202
 Vető, I. 110
 Vişan, I. 182
 Vodila, G. 110, 152
 Voytek, M. 45
 Völgyesi, P. 111
 Vreča, P. 25, 153
 Vysotskiy, S.V. 99
 Wapelhorst, E. 206
 Widory, D. 15
 Zagnitko, V. 98
 Zavšek, S. 20, 42
 Zhang, B.-L. 205
 Zigon, S. 19
 Zula, J. 20
 Zimnoch, M. 38
 Zwolinska, E. 47